Benelux meeting on systems and control, 23rd, March 17-19, 2004, Helvoirt, The Netherlands

23rd Benelux Meeting

on

Systems and Control

March 17 – 19, 2004

Helvoirt, The Netherlands

Book of Abstracts

Bram de Jager and Vincent Verdult (eds.)
Book of Abstracts 23rd Benelux Meeting on Systems and Control

Technische Universiteit Eindhoven – Faculteit Werktuigbouwkunde
Postbus 513, 5600 MB Eindhoven (The Netherlands)

ISBN 90-386-2955-9

Programmatic Table of Contents

Karel Hinnen — Delft University of Technology
Michel Verhaegen — Delft University of Technology

ThM03 — Fijnspar
Mechanical systems I
Chair: Bert Roozen — 15.30–16.45

15.30–15.55
Discrete-time sliding mode control of a direct-drive robot 79
G. van der Zalm — Technische Universiteit Eindhoven
D. Kostic — Technische Universiteit Eindhoven
B. de Jager — Technische Universiteit Eindhoven

15.55–16.20
Virtual sensors and active vibration control on a six-degrees-of-freedom vibration isolation set-up 80
H. Super — University of Twente
G. Nijsse
J. van Dijk
J.B. Jonker

16.20–16.45
Data-based design of high-performance motion controllers 81
D. Kostic — Technische Universiteit Eindhoven
B. de Jager — Technische Universiteit Eindhoven
M. Steinbuch — Technische Universiteit Eindhoven

ThM04 — Zilverspar
Control II
Chair: Anton Stoorvogel — 15.30–16.45

15.30–15.55
Decentralized control for systems with input saturation . . 82
J. Minteer — Washington State University
A.A. Stoorvogel — Delft University of Technology
A. Saberi — Washington State University

15.55–16.20
Data-based LQG control 83
W.H.T.M. Aangenent — Technische Universiteit Eindhoven
D. Kostic — Technische Universiteit Eindhoven
A.G. de Jager — Technische Universiteit Eindhoven
M. Steinbuch

16.20–16.45
Synthesis of numerical state feedback laws for singular optimal control 84
S.C. de Graaf — Wageningen University
J. D. Stigter — Wageningen University
G. van Straten — Wageningen University

ThM05 — Lijsterbes
Model predictive control I
Chair: Hans Stigter — 15.30–16.45

15.30–15.55
Receding horizon optimal control of a solar greenhouse . . 85
R. J. C. van Ooteghem — Wageningen University
J. D. Stigter — Wageningen University
L. G. van Willigenburg — Wageningen University
G. van Straten

15.55–16.20
Stabilizing receding horizon control of constrained PWA systems 86
M. Lazar — Technische Universiteit Eindhoven
W.P.M.H. Heemels — Technische Universiteit Eindhoven
S. Weiland — Technische Universiteit Eindhoven
A. Bemporad

16.20–16.45
Model predictive control for perturbed continous PWA systems 87
I. Necoara — Delft University of Technology
B. De Schutter — Delft University of Technology
T.J.J. van den Boom — Delft University of Technology
J. Hellendoorn

ThP01 — Boswilg
Fault detection
Chair: Michel Kinnaert — 17.00–18.15

17.00–17.25
Model selection for state estimation 88
R. Bos — Delft University of Technology
X.J.A. Bombois — Delft University of Technology
P.M.J. Van den Hof — Delft University of Technology

17.25–17.50
Performance evaluation for fault detection and isolation algorithms 89
Cédric Parloir — Université Libre de Bruxelles
Michel Kinnaert — Université Libre de Bruxelles

17.50–18.15
Detection and identification of two classes of actuator faults in aircraft using augmented Kalman filters 90
Redouane Hallouzi — Technische Universiteit Delft
Vincent Verdult — Technische Universiteit Delft
Robert babuska — Technische Universiteit Delft
M. Verhaegen

ThP02 — Edelspar
Identification II
Chair: Paul Van den Hof — 17.00–18.15

17.00–17.25
Bias tuning of the G-estimate in the multivariable case 91
M. Leskens — TNO Environment, Energy and Process Innovation
P.M.J. Van den Hof — Delft University of Technology
O.H. Bosgra — Delft University of Technology

17.25–17.50
Identification of Local Linear Models with Separable Least Squares 92
Jose Borges — TUDelft
Vincent Verdult — TUDelft

17.50–18.15
Computation of LTI system responses directly from input/output data 93
I. Markovsky — K.U.Leuven
J. C. Willems — K.U.Leuven
P. Rapisarda — Universiteit Maastricht

B. De Moor

ThP03 Fijnspar
Mechanical systems II
Chair: Ben Jonker 17.00–18.15

17.00–17.25
Broad-band active vibration suppression 94
A.J. den Hamer Eindhoven University of Technology
G.Z. Angelis PHILIPS Centre for Industrial Technology
N.B. Roozen PHILIPS Centre for Industrial Technology
M.J.G.v.d. Molengraft

17.25–17.50
Feedback control of broadband disturbances on a one-degree-of-freedom experimental vibration isolation set-up 95
G. Nijsse University of Twente
H. Super University of Twente
J. van Dijk University of Twente
J.B. Jonker

17.50–18.15
Self-Excited Vibrations of Drag Bits 96
Christophe Germay Universite de Liege
Dr Rodolphe Sepulchre Universite de Liege

ThP04 Zilverspar
$\mathcal{H}_2$ control
Chair: Gjerrit Meinsma 17.00–18.15

17.00–17.25
$\mathcal{H}_2$-Optimal controller synthesis - a MIMO frequency-domain solution 97
J.A. Villegas Twente University

17.25–17.50
H2-optimal control of systems with multiple i/o delays: time domain approach 98
Agoes A. Moelja University of Twente
Gjerrit Meinsma University of Twente

17.50–18.15
Shape change of tensegrity structures: design and control 99
J.J.M. van de Wijdeven Technische Universiteit Eindhoven
Bram de Jager Technische Universiteit Eindhoven

ThP05 Lijsterbes
Model predictive control II
Chair: Okko Bosgra 17.00–18.15

17.00–17.25
Structured interior-point method based MPC for nonlinear processes 100
Andrei Tiagounov Technische Universiteit Eindhoven
Jeroen Buijs Leuven Engineering School, Group T

17.25–17.50
Model predictive control for mixed urban and freeway networks 101
M. van den Berg Delft University of technology
B. De Schutter Delft University of technology
J. Hellendoorn Delft University of technology

17.50–18.15
Efficient MPC with time-varying terminal cost using convex combinations 102
Bert Pluymers Katholieke Universiteit Leuven
Johan Suykens Katholieke Universiteit Leuven
Bart De Moor Katholieke Universiteit Leuven

Friday, March 19, 2004

Mini Course: P5 Boswig
Realizations: Examples and applications
Bart De Moor (Belgium)
Chair: Vincent Verdult 8.30– 9.30

Realizations: Examples and applications 167
Bart De Moor (Belgium)

Plenary: P6 Boswig
Understanding and controlling turbulent shear flows
Bassam Bamieh (USA)
Chair: Bram de Jager 10.00–11.00

Understanding and controlling turbulent shear flows 157
Bassam Bamieh (USA)

Mini Course: P7 Boswig
The "noisy" realization problem and model reduction
Bart De Moor (Belgium)
Chair: Bram de Jager 11.30–12.30

The "noisy" realization problem and model reduction . . 167
Bart De Moor (Belgium)

FrP02 Edelspar
Identification III
Chair: Alain Vande Wouwer 14.00–15.40

14.00–14.25
Experiment design and realization for the identification of a six-degree of freedom Stewart Platform 103
Maria Isabel Parra Calvache Delft University of Technology

14.25–14.50
Measuring the transfer function and characteristic impedance of transmission lines 104
Wim De Block Vrije Universiteit Brussel

14.50–15.15
Multi-modelling of activated sludge wastewater treatment plants using data-driven techniques 105
G. Gins BioTeC - K.U.Leuven
I.Y. Smets BioTeC-K.U.Leuven
J.F. Van Impe BioTeC - K.U.Leuven
A. Geeraerd

15.15–15.40
A computational procedure for the predetermination of parameters in bioprocess models 106
Jürgen Fritz Faculté Polytechnique de Mons
Jens Haag Faculté Polytechnique de Mons
Alain Vande Wouwer Faculté Polytechnique de Mons

FrP03 Fijnspar
Process control
Chair: Gerrit van Straten 14.00–15.40

FrP04 Zilverspar
Learning control
Chair: Johan Suykens 14.00–15.15

FrP05 Lijsterbes
Distributed systems
Chair: Ruth Curtain 14.00–15.40

FrP06 Vlier
Computation and control
Chair: Vincent Blondel 14.00–15.40

P8 Restaurant
Best Junior Presentation Award ceremony
Chair: Okko Bosgra 15.45–16.00

Part 1

Contributed Lectures

Efficient Microscopic Simulation of Large Scale Highway Traffic Flows

Sven Maerivoet and Bart De Moor

Katholieke Universiteit Leuven
Department of Electrical Engineering ESAT-SCD (SISTA)
Kasteelpark Arenberg 10, B-3001 Leuven
{sven.maerivoet,bart.demoor}@esat.kuleuven.ac.be
Phone: +32 (0) 16 32 17 09 / Fax: +32 (0) 16 32 19 70
http://www.esat.kuleuven.ac.be/scd

1. Introduction

As traffic policy makers get more and more confronted with increasing global congestion on the road networks, controlling the traffic flows becomes a corner stone in the optimal usage of the existing road infrastructure.

Today, a main challenge is the construction of macroscopic and microscopic models that lend themselves to a faithful representation of road traffic, as these models are used in several key aspects in the control of traffic flows [1].

Within this context, our research is aimed at assisting traffic engineers who wish to evaluate what-if scenarios and/or perform real-time control of traffic flows. Whereas the former requires a sufficiently detailed model, the latter calls for an efficient implementation that allows fast simulations. The challenge thus consists of the development of a flexible testbed environment that is capable of providing us with a detailed simulation model of a real-world road network (which is, in our case, the Flemish primary highway network) [2].

2. Microscopic traffic flow simulation

In our research, we consider traffic flow models as being microscopic in nature. Each vehicle in a traffic flow is modelled individually, resulting in a detailed description of the dynamical processes behind a traffic flow.

The class of microscopic traffic flow models that we employ, are the traffic cellular automata (TCA) models. They represent traffic flows using very simplified models that have, on a microscopic scale, a rather low accuracy [3]. This in turn has an important advantage: they provide an efficient and fast performance when used in computer simulations. TCA models explicitly describe local interactions between individual vehicles in a traffic flow, by means of rulesets that reflect the rule based behaviour of a cellular automaton evolving in time and space (i.e., the road network).

3. The quest for speed

Although these TCA models allow for fast computations, they are nevertheless computationally very expensive because they are based on behavioural submodels that need to be applied to each vehicle at each timestep. We thus need to find the most optimal solution in terms of time and space complexity. A logical step in this direction, is an efficient parallellisation scheme that lowers the computational overhead involved. This can be accomplished by using distributed computing, where we partition the road network in several distinct geographical regions that are assigned to different machines which run in parallel.

4. Practical implementation

We automatically gain platform independency using Java. The challenge now is to get reliable and efficient (i.e., faster than real-time) operation of a very heterogeneous computing environment. To this end, the simulator consists of one master, controlling several different workers that efficiently simulate local traffic flows.

Using this fast integrated simulation environment, we can evaluate different scenarios, or even use it as a mirror of the real-world when implementing traffic control measures.

References

[1] "*Sustainability Effects of Traffic Management Systems*", PODO-II / DWTC-CP/40 project, First Intermediary Scientific Report, ed. Sven Maerivoet, january 2003.

[2] Sven Maerivoet and Bart De Moor, "*Development of an Improved Traffic Cellular Automaton Model for Traffic Flows on a Highway Road Network*", Proceedings of the 10th World Congress and Exhibition on Intelligent Transport Systems and Services, Madrid, Spain, november 2003.

[3] Kai Nagel and Michael Schreckenberg, "*A cellular automaton model for freeway traffic*", Journal de Physique I France, vol. 2, pages 2221-2229, 1992.

Sending and Receiving Functions in Macroscopic Stochastic Hybrid Models for Freeway Networks

Lyudmila Mihaylova

SYSTeMS, Universiteit Gent
B-9052 Zwijnaarde, Belgium
mila.mihaylova@ieee.org

René Boel

SYSTeMS, Universiteit Gent
B-9052 Zwijnaarde, Belgium
rene.boel@ugent.be

1 Introduction

Traffic flow on freeways is a complex process and its on-line management incorporates many aspects: analysis of the traffic phenomena and building up adequate traffic and sensor models, development of cost-effective and reliable data processing techniques for traffic state estimation and control [1]. Perturbations are propagated from upstream to downstream sections via *forward waves*. Different phenomena are observed in jammed mode. Drivers are slowing down far before the congestion zone which increases the traffic density upstream provoking a *backward wave*.

We represent the freeway traffic as a network of stochastic dynamic components, each component describing a different section of the network. It brings modularity, flexibility and scalability potential of the decentralized architectures, improves the system predictability.

2 Traffic Modelled as a Stochastic Hybrid System Using Sending and Receiving Functions

The traffic is a *stochastic hybrid system*, i.e. each traffic section possesses continuous and discrete states, interacting with variables from neighboring sections. *Continuous variables* in a section are the average speed and the average number of cars. *Modal (discrete) state variables* describe the abrupt changes in the traffic regimes (number of lanes, weather conditions or controlled events such as change of traffic lights).

A stochastic macroscopic hybrid model of the freeway traffic is developed. Each section i is here described by variables at possibly *asynchronous* points in time. The state vector contains the number $N_{i,k}$ of vehicles inside a section i at time t_k, and their average speed $v_{i,k}$. The dynamic evolution of the traffic state of a link depends on the interaction between neighbor links: on the inflow and outflow at upstream and downstream boundary of the link which can be described by dynamically changed sending and receiving functions. The *sending function* is a random variable expressing how many among $N_{i,k}$ vehicles can leave section i at time instant t_k. The *receiving function* gives the number of vehicles that can enter section $i+1$ at the next time instant t_{k+1}. The flow-density diagram plotted based on a model with sending and receiving functions (Fig. 1) has a bell-shaped form and the scattered zone in it represents the congestion mode. It describes well both the *forward* propagation of traffic perturbations from upstream to downstream sections and the perturbations' propagation to *backwards* in the presence of congestions.

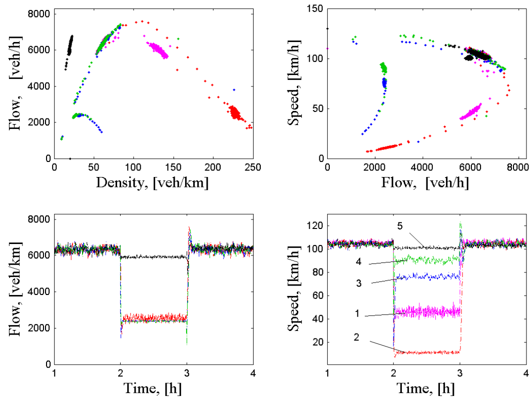

Figure 1: Traffic modelled by sending and receiving functions

3 Conclusions

This paper presents a macroscopic stochastic hybrid model of traffic suitable for on-line flow estimation, mode detection and for ramp metering control. It is general and applicable to both freeways and urban networks with different topologies and different types of sensors.

References

[1] Helbing, D., Traffic and Related Self-Driven Many-Particle Systems,*Rev. of Mod. Phys.*, Vol.73, pp.1067-1141, 2001.

Acknowledgments. Financial support by the project DWTC-CP/40 "Sustainability effects of traffic management", Belgium is gratefully acknowledged, and also by the Programme on Inter-University Poles of Attraction initiated by the Belgian State, Prime Minister's Office for Science, Technology and Culture.

Validation of advanced driver assistance systems with VEHIL

Olaf Gietelink, Jeroen Ploeg
Advanced Chassis and Transport Systems
TNO Automotive
P.O. Box 756, 5700 AT Helmond
The Netherlands
Email: gietelink@wt.tno.nl

Bart De Schutter, Michel Verhaegen
Delft Center for Systems and Control
Delft University of Technology
Mekelweg 2, 2628 CD Delft
The Netherlands
Email: b.deschutter@dcsc.tudelft.nl

1 Introduction to advanced driver assistance systems

With the increasing demand for safer passenger vehicles, the development of Advanced Driver Assistance Systems (ADASs) is of major interest to the automotive industry. State-of-the-art ADASs are adaptive cruise control and pre-crash sensing systems. They not only improve the driving comfort, but can also assist the driver in reacting to dangerous situations and collision avoidance.

The complexity of these intelligent vehicle control systems is however in contradiction to the increasing demand for reliability and safety. To improve fault management often redundant components and fault-tolerant controllers are implemented in ADASs. In practice, it is however difficult to choose the right measures and to validate their effectiveness. Currently, simulations and prototype test drives are used to validate an ADAS, but these tests can be unreliable and costly. An efficient methodology and new design tools are thus required for validation of the safety and reliability of an ADAS under the influence of a variety of faults.

2 Vehicle-hardware-in-the-loop testing

For this purpose TNO Automotive has developed VEHIL (VEhicle-Hardware-In-the-Loop), a test rig for intelligent vehicles [1]. VEHIL makes it possible to conduct hardware-in-the-loop experiments with full-scale intelligent vehicles in a laboratory environment. A virtual environment is defined in which the vehicles, the infrastructure and their interactions are simulated. The full-scale intelligent vehicle is placed on a chassis dynamometer that is interfaced with this virtual environment. Surrounding traffic participants are represented by autonomous robot vehicles (so-called moving bases) that carry out the relative motions to the intelligent vehicle. In this way the ADAS can be evaluated as if the vehicle is actually driving on the road, where the absolute velocity is removed from the test. A photo of the laboratory setup is shown in Figure 1.

3 Randomized algorithms for ADAS analysis

In VEHIL the control system can be validated with respect to environment sensor (radar) faults that can be introduced in a controlled way. It is however impossible to exhaustively test the ADAS for every fault type under every operating condition. We propose a new methodology that provides a suitable test program in order to sufficiently (but also efficiently) cover the entire 'fault space' (the combined set of possible failure modes and complex operating conditions). For this purpose algorithms are developed, in order to construct an optimum set of VEHIL tests to sufficiently prove the reliability and safety of the ADAS.

Figure 1: Laboratory setup with intelligent vehicle (left), moving base (right) and chassis dynamometer.

This approach relies on randomized algorithms that form the basis for off-line Monte Carlo simulations with the ADAS control system. The strength of this approach is that the control system analysis does not depend on the level of complexity of the underlying system (in contrast to a deterministic approach). The disadvantage is that uncertainty is associated with the estimated level of reliability, since a random sample is chosen to represented the fault space.

When simulations have indicated the most critical scenarios (in terms of safety and reliability), a selection is made to be replayed in the VEHIL facility. With this practical evaluation the assessment can be made more reliable.

Acknowledgments

Research sponsored by TNO and TRAIL Research School.

References

[1] O.J. Gietelink, J. Ploeg, B. De Schutter, and M. Verhaegen. VEHIL: Test facility for fault management testing of advanced driver assistance systems. In *Proc. of the 10th World Congress on Intelligent Transport Systems and Services (ITS)*, Madrid, Spain, 2003. Paper 2639.

Stability analysis of second order traffic flow models

B. Haut G. Campion G. Bastin

Abstract

In order to overcome the limitations of the standard first order model of traffic flow (LWR model), various second order models involving relaxation and/or anticipation terms were introduced in the literature. These models have the particularity to possess an equilibrium which can be unstable if certain so-called subcharacteristic conditions are not satisfied. It can be shown that these conditions connect the characteristic velocities of the second order model to the characteristic velocity of the LWR model, and may be interpreted as a "competition" between the relaxation and the anticipation term. The subcharacteristic conditions are also necessary to guarantee that the first order LWR model is a valid approximation of second order models. These stability subcharacteristic conditions are often assumed to be naturally satisfied although there is no a priori physical reason justifying such an assertion. It is therefore of interest to analyse the system behaviour, and namely the propagation and evolution of disturbances, when these conditions are not satisfied. The study of these instabilities provide a possible interpretation of the emergence of jams and stop-and-go effects in traffic flow.

Implications of the capacity drop phenomenon for freeway traffic control

Andreas Hegyi
Delft Center for Systems and Control
Delft University of Technology
Mekelweg 2, 2628 CD Delft
The Netherlands
email: a.hegyi@dcsc.tudelft.nl

Bart De Schutter
Delft Center for Systems and Control
Delft University of Technology
Mekelweg 2, 2628 CD Delft
The Netherlands
email: b.deschutter@dcsc.tudelft.nl

Hans Hellendoorn
Delft Center for Systems and Control
Delft University of Technology
Mekelweg 2, 2628 CD Delft
The Netherlands
email: j.hellendoorn@dcsc.tudelft.nl

Abstract

The capacity drop phenomenon on freeways has been confirmed in several empirical studies for on-ramps [1] and shock waves [2]. In both cases the capacity drop refers to the phenomenon that the outflow of a traffic jam is significantly lower than the capacity of the freeway under free-flow conditions. Consequently, the outflow can be restored to the free flow capacity only if the traffic jam is resolved. In order to resolve the traffic jam, the inflow to the jammed area must be lower than the outflow of the area, which means that the traffic control measures must be able to limit the inflow of the area sufficiently.

Figure 1: Speed limits on the A13 freeway at Overschie.

In this contribution we apply this *flow limitation condition* to traffic scenarios where dynamic speed limits (as shown in Figure 1) and ramp metering (as shown in Figure 2) are used as traffic control measures. The scenarios include: (1) dynamic speed limits to suppress shock waves, (2) ramp metering to eliminate a freeway jam at an on-ramp, (3) combined dynamic speed limits and ramp metering to eliminate a freeway jam at an on-ramp. We also show that in the last case the combination of dynamic speed limits with ramp metering can solve traffic jams for a wider range of traffic scenarios than ramp metering alone (which is currently the typical situation in practice).

Figure 2: Ramp metering on the A13 freeway near Delft-Zuid.

Acknowledgments

Research supported by the AVV Traffic Research Centre of the Dutch Ministry of Transport, Public Works and Water Management, and the TU Delft spearhead program "Mobility of People and Transportation of Goods".

References

[1] M. J. Cassidy and R. L. Bertini. Some traffic features at freeway bottlenecks. *Transportation Research Part B*, B33:25 – 42, 1999.

[2] B. Kerner and H. Rehborn. Experimental properties of phase transitions in traffic flow. *Physical Review Letters*, 79(20):4030–4033, November 1997.

Introduction to an integrated design for motion systems using over-actuation

M.G.E. Schneiders*, M.J.G. van de Molengraft, M. Steinbuch

*corresponding author:
Eindhoven University of Technology, Dept. of Mechanical Engineering,
P.O. Box 513, 5600 MB Eindhoven, The Netherlands
e-mail: m.g.e.schneiders@tue.nl

1 Introduction

The objective of a motion system is to perform a programmed motion task with the end-effector of the system. Traditionally these systems contain a number of actuators equal tot the degree of free rigid-body modes. Since all mechanical structures have finite stiffness, the total performance of the system will suffer from resonances. To drive a mechanical structure according to a predefined setpoint (feedforward), minimal excitation of resonances modes is obtained by actuator placement near the nodal points of the most significant resonant modes (minimal modal controllability). To attenuate excited resonance modes due to disturbances (feedback regulation), actuators are best located were the resonance modes can be influenced as much as possible (maximum controllability). Unfortunately, the feedback path and the feedforward path require different placement of the actuators to work optimally. Optimizing actuator placement for both paths is contradictorily, at least in traditional designs.

2 Objective

Allowing more actuators in the design than free rigid-body modes (*over-actuation*) makes it possible to overcome this limitation. The objective is to both minimize modal controllability in the feedforward path and maximize the modal controllability in the feedback path by applying over-actuation. This can result in higher levels of performance without *rigidizing* the mechanical construction (increasing stiffness). This means less moving mass, so less energy dissipation.

3 New approach

Starting-point of the procedure is modal knowledge of the system: eigenfunctions or the mode shapes of the most important resonances must be known. Next the design procedure consist of 3 steps. First, actuator placement (p_i) is determined according to maximization of a controllability measure. Next, for the feedback design (C_{fb}), standard concepts in vibration control can be used. Third step is the design of the feedforward path. A static gain relation (K_{ff}) between the actuators is determined, such that the excitation of the most dominant modes is minimized. Further feedforward design (C_{ff}) is now straightforward: acceleration-feedforward for each free rigid-body mode.

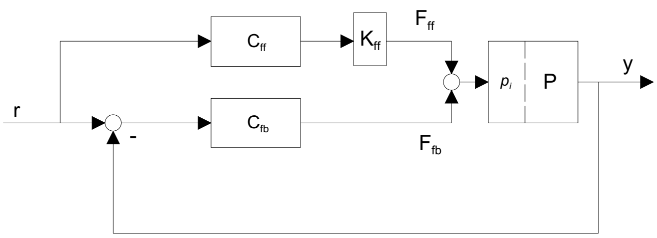

4 Discussion and results

An over-actuated design approach makes it possible to decouple the controllability of resonance modes for the feedback and feedforward path: both feedback and feedforward behavior is improved. Damping is more efficiently added by the feedback and the feedforward path shows less flexible behavior. The largest benefit of this approach is the possibility to design motion systems with higher accuracy and better disturbance attenuation without increasing mechanical stiffness and moving mass. On the other hand, it is also possible to design more lightweight motion systems by the use of over-actuation while keeping up tracking performance.

5 Future work

If disturbances are included in the design, it is possible to impose performance criteria on the feedback controller. Together with setpoint specifications, an integral optimization of the actuator placement is possible, allowing for both criteria. Furthermore, feedback design should be included in the optimization, so also sensor placement (observability) has to be included.

Exploration of multivariable control for motion systems

Matthijs Boerlage‡, Georgo Angelis†, René van de Molengraft‡, Maarten Steinbuch ‡
† PHILIPS Centre for Industrial Technology (CFT)
Mechatronics Research
P.O. Box 218, SAQ-2122, 5600 MD Eindhoven, The Netherlands
‡ Eindhoven University of Technology
Faculty of Mechanical Engineering, Control Systems Technology Group
P.O. Box 513, 5600 MB Eindhoven, The Netherlands
Email: M.L.G.Boerlage@student.tue.nl, Georgo.Angelis@philips.com

This presentation gives an overview of an exploratory study on the application of multivariable control techniques for electromechanical motion systems currently used at Philips CFT. The objective is to extend SISO manual frequency response function based loopshaping techniques towards MIMO control problems. Cases will be presented where multivariable control techniques outperform conventional scalar techniques.

A major difference of multivariable systems compared to scalar systems is the property of directionality, see e.g. [5]. Directionality has a major influence throughout the control problem. This means that not only the multivariable nature of the plant but also the multivariable nature of disturbances and performance objectives must be taken into account. When designing a multivariable controller, directionality properties may be exploited.

Integral relations for multivariable systems, see e.g. [2] or [1] point out that for some cases effects of non-minimum phase behavior in the plant may be reduced when multivariable control is applied. Then a so-called *spatial tradeoff* of sensitivities is possible in addition to the frequency wise trade-off as in scalar systems (water-bed effect). However, motion systems at Philips CFT do not have such defects, hence this spatial trade-off has negligible effect. As motion systems typically show dominant rigid body behavior, in the frequency region of interest, static decoupling procedures may be applied. Then, from a plant point of view, decentralized control (sequentially designed scalar controllers) leads to satisfactory performance. Decentralized controllers can be designed using manual loopshaping techniques, see e.g. [6]. These multivariable controllers closely resemble those derived using characteristic loci techniques, see e.g. [4], [3].

A new area, quite unexplored, is the use of the multivariable character of disturbances. In many practical applications disturbances are highly coupled as they often relate to the same underlying physical process, e.g. floor vibrations, pumps, reaction forces on metro frames, etc. Tools are proposed to derive multivariable properties of such disturbances. Furthermore, multivariable control solutions based on manual loopshaping are presented that exploit these properties.

Next, an overview is given of manual loopshaping techniques for non-square multivariable design. Cases are presented that show performance limiting properties (e.g. fast-slow systems, mode dynamics,etc.). These cases illustrate that performance can be increased using non-square multivariable control. These control design techniques are strongly related to the conventional scalar loopshaping procedures and offer a relatively simple way to use the power of multivariable control in a practical environment.

References

[1] J. Chen, ‘Sensitivity Integral Relations and Design Trade-Offs in Linear Multivariable Feedback Systems’, *IEEE Trans. Autom. Control*, 1996, Vol. 40, No. 10. pp.1700-1716.

[2] G. Gomez, G. Goodwin ‘Integral Constraints on Sensitivity Vectors for Multivariable Linear Systems’, *Automatica*, 1996, Vol. 32, No. 4. pp.499-518.

[3] J. Maciejowski, ‘Multivariable feedback design’, Addison-Wesley, 1989.

[4] H. Rosenbrock, ‘Computer-aided control system design’, Academic Press, 1974.

[5] S. Skogestad, I. Postlethwaite, ‘Multivariable feedback control, analysis and design’, John Wiley & Sons, 1996.

[6] M. Steinbuch, M.L.Norg, ‘Advanced motion control: an industrial perspective’, *Eur. J. of Control*, 1998, pp.278-293.

Experiments for high-dimensional Learning FeedForward Control,
with an on-line support vector based function approximator

Bas J. de Kruif
Drebbel Institute for Mechatronics
b.j.dekruif@utwente.nl

Theo J. A. de Vries
Drebbel Institute for Mechatronics
t.j.a.devries@utwente.nl

1 Introduction

Previous work on Learning FeedForward Control (LFFC) showed that this control scheme was able to significantly reduce the tracking error [1]. The LFFC-scheme identifies state-dependent effects like friction as function of its state, and uses this approximation to compensate for the influence of it. A function approximator is required to identify an effect as function of its states. Until now, the used function approximator was a B-spline network. This network is prone to the curse of dimensionality and can therefore only approximate effects that depend on one state.

In the past years of research a different function approximator is constructed that is less prone for this curse. This approximator is tested in an on-line LFFC setting in which the effects depend on a maximum of 9 variables.

2 Function Approximation

The constructed function approximator is based on the Support Vector Machine (SVM) introduced by Vapnik [2]. It uses a subset of the samples to represent the data and so to predict for a newly encountered samples. The samples that are used to represent the data are called *key samples.* The interpolation between the samples is determined by a kernel function. However, for on-line applications, the approximator has to cope with a data stream while SVM finds an approximation based on a batch. In the stream, the correct samples to represent the complete data set have to be found. To come to an on-line approximator the following ideas are used:

- Summarise the data by a subset of key samples.
- Assign a weight to each of these key samples that indicate the multitude of data it represents.
- Expand the subset if it cannot explain the new training sample with some probability.
- Alter the output of a key sample as a result of new training data.

The calculations necessary for the implementation of these ideas are recursive. The resulting approximator has the following properties:

- The structure is adapted by the key samples; a more difficult relation results in more key samples.
- Overfitting is countered due to the inclusion based on probabilities.
- The approximator is capable of handling high input dimensions due to SVM approach.
- Superfluous key samples are omitted to save storage space.
- Forgetting and regularisation are incorporated.

3 Experiments

The experiments are performed on a mechanical setup. This setup consist of three coupled linear motors. To compensate for the state dependent effects, three inputs for each moving motor are required for the feedforward controller. The advantage of this setup is that by allowing one, two or three motors to move, the number of inputs to the feedforward controller, and therefore the function approximator, alters.

The results are summarised in table 1. It can be seen, that the learning significantly reduces the tracking error. The performed motion was a *non-repetitive* concatenation of third order paths. The residual after learning consisted mainly of vibrations of the setup which can not be compensated for by this control scheme.

Table 1: RMS of the tracking error

	3 inputs RMS [μm]	**6 inputs** RMS[μm]	**9 inputs** RMS[μm]
no learning	170	182	176
with learning	18	25	32

4 Summary

Based on the experiments it was found that the learning control scheme is applicable to compensate for state dependent effects. Due to the introduced function approximator the number of inputs can become rather large. Nine inputs are tested with good results. The limitation of this control scheme are the residual vibrations. It is recommended that in future work these vibrations are dealt with.

References

[1] W. J. R. Velthuis, *Learning Feed-Forward Control, Theory, Design and Applications.* PhD thesis, University of Twente, Enschede, 2000.

[2] V. N. Vapnik, *The Nature of Statistical Learning Theory,* 2nd edition, Springer-Verlag, New York, 2000.

The RRR-robot Feedback Control Design via Iterative Feedback Tuning

T.A.E. Oomen, D. Kostić, B. de Jager, and M. Steinbuch
Department of Mechanical Engineering, Technische Universiteit Eindhoven
T.A.E.Oomen@student.tue.nl, D.Kostic@tue.nl, A.G.de.Jager@wfw.wtb.tue.nl, M.Steinbuch@tue.nl

Introduction

Control design can be model-based or data-based. A model-based design can deliver a high performance controller if the implemented model is an accurate description of the plant. Inaccuracies in the model limit the controller performance and may even lead to instability. It is sometimes time consuming and costly to model the plant accurately. Moreover, if the model is complex, the controller can be too complex for real time implementation. In data-based control design, the plant modelling step is omitted. Instead, the controller is derived using experimental data. In this work, a data-based control approach, called Iterative Feedback Tuning (IFT) [1], is investigated. This approach can be used to tune the parameters of a controller with a fixed structure.

Approach

Feedback design using the IFT approach begins with the definition of a performance criterion. Typically, the criterion simultaneously penalizes the difference between the desired and actual plant output (error) and the input to the plant. Furthermore, the designer selects a controller class of desired complexity with some parameters free to tune, *e.g.* a PID controller. The objective of IFT is to minimize the criterion by tuning the free controller parameters. The optimization is performed by an iterative method, which requires knowledge of the gradient of the criterion with respect to the controller tuning parameters. The key feature of IFT is the estimation of this gradient directly from the experimental data.

Experimental setup

The IFT algorithm is applied on a direct-drive robot. This robot has three revolute joints (RRR kinematics) and it exhibits strongly nonlinear dynamics. In previous work [2], a nonlinear model-based feed-forward compensation has already been designed. The dynamics that remain after compensation are decoupled and mostly linear. These remaining dynamics have already been identified and modelled. In this work, a feedback controller is designed for the remaining dynamics that correspond to the first robot joint, by using IFT. Only input-output data from the plant is used by the IFT algorithm, the model is merely used for simulation purposes.

Results

The IFT algorithm selected is adequate for the considered robot control problem. At each iteration step, two experiments are performed. The first experiment is performed under normal operating conditions. The second experiment is a special, dedicated experiment, where the error signal of the first experiment is used as reference signal. After appropriate processing of the process output of this special experiment, the gradient of the criterion with respect to the controller parameters is obtained. Subsequently, the controller parameters are updated. This algorithm is tested in simulations, based on a high-order linear model of the remaining dynamics. Next, the algorithm is implemented on the robot. In both cases, a minimum is found after several iterations. Finally, the controllers obtained during simulations and experiments are evaluated. It turns out that the third-order discrete-time controller, obtained with the IFT algorithm, results in increased performance compared to the initial, weakly tuned PD controller, see figure 1. The resulting controllers during simulations and experiments are not identical. Differences are explained by unmodelled dynamics.

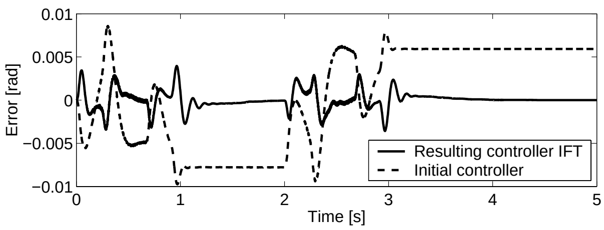

Figure 1: Tracking error during experiments

References

[1] H. Hjalmarsson, M. Gevers, S. Gunnarsson, O. Lequin, "Iterative Feedback Tuning: Theory and Applications," IEEE Control Systems Magazine, Vol. 18, no. 4, pp. 26-41, 1998.

[2] D. Kostić, B. de Jager, M. Steinbuch, "Experimentally Supported Control Design for a Direct Drive Robot,", Proc. of the 2002 IEEE Int. Conf. on Control Applications, Vol. 1, pp. 186-191, 2002.

Implementing control algorithms on embedded platforms[1]

J.H. Sandee, P.P.J. van den Bosch, W.P.M.H. Heemels
Control Systems Group, Department of Electrical Engineering
Technische Universiteit Eindhoven, P.O. Box 513, 5600 MB Eindhoven, The Netherlands
Email: j.h.sandee@tue.nl

1 Introduction

In the design of complex embedded dynamical systems the interaction between control and software plays an important role. The control algorithms that are obtained from models and experiments on dedicated high performance hardware, have to be implemented on embedded hardware with processor power to be shared among various other applications.

2 Requirements of standard control

A control algorithm poses severe requirements on the embedded software, namely both a high and an accurate sample frequency. A high sample frequency is needed to perform measurements and to update actuator signals. An accurate sample frequency, so no jitter, is required because control laws simply assume this. An example of a standard implementation of a control algorithm is given in fig.1.

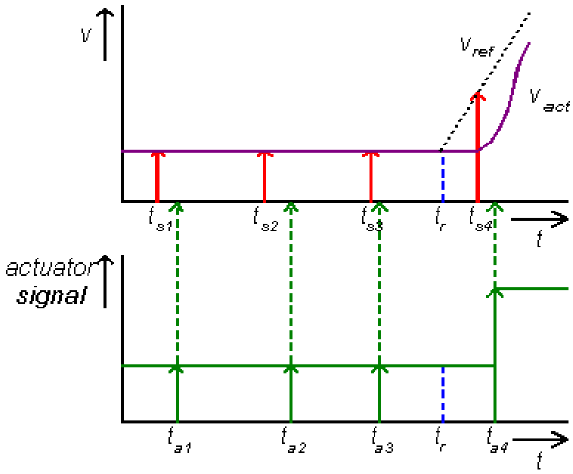

Figure 1: Standard control behavior

At a specified frequency, samples are taken (t_{s1}, t_{s2}, etc). After this the control signal is calculated and applied with some delay (t_{a1}, t_{a2}, etc). A high sample rate is required to keep track with fast changing reference values and/or disturbances. Moreover, a small sample time reduces the delay owing to sampling a time continuous process. Jitter introduces errors owing to differences between the assumed sample time and the real sample time, such that the calculated actuator signal is no longer appropriate when it is really applied.

3 Possible solution directions

Most control algorithms, like the one depicted in fig.1, make use of both observer and controller behaving synchronously in time. When implementing the control algorithm on embedded platforms, the need for asynchronous observers and controllers seems to be arising, or at least some method to cope with the variations in the sampling rate. Already quite some effort has been spent in investigating asynchronous observers in combination with a fixed rate controller, see e.g. [1]. Less effort has been spent in the field of asynchronous controllers [2]. The advantage of having both the measurement and the actuator signal update not equidistant in time, is the ability to perform control actions at moments when very accurate and relevant measurement data comes available. Returning to the example depicted in fig.1, it can be seen that the best moment for an asynchronous controller to update the control signal would be time t_r. An intelligent sensor could be used to interrupt the software at the moment the error exceeds a specified boundary. Another possibility to reduce the sampling frequency could be to generate an actuator signal that is not time-discrete, but piecewise linear or even of higher order. At last, the influence of jitter can be reduced or can even be avoided when the correct value of the actuator signal can be fast retrieved at the moment in time the actuator signal is executed.

4 Conclusion

The suggested control algorithms can effectively ease the strong requirements on accurate sampling frequencies that the control community lays upon the embedded software.

References

[1] Philips, A.M., Tomizuka, M., Multirate estimation and control under time-varying data sampling with applications to information storage devices. *Amer. Control Conf., pp. 4151-4144, vol. 6, 1995.*

[2] Heemels, W.P.M.H., Gorter, R.J.A., et al, Asynchronous measurement and control: a case study on motor synchronization. *Control Eng. Pract. 7, pp. 1467-1482, 1999.*

[1]This work has been carried out as part of the Boderc project under the responsibility of the Embedded Systems Institute. This project is partially supported by the Netherlands Ministry of Economic Affairs under the Senter TS program.

Towards a model for Indole-3-Acetic Acid (IAA) production by *Azospirillum brasilense* Sp245

A. Cappuyns[1], I. Smets[1], K. Bernaerts[1], O. Ona[2], J. Vanderleyden[2], E. Prinsen[3] and J. Van Impe[1]
[1]BioTeC–Katholieke Universiteit Leuven, W. de Croylaan 46, B-3001 Leuven (Belgium)
astrid.cappuyns@cit.kuleuven.ac.be - jan.vanimpe@cit.kuleuven.ac.be
[2]CMPG–Katholieke Universiteit Leuven, Kasteelpark Arenberg 20, B-3001 Leuven (Belgium)
[3]Department of Biology, University of Antwerp, Universiteitsplein 1, B-2610 Antwerpen (Belgium)

1 Introduction

The nitrogen fixing bacteria *Azospirillum* offers interesting perspectives for alternative fertilization since inoculation with these bacteria positively affects the plant growth [1]. Studies have shown that the growth promoting power after *Azospirillum* inoculation can probably be attributed to the production of indole-3-acetic acid (IAA) [3]. The aim of this study is to characterize and quantify the IAA production by *Azospirillum brasilense* Sp245 on a macroscopic level. In order to study the IAA production, batch experiments were performed with L-malate as sole carbon source. Tryptophane (Trp), which is necessary for IAA production, was also added at the beginning of the batch experiments.

2 Modelling of growth and IAA production

Since there is no evidence that malate consumption or biomass growth is influenced by the presence of IAA or Trp in the medium, the growth process is tackled first as a separate phenomenon. When focussing on mass balance equations for batch reactors, the only term that needs to be specified is the reaction term since no transport has to be taken into account. For modelling the specific growth rate μ, a simple monotonically increasing function, i.e., the Monod equation is proposed. The link between the specific growth rate and the substrate consumption is represented by the so-called linear law in which maintenance is neglected.
For the IAA production, two models structures are proposed. In the first model hypothesis, IAA is formed from Trp and biomass serves as (bio)catalyst. In the second hypothesis, production of IAA is also growth related.

3 Discussion of the preliminar results

When Monod type kinetics have to be identified from batch experiments, it is known that the parameters will be highly correlated and a unique identification will be hard since the cost surface is littered with local minima. To overcome this identification problem, further experiments have to be carried out. Performing a fed batch experiment with a very low feed rate in which malate is present, enables to clarify which parameter set is more reliable. A more rigorous approach is based on optimal experimental design (OED). With OED an optimal input (i.e., feeding profile) can be designed, that ensures high information content of the data with respect to uncorrelated, unique parameter estimation [4].
For the IAA production process, no distinction between the two hypotheses (growth dependency or not) could be made on the basis of the available data. To overrule or validate the hypothesis that IAA production is growth related, the time instant at which the malate becomes depleted must be different from the instant at which Trp becomes exhausted. This can be achieved by performing a simple batch experiment with other initial malate and Trp concentrations. Also for this type of model structure discrimination, techniques of optimal experimental design can be applied (eg., [2]).

4 Conclusions

In this research, two prototype models for the production of IAA by *Azospirillum brasilense* Sp245 are proposed. Based on these prototype models and computer simulations, experiments are proposed that allow better parameter estimation and discrimination between the two hypotheses related to IAA production. Further research will focus on accurate parameter estimation and model structure discrimination by means of optimal experimental design and the realization of the proposed (more informative) experiments.

Acknowledgements. Ilse Smets and Kristel Bernaerts are Postdoctoral Fellows with the Fund for Scientific Research Flanders (FWO). Work supported in part by Projects FWO-G.0085.03, IWT-GBOU-project 20160, OT/99/24 and OT/03/30 of the Research Council of the Katholieke Universiteit Leuven and the Belgian Program on Interuniversity Poles of Attraction, initiated by the Belgian State, Prime Minister's Office for Science, Technology and Culture. The scientific responsibility is assumed by its authors.

References

[1] Baldani, V.L.D., Baldani, J.I. and Döbereiner, J. (1983). Effects of *Azospirillum* inoculation on root infection and nitrogen incorporation in wheat. *Canadian Journal of Microbiology* **29**, 924-929.

[2] Munack, A. (1992). Some improvements in the identification of bioprocesses. In: *Modelling and Control of Biotechnical processes* (M.N. Karim and Stephanopoulos, Eds). pp. 89-94 . Pergamon Press, Oxford.

[3] Okon, Y. and Vanderleyden, J. (1997). Root associated *Azospirillum* can stimulate plants. *ASM News* **63**, 366-370.

[4] Versyck, K.J. , Claes, J.E. and Van Impe, J.F. (1997). Practical identification of unstructured growth kinetics by application of optimal experimental design. *Biotechnology Progress* **13**(5), 524-531.

Systematic decoupled identification of pseudo-stoichiometry, lysis rate and kinetics for a xylanase production

A. Grosfils[a], A. Vande Wouwer[b] and Ph. Bogaerts[a]
[a] Service de Chimie générale et Biosystèmes
Université Libre de Bruxelles
CP 165/61, Av. F.-D. Roosevelt, B-1050 Bruxelles,
Belgium
aline.grosfils@ulb.ac.be
philippe.bogaerts@ulb.ac.be

[b] Service d'Automatique, Faculté Polytechnique de Mons,
Boulevard Dolez, 31,7000 Mons,
Belgium
alain.vandewouwer@fpms.ac.be

Abstract

Macroscopic models of bioprocesses (cultures of bacteria, yeast or animal cells in bioreactor) are very useful to build engineering tools like simulators, software sensors or controllers. This kind of models consists of a system of mass balances for the macroscopic species (biomass, main substrates and products of interest) involved in a reaction scheme [1]. Such a reaction scheme, that describes the main phenomena occurring in the culture, is built of a reduced number of irreversible reactions. The choice of these reactions is an important prerequisite. Unfortunately, this first stage in bioprocess modeling is often achieved on a trial and error basis which may be very time consuming and may result to the choice of an unsuitable reaction scheme. In order to avoid these problems, a systematic procedure to generate all the C-identifiable reaction schemes, given a set of components whose measurements are available, was developed in [2]. This procedure is based on the decoupled identification method proposed in [1] which allows the pseudo-stoichiometric coefficients to be estimated independently of the kinetics. Moreover, it uses the necessary and sufficient condition of identifiability of the pseudo-stoichiometric coefficients presented in [3]. Based on maximum likelihood estimators [4, 5], the systematic procedure estimates easily the pseudo-stoichiometric coefficients of each identifiable reaction scheme taking into account all the measurements errors.

In this study, this procedure is used to determine the most-likely macroscopic reaction scheme representing a bioprocess used by the Beldem Company (Andenne, Belgium), in which bacteria produce an enzyme by consumption of two substrates. Moreover, an extension of the procedure is presented, which allows the cell lysis rate to be estimated, when non-lysed cell measurements only are available (by dry cell weight measurements).

Acknowledgements

The authors are grateful to the Beldem Company (Andenne, Belgium) for its collaboration and to F.R.I.A. for its financial support.

References

[1] G. Bastin and D. Dochain (1990). On-line estimation and adaptative control of bioreactor. Elsevier, Amsterdam.

[2] Ph. Bogaerts and A. Vande Wouwer (2001). Systematic generation of identifiable macroscopic reaction schemes. *Proceedings of the 8th International Conference on Computer Applications in Biotechnology (CAB8),* Quebec City, 13-18.

[3] L. Chen and G. Bastin (1996). Structural identifiability of the yield coefficients in bioprocess models when the reaction rates are unknown. *Math. Biosci.*, 132, 35-67.

[4] Ph. Bogaerts, J-L. Delcoux and R. Hanus (2003). Maximum likelihood estimation of pseudo-stoichiometry in macroscopic biological reaction schemes. *Chemical Engineering Science*, 58, 1545-1563.

[5] Ph. Bogaerts and R. Hanus (2000). Macroscopic modelling of bioprocess with a view to engineering applications. In: *Focus on Biotechnology* (Ph. Thonart and M. Hofman, Ed.) Vol.IV (Engineering and manufacturing for biotechnology). Kluwer Academic Publishers.

Existence, uniqueness and stability of the equilibrium points of a SHARON bioreactor model

Eveline I.P. Volcke[(1)], Mia Loccufier[(2)], Peter A. Vanrolleghem[(1)] and Erik J.L. Noldus[(2)]

[1] Department of Applied Mathematics, Biometrics and Process Control (BIOMATH)
Ghent University (UGent), Coupure Links 653, 9000 Gent, Belgium
e-mail: Eveline.Volcke@biomath.ugent.be

[2] Department of Electrical Energy, Systems and Automation (EESA)
Ghent University (UGent), Technologiepark 913, 9052 Zwijnaarde, Belgium

1 Introduction

The existence, uniqueness and stability of the equilibrium points of a bioreactor for nitrogen removal are investigated. The process under study is the SHARON process for coupling with an Anammox process, a promising technique for biological nitrogen removal from ammonium-rich wastewater streams.

In the SHARON (Single reactor High activity Ammonium Removal Over Nitrite) process, ammonium is converted to nitrite while further conversion of nitrite to nitrate is prevented. This is realized by operating the reactor at a suitable dilution rate. At the prevailing high temperature (about 35°C) and neutral pH (about 7), ammonium oxidizing biomass grows faster than nitrite oxidizing biomass. The dilution rate is chosen low enough to maintain ammonium oxidizers in the reactor, but also high enough to ensure wash-out of the nitrite-oxidizing biomass.

In the subsequent Anammox (Anaerobic Ammonium Oxidation) process, ammonium and nitrite are combined to form nitrogen gas. In order to obtain both a good conversion efficiency and to prevent inhibition of the Anammox process, the SHARON reactor must be operated in such a way that its effluent contains a nitrite:ammonium ratio of 1:1.

2 Problem statement and simplified model description

The question rises whether the nitrite:ammonium ratio obtained in the SHARON process is unique and stable for constant input variables, being the dilution rate (u_0) and influent concentrations of (total) ammonium (u_1), (total) nitrite ($u_2 = 0$), ammonium oxidizing biomass (u_3) and nitrite oxidizing biomass (u_4).

The SHARON reactor is assumed to be controlled at a constant pH. In this way, pH effects associated with conversion don't have to be taken into account and only four state variables have to be considered: the reactor concentrations of ammonium (x_1), nitrite (x_2), ammonium oxidizing biomass (x_3) and nitrite oxidizing biomass (x_4). The simplified process is described by a fourth order system of nonlinear differential equations:

$$\dot{\mathbf{x}} = (\mathbf{u} - \mathbf{x}) \cdot u_0 + \mathbf{M} \cdot \rho(\mathbf{x})$$

with $\mathbf{x} \triangleq [x_1 \ldots x_4]^T$, $\mathbf{u} \triangleq [u_1 \ldots u_4]^T$, $\mathbf{M} \in \mathbb{R}^{4\times 2}$ the (constant) stoichiometric matrix and $\rho(\mathbf{x}) \in \mathbb{R}^{2\times 1}$ the vector of specific growth rates, that is a nonlinear function of the state variables. Note that for constant values x_i, the nitrite:ammonium ratio in the SHARON effluent is also constant.

3 Research method

Sufficient conditions for the existence of a unique equilibrium point in the system's state space are formulated using a contraction mapping theorem. It is shown that for any given constant $\mathbf{u}$ there exists a lower bound on u_0 that ensures the existence and uniqueness of the equilibrium. Algorithms are developed to compute the lower bound and to find the equilibrium for given values of dilution rate u_0 and influent concentrations $\mathbf{u}$.

Further, the local asymptotic stability of the equilibrium points is studied in terms of the model parameters and input variables. Again a lower bound on u_0 is computed that ensures local asymptotic stability of the equilibrium.

4 Results and future research

Numerical results suggest that the reactor's operation with a unique equilibrium state only occurs for very large values of the dilution rate, corresponding with wash-out of both ammonium and nitrite oxidizers, i.e. the trivial equilibrium point where the reactor fails.

Useful working conditions require operational modes with at least three equilibrium states: a technically useful stable set point, a stable wash-out state and an unstable equilibrium in between. This mode of operation is currently under investigation.

Robust Control with Youla Parametrization of Fed-Batch Cultures of *S. Cerevisiae*

F. Renard, A. Vande Wouwer
Laboratoire d'Automatique,
Faculté Polytechnique de Mons,
Bd Dolez 31, B-7000 Mons, Belgium
(E-mail : Frederic.Renard@fpms.ac.be)

D. Dumur
Supélec, Service Automatique
Plateau de Moulon
3 rue Joliot-Curie, F-91192 Gif sur Yvette cedex,
France (E-mail : didier.dumur@supelec.fr)

S. cerevisiae are among the most popular industrial microorganisms for their robustness and ability to utilize cheap materials for growth and production. They have been used since the very early days of microbial fermentation history for brewing wine and beer. Recently, with achievement of modern gene technology, *S. cerevisiae* can be used as host organisms for production of recombinant proteins (production of insulin, vaccines, …).

Due to the economic importance of these products, there is an obvious motivation to maximize the biomass productivity of the process. One method commonly used to ensure the optimal productivity operating conditions consists in controlling the ethanol concentration at a constant low value. Several methods have been proposed to control the ethanol concentration (see e.g. [1] or [2]) but these control schemes often require an extensive knowledge of the reaction scheme stoichiometry and several on-line measurements (OUR, CPR, dissolved oxygen and carbon dioxide, …).

This study suggests a strategy for robust control of the ethanol concentration assuming the knowledge of only one stoichiometric coefficient and only one on-line measurement (ethanol concentration). Following the reasoning of Valentinotti [5], two simple linear models are derived from the global nonlinear model of Sonnleitner and Käppeli [4]. The first model depicts the relationship between the substrate feed and the ethanol production, while the second model describes the exponential cell growth. Therefore as far as the regulation of ethanol concentration is concerned, the exponential cell growth can be considered as a disturbance to be rejected.

Then, an original control strategy which uses a RST controller with a particular Youla parametrization is developed. The Youla parameter is chosen in order to reach two objectives:

- an asymptotic rejection of the exponential growth disturbance [5].
- an improvement of the robustness towards unstructured uncertainties and the respect of temporal constraints on the response to disturbances [3].

A particular structure of the Youla parameter is chosen in order to take account of these two objectives with two stable transfer functions Q_1 and Q_2. The design of Q_1 is based on the internal model principle whereas Q_2 results from a convex optimisation problem expressing the frequency and temporal constraints of the second objective.

The proposed strategy is tested in simulation with fed-batch cultures of *S. cerevisiae.* The exponential substrate uptake for cell growth is taken as a disturbance to be rejected asymptotically by a suitable choice of the Youla parameter. As the growth rate can evolve during the culture, an adaptive version of the robust control algorithm is considered.

References

[1] Chen, L., G. Bastin and V. van Breusegem (1995). *A case study of adaptive nonlinear regulation of fed-batch biological reactors.* Automatica 31(1), 55-67.

[2]Pomerleau, Y. (1990). Modélisation et commande d'un procédé 'fed-batch' de culture des levures à pain. Ph.D. thesis. Dept. génie chimique, Université de Montreal, Canada.

[3]Rodriguez, P., Dumur, D., Mendes, E. (2003). *A GPC controller robustification towards measurement noise and parameter uncertainty constraints*. In ECC'03, Cambridge.

[4] Sonnleitner, B., Käppeli, O. (1986). *Growth of Saccharomyces cerevisiae is controlled by its limited respiratory capacity : Formulation and verification of a hypothesis.* Biotechnol. Bioeng. 28, 927-937.

[5] Valentinotti, S., Srinivasan, B. and al (2003) *Optimal operation of fed-batch fermentations via adaptive control of overflow metabolite.* Control Eng. Practice. 11, 665-674.

WATERGY, towards a closed greenhouse in semi-arid regions; a model based identification experiment

S.L. Speetjens, J.D. Stigter, G. van Straten
Systems and Control Group
Wageningen University
P.O. Box 43, 6700 AA Wageningen
The Netherlands
Email: Bas.Speetjens@wur.nl

The main aim of the Watergy project is the development of a new humid air solar-collector system that follows the principle of a thermosyphon. This means that the sun is the driving force for the airflow in the system, making it (in theory) completely independent of external energy input. The aims of the Watergy project are the following:
- Understanding of solar thermal properties of the system
- Greenhouse (and building) heating and cooling
- Optimisation of crop production
- Reduction of building mass
- Enhanced water efficiency
- Solar based water treatment
- Model based control

The system functions as follows: during the day the greenhouse air is heated by the sun. As an effect, the air starts to rise. Inside the central chimney the air is cooled with a large heat exchanger, causing the air to fall down and the whole process is repeated. The energy gained at cooling the air is stored for later use. During the night, the flow direction of the air is in the opposite direction; the heat exchanger inside the chimney can heat the air.
Two prototypes will be constructed in the next year: one in Southern Europe in the shape of a closed greenhouse to cool the inside air and produce energy in the form of clean water and heat stored to be used during the night. The North European variant puts more emphasis on integral building design, combining a building with a winter garden. The function of this winter garden is to extract heat, store it and use it to heat the building during the day, night or in another season.
The system can be controlled in several ways; the central chimney with the heat exchanger is the heart of the climate control. Heating and cooling is performed here and the airflow through the system depends on the buoyancy generated here. Water evaporation by plants and additional surface in the shape of an 'inner roof' cools the greenhouse air further. This water condenses inside the heat exchanger and can be re-used.
In order to control the climate in the prototypes, several ways of model based control will be tested. The model used in this type of control are either physics or data based, but a combination is also possible [1]. Application of this approach in (greenhouse) control is quite new; it has only been tested in a few case studies, though with very good results [2]. In a local experimental set-up, the performance and characteristics of the central heat exchanger are tested. A system model will be identified and parameters will be estimated.
The paper will shortly introduce the basics of the Watergy concept, after which the application of Data Based Mechanistic Modelling in greenhouse control will be discussed. The results of the local heat exchanger experiment as well as the expectations of application of this theory in the full scale prototype will play an important part in this discussion. The model used will be data based and will be extracted from measurements taken in the greenhouse.

References

[1] P.C. Young "Databased mechanistic modelling of environmental, ecological, economic and engineering systems," Environmental Modelling and Software, Volume 13, Pages 105 - 113, 1998.

[2] P.C. Young, M.J. Lees, A. Chotai, W. Tych, Z.S. Chalabi, "Modelling and PIP control of a glasshouse microclimate," Control Engineering Practice, Volume 2, Issue 4, Pages 591 - 604, 1994.

Compartmental and (min,+) modelling of network elements in communication systems.

Vincent Guffens, Georges Bastin
Centre for Systems Engineering and Applied Mechanics (CESAME)
Université Catholique de Louvain
Belgium, 1348 Louvain-La-Neuve
{guffens, bastin}@auto.ucl.ac.be

Hugues Mounier
Ecole Nationale Supérieure des Mines de Paris
Centre d'Automatique et de Robotique (CAOR)
60 Bd. Saint-Michel, 75006 Paris
mounier@caor.ensmp.fr

1 Abstract

(Min,+) algebra has proved to be useful in describing communication networks where packet flows are reshaped by some service disciplines (see e.g. [5]). On the other hand, continuous fluid flow models are currently used to analyse the behaviour of communication networks. The purpose of this contribution is to investigate the connections between these two approaches through a specific case study : a chain of routers under hop-by-hop control. In an introductory example a simple constant bit rate buffer is analysed and its (Min,+) representation is shown to be equivalent to a fluid flow model commonly found in the literature ([3],[2]). The limitation of this simple model in the context of stochastic queueing networks is illustrated and an alternative model is proposed [4]. This alternative model is then used for the design of a hop-by-hop feedback control law in a chain topology. A (Min,+) transfer function is derived for this chain (following a similar derivation in [1]) and the result is compared with a compartmental analysis of the equivalent fluid model.

References

[1] R. Agrawal, R. L. Cruz, C. Okino, and R. Rajan. Performance bounds for flow control protocols. IEEE/ACM transactions on networking, 7(3):310 323, 1999.

[2] Jean-Chrysostome Bolot and A. Udaya Shankar. Analysis of a fluid approximation to flow control dynamics. In INFOCOM (3), pages 2398 2407, 1992.

[3] C. G. Cassandras, Y. Wardi, B. Melamed, G. Sun, and C. G. Panayiotou. Perturbation analysis for online control and optimization of stochastic fluid models. IEEE transaction on automatic control, 47(8):1234 1248, 2002.

[4] V. Guffens, G. Bastin, and H. Mounier. Using token leaky buckets for congestion feedback control in packets switched networks with guaranteed boundedness of buffer queues. In proc. of ECC03 Cambridge, UK, 2003.

[5] J.Y. Leboudec and P. Thiran. Netowrk Calculus, A Theory of Deterministic queueing system for the Internet. Springer Verlag, 2002.

A model for network congestion control

J.M. Schumacher, I.A. Korostil
Department of Econometrics and Operations Research
Tilburg University
{j.m.schumacher,i.korostil}@uvt.nl

1 Abstract

Many models for network usage can be described in terms of users who have access to several resources. For instance, users may be origin-destination pairs in a traffic network model, and in this case resources are the links between crossings. In the context of production planning, users may be products and resources may be machines. We might even model the submission system of scientific papers by defining authors to be users and journals to be resources. The use of a given resource generates a certain cost for the user, for instance in terms of incurred delay; this cost depends in general on the load that is placed on the resource by all users.

Congestion is an important problem in many networks. One may try to control congestion by providing incentives for users. In doing this, one has to take into account the behavior of users in determining their demand for services from the resources available to them. Models for congestion control aim to describe this behavior. A model of the desired type may be set up as follows.

Suppose that we have p users and m resources. Introduce the following quantities:

- $l_{ij}(t)$ = load per unit of time placed by user i on resource j at time t;
- $q_{ij}(t)$ = cost incurred at time t by user i when applying to resource j;
- $d_i(t)$ = total demand of user i at time t;
- $a_i(t)$ = cost accepted by user i at time t.

The above quantities are summarized in a *load matrix* $L(t) \in \mathbb{R}_+^{p\times m}$ (load is taken to be nonnegative), a *cost matrix* $Q(t) \in \mathbb{R}^{p\times m}$, a *demand vector* $d(t) \in \mathbb{R}^p$, and an *accepted cost vector* $a(t) \in \mathbb{R}^p$. The term "cost" need not be interpreted in a monetary sense; rather it should be viewed as a measure of the (un)attractiveness of a given resource to a given user, given all incentives and disincentives such as delay. The cost matrix may depend on a state vector $x(t)$ and a control input $u(t)$ as follows:

$$\dot{x}(t) = F(x(t), L(t), u(t)) \tag{1a}$$

$$Q(t) = H(x(t), L(t), u(t)). \tag{1b}$$

For instance, the state variable $x(t)$ may be a measure of congestion.

To describe the behavior of users, we assume that the Wardrop principle holds at every time instant t. In other words, given a demand level, each user distributes its load over resources in such a way that all resources that are used generate the same cost (this is the accepted cost), and there is no resource that is not used and that would generate a lesser cost. This behavioral principle, together with the nonnegativity of the load, can be expressed in matrix terms by

$$0 \le L(t) \perp Q(t) - a(t) \cdot \mathbb{1}^T \ge 0 \tag{1c}$$

where the "perp" relation is understood in the sense of the inner product $\langle A, B\rangle = \mathrm{tr}(A^T B)$ for $A, B \in \mathbb{R}^{p\times m}$. To close the model, we furthermore need the accounting relation

$$L(t)\mathbb{1} = d(t) \tag{1d}$$

as well as a "constitutive relation" between the demand and the accepted cost which we take to be of the form

$$R(d, a) = 0 \tag{1e}$$

where R is a mapping from $\mathbb{R}^p \times \mathbb{R}^p$ to $\mathbb{R}^p$. The system (1) is of the form of a *controlled cone complementarity system* [1], where the "dual cone" of a given cone $\mathcal{C}$ is defined by $\mathcal{C}^* = \{z \mid \langle w, z\rangle \ge 0 \text{ for all } w \in \mathcal{C}\}$:

$$\begin{aligned} \dot{x}(t) &= f(x(t), z(t), u(t)) \\ w(t) &= h(x(t), z(t), u(t)) \\ \mathcal{C} \ni w &\perp z \in \mathcal{C}^*. \end{aligned}$$

To write (1) in the above form, define in particular:

$$\begin{aligned} z &= (L, a) \in \mathbb{R}^{p\times(m+1)} \\ w &= \big(H(x, L, u) - a \cdot \mathbb{1}^T, R(L\mathbb{1}, a)\big) \in \mathbb{R}^{p\times(m+1)} \\ \mathcal{C} &= \mathbb{R}_+^{p\times m} \times \{0\} \subset \mathbb{R}^{p\times(m+1)}. \end{aligned}$$

Due to the so-called Braess paradox, it may happen in models of this type that overall cost is reduced by increasing the cost of some resources.

References

[1] M. K. Çamlıbel, W. P. M. H. Heemels, A. J. van der Schaft, J. M. Schumacher. Switched networks and complementarity. *IEEE Transactions on Circuits and Systems I 50* (2003), 1036-1046.

A Cellular Localisation Technology: Multi Cell-ID

Nico Deblauwe, Leo Van Biesen

Vrije Universiteit Brussel, dept. ELEC, Pleinlaan 2, 1050 Brussels, BELGIUM
e-mail: ndeblauw@vub.ac.be

ABSTRACT – This paper describes the approach for the research on a cellular localisation method, called Multi-Cell-ID. Main advantages are the instant applicability, without the need for changes to the network architecture and moderate to high localisation precision (aimed to be 100m).

I. INTRODUCTION

This paper describes a work plan aimed at improving the resolution of cellular localisation technologies. Multi Cell-ID aims to be low-cost (few network changes) and yet, thanks to spatial propagation models and measurement post-processing, as precise as currently available but more complex and expensive methods.

First the general framework of the research field – Location Based Services (LBS) – is sketched. Then the technical side is explained: the proposed technique and the research approach.

II. LOCATION BASED SERVICES

Generally spoken, the term LBS refers to mobile services in which the user location information is used in order to add value to the service as a whole.

The services can be categorised in 4 groups: information services (restaurant finder, navigational aids), trigger services (automated advertising, enhanced call routing), tracking services (fleet management, buddy services) and assistance services (emergency notification, roadside assistance).
Technically, 3 different components can be differentiated for LBS: localisation (user's position), communication (receive and send information) and application (user's input and/or actions). Amongst the techniques that allow localisation, we have satellite (GPS, Galileo…), cellular (Cell-ID, E-OTD…) and dead reckoning (using motion sensor input).

The remainder of this paper focuses on cellular localisation techniques.

III. MULTI CELL-ID

With the Cell-ID technique, a mobile phone is linked to a zone around the Base Transceiver Station (BTS) it is connected to. Using the BTS antenna sector information (when available) and/or the received power in the mobile allows to narrow down this zone. This is called the Enhanced Cell-ID (E-Cell-ID) technique .
Instead of using only the active cell for the localisation, other cells – or (the power of) their broadcast signals, more precisely – will be used [Wong 00]. This will result in a higher precision position estimate.

This research is supported by a grant of the Flemish Institute for the improvement of the scientific-technological research in industry (IWT).

IV. RESEARCH APPROACH

The development of this technique can be divided in 3 parts:

- The basic technique: a spatial propagation model will be developed. Besides explaining the propagation time, it will also be able to explain the travel path loss. Based on measurements at some selected sites, a simulator will be set up for verifying the propagation model. Goal of this part is to be able to find a function that links a distance and orientation to an antenna to the received power, thus enabling cellular localisation.
- Resolution enhancement: having the power as only measure isn't likely to deliver a sufficient high resolution. Therefore techniques to improve this resolution will be investigated. Especially the effects caused by short term fading need to be taken into account.
- Creating a concrete application: based on the previous, research will be undertaken to construct a working localisation application for GSM.

VI. CONCLUSIONS

In this paper, the potential of localisation by means of a the Multi Cell-ID method is showed, as well as a possible path for the research.

REFERENCES

[Wong 00] Chris L.C. Wong, M.C. Lee, Raymond K.W. Chan, "*GSM-based Mobile Positioning using WAP*", September 2000, IEEE Proc Wireless Communications and Networking.

ACKNOWLODGEMENT

Proximus, for their agreement to help and cooperate with the network measurements.

Boderc: Multi-disciplinary Modelling of Embedded Dynamical Systems[1]

Björn Bukkems,† René van de Molengraft,‡ and Maarten Steinbuch§
Dynamics and Control Technology Group, Department of Mechanical Engineering
Technische Universiteit Eindhoven, P.O. Box 513, 5600 MB Eindhoven, The Netherlands
Email: (†b.h.m.bukkems, ‡m.j.g.v.d.molengraft, §m.steinbuch)@tue.nl

1 Introduction

The design of modern embedded dynamical systems, like e.g. high-speed digital printing equipment, is highly dependent on the integration of knowledge from different disciplines like mechanics (M), electronics (E) and software engineering (I). All three disciplines have their own formalisms and need to cooperate closely in order to model embedded dynamical systems. The latter is subject of this presentation.

2 Objectives

The topic of the Boderc research project is to develop methods that can effectively bridge the gap between the different disciplines, taking into account demanding industrial circumstances. The multi-disciplinary integration, schematically depicted in Fig. 1, is the breakthrough that is needed to be able to develop complex embedded dynamical systems for a reasonable price in a reasonable time.

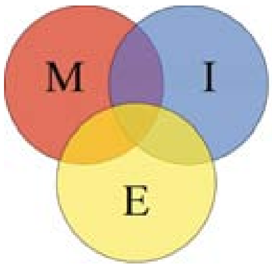

Figure 1: Schematic representation of the multi-disciplinary integration

3 The research project

The Boderc project is a large-scale research project that is coordinated by the Embedded Systems Institute, which carries the project management responsibility. In the project, four academic partners and five partners from industry are represented, of which Océ Technologies is the so-called carrying industrial partner that defined the problem statement and provides all background information to perform the project. Currently, the exploration and application project activities are performed on the Océ VarioPrint™ 2090, depicted in Fig. 2.

Figure 2: The Océ Varioprint™ 2090

During the first part of the first project year, the experimental set-up and its measurement environment have been reaized. Also tool selection for modelling, analysis, and validation, and requirements modelling have been carried out. The second part of the first project year is used for modelling selected aspects of the paper throughput path of the printer in multi-disciplinary groups. The goal of working with people from other disciplines is to understand each others way of thinking and modelling, and to explore the possibilities of combining information from the disciplines into executable models. In this presentation, the first explorations about the multi-disciplinary modelling activities are discussed, and problems, challenges, and ideas for future work are considered.

4 Conclusions

The Boderc project aims at addressing and solving the shortcomings in the design of embedded dynamical systems. Multi-disciplinary modelling, including the supporting tools, plays an essential role in the chosen approach. The first explorations on modelling activities in multi-disciplinary groups are discussed.

[1]This work has been carried out as part of the Boderc project under the responsibility of the Embedded Systems Institute. This project is partially supported by the Netherlands Ministry of Economic Affairs under the Senter TS program.

Multidisciplinary modelling [1]

Marieke Cloosterman, Nathan van de Wouw, Henk Nijmeijer
Department of Mechanical Engineering, Technische Universiteit Eindhoven
P.O. Box 513, 5600 MB Eindhoven, The Netherlands
Email: (m.b.g.cloosterman, n.v.d.wouw, h.nijmeijer)@tue.nl

1 Introduction

In the Boderc (Beyond the ordinary: design of embedded real time control) project people from the disciplines mechanics, electronics and software work together to investigate how this multidisciplinary combination can improve or accelerate the development of an embedded system. As first step a modelling exercise for an Océ printer is performed. A part of the printer is chosen and modelled from the viewpoint of the different disciplines. It seems that if each discipline uses its own modelling method, different levels of abstraction in the models occur. Moreover, also the usefulness and goals of modelling are different. The approach taken to deal with these problems will be described in the next paragraphs.

2 Modelling

For the model one specific unit of the printer is used, in which the three mentioned disciplines meet. Per discipline, known methods are used. In the total model, the relations between the disciplines are described as inputs or outputs for the mono-disciplinary sub-models. This way of working supports communication between the disciplines and helps to determine their influences on each other. A general example is given in figure 1.

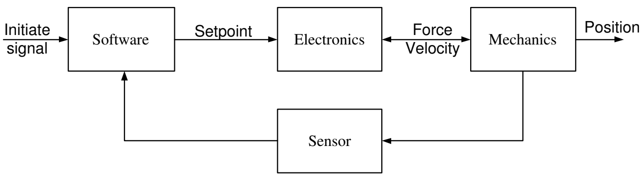

Figure 1: *Combination of three disciplines*

The three blocks represent the models as used in each discipline. The electronics and mechanics are modelled using differential equations. For the software, a model describing timing with perturbations due to interrupts of other machine parts is built. The arrows indicate the connection between the disciplines. From software to electronics the link is e.g. a setpoint which is sent to a motor. From electronics to mechanics, the arrow represents a force or torque. The mechanics itself also influences the electronics, therefore the link between these two disciplines also contains a velocity or angular velocity. From mechanics to software the link is an electrical sensor, which measures the position, such that the controller output can be computed. A second possibility is a sensor, that gives only a signal (interrupt) if a desired position is achieved.

The total model is used to determine the influences of parameter changes in one sub-model on the behaviour of the system within other disciplines and finally the total model output.

3 Encountered problems

Besides the problem of different levels of abstraction for the models within each discipline, also the notion of time is different. Software uses an internal time, while in electronics and mechanics the states are computed by solving differential equations for given initial conditions at a given time. If the software is interrupt based, it is event driven, while the hardware is very often dependent of its state at a certain time, thus being more time driven. This combination of time and event driven systems and the use of both continuous and discrete time models may result in complex models, which are difficult to analyse.

4 Conclusion

The used method, where the models from the different disciplines are coupled with in- and outputs, is useful to simulate the behaviour of a multidisciplinary model and to determine the influences of the mono-disciplinary models on each other. The levels of abstraction can differ between the disciplines, dependent on the couplings used. An additional advantage is that communication between the disciplines is supported by using the scheme of figure 1.

5 Future research

The combination of time-driven and event-driven submodels results in a hybrid overall model. Future work will focus on analysis methods for such hybrid models.

[1]This work has been carried out as part of the Boderc project under the responsibility of the Embedded Systems Institute. This project is partially supported by the Netherlands Ministry of Economic Affairs under the Senter TS program.

A fishery management game

J.C. Engwerda
Tilburg University, Department of Econometrics and O.R.
P.O. Box 90153, 5000 LE Tilburg, The Netherlands
email: engwerda@kub.nl

Keywords:
Indefinite linear quadratic differential games, Nash equilibrium, Solvability conditions, Riccati equations, Robustness, Policy games

Abstract

In this presentation we illustrate the consequences of taking deterministic noise into account in a simple fishery management problem.

Starting with a simple linear quadratic game formulation of the problem, we show which potential consequences there are of taking deterministic noise into account by the players of this game.

This problem fits into the general framework of linear quadratic differential games studied by Engwerda in [1.]. That is, the problem where two individual players like to minimize an indefinite linear quadratic function, i.e.

$$J_i = \int_0^\infty \{x^T(t)Q_i x(t) + u_i^T R_i u_i(t) - w^T V_i w\} dt,$$

subject to

$$\dot{x} = Ax + B_1 u_1 + B_2 u_2 + Ew, x(0) = x_0.$$

Here $w \in L_2^q(0,\infty)$ represents an unknown disturbance, x denotes the state of the system and u_i is the control of player i. Furthermore, Q_i are assumed to be symmetric; R_i and V_i positive definite. V_i expresses the risky attitude of player i.

The several different behavior that can occur in our simple model basically depends on the relationship between certain model parameters. We will see, e.g., that for certain parameter sets there will be no effect of considering noise on the equilibrium catching rates of the fishermen. Whereas, for other parameter sets noise expectations do play a role on the equilibrium strategies. New equilibria may appear, or, old ones may disappear. Furthermore, in some equilibria the fishermen take into account in their fishing strategy the expectations about the noise of their collegue. In general, the reaction by the fishermen to an expected more disturbed fish stock growth is to increase the catching rate of fish.

References

1. Engwerda J.C., 2004, Linear-Quadratic Differential Games, to appear.

Controllability of polynomial-shift inverse iteration

Jens Jordan (communicated by Uwe Helmke)
Department of Mathematics
University of Würzburg
97074 Würzburg Germany
jordan@mathematik.uni-wuerzburg.de

1 Introduction

A common way to compute eigenvectors of a square real or complex matrix $\mathbf{A} \in F^{n\times n}$ ($F = R$ or $F = C$) is to apply the **inverse iteration** on an arbitrary initial subspace x_0. The efficiency of this algorithm is based on the use of shifts. In fact, using shift strategies one can speed up the convergence of the algorithm from linear convergence rates to quadratic ones (see for example [1] or [4]). Such spectral shift parameters act as control variables. Therefore the shifted algorithm can be formulated as a discrete-time control system on the projective space PF^{n-1}. Thus, the algorithms can be analyzed from the viewpoint of nonlinear control theory. A natural question in this context is under which conditions the system is controllable i.e. for which system matrices $\mathbf{A}$ there exists an initial point $x_0 \in PF^{n-1}$, such that every other point can be reached arbitrarily close in finite many steps.
In [2] Helmke and Fuhrmann showed that controllability is a generic feature in the complex case. They give a complete characterization in terms of the Jordan canonical form of the system matrices $\mathbf{A}$. The case $F = R$ turned out to be much more complicated. In [3] necessary and sufficient conditions for controllability are discussed, but in general it is still unknown if controllability is a generic condition or not. Nevertheless one can affect controllability by adding collateral shift options. In the following we want to discuss one possible variation of the algorithm and show controllability.

2 Polynomial-shift inverse iteration

Let $\mathbf{A}$ be a square matrix and x_0 an initial point of the projective space PF^{n-1}. The shifted inverse iteration can be formulated in the following way:

$$x_0 \in PF^{n-1}, \qquad x_{t+1} = (\mathbf{A} - u_t\mathbf{I})^{-1}x_t \tag{1}$$

with control parameters $u_t \in U = F \setminus \sigma(\mathbf{A})$. We want to discuss a slight variation of this algorithm. Besides the common Inverse Iteration steps we allow also an additional kind of algorithm steps. Let $U_\alpha := U = F \setminus \sigma(\mathbf{A})$ and

$$U_\beta := \{(u,v) \in F^2 \,|\, \mathbf{A}^2 + u\mathbf{A} + v\mathbf{I} \in \mathbf{GL}_n(F)\}$$

be two sets of control parameters. We define:

$$p_\alpha : U_\alpha \to \mathbf{GL}_n(F), \quad p_\alpha(u) = \mathbf{A} - u\mathbf{I}$$

and

$$p_\beta : U_\beta \to \mathbf{GL}_n(F), \quad p_\beta(u,v) = \mathbf{A}^2 + u\mathbf{A} + v\mathbf{I}.$$

We baptize the following discrete-time control system **polynomial-shift inverse iteration**:

$$x_0 \in PF^{n-1}, \qquad x_{t+1} := p_t(u_t)^{-1}x_t \tag{2}$$

with $(p_t, u_t) \in \{(p_\alpha, U_\alpha), (p_\beta, U_\beta)\}$. Note that system (2) is equivalent to system (1) in the complex case.

By $R(x_0)$ we denote the reachable set of the initial point $x_0 \in PF^{n-1}$, i.e. the set of all points $x \in PF^{n-1}$ which can be reached by finite many algorithm steps. Thus, system (2) is controllable if there exist a initial point $x_0 \in PF^{n-1}$ such that the reachable set of x_0 is dense in PF^{n-1}, i.e. $\overline{R(x_0)} = PF^{n-1}$.

Even for $F = R$ it turns out that, the set of matrices which induces a controllable system of type can be characterized.

Theorem: *System (2) is controllable if and only if the system Matrix is cyclic, i.e. there exists an vector $x \in F^n$ such that $\{x, \mathbf{A}x, \ldots, \mathbf{A}^{n-1}\}$ is a basis of F^n.*

The set of cyclic matrices is open and dense in $F^{n\times n}$. Thus controllability is a generic property for the polynomial-shift inverse iteration.

References

[1] S. H. Crandall "Iterative procedures related to relaxation methods for eigenvalue problems", Proc. Roy. Soc. London **207**, 1951, pp 416-423.

[2] U. Helmke, P.A. Fuhrmann "Controllability of matrix eigenvalue algorithms: the inverse power iteration," System & Control Letters **41**, 2000, pp 57-66.

[3] U. Helmke, F. Wirth "On controllability of the real shifted inverse power iteration," System & Control Letters **43**, 2001, pp 9-23.

[4] B. N. Parlett "The symmetric eigenvalue problem", Classics in applied mathematics, vol 20, SIAM, Philadelphia, 1998.

Acknowledgement: The author was supported by the Control Training Site(CTS).

Coprime factorization of irrational transfer functions

Mark R. Opmeer
Departement of Mathematics
University of Groningen
P.O. Box 800 9700AV Groningen
The Netherlands
opmeer@math.rug.nl

Ruth F. Curtain
Departement of Mathematics
University of Groningen
P.O. Box 800 9700AV Groningen
The Netherlands
R.F.Curtain@math.rug.nl

1 Introduction

Coprime factorizations of transfer functions have been studies for some 30 years now. One of its main contributions to systems theory is the Youla-Jabr-Bongiorno-Kucera parametrization of all stabilizing controllers for a given plant which is given in terms of a coprime factor and the corresponding Bezout factors.

There is a strong connection between coprime factorization and linear quadratic regulator theory which can be used to calculate the coprime factorization and the Bezout factors in terms of the matrices A, B, C, D from a state space realization of the transfer function.

Using this connection we show that transfer functions of certain infinite-dimensional discrete-time state-space systems have a coprime factorization.

2 Definitions

A function is called *proper* if it is analytic and bounded on a disc centered at the origin. A function is called *stable* if it is analytic and bounded on the unit disc. A function P is called *inner* if it is stable and $P(s)^*P(s) = I$ for almost all s on the unit circle. A *right-factorization* of a proper function G is a pair of stable functions M, N such that M^{-1} is proper and $G = NM^{-1}$. The factorization is called *normalized* if the function $[M; N]$ is inner. The factorization is called *coprime* if there exist stable functions X, Y such that $XM - YN = I$. This X and Y are called the *Bezout factors*.

A discrete-time linear state space system is a dynamical system of the form

$$x_{n+1} = Ax_n + Bu_n, \quad x(0) = x_0, \quad y_n = Cx_n + Du_n,$$

where A, B, C, D are bounded operators on separable Hilbert spaces. The *transfer function* is defined to be $D + Cz(I - zA)^{-1}B$. It is well-known that this transfer function is proper and that every proper function is the transfer function of some discrete-time linear state space system. We say that a system satisfies the finite cost condition (FCC) if for every initial state x_0 there exists a square summable input such that the corresponding output is square summable. A system is said to satisfy the dual finite-cost condition (dFCC) if its dual system (A^*, C^*, B^*, D^*) satisfies the FCC.

3 Results

The following theorems hold.

Theorem 1 *The transfer function of a discrete-time linear state space system for which the FCC is satisfied and whose input space is finite-dimensional has a normalized coprime factorization which is given by the standard formulas.*

Theorem 2 *The transfer function of a discrete-time linear state space system for which the FCC and the dFCC is satisfied has a normalized coprime factorization which is given by the standard formulas.*

The proof of Theorem 1 is based on a state space characterization of inner functions and the Corona theorem (see [1]). The proof of Theorems 2 is based on Nehari's theorem (see [2]). Similar results hold in continuous-time (see [3], [2] and also [4]).

References

[1] M.R. Opmeer and R.F. Curtain, LQG-balancing for discrete-time infinite-dimensional linear systems, submitted.

[2] R.F. Curtain and M.R. Opmeer, The suboptimal Nehari problem for stable infinite-dimensional systems: the vector-valued case, manuscript.

[3] K.M. Mikkola, Riccati equations and optimal control for well-posed linear systems, submitted.

[4] M.R. Opmeer and R.F. Curtain, LQG-balancing for continuous-time infinite-dimensional linear systems, manuscript.

State construction and systems equivalence

A. A. Julius
Dept. Applied Mathematics
University of Twente
The Netherlands
a.a.julius@math.utwente.nl

A. J. van der Schaft
Dept. Applied Mathematics
University of Twente
The Netherlands
a.j.vanderschaft@math.utwente.nl

Abstract

This talk concerns our study of the so called *state maps* in the behavioral approach to systems theory. The discussion is a continuation of some preliminary development presented in [1].

The concept of *states* or *state variables* is present in almost all branches of dynamical systems theory. In areas as remotely connected as discrete event systems and linear time invariant systems we can observe that the notion of *states* is present. One may think that this is a mere coincidence, but this is not true. The different notions of states have something in common. They are all connected by the so called *state property*. In short (and perhaps rather inaccurately), one can say that a quantity or variable possesses the state property if it captures the necessary information about the evolution of the dynamical system. There is of course a more mathematically formal and rigor formulation of this property, for example in [2].

It is quite a common view in the field of dynamical systems that states are understood to be internal. When the system is interconnected with other systems, states usually do not appear explicitly in the description of the interconnection. Nevertheless, they play an arguably central role in characterizing the compatibility of the interconnection. We shall not discuss this issue further, and the interested reader is referred to [3] and [1].

Following the earlier development in [1], our point of view, which is based on the behavioral approach, is that states are constructed out of the system trajectories (the behavior). In the behavioral point of view, the behavior (i.e. the collection of all possible trajectories) defines/identifies the system. Of course, it is required that the trajectories bear all information/variables on everything relevant to the discussion. Irrelevant variables/information, which in the case of linear behaviors are called *latent variables*, can be eliminated. See [2] for more about this.

Having stated the previous paragraph, we should also remark that external behavior (i.e. the collection of external trajectories) does not always define the system. In some analysis, for example in the field of discrete event systems, the states are also relevant. In this case, the external behavior and the states define the system.

In this talk, we also discuss the concept of minimal state map from the general behavioral point of view. This is done by introducing a simple definition of partial ordering among state maps. With this partial ordering, comes the lattice structure of state maps, and with that minimal and maximal state maps are defined. The definition of minimality here coincides with well known definitions, for example the state space with minimal dimension in linear systems. We shall also discuss some additional properties of state maps, and how state maps that satisfy the properties are positioned in the lattice.

We shall also study bisimulations between systems, cast in the general behavioral framework. Our main subject of study is the relation between bisimulation and external behavior equivalence. Bisimulation as a notion of equivalence between dynamical systems has its root in discrete event systems. See, for example, the excellent introduction in [4]. The concept is centered around equivalence between the states of the systems. Therefore, when studying bisimulation, the states and the external trajectories define the systems under study. The study of bisimulation for dynamical systems has been done, for example in [5] and [6].

References

[1] A.A. Julius and A.J. van der Schaft, *Compatibility of behavior interconnections*, in Proc European Control Conference 2003, Cambridge, UK, 2003.

[2] J.W. Polderman and J.C. Willems, *Introduction to mathematical systems theory: a behavioral approach*, Springer, New York, 1998.

[3] J.C. Willems, *On interconnections, control and feedback*, IEEE Trans. Automatic Control, **42(3)**, pp 326-339, 1997.

[4] R. Milner, *Communication and concurrency*, Prentice Hall Int'l, 1989.

[5] G.J. Pappas, *Bisimilar linear systems*, Automatica, **39**, pp 2035-2047, 2003.

[6] A.J. van der Schaft, *Bisimulation of dynamical systems*, to appear in Proc. Hybrid Systems: Computation and Control 2004, Philadelphia, USA, 2004.

Interconnections of Dirac Structures

Ramkrishna Pasumarthy and Arjan J van der Schaft
Faculty of EEMCS
University of Twente
PO Box 217, 7500AE Enschede
The Netherlands
(R.Pasumarthy, a.j.vanderschaft)@math.utwente.nl

1 Abstract

Port based modeling of physical systems leads to port-Hamiltonian systems, which are defined with respect to a geometric structure called Dirac structures. A power conserving interconnection of a number of port-Hamiltonian systems leads to another port-Hamiltonian system with Dirac structure defined by the interconnection of Dirac structures of the subsystems. We study interconnection of Dirac structures in the mixed finite and infinite dimensional case i.e. interconnection of a finite dimensional system(s) with infinite dimensional system(s). Also necessary and sufficient conditions for the achievability of Dirac structures as in the finite dimensional case are extended to the mixed finite and infinite dimensional case. This theory is studied in particular with respect to the transmission line

References

[1] A.J. van der Schaft, "*L_2-Gain and Passivity Techniques in Nonlinear Control*, Springer-Verlag, 2000.

[2] A.J. van der Schaft, B.M Maschke, "Hamiltonian formulation of disrtibuted parameter systems with boundary energy flow, *Journal of Geometry and Physics vol.42* pp.166-194, 2002

[3] A.J. van der Schaft, J. Cervera, "Composition of Dirac structures and control of port-Hamiltonian Systems , *Proceedings 15th International Symposium on Mathematical Theory of Networks and Systems (MTNS 2002)*, Eds. D.S.Gilliam, J.Rosenthal, South Bend, August 12-16, 2002.

[4] H.Rodriguez, A.J. van der Schaft, R.Ortega "On stabilization of nonlinear distributed parameter port-Hamiltonian systems via energy-shaping, Technical report Feb.2001 in: , *Proceedings of the 40th IEEE Conference on Decision and Control*, Orlando, FL, December 2001

Energy management for vehicle power nets: Finding ultimate performance using Dynamic Programming

J.T.B.A. Kessels, M. Eifert,
W.P.M.H. Heemels, P.P.J. van den Bosch
Department of Electrical Engineering
Technische Universiteit Eindhoven
P.O. Box 513, 5600 MB Eindhoven
The Netherlands
E-mail: J.T.B.A.Kessels@tue.nl

Michiel Koot,
Bram de Jager
Department of Mechanical Engineering
Technische Universiteit Eindhoven
P.O. Box 513, 5600 MB Eindhoven
The Netherlands

1 Introduction

Today's passenger cars are equipped with many electric devices, offering people a high standard on safety and comfort. In future vehicles, it is expected that the electric power requirements will grow further [1]. Think for example of (mild) hybrid electric vehicles where electric power is used for vehicle propulsion, but also the drive-by-wire concept where mechanical or hydraulic systems are replaced by electric devices. As these power demands become more dominant in the total energy consumption of a vehicle, also the need for Energy Management (EM) will grow.

2 Problem definition

The EM strategies that are considered here will focus on vehicles with a conventional drive train. However, the 14V power net has been replaced by a 42V power net including an advanced alternator that offers more freedom in controlling the power flow towards the power net. The EM strategy exploits this degree of freedom, such that the vehicle's overall power requirements are fulfilled more efficiently.

3 Control objective

The control objective is to reduce the energy losses in the vehicle and hence, minimize the total fuel consumption. The fuel consumption is calculated from the engine's fuel map and depends on two variables: the power delivered to the drive train plus alternator: $P_d + P_a$ and the speed of the engine ω. Assuming that the driver dictates a certain speed profile (here the NEDC driving cycle), both $P_d(t)$ and $\omega(t)$ are exactly defined along the driving cycle. This leaves only P_a as the manipulated variable respecting several constraints (e.g. maximum alternator power) and influences closely related dependencies such as the energy level E_s in the battery. Given a driving cycle over t_e seconds, the following optimization problem can be formulated:

$$\min_{P_a} J(P_d + P_a, \omega) = \int_0^{t_e} fuelrate(P_d + P_a, \omega)\mathrm{d}t$$

$$\text{subject to:} \quad \begin{array}{ccccc} P_{a,\min} & \leq & P_a & \leq & P_{a,\max} \\ E_{s,\min} & \leq & E_s & \leq & E_{s,\max} \end{array}$$

Note that this is a non-linear optimization problem due to the selected engine- and battery model. A technique called Dynamic Programming [2] has been used to find an optimal solution. Therefore, the optimization problem is transformed into a time-discrete description where the states of the system and the manipulated variables are mapped on a dense grid. This approximation reduces the original problem, such that a solution is found in an acceptable amount of time.

4 Results

It turns out that the performance of EM is closely related to the engine's fuel map where nonlinearities should be present. Also the energy efficiency of the battery influences the decision whenever it is profitable to generate electric energy in advance. Applying Dynamic Programming learns that fuel reductions of 2.5% can be expected. It should be emphasized that this number depends heavily on environmental parameters such as driving cycle, electric load request, etc.

5 Further research

Within the scope of the project, further research is expected on the following topics:

- Analyze the optimal solution to find heuristic rules for implementing an on-line control algorithm.
- Include additional features to improve the overall performance of the strategy (e.g. stop-start function).

References

[1] J.G. Kassakian, J.M. Miller, N. Traub, “Automotive electronics power up”, IEEE spectrum, pp. 34-39, May 2000.

[2] D.P. Bertsekas, “Dynamic programming and optimal control”, Athena Scientific, 1995.

Measurement and Control of slip in a Continuously Variable Transmission

Bram Bonsen
Eindhoven University of Technology
Den Dolech 2, 5600MB Eindhoven, The Netherlands
b.bonsen@tue.nl

1 Introduction

Continuously Variable Transmission (CVT's) are increasingly used in automotive applications. They have an advantage over normal automatic transmissions, namely the ratio coverage of the CVT is much greater and more versatile. This enables the engine to operate at a more economic working point. Unfortunately the big advantage is largely lost due to inefficiencies in the variator in the CVT. High clamping force levels are applied to prevent slip from occurring, which could damage the pulleys and the belt. However, high clamping forces increase wear and fatigue and increase internal friction in the belt. Furthermore a higher clamping force causes more actuation losses due to hydraulic leakage[1]. Lowering the clamping force therefore increases the efficiency of the variator, but also increases the risk of damage.

2 Modelling slip

Slip is defined relative to the rotational speed of the primary axis. The reason for this is the slip mechanism in the microslip area.

$$\nu = \frac{r_s}{r_g} - 1 \quad (1)$$

$$r_s = \frac{\omega_s}{\omega_p} \quad (2)$$

$$r_g = \frac{R_p}{R_s} \quad (3)$$

$$T_{cvt} = \frac{2F\mu R}{\cos\alpha} \quad (4)$$

The speed ratio r_s is calculated using the rotational speeds of the primary and secondary axes. The geometric ratio r_g is measured indirectly via the pulley position.
A dynamic model can be derived:

$$\dot{\nu} = \frac{\dot{r}_s r_g - r_s \dot{r}_g}{r_g^2} \quad (5)$$

$$\dot{r}_s = \frac{\dot{\omega}_s \omega_p - \omega_s \dot{\omega}_p}{\omega_p^2} \quad (6)$$

$$\dot{r}_g = \kappa \omega_p \Delta F \quad (7)$$

The derived dynamic model for slip in a variator is nonlinear[3][2]. In order to analyse the system for control purposes the system is linearized. To do this the system is written in State-Space format. For the linearization two different situations are distinguished. The first case is the part of the tractioncurve that is decreasing with slip. This is the microslip area of the tractioncurve. In macroslip the tractioncurve is flat. The nonlinear state space description with $x = [\omega_p, \omega_s, r_g]^T$ and $u = [Td, Te, F, \Delta F]^T$ is:

$$\dot{x} = f(x,u) = \begin{bmatrix} \frac{2FR_s\mu}{\cos\alpha J_s} - \frac{T_d}{J_s} \\ \frac{T_e}{J_e} - \frac{2FR_p\mu}{\cos\alpha J_e} \\ \kappa \Delta F w_p \end{bmatrix} \quad (8)$$

To linearize the system the geometric relationship between R_p, R_s and r_g is used. R_p and R_s are characterized as a second order polynomial of r_g. The function for $\mu(\nu)$ is taken piecewise linear, this is indicated by the index i. The system can be linearized around a certain working point $x_0 = [\omega_{s0}, \omega_{p0}, r_{g0}]^T$.

$$\mu = k_{1i}\nu + k_{2i} \quad (9)$$

$$\dot{\hat{x}} = A\hat{x} + B\hat{u} \quad (10)$$

Where $\hat{x} = x - x_0$ and $\hat{u} = u - u_0$. The linearized matrices A and B can now be found to be:

$$A = \frac{2F_0}{\omega_{p0} r_{g0} \cos\alpha} \begin{bmatrix} \frac{R_{s0}k_{1i}}{J_s} & -\frac{\omega_{s0}R_{s0}k_{1i}}{\omega_{p0}J_s} & \dots \\ -\frac{R_{s0}k_{1i}r_{g0}}{J_e} & \frac{\omega_{s0}R_{s0}k_{1i}r_{g0}}{\omega_{p0}J_e} & \dots \\ 0 & \kappa_0 \Delta F_0 & \dots \end{bmatrix}$$
$$\begin{bmatrix} \dots & \frac{\omega_{p0} r_{g0}^2 \frac{dR_s}{dr_g}\mu - R_s k_{1i}\omega_s}{r_g J_s} \\ \dots & \frac{-\omega_{p0} r_{g0} R_{s0}\mu - r_{g0}^2 \omega_p \frac{dR_s}{dr_g}\mu + R_{s0}k_{1i}\omega_{s0}}{J_e} \\ \dots & 0 \end{bmatrix} \quad (11)$$

$$B = \begin{bmatrix} -\frac{1}{J_s} & 0 & \frac{2R_{s0}\mu}{J_s\cos\alpha} & 0 \\ 0 & \frac{1}{J_e} & -\frac{2R_{p0}\mu}{J_e\cos\alpha} & 0 \\ 0 & 0 & 0 & \kappa_0\omega_{p0} \end{bmatrix} \quad (12)$$

References

[1] H. Faust, M. Homm, and F. Bitzer. Wirkungsgradoptimiertes cvt-anpresssystem. *7. LuK Kolloquium 2002*, pages 61–73, 2002.

[2] A. Tonohata M. Adachi H. Asayama, J. Kawai. Mechanism of metal pushing belt. *JSAE Review 16*, pages 137–143, 1995.

[3] D. Kobayashi, Y. Mabuchi, and Yoshiaki Katoh. A study on the torque capacity of a metal pushing v-belt for cvt's. *SAE Technical papers*, 1998.

Energy management for vehicle power nets: using model predictive control

Michiel Koot*[1], Bram de Jager[1], Maarten Steinbuch[1],
John Kessels[2], Maurice Heemels[2], Paul van den Bosch[2]
Technische Universiteit Eindhoven
Dept. of [1]Mechanical Engineering, [2]Electrical Engineering
P.O. Box 513, 5600 MB Eindhoven, The Netherlands
*corresponding author: m.w.t.koot@tue.nl

1 Introduction

In the near future a significant increase in electric power consumption in vehicles is expected. Reasons for this are the increasing standards for safety and comfort and the replacement of mechanical and hydraulic systems by electric ones.

To limit the associated fuel consumption, smart strategies for the generation, storage/retrieval, distribution and consumption of the electric power can be used that:

- exploit the fact that the cost for generating electricity varies with the operating point of the engine,
- make use of the possibility to temporarily store electric energy in a storage device.

2 Problem statement

The goal of this project is to develop a smart energy management system that uses knowledge on the component characteristics and the mechanical and electric power requests, in order to generate electric energy at lower costs.

3 Vehicle

The power flow in a conventional vehicle with an alternator and a battery can be represented according to Figure 1.

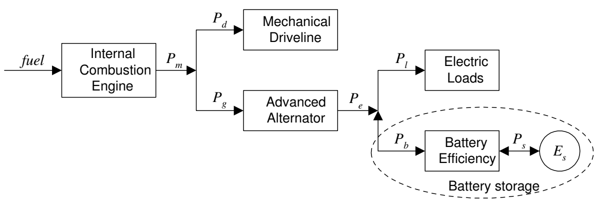

Figure 1: Power flow in the vehicle

The engine torque is split between the mechanical drive line and the alternator. The alternator torque depends on the electric power drawn from it.

4 Control strategy

The energy management problem is written as an optimization problem, where the cost function expresses the relation between generated power and fuel use. The constraints incorporate the physical limitations of the components. [1, 2, 3]

A Model Predictive Control framework is used, such that the optimization problem is solved over a receding prediction horizon.

5 Implementation

A Hardware in the Loop test setup has been built for evaluation of different control strategies. In this test setup the mechanical parts of the vehicle are simulated, whereas some components of the electric power net are physically present.

6 Results

Fuel savings are obtained of about 1-2 % of the total fuel consumption for the NEDC driving cycle in combination with electric loads of 500 to 2000 W. [3]

7 Further Research

- Extension to a parallel hybrid electric vehicle where the generator can also be used as a motor.
- Minimizing peak power demands using priority control. This power scheduling system can postpone or quicken certain energy requests.

References

[1] E. D. Tate and S. P. Boyd, *Finding ultimate limits of performance for hybrid electric vehicles*, SAE Paper 2000-01-3099.

[2] Bram de Jager, *Predictive storage control for a class of power conversion systems*, Proceedings of the ECC 2003, Cambridge, UK.

[3] M. Koot, J. Kessels, B. de Jager, M. Heemels, and P. van den Bosch, *Energy Management for Vehicle Power Nets*, Submitted to the ACC 2004, Boston, USA.

Modeling and simulation of an electro-mechanical CVT

Tim Klaassen
Eindhoven University of Technology
Den Dolech 2, 5600 MB Eindhoven, The Netherlands
T.W.G.L.Klaassen@tue.nl

1 INTRODUCTION

The pulleys of a pushbelt or chain type CVT are actuated axially to adjust transmission ratio and to apply slip-preventing belt clamping force. In conventional CVTs this is done using hydraulics. Hydraulic losses are however substantial. To reduce the energy consumption, a electro-mechanical CVT, as shown in Figure 1, is developed. This system has the advantage that only mechanical power is needed when the CVT is shifting or the clamping force is changed. Another advantage is that the CVT transmission ratio and the clamping force can be set independently.
For simulation, control design and testing, a multi-body model of this system is implemented in Adams software. The main part of the model is the ariator, which is discussed in the next section. The model also incorporates friction losses in bearings, gears and spindles. Furthermore electromotor models and some characteristic properties of the driveline are implemented, such as engine data and a torque converter.

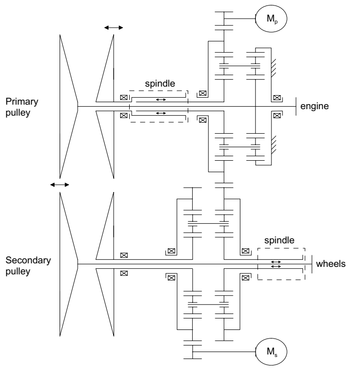

Figure 1: Alternative Variator Actuation concept

2 MULTI-BODY MODEL

The belt is not implemented as a multi-body system. This would introduce many degrees of freedom, and simulation would be very slow. The coupling between the primary and secondary pulley is implemented using a velocity controller and is represented in Figure 2. The maximum torque that can be transmitted depends on the clamping force between the sheaves and the belt. Experiments show that, when torque is transmitted, there is always slip between the belt and the pulleys [1]. By saturating the control torque on the maximum belt torque T_{belt}, a realistic variator behavior is obtained.

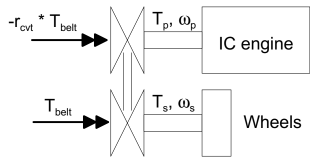

Figure 2: Variator implementation

The clamping forces between the belt and pulleys are calculated using the model by Kobayashi, presented in [3]. This model gives an insight on the tensile and compressive forces acting within the bands and between the blocks of the belt.
Transient variator models like Ide's model [2] or Shafai's model [4] state that there is a damping force relative to the shifting speed. This damping is implemented on the moveable pulley sheaves.

3 RESULTS

The model presented shows a very realistic behavior. Simulations show very low power consumption of both electro motors during FTP and NEDC driving cycles in comparison with a conventional CVT. By decoupling the ratio and clamping force control, a high actuation performance with a high closed loop bandwidth and a small steady-state error can be obtained.

References

[1] B. Bonsen, T.W.G.L. Klaassen, K.G.O. van de Meerakker, P.A. Veenhuizen and M. Steinbuch, Analysis of slip in a continuously variable transmission, in Proc. of Imece 2003, Washington USA, 2003

[2] T. Ide, A. Udagawa, and R. Kataoka, A dynamic response analysis of a vehicle with a metal V-belt CVT, in Proc. of the 2nd Internat. Symp. on Advanced Vehicle Control (AVEC94), vol. 1, pp. 230235. Tsukuba, Japan, 1994.

[3] D. Kobayashi, Y. Mabuchi and Yoshiaki Katoh, A Study on the Torque Capacity of a Metal Pushing V-Belt for CVTs, in SAE Technical papers, nr. 980822, 1998

[4] E. Shafai, M. Simons, U. Neff, and H.P. Geering, Model of a continuously variable transmission, in Proc. of the 1st IFAC Workshop on Advances in Automotive Control, pp. 99107, 1995.

Variance analysis of frequency response function measurements using periodic excitations

T. D'haene (1), R. Pintelon (1), J. Schoukens (1), E. Van Gheem (2)
Vrije Universiteit Brussel, dept. ELEC(1), META(2) Pleinlaan 2, B1050 Brussels, Belgium
email: Tom.Dhaene@vub.ac.be

I. INTRODUCTION

The influence of disturbing noise and non-linear distortions on frequency response function (FRF) measurements using periodic excitations has been studied in detail in the literature[1,2,3]. A variance analysis method (1) has been developed [4] that allows to detect and quantify the non-linear distortions G_S and the disturbing noise N_G. Here the device under test is excited with an odd random phase multisine with a random harmonic grid. P consecutive periods of the steady state response are measured and this experiment is repeated for M different realisations of the phases of the multisine. This results in the following sample variances:

$$\begin{aligned} \hat{\sigma}^2_{G,1} &\to \sigma^2_S/M + \sigma^2_n/MP \\ \hat{\sigma}^2_{G,2} &\to \sigma^2_n/MP \end{aligned} \tag{1}$$

where $\sigma^2_n = var(N_G^{[m,p]})$, $\sigma^2_S = var(G_S^{[m]})$, for $m = 1,...,M$ and $p = 1,...,P$

However in the presence of non-synchronous periodic disturbances $N_t^{[m,p]}$ such as the 50Hz mains and its harmonics it has been observed in [5] that $\hat{\sigma}^2_{G,1}$ can be smaller than $\hat{\sigma}^2_{G,2}$ and hence $\hat{\sigma}^2_S < 0$, which is an undesired property.

II. THE VARIANCE ANALYSIS PROCEDURE

In this paper the variance analysis (2) is generalised to detect and quantify the following non-stationary disturbances: (i) non-synchronous periodic signals, for example the 50Hz mains and its harmonics, and (ii) non-stationary behaviour of the device under test, for example phase or frequency modulation.

$$\begin{aligned} \hat{\sigma}^2_{G,1} &\to \sigma^2_S/M + \sigma^2_n/MP + \sigma^2_t/MP^2 \\ \hat{\sigma}^2_{G,2} &\to \sigma^2_n/MP + \sigma^2_t/MP \\ \hat{\sigma}^2_{G,3} &\to \sigma^2_S/MP + \sigma^2_n/MP + \sigma^2_t/MP \end{aligned} \tag{2}$$

where $\hat{\sigma}^2_S$ and $\hat{\sigma}^2_n$ are defined in (1) and with $\sigma^2_t = var(N_t^{[m,p]})$

III. SIMULATION

In this simulation, we consider a system with a third order non-linearity in the presence of disturbing noise and 2 different non-synchronous periodic components:

$$y(t) = z(t) + 0.1z(t)^3 + \sin(2\pi f_1 t) + \sin(2\pi f_2 t) + 0.01n(t) \tag{3}$$

with $P = 50$, $M = 5$, $f_1 = 500\text{Hz}$, $f_2 = 2300\text{Hz}$ and $n(t)$ normally distributed white noise.

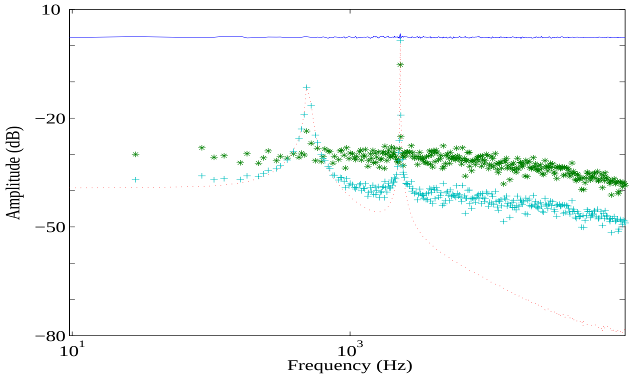

FIG. 1. The top blue line: the best linear approximation of the system, the dotted line: $\hat{\sigma}_{G,2}$, the +: $\hat{\sigma}_{G,3}$. the *: $\hat{\sigma}_{G,1}$

This simulation shows that even for large values of the number of periods P, $\hat{\sigma}^2_{G,2}$ becomes larger than $\hat{\sigma}^2_{G,1}$ in the neighbourhood of the frequencies f_1 and f_2. Due to these frequencies the estimate $\hat{\sigma}^2_S$ (1) would be negative, although the significant presence of the non-linearities. The contribution of this paper is to overcome this problem via the generalised variance analysis (2).

This work is sponsored by the Fund for Scientific Research (FWO-Vlaanderen), the Flemish Government (GOA-IMMI) and the Belgian Program on Interuniversity Poles of Attraction initiated by the Belgian State, Prime Minister's Office, Science Policy programming (IUAP V/22).

IV. REFERENCES

[1] R. Pintelon and J. Schoukens (2001). System Identification. A frequency domain approach. *IEEE press*, New Jersey.

[2] J. Schoukens, T. Dobrowiecki, R. Pintelon (1998). Identification of linear systems in the presence of non-linear distortions. A frequency domain approach. *IEEE Trans. on Automatic Control*, vol 43, no 2, pp. 176-190.

[3] Pintelon R. and J. Schoukens (2002). Measurement and modeling of linear systems in the presence of non-linear distortions. *MSSP*, vol.16, no. 5, pp. 785-801.

[4] Pintelon R., G. Vandersteen, L. De Locht, Y. Rolain and J. Schoukens (2004). Experimental characterization of operational amplifiers: a system identification approach - Part I: theory and simulations, *IEEE Trans. Instrum. Meas.*, vol. 53, no 3.

[5] Pintelon R., Y. Rolain, G. Vandersteen, and J. Schoukens (2004). Experimental characterization of operational amplifiers: a system identification approach - Part II: calibration and measurements, *IEEE Trans. Instrum. Meas.*, vol. 53,

Creating Spectrally Pure Signals for ADC-testing

D. Rabijns, W. Van Moer and G. Vandersteen.
Vrije Universiteit Brussel (Dept. ELEC/TW); Pleinlaan 2; B-1050 Brussels (Belgium)
Phone : +32.2.629.29.79; Fax : +32.2.629.28.50; Email : Daan.Rabijns@vub.ac.be

Abstract - **For accurate testing of analog-to-digital converters (ADC), the spectral purity of the input signal is utterly important. This paper describes a method to create very pure signals, such as sine waves, dual-tones or multi-tones, using only power measurements. The signals are generated with an arbitrary waveform generator (AWG). Any unwanted spectral line is removed, independent of its exact origin. This allows to apply the correct signal to the ADC under test, even if the signal source is not perfect or is followed by filters or amplifiers with a small non-linear distortion. Measurements are used to demonstrate the capabilities of the method.**

I. Introduction

Signal generators are imperfect devices. Besides the wanted spectrum, unwanted spectral contributions appear and the generated spectrum becomes non-ideal. This is especially true if the generator is followed by filters, amplifiers,... In those cases, the difference between the exact spectrum required to excite the analog-to-digital converter (ADC) and the one actually applied can be unacceptable large. These unwanted spectral contributions make it very difficult to measure the response of an ADC properly.

The method described in this paper corrects distorted spectra. The input spectrum of the used AWG is modified to cancel out every undesired spectral peak in the signal applied to the ADC under test. This is possible because a well designed AWG is mainly linear.

Measurements are performed with a spectrum analyzer, which both has a very low noise floor and can work at higher frequencies, allowing the compensation of very small harmonics. This is also an advantage from metrologic point of view, since the operation of an ADC is very similar to an AWG and may contain common flaws, whereas a spectrum analyzer is based on a totally different working principle.

II. Proposed Method

The method to obtain compensation is very simple and will be explained in detail in the presentation. It requires no modelling, only measurements and very few assumptions are made.

III. Measurements

The first example is the creation of a pure sine wave. The AWG used 4096 points and a sample frequency of 10 MHz. For this example, line 30 was excited, which results in a sine wave with a frequency of 73,242 kHz. To determine the phase, seven recursions were used. For the amplitude and gain, only 5 recursions were necessary. The results (see figure 1) show that unwanted spectral lines, including the one at DC are all suppressed by at least 80 dB.

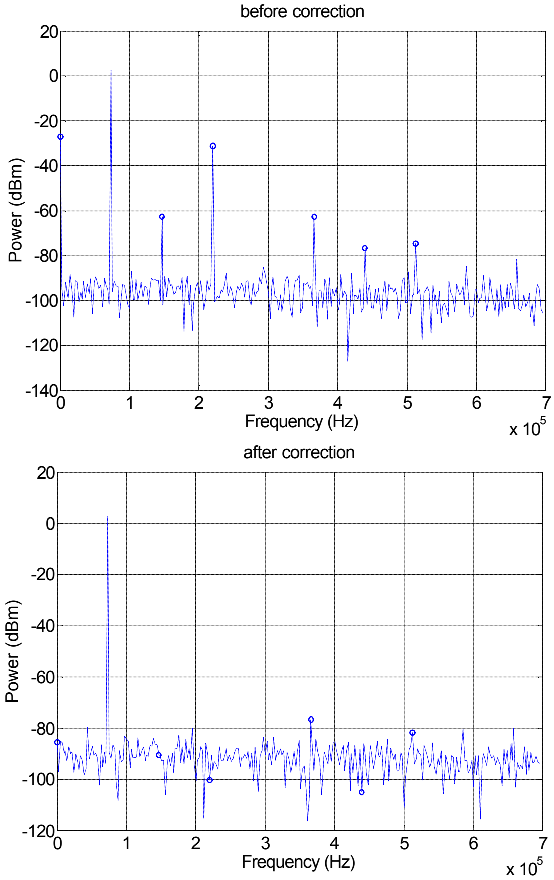

Fig.1 Spectrum of a generated sine wave before and after correction (o : lines to which correction was applied)

Acknowledgment

This research was supported by a grant of the Flemish Institute for the improvement of the scientific-technological research in industry (IWT), the Belgian National Fund for Scientific Research, Flanders, the Flemish government (GOA_IMMI), and the Belgian government as a part of the Belgian program on Interuniversity Poles of attraction (IUAP-5/22) initiated by the Belgian State, Prime Ministers Office, Science Policy Programming.

References

[1] Rabijns D., G. Vandersteen, W. Van Moer, Y. Rolain and J. Schoukens, "Creating spectrally pure signals for ADC-testing", IMTC 2003 Conference proceedings, Vail, USA, 2003

Fast Measurement of Quantization Distortions in DSP Algorithms

Johan Paduart, Johan Schoukens, Yves Rolain
Vrije Universiteit Brussel, dep. ELEC, Pleinlaan, 2 1050 Brussels, BELGIUM e-mail: johan.paduart@vub.ac.be

I. INTRODUCTION

Digital Signal Processing systems have the advantage of being flexible compared to analog circuits, but they introduce calculation errors. These errors induce a non ideal behaviour of the output like the presence of quantisation noise, limit cycles, chaotic and even nonlinear behaviour. Therefore it is necessary to check for the presence of these effects and to quantify them in order to be sure that the design specifications are still met. A single experiment showing and quantifying all errors at the same time is possible by applying a multisine with well chosen amplitude spectrum instead of using single sines. The amplitude of the multisine can be composed in such a way that the RMS value of the multisine is about the same as the RMS value of the expected input signal of the system, in order to have a realistic idea of the level of nonlinear distortions that will arise in later use. At the unexcited frequencies of the multisine, the nonlinear behaviour at the output of the DSP system will be detected. Moreover, by looking at variations in the output from one period to another, also the presence of a chaotic/quasiperiodical contribution will be seen.

II. DSP ERRORS

A fixed point DSP system will be used to illustrate the results. The advantages of a fixed point representation in a DSP system are well known, however, there are some serious drawbacks: finite precision and finite range for the internal representation of the processed samples. A lowpass filter, implemented in Direct Form II with 16 bit accumulators and 8 bit memory and with respectively 4 and 2 bits headroom serves as an example. The different kinds of distortion can be detected and quantized:

• *Truncation errors of the filter coefficients*

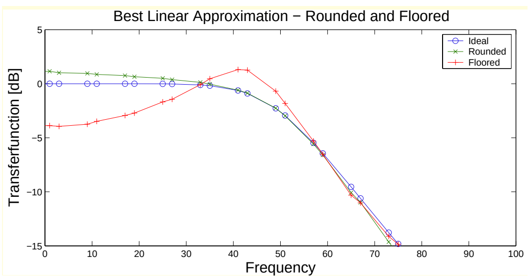

FIG. 1. Distortion of the transferfunction due to pole dislocation

It is obvious that the truncation method of the filter coefficients has an influence of the realised transfer function. (FIG. 1.)

• *Finite Precision Distortion*

The level of nonlinear distortion components at the output due to the finite precision of the arithmetic and storage operations can be investigated from the same data (FIG. 2.), on the non excited frequency lines of the applied multisine.

• *Finite Range Distortion*

The two approaches that can be used to deal with the finite range (two's complement overflow and saturation) are compared

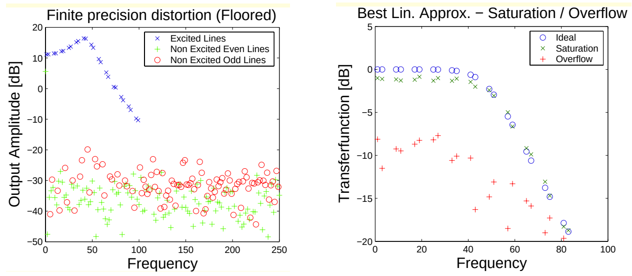

FIG. 2. Finite precision distortion and overflow methods

The simulation clearly shows heavy distortion of the transfer function in the case of two's complement overflow (FIG. 2.), while the distortion in case of saturation is much smaller.

• Chaos

Chaotic behaviour can occur with two's complement overflow when no special precautions are taken concerning the filter coefficients [5]. For high order systems, the analysis is not simple. Quasiperiodical solutions can be detected by comparing successive periods of the output of the multisine.

This work was supported by the FWO-Vlaanderen, the Flemish community (Concerted action ILiNoS), and the Belgian government (IUAP-V/22).

References

[1] Full Abstract: ftp://elecftp.vub.ac.be/Papers/JohanPaduart/TNBenelux_04_Paduart.pdf
[2] J. Schoukens, J. Swevers R. Pintelon H. Van der Auweraer, Excitation design for FRF measurements in the presence of nonlinear distortions. *Proceedings of ISMA2002*, Vol. 2, 951-958.
[3] J. Schoukens J. , T. Dobrowiecki, and R. Pintelon. Identification of linear systems in the presence of nonlinear distortions. A frequency domain approach. *IEEE Trans. on Automatic Control*, Vol. 43, No.2, pp. 176-190, 1998.
[4] R. Pintelon, J. Schoukens, *System Identification. A Frequency domain approach*. IEEE Press, New Jersey.
[5] Leon Chua, Tao Lin - Chaos in Digital Filters, *IEEE Transactions on Circuits and Systems,* Vol.35 No 6, 1988.
[6] Thompson, J. M. T., and H. B. Stewart, *Nonlinear Dynamics and Chaos*, New York: John Wiley & Sons, 1986.
[7] A.V. Oppenheim and R.W. Schafer, *Digital Signal Processing*, Prentice Hall, 1975

Least costly identification for control

Xavier Bombois
Delft Center for Systems and Control
Delft University of Technology
Mekelweg 2, 2628 CD Delft
The Netherlands
Email: x.j.a.bombois@dcsc.tudelft.nl

Gérard Scorletti
LAP ISMRA, Caen, France

Paul Van den Hof
DCSC, Delft, The Netherlands

Michel Gevers
CESAME, Louvain-la-Neuve, Belgium

In the industrial practice, a controller for a real-life system G_0 is generally designed using a model $\hat{G}$ of G_0 identified using data collected on the true system. When designing the identification experiment, the control engineer generally faces the problem of making a trade-off between its desire of obtaining as much information as possible about the true system by using a very long identification experiment and a very powerful input signal, and the economical constraint asking her/him to reduce as much as possible the costs of the identification by keeping this identification short and by exciting G_0 with a low power signal. In this paper, we propose an elegant solution to that problem of trade-off by determining the least costly identification experiment for control. The least costly identification experiment for control is here defined as the experiment on G_0 (with a fixed length of measurement data) where the input signal $u(t)$ is the one whose total power P_u (i.e. $P_u = (1/2\pi)\int \Phi_u(\omega)d\omega$) is minimized under the constraint that the identification still delivers a model $\hat{G}$ sufficiently close to G_0 for the controller $\hat{C}$ designed with $\hat{G}$ to stabilize and to achieve sufficient performance with G_0. The desired performance on G_0 will be expressed by magnitude bounds on one (or several) closed-loop transfer functions of $[\hat{C}\ G_0]$ (H_∞ performance constraints). Note that, to remain brief, we will focus on the design of the input signal $u(t)$, given a fixed data length, since this variable is generally the variable considered in experiment design. However, our results can be easily extended to the design of the shortest identification experiment for control, given a fixed $u(t)$.

In this abstract, we thus propose a new framework in order to design the identification experiment when the model has to be used for control. This framework consists of designing the cheapest identification experiment (i.e. the experiment with the less powerful input signal) to ensure that the identified model delivers a satisfying controller for the unknown true system. This framework is a novelty since the optimal identification experiment had been until now defined as the experiment for which a measure of the performance degradation between the loops $[\hat{C}\ G_0]$ and $[\hat{C}\ \hat{G}]$ was minimized under a constraint on the power of $u(t)$. Multiple examples of such an approach can be found in the literature. The major difference between the framework developed until now in the literature and our new framework is that, in the first, the authors seek the best performance with $\hat{C}$ for a given cost of the identification while, in the latter, we seek the minimal cost for the identification to obtain the desired performance with $\hat{C}$.

Due to the novelty of the framework, the existing techniques for the design of an identification experiment were not appropriate for the design of the least costly identification experiment for control. Consequently, besides the contribution related to the definition of this new framework, a second (more technical) contribution is to propose a methodology in order to determine the least costly identification experiment for control (and more particularly the input signal corresponding to this identification experiment). This methodology consists of two distinct steps. In a first step, we determine how far the true system G_0 may be from the identified model $\hat{G}$ for the $\hat{G}$-based controller $\hat{C}$ to be still a satisfying controller for G_0. The second step is then the actual design step. Indeed, in this second step, we design the identification input signal $u(t)$ with the minimal total power P_u such that, at a self-chosen probability level, the obtained modeling error is smaller than the larger admissible error determined in the first step.

Brain activation detection from magnitude fMRI data using a generalized likelihood ratio test

Arjan den Dekker
Delft Center for Systems and Control
Delft University of Technology
Mekelweg 2, 2628 CD Delft
The Netherlands
Email: a.j.dendekker@dcsc.tudelft.nl

Jan Sijbers
Vision Lab, Department of Physics
University of Antwerp
Groenenborgerlaan 171, 2020 Antwerp
Belgium
Email: jan.sijbers@ua.ac.be

1 Introduction

Functional magnetic resonance (fMRI) studies intend to answer neuroscience questions by statistically analyzing a set of acquired images. Thereby, the aim is to determine those regions in the brain image in which the signal changes upon stimulus presentation. Although MR data are intrinsically complex valued, most tests are commonly applied to magnitude MR images, because these images have the advantage to be immune to incidental phase variations due to various sources. A consequence of transforming the complex valued images into magnitude images is a change of the probability density function (PDF) of the data under concern. Whereas complex data are Gaussian distributed, magnitude data are Rician distributed [1]. Nevertheless, tests applied to magnitude data generally rely on the (false) assumption of Gaussian distributed data. If the signal-to-noise ratio (SNR) of the data is high, this may be a valid assumption since the Rician PDF tends to a Gaussian PDF at increasing levels of the SNR. However, at low SNR, the Rician PDF significantly deviates from a Gaussian PDF. In this paper, we propose a Generalized Likelihood Ratio Test (GLRT) for magnitude fMRI data that fully exploits the knowledge of the Rician PDF.

2 The Generalized Likelihood Ratio Test

Let $\boldsymbol{m} = (m_1, ..., m_N)^T$ be a magnitude data set of which the joint PDF depends on the vector $\boldsymbol{\theta} = (\theta_1, ..., \theta_k)^T$ of unknown parameters. Suppose that we wish to test the composite null hypothesis:

$$H_0 : \theta_1 = \theta_1^0, \cdots, \theta_r = \theta_r^0, \theta_{r+1}, \cdots, \theta_k \tag{1}$$

where $\theta_1^0, ..., \theta_r^0$ are known and $\theta_{r+1}, ..., \theta_k$ are left unspecified, against the alternative composite hypothesis H_1 under which all parameters $\theta_1, ..., \theta_k$ are left unspecified. The generalized likelihood-ratio (GLR) λ is then defined as follows:

$$\lambda(\boldsymbol{m}) = \frac{\sup\limits_{\theta_1, \cdots, \theta_k} L(\theta_1, \cdots, \theta_k; \boldsymbol{m})}{\sup\limits_{\theta_{r+1}, \cdots, \theta_k} L(\theta_1^0, \cdots, \theta_r^0, \theta_{r+1}, \cdots, \theta_k; \boldsymbol{m})} \tag{2}$$

where the denominator of λ is the likelihood function evaluated at the Maximum Likelihood (ML) estimator of $\boldsymbol{\theta}$ under H_0, whereas the numerator of λ is the likelihood function evaluated at the ML estimator of $\boldsymbol{\theta}$ under H_1. H_0 is to be rejected if and only if $\lambda \geq \lambda_0$, where λ_0 is some user specified threshold. The false alarm rate P_F is given by the probability that the test will decide H_1 when H_0 is true. The *detection rate* P_D is given by the probability that the test will decide H_1 when H_1 is true. It can be shown that, asymptotically, the test statistic $2 \ln \lambda$ possesses a chi-square distribution with r degrees of freedom when H_0 is true. This allows one to determine the proper threshold needed to achieve a desired P_F. We considered the problem of testing whether the response of a magnitude MR data set $\boldsymbol{m}$ of sample size N to a known reference function $\boldsymbol{r} = (r_1, ..., r_N)^T$ is significant. The noiseless magnitude data set was assumed to be described by the $N \times 1$ deterministic signal vector:

$$\boldsymbol{z} = a\mathbf{1} + b\boldsymbol{r} \tag{3}$$

with $\mathbf{1}$ an $N \times 1$ vector of ones. Hence, $\boldsymbol{z}$ is a constant baseline on which a reference function $\boldsymbol{r}$ with amplitude b is superimposed. In the absence of activity, b equals zero, such that $\boldsymbol{z} \equiv a\mathbf{1}$. The hypothesis that $b = 0$ (H_0) is tested against the hypothesis that $b \neq 0$ (H_1).

3 Results

Extensive Monte Carlo simulation experiments were set up to test the performance of the GLRT. Thereby, the offset as well as the amplitude of the reference function was estimated using ML estimation [2]. Experiments were run for various reference functions, for various values of the SNR and for various values of N. The results reveal that, for a fixed false alarm rate, the proposed GLRT outperforms existing statistical tests applied to magnitude MR data in terms of detection rate.

References

[1] A. Macovski, Magnetic Resonance in Medicine **36**, 494-497, 1996.

[2] J. Sijbers, A.J. den Dekker, E. Raman, and D. Van Dyck, International Journal of Imaging Systems and Technology **10**(2),109-114, 1999.

Asynchrony between position error and retinal slip signals in 2D catch-up saccades

C. Schreiber, M. Missal and P. Lefèvre
CESAME and lab. neurophysiology, UCL, Belgium
schreiber@auto.ucl.ac.be

1 Introduction

When primates track a moving visual stimulus, they combine two different types of eye movements to orient their visual axis: smooth pursuit and catch-up saccades. Saccades are rapid eye movements that can reach velocities as high as 500^o/s. They allow to orient the fovea (the highest acuity zone of the retina) to the target. They are controlled without any visual feedback, because the visual delays are too long compared to their duration. Smooth pursuit is characterized by slower movements. They can reach maximum velocities of 50^o/s and allow to track a moving visual target. In contrast with saccades, they are controlled by continuous visual feedback.

Horizontal catch-up saccade have been studied in details. Their programming uses both information about position error (PE) and retinal slip (RS)[1]. Visual tracking in two dimensions (2D) allows to better assess the interaction between position and velocity errors by exploring different orientations of PE and RS vectors.

2 Methods

We measured 2D eye movements in 7 human subjects (search coil technique).

Control trials were composed of 2 fixation periods (duration [700..1300ms]). The first position of fixation was at the center of the screen, and the second position was randomly chosen in a 20 sided square.

Each double-step-ramp trials started with a 2D Rashbass step-ramp stimulus (velocity [10..20^o/s], direction [0..360^o], duration [600..1100ms]) [2]. This was followed by a second step-ramp of the target (duration, [500..700ms]). Both the direction of the position step (PS, [-10..10^o]) and the velocity step (VS, [-40..40^o/s]) varied randomly in 2D. We analyzed the first catch-up saccades after the second step of the target.

3 Results

We could divide the data in two categories of catch-up saccades, single-peaked saccades (n=12833) and double-peaked saccades (n=1555). The proportion of double-peaked saccades versus single-peaked saccades increased with RS ($\sim$ 35% for RS>50^o/s). A multiple linear regression analysis was performed to find the parameters determining the amplitude of catch-up saccades. We confirmed that both PE and RS were used in single-peaked saccades programming. In contrast, for double-peaked saccades, the first part of saccades (Amp_1) presented a better correlation with PE whereas the second part (Amp_2) presented a better correlation with RS:

$$\begin{array}{ll} Amp_1 = 0.80 * PE + 0.06 * RS, & R = 0.94, n = 1555, \\ & R_{PE} = 0.90, \\ & R_{RS} = 0.63, \\ Amp_2 = 0.21 * PE + 0.10 * RS, & R = 0.91, n = 1555, \\ & R_{PE} = 0.57, \\ & R_{RS} = 0.85. \end{array}$$

Thus, double-peaked saccades illustrate that PE and RS are not necessarily integrated simultaneously in catch-up saccades programming.

In order to show such asynchrony between PE and RS for the single-peaked catch-up saccades, we studied their curvature. The curvature of control saccades, defined as the angle between the initial and final saccadic orientations, depended on the global saccadic orientation. The catch-up saccade curvature was modulated by the relative orientation of PE and RS around control values. More precisely, the angle between the initial and final saccadic orientations depended linearly on the angle θ between the orientations of PE and RS. This dependence was greater when RS increased. For saccades oriented in the upper-right quadrant, we obtained:

$$\begin{array}{ll} Curv = -29.75, & controls, n = 657, \\ Curv = -28.2 + 0.08 * \theta, & RS < 20^o/s, n = 656, \\ & R = 0.21, \\ Curv = -23.7 + 0.29 * \theta, & RS > 20^o/s, n = 572, \\ & R = 0.53. \end{array}$$

In conclusion, the combination of position error and retinal slip allows the saccadic system to accurately catch a moving target even when these signals are not synchronized. This difference in timing suggests different neuronal pathways for the processing of PE and RS.

References

[1] De Brouwer S, Missal M, Barnes G, Lefevre P, Quantitative analysis of catch-up saccades during sustained pursuit, J Neurophysiol, 87:1772-1780 , 2002.

[2] Rashbass C, The relationship between saccadic and smooth tracking eye movements, J Physiol (Lond), 159:326:338, 1961.

A biomolecular pathway of vascular wall integrity as a hybrid piecewise constant system

Mark Musters
Department of Electrical Engineering
Eindhoven University of Technology
P.O. Box 513, 5600 MB Eindhoven
The Netherlands
Email: m.w.j.m.musters@tue.nl

Jorn op den Buijs
Department of Electrical Engineering
Eindhoven University of Technology
P.O. Box 513, 5600 MB Eindhoven
The Netherlands
Email: j.o.d.buijs@tue.nl

Natal van Riel
Department of Electrical Engineering
Eindhoven University of Technology
P.O. Box 513, 5600 MB Eindhoven
The Netherlands
Email: n.a.w.v.riel@tue.nl

1 Introduction

In man, blood vessels are lined by a thin layer of endothelial cells. Regulation of endothelial cell division is one of the numerous functions of the protein transforming growth factor-β_1 (TGF-β_1) [1]. Recent experimental findings suggest that endothelial cells become insensitive to TGF-β_1 at an advanced age, which might explain the endothelial malfunctioning in various cardiovascular diseases, e.g. atherosclerosis. Computational modelling can contribute to our understanding of these physiological processes. Nowadays, most biological computer models consist of highly non-linear differential equations due to so-called sigmoid functions in signalling pathways and enzyme processes:

$$f(x) = \frac{x^{\nu}}{K^{\nu} + x^{\nu}}, \qquad (1)$$

with x [in M] the substrate concentration; K [in M] and ν are the “half-maximum” concentration and the so-called cooperativity coefficient, respectively. However, little experimental data confirm the sigmoid curve’s exact shape and data is lacking to determine K and ν [2]. For high ν-values, sigmoid functions show switching behaviour, which can be modelled as a two-step piecewise constant system. Replacing the non-linear sigmoid function with linear equations makes the system more suitable for analysis, e.g. reachability and stability [3]. On the contrary, the change from a non-linear system to a piecewise system could result in approximation errors. We show in this paper that a 2-step abstraction approaches the sigmoid function in a biological model very well for high ν-values ($\nu > 10$) and is still reasonable at lower ν-values.

2 Model

The TGF-β_1 pathway consists of various interacting concentrations, which are assumed to be homogenously distributed in the extracellular compartment (LTGF-β_1 and TGF-β_1) and cytoplasm (R-SMAD and mRNA) of the endothelial cell. An inhibiting substrate (I-SMAD) is located in the nucleus of the cell, which shuttles into the cytoplasm as soon as the TGF-β_1 activation is sufficiently high to exceed a threshold. The dynamics of the concentrations were described with five ordinary differential equations that contain both a positive and a negative feedback; the shuttling of I-SMAD is modelled with a sigmoid function and as a 2-step piecewise constant function:

$$\dot{\mathbf{x}} = \mathbf{A}\mathbf{x}, \qquad (2)$$

$$\mathbf{A} = \begin{bmatrix} -k_1 & 0 & 0 & 0 & k_5 \\ k_1 & -k_2 & 0 & 0 & 0 \\ 0 & k_2 & -k_{d1} - k_4(x_4) & 0 & 0 \\ 0 & 0 & k_3 & -k_{d2} & 0 \\ 0 & 0 & k_3 & 0 & -k_{d3} \end{bmatrix}, \qquad (3)$$

with $\mathbf{x} =$ [LTGF-β_1,TGF-β_1,R-SMAD,I-SMAD,mRNA]^T. The parameter $k_4(x_4)$ is in the non-linear model simulated as a sigmoid function (Eq. 1), multiplied by a maximum rate constant, k_{max}. The 2-step piecewise constant approach is described as follows:

$$k_4(x_4) = \begin{cases} 0 & \text{for } x_4 \le K \\ k_{max} & \text{for } x_4 > K \end{cases}, \qquad (4)$$

with K [in M] is the threshold concentration.

Simulation
Normalised concentrations were used. Multiple simulations were performed with both models by varying the k-values between 0 and 1, because no physiological relevant values could be obtained from literature. Furthermore, the ν-values of the non-linear model were simulated between 1 and 100. At t = 0, LTGF- β_1 was set to one, the other concentrations were initially zero. The time-concentration plots from all simulations of both models were compared to each other.

3 Conclusion

For high ν-values (> 10), the non-linear model and the piecewise approach show good resemblance. However, for lower ν-values, the piecewise graphs deviate slightly from the non-linear system. Therefore, we propose to substitute the 2-step piecewise constant for an *n*-step piecewise affine system for lower ν-values. Moreover, we will perform stability and reachability analysis of these piecewise systems in future studies. In conclusion, a piecewise approximation of a non-linear biological pathway is a plausible alternative for high ν-values.

References

[1] Derynck *et al. Nature* **425**: 577-584, 2003.
[2] Alur *et al. Comp.Sci. Eng.*, **1**: 2-13, 2002.
[3] Belta *et al. Proc. 40th IEEE CDC*: 869-874, Dec. 2001.

Using Metabolic Flux Analysis for the Modelling of a Cell Culture during the Apoptose Phase

A. Provost, G. Bastin
CESAME
Université catholique de Louvain, B-1348 Louvain-la-Neuve, Belgium
Email: bastin,provost@auto.ucl.ac.be

Y.-J. Schneider
Cell Biochemistry Laboratory
Université catholique de Louvain, B 1348 Louvain-la-Neuve, Belgium

S.N. Agathos
Unit of Bioengineering
Université catholique de Louvain, B-1348 Louvain-la-Neuve, Belgium

Abstract

In previous works, the modelling of CHO cells during the growth phase has been obtained by performing a Metabolic Flux Analysis on a given metabolic network (Fig. 1) supposedly governing the growth machinery.

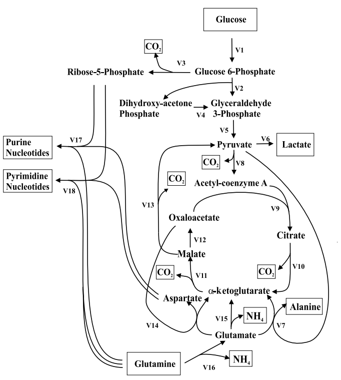

FIG. 1: Metabolic network for the growth phase.

Then the metabolic network was translated into a set of macro-reactions :

$$
\begin{aligned}
Glucose &\longrightarrow 2\, Lactate \\
Glucose &\longrightarrow 6\, CO_2 \\
Glutamine &\longrightarrow Alanine + 2\, CO_2 + NH_4 \\
Glutamine &\longrightarrow Lactate + 2\, CO_2 + 2\, NH_4 \\
Glutamine &\longrightarrow 5\, CO_2 + 2\, NH_4 \\
Glucose + 3\, Glutamine &\longrightarrow Purine + 2\, CO_2 + NH_4 \\
Glucose + 2\, Glutamine &\longrightarrow Pyrimidine + 2\, CO_2 + NH_4
\end{aligned}
$$

by first deducing the so-called elementary flux modes. From there a classical model was elaborated and used to obtain simulation results.

The main idea in this contribution is to use the same methodology for the apoptose phase. A metabolic network (see Fig. 2) is proposed for modelling this particular stage of the cell life. Then a Metabolic Flux Analysis is performed and the elementary fluxes related to the apoptose phase are computed. Subsequently, the set of macro-reactions corresponding to the apoptose phase is deduced :

$$
\begin{aligned}
Lactate &\longrightarrow 3\, CO_2 \\
Alanine &\longrightarrow 3\, CO_2 + NH_4 \\
Glutamine &\longrightarrow 5\, CO_2 + 2\, NH_4
\end{aligned}
$$

The transition between the two phases is described by smoothly switching between the two metabolic networks and the two corresponding models. The results are presented in Fig. 3

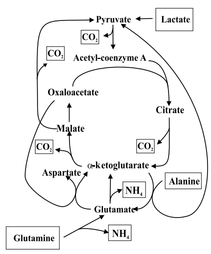

FIG. 2: Metabolic network for the apoptose phase.

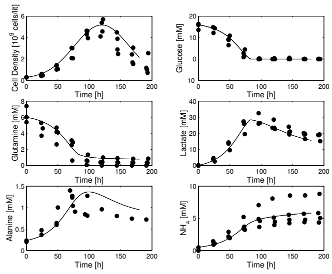

FIG. 3: Experimental data and simulation results.

Contribution to dynamic modelling of a cement kiln

A.C. Witsel, C. Renotte, M. Remy

Laboratoire d'Automatique, Faculté Polytechnique de Mons
Boulevard Dolez,31, 7000 Mons, Belgium
E-mail : Anne-Catherine.Witsel@fpms.ac.be

Abstract

The three basic processes in the cement manufacturing industry are preparing the raw material mix, baking the raw materials and grinding the final product. Of these three processes, the burning process is the most important and the most difficult step. Indeed the quality of the cement produced is essentially determined by the temperature in the kiln where the raw mix is transformed in clinker.

The clinker burning process is a very complex dynamical process due to the heat exchanges and the series of chemical reactions taking place therein. The complexity of the phenomena makes the process quite misunderstood and the cement kiln complicated to control. A dynamic model of the cement kiln can therefore be very useful to understand its behaviour in more details and to design more sophisticated control strategies.

In the literature, few dynamic models of the cement kiln are proposed. The models of Blumberg [1] and Spang [3] are quite complete and are both based on the work of Lyons [2]. The partial differential equations used by Spang [3] are very similar to those of Lyons [2] but the author adds a dynamic model of the flame. In order to reduce the computational load, simplifying assumptions have been made. On the other side, Blumberg's [1] model takes more phenomena into account but represents the kiln by a finite number of sections. This representation leads to formulate the model equations in a finite-difference form rather than by a set of partial differential equations, ordinary differential equations being easier to solve.

In this contribution, the dynamic model of Spang [3] is chosen and studied. The computational power now available allows the use of a more complicated model. The structure of the model is therefore modified on the base of Blumberg's work to take more phenomena into account and incorporate time-varying parameters. The partial differential equations describing the model are implemented using the method of lines.

Several simulations have been performed for different loading conditions and values of the parameters. The results give interesting informations on the general behaviour of the kiln and on the input/output relations. Potential control and measured variables can also be chosen from the simulation for control purpose.

Acknowledgements

A.C. Witsel is a research fellow of the Belgian F.R.I.A. (Fonds pour la formation à la Recherche dans l'Industrie et dans l'Agriculture)

References

[1] Blumberg J.M., *Modelling and control of the cement manufacturing process*, The University of Manchester – PhD thesis, 1970.

[2] Lyons J.W., Min H.S., Parisot P.E., Paul J.F., *Experimentation with a wet-process rotary cement kiln via the analog computer*, I & E C Process Design and Development, Vol. 1, No. 1, Jan 1962.

[3] Spang H.A., *A dynamic Model of a cement kiln*, Automatica, Vol. 8, pp 309-323, Pergamon Press, 1972.

The influence of amplitude and phase variations on a resonant cavity

C.M.M. van Lierop, P.P.J. van den Bosch
Department of Electrical Engineering
Technische Universiteit Eindhoven
P.O. Box 513, 5600 MB Eindhoven
The Netherlands
Email: C.M.M.v.Lierop@tue.nl

F.B. Kiewiet, O.J. Luiten, M.J. van der Wiel
Department of Applied Physics
Technische Universiteit Eindhoven
P.O. Box 513, 5600 MB Eindhoven
The Netherlands
Email: F.B.Kiewiet@tue.nl

1 Introduction

At Eindhoven University of Technology a project has been started to build a combined DC/RF accelerator. The RF accelerator cavity is an RF coupled resonant structure which creates a longitudinal electric field of standing waves (along the axis of the cavity). A pulsed laser is used to create a short bunch of electrons. For optimal acceleration the electrons must be created at the right phase of the RF field. In order to achieve this the laser pulses have to be synchronized to the RF signal. The RF cavity is filled with energy by a pulsed klystron tube (which is an RF amplifier just like for instance a magnetron). To create an RF power pulse the power input of the klystron tube is pulse modulated. The modulator creates a pulse of approximately $20MW$ with a duration of $4\mu s$. The RF power pulse at the output of the klystron has a peak power of approximately $10MW$.

2 Problem definition

Usually the modulator is designed to deliver a flat top power pulse. In the setup which is built at Eindhoven University of Technology a different approach is used. Instead of using a modulator creating a flat top pulse the modulator was designed to create an “exponentially shaped” pulse. The reasons for choosing an “exponentially shaped” pulse instead of a flat top pulse are: Only one short electron bunch is accelerated per RF power pulse (which consumes only a very small fraction of the power) so there is no need for a constant output power. The modulator becomes very compact because it contains less large high voltage and high power components. The modulator becomes more reliable mainly because it contains less capacitors. The setup becomes cheaper.

The choice of an “exponentially shaped” pulse introduces extra dynamics into the system. To evaluate the influence of these dynamics on the performance of the system a thorough identification of the non-linear system dynamics had to be performed [1].

3 System identification and analysis

Though there are advantages, there are also problems connected with using an “exponentially shaped” pulse to power the klystron tube. Firstly, the tube introduces a phase change

$$\phi(t) = \frac{d\omega_0}{v_e(t)}$$

where d is the length of the tube and ω_0 is the input frequency. This is caused by the changing electron speed $v_e(t)$ in the klystron. Since the RF accelerator cavity has an extremely small absorption bandwidth (a loaded quality factor Q of 7000) the changing delay causes the cavity to be shifted off resonance which means that the maximum RF field in the cavity will be smaller.

The second effect is that because of the changing frequency the phase of the RF field inside of the cavity will have a small time-dependency which could increase the phase jitter between the laser and the RF field inside the cavity. This might spoil the stability of the accelerator.

The third effect is caused by the shape of the pulse itself. Since the cavity has a very high quality factor $Q = 7000$ it has a limited bandwidth which prevents it from reaching its maximum (steady state) value. This also results in a decrease of the maximum RF field inside the cavity.

4 Conclusions

The overall decrease of the electric RF field inside the cavity when using an “exponentially shaped” modulator pulse, equals approximately 10% of which approximately 5% is caused by the klystron output frequency change. The 5% loss of electric field due to phase changes is actually much less than the initial guess. This is caused by the relativistic effect since it reduces the phase variations around maximum (it can be seen as a saturation effect). The phase jitter is slightly larger when using an “exponentially shaped” modulator pulse instead of a flat modulator pulse. The total time jitter resulting from the phase jitter has a standard deviation of approximately $3.9 \cdot 10^2 fs$. When using a flat top pulse the standard deviation of the total jitter could have been approximately 25% smaller.

References

[1] C.M.M. van Lierop, “The influence of amplitude and phase variations on a resonant cavity.” Master’s thesis, Eindhoven University of Technology, 2003.

Modelling for control of a centrifugal compression system

Jan van Helvoirt*, Bram de Jager, Maarten Steinbuch
Department of Mechanical Engineering
Technische Universiteit Eindhoven
P.O. Box 513, 5600 MB Eindhoven
The Netherlands
email: *J.v.Helvoirt@tue.nl

Introduction

The performance and operating range of centrifugal compressors is limited by the occurrence of an aerodynamic instability called *surge*. This instability can lead to severe damage of the machine due to large mechanical and thermal loads. A way to cope with this instability is active control. In this approach, perturbations are fed back into the flow field in order to modify the dynamics of the compression system. Such techniques can extend the stable operating range towards lower mass flows, which makes the compressor more versatile. See also Figure 1. Furthermore it enables the safe operation of the compressor near the surge point.

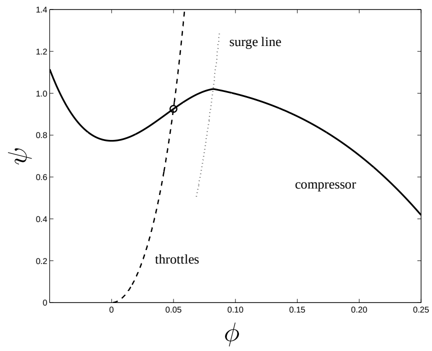

Figure 1: Compressor curve with unstable operating point.

Compression system model

The suggested approach is applied to an experimental compression system with a rated power of 250 kW. To describe the dynamic behaviour of the examined compression system, the model suggested in [1] is used. The lumped parameter model is schematically shown in Figure 2. By introducing a dimensionless mass flow ϕ, pressure rise ψ, and time scale $\tilde{t}$, the following set of equations is obtained

$$\frac{d\phi_c}{d\tilde{t}} = B(\psi_c - \psi) \tag{1}$$

$$\frac{d\psi}{d\tilde{t}} = \frac{F}{B}(\phi_c - \phi_l - \phi_s) \tag{2}$$

where ψ_c represents the nonlinear steady-state compressor pressure rise shown in Figure 1. The parameters ϕ_l and ϕ_s represent relations for the throttle mass flows.

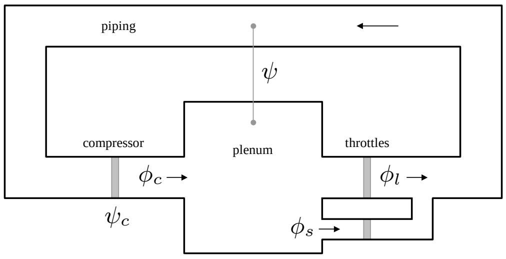

Figure 2: Lumped parameter compression system model.

Model validation

In order to validate the obtained model, simulation results are compared with experimental surge measurements. Figure 3 shows that both the amplitude and frequency of the surge oscillations are captured well by the model. Furthermore, a sensitivity analysis is carried out. This analysis provides measures for the relative importance of the various model parameters. The results also form the starting point for the analysis of the linearized model and the design of a stabilizing feedback controller.

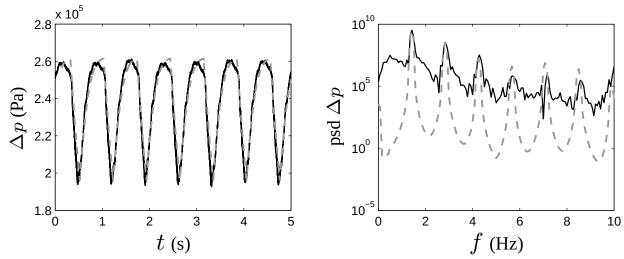

Figure 3: Comparing simulations (- -) with experimental data (–).

Acknowledgement

This research is done in cooperation with TNO TPD and is supported by Siemens Demag Delaval Turbomachinery B.V.

References

[1] Greitzer, E.M. (1976), 'Surge and rotating stall in axial flow compressors. Part I: Theoretical compression system model', ASME J. Eng. for Power, **98**(2), 190–198.

Modeling of an ink-jet printhead

Matthijs Groot Wassink
Delft Center for Systems and Control
Mekelweg 2, 2628 CD Delft, The Netherlands
Email: m.b.grootwassink@dcsc.tudelft.nl

Sjirk Koekebakker
Océ-Technologies B.V. Group Research
PO Box 101, 5900 MA Venlo, The Netherlands
Email: koek@oce.nl

Keywords

Ink-jet technology, control, physical modeling, model validation.

Abstract

Inkjet is an important keytechnology, both from an industrial point of view and from an academic research perspective. Applications of this technology cover a wide range varying from printing applications, the production of PolyLEDs, and the production of biochips used for medical research, see e.g. [1] and [2]. Each specific field of application has its own performance requirements to the fluidjet printhead. First, specifications in terms of timing, positioning, and volume have to be met. Often, these criteria are quite tight. For applications of Océ one can think of an accuracy to be met in terms of fractions of microseconds, micrometers and picoliters. Second, requirements play a role concerning reproducibility in face of aging, material variations, and the like. In the future, these performance criteria become even tighter. The requirements for future applications motivate ongoing research into inkjet technology.

A typical design of a printhead comprises several piezoactuated channels in parallel. Given a certain design of these channels, the piezoactuators are provided with pulses (wave forms), whose shape has been the result of a design, such that the requested drop on demand results. From a control perspective, these designs amount to a passive control strategy. A switch from passive to active control of a printhead can break current boundaries that are associated with this open-loop control: one can think of for example higher jet-frequencies and drop-size modulation. To make optimal use of abilities of active control, a mechatronic redesign of the printhead is required. For one, proper sensor functionality should be built in. However, performing a redesign and application of control requires the availability of a suitable model.

At Océ, a number of models are available, two of which are most important. The first one is an acoustic model based on [3]. However, this model is inaccurate with respect to the fluid-dynamics due to the simplifying assumption that the printhead only involves acoustics. The second model is a finite volume model in Flow-3D ([4]). A major drawback of this model is that it requires large computational times. Since both models are not suited for the redesign and control purposes in mind, a new dynamical model is developed based on physical insight. The results of these modeling efforts are presented and discussed. In the future, these insights will be used for control and redesign of the ink-jet printhead.

References

[1] R. Bennett, “Precision Industrial Ink-jet Printing Technology for Full Color PLED display and TFT-LCD manufacturing,” Proc. of the 3rd International Display Manufacturing Conf.,2003.

[2] P.W. Cooley and D.B. Wallace and B.V. Antohe, “Application of Ink-jet Printing Technology to BioMEMS and Microfluidic Systems,” Proc. SPIE Microfluidics and BioMEMS Conference, 2001.

[3] W.M. Beltman, “Viscothermal wave propagation including acousto-elastic interaction,” University of Twente, 1998.

[4] Flow Science Inc., “Flow-3D Release 8.0: User Manual,” Santa Fe, New Mexico, 2002.

Open Loop Stabilization of Periodic Orbits in a Wedge Billiard

Renaud RONSSE
Montefiore Institute, B28
Universite de Liege
Grande Traverse, 10
B-4000 Liege
Belgium
R.Ronsse@ulg.ac.be

Philippe LEFEVRE
CESAME
Universite Catholique de Louvain
Avenue Georges Lemaitre, 4
B-1348 Louvain-la-Neuve
Belgium
lefevre@csam.ucl.ac.be

Rodolphe SEPULCHRE
Montefiore Institute, B28
Universite de Liege
Grande Traverse, 10
B-4000 Liege
Belgium
R.Sepulchre@ulg.ac.be

This study aims at a deep parametric description of the open-loop properties of an impact system: the *wedge billiard*.

The model of a ball non-elastically bouncing on a sinusoidally vibrating table provides one of the simplest illustrations of a dynamical system exhibiting rich nonlinear phenomena such as period doubling and chaotic behavior ("bouncing ball" dynamics, see Holmes (1982) for a review). This model uses open-loop sinusoidal excitement as an input command *stabilizing* several periodic motions, depending on the vibration amplitude and frequency. Our aim is to transpose these results to a more complex system based on the *wedge billiard* configuration (Lehtihet and Miller, 1986), see Figure 1: the ball moves in the plane (2D juggling) under the action of a constant gravitational field and undergoes collisions with two intersecting edges.

The complexity of the wedge billiard is intermediate between the 1D bouncing ball and the classical 3D juggling skill (Sternad, 1999) – with the edges viewed as an idealization of the juggler's two arms – involving some critical "juggling" constraints, such as synchronism of both hands and spatial constraints (if more than one ball are juggled). P.J. Beek and his team studied extensively the cascade juggling skill (see Post et al., 2000, and references therein) which is typically characterized by these constraints.

Recently, Sepulchre and Gerard (2003) studied closed-loop control of periodic orbits in the wedge billiard. We use here an open-loop sinusoidal excitation of both edges to stabilize particular orbits. The bifurcation parameters are not only the vibration amplitude and frequency (as in the bouncing ball model) but also a critical parameter for the wedge system: the angle θ (see Lehtihet and Miller, 1986). Phase-lag between the edges will also be investigated to select particular orbits.

An experimental setup is currently built in our lab. It is based on a tilted air-hockey table ensuring a frictionless puck motion. We will describe the technical features of this setup and present some preliminary experimental results.

Our further research will be based on the human ability to exploit these open-loop stability properties when performing this task, as Sternad et al. (2001) did previously with the bouncing ball.

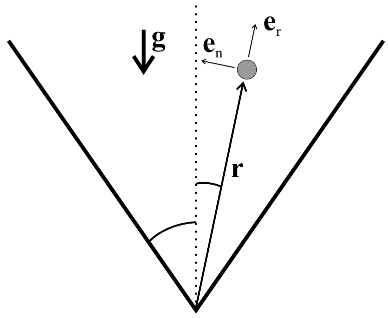

Figure 1: Wedge billiard.

References

P. J. Holmes. The dynamics of repeated impacts with a sinusoidally vibrating table. *J. Sound Vibration*, 84(2): 173–189, 1982.

H. E. Lehtihet and B. N. Miller. Numerical study of a billiard in a gravitational field. *Phys. D*, 21(1): 93–104, 1986.

A. A. Post, A. Daffertshofer and P. J. Beek. Principal components in three-ball cascade juggling. *Biol Cybern*, 82(2): 143–52, 2000.

R. Sepulchre and M. Gerard. Stabilization of periodic orbits in a wedge billiard. In *42nd IEEE Conference on Decision and Control*. Hawaii, 2003.

D. Sternad. Juggling and bouncing balls: Parallels and differences in dynamic concepts and tools. *International Journal of Sport Psychology*, 30(4): 462–489, 1999.

D. Sternad, M. Duarte, H. Katsumata and S. Schaal. Bouncing a ball: tuning into dynamic stability. *J Exp Psychol Hum Percept Perform*, 27(5): 1163–84, 2001.

Phase Locking in a Ring of Oscillators

Jonathan Rogge
Technologiepark Zwijnaarde 914
9052 Zwijnaarde, Belgium
jonathan.rogge@ugent.be

Dirk Aeyels
Technologiepark Zwijnaarde 914
9052 Zwijnaarde, Belgium
dirk.aeyels@ugent.be

1 Introduction

In nature many examples of oscillating systems coupled into a ring formation can be found. Such a structure is used to explain the gaits of n-legged animals [1], and to model the twining of plants [2] and rings of semiconductor lasers [3]. In this paper the cells are coupled unidirectionally, i.e. the i-th oscillator is influenced by the $(i+1)$-th oscillator for $i = 1, \ldots, N$, and the N-th one is influenced by the first. This way of coupling can be used to model a cyclic pursuit strategy of robots. In [4] such a strategy is modeled without the use of limit cycle oscillators. The present paper indicates the stability properties of the equilibrium solutions.

2 System dynamics

Some simplifying assumptions are made in the construction of the model. Each oscillator is assumed to exhibit a periodic behavior when not coupled to other oscillators. It is assumed that these oscillators still behave periodically when coupled, and that the only property that is influenced by the coupling is the speed of the periodic motion of each oscillator. With these assumptions it is possible to create a model where the state of each oscillator is represented by one scalar variable θ, *the phase* of the oscillator. The phase of the i-th oscillator, when uncoupled, evolves in time according to the differential equation $\dot{\theta}_i = \omega_i,\ \theta_i \in S^1$. In this equation $\omega_i \in \mathbb{R}$ is the *natural frequency* of the i-th oscillator; it indicates the speed of the periodic motion. The phase of an oscillator can be visualized as a point moving around on the unit circle. When the oscillator is uncoupled, this point moves around with a constant velocity. The system equations of the coupled oscillators become

$$\begin{aligned} \dot{\theta}_i &= \omega_i + K\sin(\theta_{i+1} - \theta_i), \quad i = 1, \ldots, N-1, \\ \dot{\theta}_N &= \omega_N + K\sin(\theta_1 - \theta_N). \end{aligned} \tag{1}$$

The parameter K is called the coupling strength and N is the number of oscillators. For the sake of simplicity, the interaction is implemented by a sine function.

2.1 Identical oscillators

In the case of identical oscillators, all oscillators have the same natural frequency. Call this frequency ω. Define the phase differences $\phi_i \triangleq \theta_i - \theta_{i-1},\ i = 2, \ldots, N$ and $\phi_1 = \theta_1 - \theta_N$. Every vector $\phi = (\phi_1, \ldots, \phi_N)$ that is a permutation of a vector of the form

$$(\underbrace{\alpha, \ldots, \alpha}_{m} \underbrace{\pi - \alpha, \ldots, \pi - \alpha}_{N-m}), \tag{2}$$

with $m \in \{0, 1, \ldots, N\}$ and α the solution of $m\alpha + (N - m)(\pi - \alpha) = 2\pi l,\ l \in \mathbb{Z}$, corresponds to a phase locking solution. The solutions of interest are those of the form $\phi = (\frac{2\pi k}{N}, \ldots, \frac{2\pi k}{N}),\ k \in \mathbb{Z}$. The solution with $k = 0 \mod 2\pi$ is called the *synchronized solution*; the other solutions are the so-called *traveling wave solutions*. The velocity Ω with which such a phase locked group moves is $\sin(\frac{2\pi k}{N})K$. The stronger the oscillators attract each other, the faster they will move when the motion is a traveling wave. If the oscillators synchronize, the group velocity Ω is zero. This behavior is completely different from the case in which the oscillators are bidirectionally coupled, where Ω is zero for each phase locking solution and hence does not depend on K. Remark that in the original coordinates the group velocity is $\Omega + \omega$. For coupling strengths $K > 0$ the phase locking solutions $\phi = (\frac{2\pi k}{N}, \ldots, \frac{2\pi k}{N})$ with $\cos(\frac{2\pi k}{N}) > 0$ are locally asymptotically stable.
For $K < 0$ the phase locking solutions $\phi = (\frac{2\pi k}{N}, \ldots, \frac{2\pi k}{N})$ with $\cos(\frac{2\pi k}{N}) < 0$ are locally asymptotically stable.

2.2 Nonidentical Oscillators

If the oscillators possess different natural frequencies, phase locking solutions exist as well. Assuming that $\dot{\theta}_i = \Omega, \forall i$, leads to an equation that has to be satisfied by Ω. Once a value of Ω is obtained, the values of the phase differences can be determined via (1). For very small K no phase locking solutions exist. It is only when the coupling strength exceeds some threshold value K_p that phase locking solutions arise . Similar to the case with identical oscillators, the group velocity of the phase locked oscillators depends on the coupling strength. When K gets very large, the behavior converges to the behavior of a ring with identical cells.

References

[1] M. Golubitsky et al., Physica D 115, pp. 56-72.

[2] S. Lubkin, Bull. Math. Biol. 56, pp. 795-810.

[3] J. Silber, L. Fabiny and K. Wiesenfeld, J. Opt. Soc. Am. B 10, pp. 1121-1129.

[4] J. Marshall et al., Proc. 42nd IEEE CDC.

[5] Y. Kuramoto, Prog. Theoret. Phys. Suppl. 79, pp. 223-240.

Stabilization of periodic orbits in a wedge billiard

Manuel Gerard, Rodolphe Sepulchre
Department of Electrical Engineering and Computer Science
Université de Liège, Belgium
Manuel.Gerard@ulg.ac.be, R.Sepulchre@ulg.ac.be

1 The wedge billiard system

The wedge billiard system is depicted on the Figure 1. A point mass (ball) moves in the plane under the action of a constant gravitational field. The ball undergoes collisions with two intersecting edges, an idealization of the juggler's two arms. In the absence of control, the two edges form a fixed angle θ with the direction of gravity. Rotational actuation of the edges around their fixed intersection point is used to stabilize one particular orbit of the uncontrolled system.

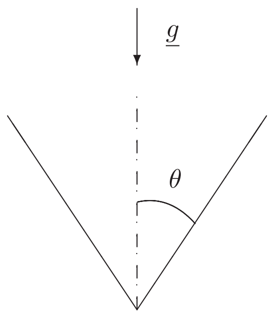

Figure 1: The wedge billiard.

When uncontrolled, the wedge billiard is a rich dynamical model leading to stabilization problems of various complexity. It was realized in [2], [6] that the wedge billiard displays a variety of dynamical phenomena as a function of the angle θ. For $\theta < 45°$, the phase space exhibits stable and chaotic behavior associated with periodic orbits of any period. For $\theta > 45°$, the motion appears completely chaotic. The value $\theta = 45°$ is very special and leads to a completely integrable system with a two-parameter family of unstable periodic orbits.

2 Stabilization problem

The stabilization problem under consideration is viewed as a benchmark for theoretical investigations of impact control problems encountered in legged robotics. The difficulty when studying these mechanisms comes from the underactuated and intermittent nature of the control.

Active stabilization of juggling machines has been addressed by [1], [3],[4], [7].

From a theoretical point of view, the stabilization of periodic orbits through impact control is rephrased as the fixed point discrete-time stabilization of the Poincar map. Hence our problem defines as the stabilization of a three-dimensional discrete-time nonlinear system.

In [5], the problem of stabilizing a period-two orbit (as depicted on the left part of Figure 2) is addressed in the case $\theta = 45°$.

The present paper will address the stabilization of a period-one orbit (see right part of Figure 2) for an arbitrary wedge angle $0° < \theta < 90°$.

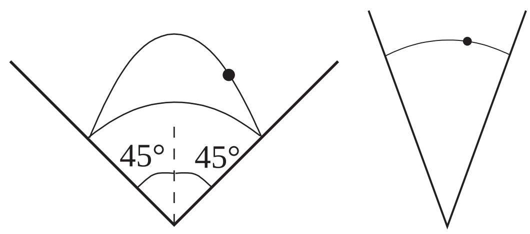

Figure 2: Period-two orbit (left, $\theta = 45°$) and period-one orbit (right).

References

[1] M. Buehler, D.E. Koditschek, and P.J. Kindlmann, *Planning and control of robotic juggling and catching tasks*, International Journal of Robotics Research **13** (1994), no. 2, 101–118.

[2] Lehtihet, H. E. Miller, and B. N., *Numerical study of a billiard in a gravitational field*, Physica **21D** (1986), 93–104.

[3] K.M. Lynch and C.K. Black, *Control of underactuated manipulation by real-time nonlinear optimization*, 9th Int. Symposium Robotics Research (Snowbird, UT), October 1999.

[4] A. A. Rizzi and D. E. Koditschek, *Progress in spatial robot juggling*, IEEE International Conference on Robotics and Automation (Nice, France), 1992, pp. 775–780.

[5] R. Sepulchre and M. Gerard, *Stabilization of periodic orbits in a wedge billiard*, IEEE 42nd Conf. on Decision and Control (Maui, Hawaii-USA), 2003, pp. 1568–1573.

[6] T. Szeredi and D.A. Goodings, *Classical and quantum chaos of the wedge billiard. i. classical mechanics*, Physical Review E **48** (1993), no. 5, 3518–3528.

[7] A. Zavala-Rio and B. Brogliato, *On the control of a one degree-of-freedom juggling robot*, Dynamics and Control **9** (1999), 67–90.

Convergence results for infinite products of stochastic matrices

Luc Moreau
Eindhoven University of Technology
Mechanical Engineering, Dynamics and Control Technology
P.O. Box 513, 5600 MB Eindhoven, The Netherlands
L.P.M.Moreau@tue.nl

1 Abstract

Recent years have witnessed an increasing interest in the interaction between information flow and system dynamics. It is further recognized that information and communication constraints may have a considerable impact on the performance of a control system. The study of these topics forms a very active area of research, giving rise to new control paradigms such as *quantized control systems*, *networked control systems* and *multi-agent (multi-vehicle, multi-robot) systems*.

An important aspect of information flow in a dynamical system is the communication topology, which determines what information is available for which component at a given time instant. We study the role of communication topology in the context of multi-agent systems. Our interest in multi-agent systems is motivated by the emergence of several applications including formation flying of UAVs (unmanned aerial vehicles), cooperative robotics and sensor networks.

In the present work we consider a group of n agents, not necessarily identical. The individual agents share a common state space and each agent updates his current state based upon the information received from other agents, according to a simple weighted average rule. The mathematical model of this multi-agent system is a linear time-varying system in discrete time with a stochastic system matrix at each time instant. Our aim is to relate the information flow and communication structure with the stability properties of this system.

The model that we consider encompasses, or is closely related to, several models reported in the literature. A prominent and well-studied example concerns synchronization of coupled oscillators, a phenomenon which is ubiquitous in the natural world and finds several applications in physics and engineering; see [3, 4] for a review and a historical account. Another interesting example concerns swarming, a cooperative behavior observed for a variety of living beings such as birds, fish, bacteria, etc. In the physics literature, swarming models are often individual-based with each individual being represented by a particle moving with constant velocity, its direction of motion being updated according to nearest neighbor coupling; see, for example, the papers [1, 5]. A third and last example of multi-agent systems that fall within the scope of the present paper are the consensus algorithms studied in [2]. Consensus protocols enable a network of dynamic agents to agree upon quantities of interest via a process of distributed decision making.

An important feature of the present work concerns the broad class of communication patterns that we consider. We allow for general, time-dependent communication patterns, not necessarily bidirectional. Unidirectional communication is important for practical applications and can easily be incorporated, for example, via broadcasting. Also, sensed information flow which plays a central role in schooling and flocking, is typically not bidirectional. In addition, we do not exclude loops in the communication topology. This means that, typically, we are considering leaderless coordination rather than a leader-follower approach. Finally, we allow for time-dependent communication patterns which are important if we want to take into account link failure and link creation, reconfigurable networks and nearest neighbor coupling.

We present necessary and/or sufficient conditions on the communication topology guaranteeing convergence of the individual agents' states to a common value. These results are, essentially, convergence results for infinite products of stochastic matrices.

References

[1] A. Jadbabaie, J. Lin, and A. S. Morse. Coordination of groups of mobile autonomous agents using nearest neighbor rules. *IEEE Trans. Automat. Control*, 48(6):988–1001, June 2003.

[2] R. O. Saber and R. M. Murray. Consensus protocols for networks of dynamic agents. In *Proceedings of the 2003 American Control Conference (ACC)*, 2003.

[3] S. H. Strogatz. From Kuramoto to Crawford: exploring the onset of synchronization in populations of coupled oscillators. *Physica D*, 143:1–20, 2000.

[4] S. H. Strogatz. *Sync: The Emerging Science of Spontaneous Order*. Hyperion, 2003.

[5] T. Vicsek, A. Czirok, E. B. Jacob, I. Cohen, and O. Schochet. Novel type of phase transitions in a system of self-driven particles. *Phys. Rev. Lett.*, 75:1226–1229, 1995.

Reachability of Affine Systems on Polytopes in the plane

L.C.G.J.M. Habets
Department of Mathematics and Computer Science
Technische Universiteit Eindhoven
P.O. Box 513, 5600 MB Eindhoven
The Netherlands
Email: luch@win.tue.nl

Abstract

In the last decade the study of hybrid systems has received considerable attention. Recently, a specific subclass of hybrid systems, so-called piecewise-affine hybrid systems, is studied quite extensively. A piecewise-affine hybrid system consists of an automaton, with at each discrete mode of the automaton an affine system on a polytope, evolving in continuous time. As soon as the continuous state reaches the boundary of the polytope, a discrete event is triggered, and the automaton switches to a new discrete mode. There the continuous state is restarted and will evolve according to the system dynamics of the affine system corresponding to the new discrete mode. In every discrete mode, the dynamics of the corresponding continuous-time affine system, and the polytope on which this system is defined, may be different.

In the analysis and control of hybrid systems, the problem of reachability plays an important role: is it possible to steer the system in such a way that every state of the system can be reached? A similar problem occurs in the problem of safety verification, where one has to guarantee that some undesirable (unsafe) states are never reached while the system is in operation. Unfortunately, the reachability problem is very difficult to solve, in general.

One of the problems in reachability analysis of piecewise-affine hybrid systems is the determination of the domain of attraction of an exit facet. Given an affine system on a polytope, the exit facets are the facets through which the state may try to leave the polytope. Since leaving through a different facet corresponds to a different transition in the automaton, reachability analysis requires that for every element in the state polytope, the corresponding exit facet is determined. More precisely, for any point in the state polytope, one should check whether the state trajectory of the autonomous affine system with this particular initial value, eventually leaves the state polytope, and if that is indeed the case, the corresponding exit facet has to be determined. It is exactly this problem of characterization of the domains of attraction of the exit facets that is the subject of this talk. In full generality this problem is difficult to solve, and therefore we confine ourselves to affine systems on polytopes of dimension 2, i.e. to the planar case. It turns out that this situation is simple enough to obtain useful results, and rich enough to gain some understanding why the problem becomes far more difficult in higher dimensions. In the planar case some results are obtained by explicitly using the geometry of the plane; in higher dimensions this way out is no longer available.

In the talk we focus on one particular discrete mode of a hybrid system, and study the continuous dynamics in this mode, described by an affine autonomous system on a polytope. First it is shown how the exit facets of this system can be recognized. Next, the state polytope is divided into three parts: solutions that remain inside the polytope forever, solutions that leave the state polytope in finite time through one of the exit facets, and solutions that touch one of the boundaries of the state polytope. For affine systems of dimension $n = 2$ (i.e. the planar case), it is shown how these sets can be determined explicitly. Eventually, this leads to a subdivision of the polytope into an invariant set (solutions that remain in the polytope forever), and into several domains of attraction of the different exit facets.

Realization Theory for Linear Switched Systems

Mihály Petreczky
Centrum voor Wiskunde en Informatica, P.O.Box 94079, 1090GB Amsterdam
M.Petreczky@cwi.nl

Abstract

The problem of constructing a control system realizing an input/output map is one of the central problems of system theory. The solution of this problem for the linear case is well-known and exploited in various branches of system and control theory. In this talk realization theory for linear switched systems will be presented. The results are parallel to those on classical linear systems, although the methods used to derive them are substantially different.

1 The framework of linear switched systems

A linear switched system Σ is a switched system in the spirit of [2] of the form

$$\begin{aligned} \frac{d}{dt}x(t) &= A_{q(t)}x(t) + B_{q(t)}u(t) \\ y(t) &= C_{q(t)} \end{aligned}$$

where $q(t) \in Q$, $q(.) : [0, +\infty) \to Q$ is piecewise-constant, $Q = \{q_1, \cdots, q_N\}$ is the set of discrete modes, $\mathcal{X}$ is the state space, $\mathcal{U}$ is the continuous input space, $\mathcal{Y}$ is the continuous output space. The sets $\mathcal{X}$, $\mathcal{Y}$ and $\mathcal{U}$ are assumed to be vector spaces and $A_q : \mathcal{X} \to \mathcal{X}$, $B_q : \mathcal{U} \to \mathcal{X}$, $C_q : \mathcal{X} \to \mathcal{Y}$ are linear mappings. The input function $u(.) : [0, +\infty) \to \mathcal{U}$ is assumed to be piecewise-continuous and bounded on any bounded interval . Denote the state trajectory from the initial state x_0 under the input $u(.) : [0, +\infty) \to \mathcal{U}$ and switching sequence $w = (q_1, t_1), \cdots, (q_k, t_k) \in (Q \times [0, +\infty))^*$ by $x_\Sigma(x_0, w, u(.)) : [0, \sum_1^k t_i] \to \mathcal{X}$. Define the corresponding output trajectory $y_\Sigma(x_0, w, u(.)) : [0, \sum_1^k t_i] \to \mathcal{Y}$ by $y_\Sigma(x_0, w, u(.))(t) := C_{q_l} x_\Sigma(x_0, w, u(.))(t)$ for $t \in \begin{cases} (\sum_1^{l-1} t_i, \sum_1^l t_i] & l > 1 \\ [0, t_1] & l = 1 \end{cases}$. Two linear switched systems Σ_1 and Σ_2 with identical continuous input and output spaces and identical set of discrete modes are said to be *input/output equivalent* if $y_{\Sigma_1}(0, w, u(.)) = y_{\Sigma_2}(0, w, u(.))$ for all continuous inputs $u(.)$ and switching sequences w. Consider the function $y : \mathcal{U}^{[0,+\infty)} \times (Q \times [0, +\infty))^* \to \mathcal{Y}^{[0,+\infty)}$ where $\mathcal{U}^{[0,+\infty)}$ stands for the set of piecewise-continuous input functions and the set $\mathcal{Y}^{[0,+\infty)}$ stands for the set of partial mappings of type $[0, +\infty) \to \mathcal{Y}$. A linear switched system Σ is said to be a *realization* of y if $y_\Sigma(0, w, u(.)) = y(u(.), w)$ for all input functions $u(.) : [0, +\infty) \to \mathcal{U}$ and switching sequences w. A linear switched system Σ is said to be *reachable* if $Reach(\Sigma) = \{x(0, w, u(.))(t_k) \mid w = (q_1, t_1) \cdots (q_k, t_k) \in (Q \times [0, +\infty))^*, u(.) \in \mathcal{U}^{[0,+\infty)}\} = \mathcal{X}$. A linear switched system Σ is said to be *observable* if $(\forall w \in Q^*, u(.) \in \mathcal{U}^{[0,+\infty]} : y_\Sigma(x_1, w, u(.)) = y_\Sigma(x_2, w, u(.))) \implies x_1 = x_2$ for all $x_1, x_2 \in \mathcal{X}$. A linear switched system is said to be *minimal* if it is reachable and observable. Two linear switched system are said to be *algebraically similar* if the matrices of the one of the systems can be converted to the matrices of the other system by means of a linear transformation between the state spaces. This transformation is independent of the discrete modes.

2 Results

In this talk two separate but related topics will be discussed. First, given a linear switched system Σ, it will be shown that there exists a linear switched system Σ_{min}, such that Σ_{min} is minimal and input/output equivalent to Σ. Moreover, any other minimal Σ' which is input/output equivalent to Σ_{min} is algebraically similar to Σ_{min}. Second, given an input/output function $y : \mathcal{U}^{[0,+\infty)} \times (Q \times [0, +\infty))^* \to \mathcal{Y}^{[0,+\infty)}$ necessary and sufficient conditions in terms of y will be presented for the existence of a switched linear system Σ such that Σ is a realization of y. The proof of the sufficiency also yields a minimal linear switched system which realizes y.

References

[1] Bronisław Jakubczyk. Existence and uniqueness of realizations of nonlinear systems. *SIAM J. Control and Optimization*, 18(4):455 – 471, 1980.

[2] Daniel Liberzon. *Switching in Systems and Control*. Birkhäuser, Boston, 2003.

[3] E.D. Sontag. *Mathematical Control Theory*. Spinger-Verlag, 1990.

[4] Zhendong Sun, S.S. Ge, and T.H. Lee. Controllability and reachability criteria for switched linear systems. *Automatica*, 38:115 – 786, 2002.

[5] H. Sussman. Existence and uniqueness of minimal realizations of nonlinear systems. *Mathematical Systems Theory*, 10:263–284, 1977.

A Bayesian Approach to the Identification of Hybrid Systems[1]

Alexander Lj. Juloski
Department of Electrical Engineering
Eindhoven University of Technology
P.O. Box 513, 5600 MB Eindhoven
The Netherlands
Email: a.juloski@tue.nl

Siep Weiland
Department of Electrical Engineering
Eindhoven University of Technology
P.O. Box 513, 5600 MB Eindhoven
The Netherlands
Email: s.weiland@tue.nl

Abstract

This presentation deals with a novel method of identification of a class of hybrid systems. We consider the problem of identifying piecewise ARX systems of the form $y(k) = f(x(k)) + e(k)$ where

$$f(x) = \begin{cases} \theta_1^\top \begin{pmatrix} x \\ 1 \end{pmatrix} & \text{if } x \in \mathcal{X}_1 \\ \vdots & \\ \theta_s^\top \begin{pmatrix} x \\ 1 \end{pmatrix} & \text{if } x \in \mathcal{X}_s \end{cases}$$

is a piece-wise affine map, $x(k)$ is a vector of regressors consisting of time-delayed output and input measurements $x(k) = \text{col}(y(k-1), \ldots, y(k-n_a), u(k-1), \ldots, u(k-n_b))$. Here, $\mathcal{X} = \bigcup_{i=1}^{s} \mathcal{X}_i$ is a bounded polyhedron, and $\{\mathcal{X}_i\}_{i=1}^{s}$ is a polyhedral partition of $\mathcal{X}$. Parameters n_a and n_b and the number of modes s are assumed to be known, or decided upon and the noise e is an i.i.d. sequence with density function p_e.

Given T measurements $(x(k), y(k))$, $k = 1, \ldots, T$, the identification problem consists of estimating the parameter vectors θ_i, for $i = 1 \ldots s$, and the specification of the regions $\{\mathcal{X}_i\}_{i=1}^{s}$ so that the measured data is explained by the piecewise ARX model in a maximum likelihood sense.

To solve the above identification problem in a numerically tractable way, we propose a Bayesian approach in which the unknown parameter vectors θ_i, $i = 1, \ldots, s$, are regarded as random variables with an *a priori* probability distribution function (pdf) p_{θ_i} that is sequentially adapted as data becomes available. This yields a recursive identification procedure in which at each time step k the likelihood that the data point $(x(k), y(k))$ belongs to mode i is computed according to the *a priori* pdf $p_{\theta_i}^{(k-1)}$ obtained from the previous time step. The data point $x(k), y(k))$ is assigned to the mode with maximum likelihood which results in an *a posteriori* pdf $p_{\theta_i}^{(k)}$. Repeating this scheme sequentially for all data points yields parameter vectors θ_i either as expected values or as maximum likelihood estimates associated with the probability distribution functions $p_{\theta_i}^{(T)}$. A schematic representation of the algorithm for the case $s = 2$ is given in Figure 1.

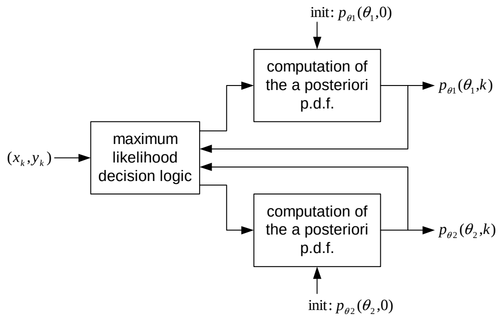

Figure 1: Schematic representation of pdf adaptation

Having the data points attributed to the modes, we apply some standard clustering techniques from pattern recognition to obtain the regions $\{\mathcal{X}\}_{i=1}^{s}$.

A numerically tractable implementation of this algorithm makes use of ideas from particle filtering for the calculation of pdf's. We will discuss these ideas in the talk. Some simulation results will be provided. We discuss advantages and disadvantages of this method, and issues such as convergence, region classification and region misclassification.

Figure 2 shows an example of a two-mode system ($s = 2$) with $n_a = n_b = 1$, $T = 100$ and with 200 particles in the initial and final estimates, respectively.

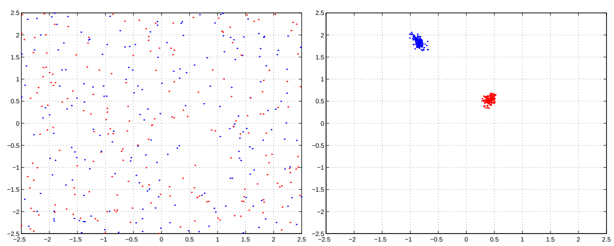

Figure 2: Particle approximation to the initial (uniform) and final pdf's (red: particles of p_{θ_1}; blue: particles of p_{θ_2})

[1]This research is financially supported by STW/PROGRESS grant EES5173

Adaptive weather forecasting using local meteorological information

T.G. Doeswijk
Systems and Control Group
Wageningen University
Mansholtlaan 10
6708 PA Wageningen
timo.doeswijk@wur.nl

K.J. Keesman
Systems and Control Group
Wageningen University
Mansholtlaan 10
6708 PA Wageningen
karel.keesman@wur.nl

1 Abstract

Many agricultural systems are influenced by weather conditions. When controlling these systems, weather forecasts can be of substantial importance, especially when anticipating control strategies are used [1]. Uncertainties in weather forecasting then play an important role.

Weather forecasts can be divided in two forecasts ranges: short term forecasts (up to 32 hours ahead) and medium range forecasts (up to 10 days ahead). The short term forecast only consists of a ”best” forecast whereas the medium range forecast consist of 52 independent forecasts with different scenarios.

A general framework is presented in which local weather forecasts are updated using local measurements. Also medium range forecasts can be updated using short term forecasts by this framework. In this case all scenarios are updated separately. Kalman filtering is used for this purpose as assimilation technique [2]. Given short term weather forecasts from the Dutch weather agency Weathernews Benelux, for location ”De Bilt”, as well as the observations for the same location, it is shown that the standard deviation can be reduced for several hours ahead. This reduction depends on the weather variable that is used. The results for 2 meter temperature forecasts are presented in figure 1. For 2 meter temperature it is shown that assimilating short term forecasts into medium range forecasts lead to a decrease of the standard deviation up to 1 day ahead.

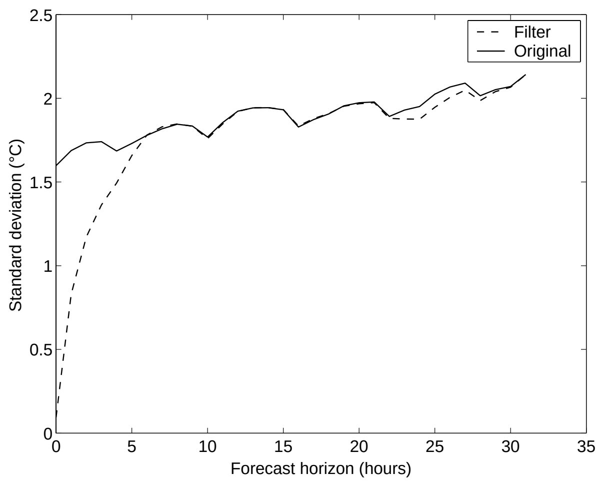

Figure 1: standard deviation of the short term forecast error for 2 meter temperature

References

[1] K. J. Keesman, D. Peters, and L. J. S. Lukasse. Optimal climate control of a storage facility using local weather forecasts. *Control engineering practice*, 11(5):505–516, 2003.

[2] A. Gelb. *Applied Optimal Estimation*. MIT Press, Cambridge, Massachusetts, 1974.

Expert system for road temperature prediction during Winter

S.Beguin, G.Bastin, V.Wertz
CESAME Research Center
Université catholique de Louvain
4 av. Georges Lemaître 1348 Louvain-la-Neuve
Belgium
Email: {beguin,bastin,wertz}@auto.ucl.ac.be

A few years ago, the roads in Wallonie (Belgium) have been equipped with meteorological stations that measure many meteorological data such as air temperature, subsurface temperature, road state, wind direction etc. The people in charge of those stations would like now to exploit those data in an intelligent way. Among possible applications is the construction of an expert system which would act as a computer-aided decision making tool to estimate the need to spread salt on the roads to prevent the apparition of ice. Our work aims at studying the feasability of such a project.

We focused on two precise problems :

1 Prediction of the temperature of the surface of the road

A systematic study [1] has lead us to identify the best possible linear prediction models with respect to the available data. It appears that good prediction performances are achieved when considering a 3 hours horizon. We expressed our results in terms of RMSE (*Root Mean Square Error*) which is defined as follows:

$$RMSE = \sqrt{\frac{\sum_{i=1}^{N}(\hat{T}_{surf_i} - T_{surf_i})^2}{N}}$$

Figure 1 shows the comparison between the RMSE of the predictions given by the "Wing Météo" ('G4 predictions') and the RMSE of our Auto-Regressive models of order 9, for the station of Berloz.

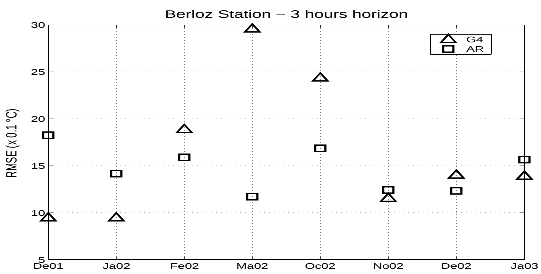

Figure 1: Comparison between G4 results and AR results for a 3 hours horizon

However, longer horizon prediction will only be possible if weather forecasting from the IRM (Institut Royal de Météorologie) can be included in the model. Figure 2 shows the comparison between G4 results and our Auto-Regressive models of order 5 for a 6 hours horizon, also for the station of Berloz.

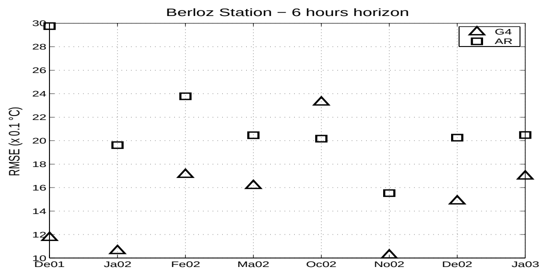

Figure 2: Comparison between G4 results and AR results for a 6 hours horizon

2 Nonlinear classifier

We also built a LS-SVM nonlinear classifier [2] that predicts directly the state of the road (icy or not). The first major difficulty is the lack of data examples when ice is present (it is quite a rare event compared to absence of ice). This could lead us to bad results in classification. Our solution was to reduce the number of events without ice by randomly selecting a subset of these events, in order to obtain similar numbers of the events of each of the two classes. The second difficulty is that data do not explicitly mention whether the absence of ice is natural or due to previous spreading of salt. We then built a model which would try to estimate the "initial" state of the road, that is the state which we would observe without spreading any salt on the roads. This model was based on the values of the surface temperature, the congelation temperature, and the humidity of the road.

References

[1] L. Ljung, System Identification: Theory for the User, Prentice-Hall, 1987.

[2] Suykens, J. A. K. and Vandewalle, J.: Least squares support vector machine classifiers. Neural Processing Letters, 9(3):293–300, 1999.

Short Term Load Modeling and Clustering

Marcelo Espinoza
Kasteelpark Arenberg 10, 3001 Leuven, Belgium
marcelo.espinoza@esat.kuleuven.ac.be

Bart De Moor
Kasteelpark Arenberg 10, 3001 Leuven, Belgium
bart.demoor@esat.kuleuven.ac.be

Abstract

The modeling and forecasting of the load is currently an important area of quantitative research [5, 1]. The short term modeling is usually applied on a daily basis on every major dispatch center and by grid managers [4], and there exist an important research literature where different methods are applied with excellent results [6, 2]. A second important topic is the characterization of the load in terms of its typical features, and the task is to extract this information from the model in order to identify if a post can be assigned to any of the categories of industrial, residential or business-commercial customers.

Within the context of an applied research project, we have developed a methodology based on traditional econometrics that can tackle the problem of individual load modeling using a vector auto-regression structure. By a simple extension, this model can be used to identify the typical daily shapes for each post after removing the seasonal and weather effects. The set of all daily shapes computed in this way can be used in a clustering exercise for a given set of more than 200 available posts.

Each hourly load series is modeled by using a Periodic Autoregressive (PAR) model [3] consisting of a set of 24 equations, one for each hour of the day. Each equation contains 48 lagged values of the load plus calendar variables and temperature-related variables. The hourly periodicity is captured by the coefficients of the system, leading to a diagonal structure that can be estimated using ordinary least squares (OLS). In our setting, exactly the same specification has been applied to all posts, obtaining different forecasting performances for different posts. An example is given in Figure 1.

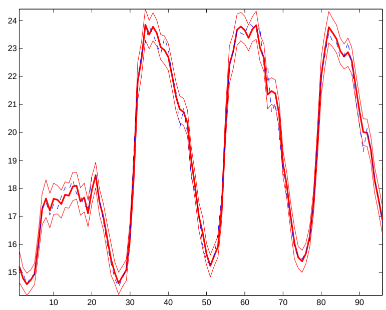

Figure 1: Out-of-sample hourly predictions (thick), confidence intervals (thin) and true values (dashed) for a selected post over a period of 96 hours.

By using $\boldsymbol{Y}_d$ as the collection of the 24 hourly values of the load for day d, the PAR model can be written in vector form as $\Phi_0 \boldsymbol{Y}_d = \boldsymbol{C} + \Phi_1 \boldsymbol{Y}_{d-1} + \Phi_2 \boldsymbol{Y}_{d-2} + \Phi_3 \boldsymbol{X}_d + \boldsymbol{\varepsilon}_d$. After removing the exogenous effects of weather and calendar information contained in the matrix $\boldsymbol{X}_d$ it is possible to compute a convergence vector $\boldsymbol{Y}^* = \{\Phi_0 - \Phi_1 - \Phi_2\}^{-1}\boldsymbol{C}$. In our setting, this 24-valued vector $\boldsymbol{Y}^*$ can be interpreted as the typical load daily shape for each post, cleaned out from the seasonal and weather influences. By using all the computed (and normalized) $\boldsymbol{Y}^*$ in a kernel-based clustering exercise [7], several shapes categories can be identified (Figure 2).

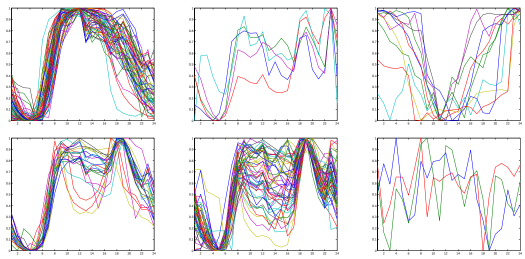

Figure 2: Identified Clusters based on Typical Shapes

References

[1] Bunn, D. "Forecasting Load and Prices in Competitive Power Markets,", Invited Paper, *Proceedings of the IEEE*, Vol 88, No.2, 2000.

[2] Fay, D., Ringwood, J., Condon, M. and Kelly, M. "24-h Electrical Load Data-A Sequential or Partitioned Time Series?," *Neurocomputing* 55, 469-498, 2003.

[3] Guthrie, G. and Videbeck, S. "High Frequency Electricity Spot Price Dynamics: An Intra-Day Markets Approach," New Zealand Institute for the Study of Competition and Regulation, 2002.

[4] Mariani, E. and Murthy, S.S. *Advanced Load Dispatch for Power Systems*. Advances in Industrial Control, Springer-Verlag, 1997.

[5] Ramanathan, R., Engle, R., Granger, C.W.J., Vahid-Aragui, F., Brace, C. "Short-run Forecasts of Electricity Load and Peaks," *International Journal of Forecasting* 13, 161-174, 1997.

[6] Steinherz, H., Pedreira and Castro, R. "Neural Networks for Short-Term Load Forecasting: A Review and Evaluation,"*IEEE Transactions on Power Systems*, Vol.16. No.1,2001.

[7] Girolami,M. "Mercer Kernel Based Clustering in Feature Space," *IEEE Transactions on Neural Networks*, 2001.

Friction compensation in a controlled one-link robot using a reduced-order observer

N. van de Wouw, N.J. Mallon, H. Nijmeijer
Eindhoven University of Technology, Department of Mechanical Engineering,
P.O. Box 513, 5600 MB Eindhoven, The Netherlands.
e-mail: N.v.d.Wouw@tue.nl, N.J.Mallon@tue.nl, H.Nijmeijer@tue.nl

1 Introduction

The positioning performance of many controlled mechanical systems, such as robots and optical disc drives, is limited by the presence of dry friction. One possible strategy to tackle this problem is model-based friction compensation [1]. In this paper, friction compensation in a controlled one-link robot using a reduced-order observer is studied. Since friction is generally velocity-dependent and controlled mechanical systems are often only equipped with position sensors, friction compensation requires velocity-estimation. Here, a reduced-order observer is used for this purpose. Both the case of exact friction compensation and non-exact friction compensation is investigated. In case of exact friction compensation, design criteria in terms of controller and observer parameter settings guaranteeing global exponential stability of the set-point are proposed. Moreover, in case of non-exact friction compensation it is shown that undercompensation leads to the existence of an equilibrium set and overcompensation leads to limit cycling. These results are obtained both numerically and experimentally.

2 Friction compensation strategy

In figure 1, the friction compensation strategy incorporating the reduced-order observer and a proportional-derivative controller is depicted schematically and is applied to a one-link robot (inertia J, position q and friction torque F_f).

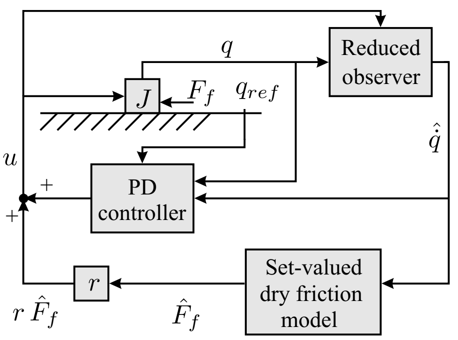

Figure 1: Friction compensation strategy.

3 Exact friction compensation

In the case of exact friction compensation ($r = 1$ in figure 1), conditions in terms of the controller and observer parameters are derived, which ensure global exponential stability of the set-point q_{ref}. These conditions can be used as design criteria for the friction compensation strategy as proposed in figure 1. When these conditions are not satisfied an equilibrium set exists, possibly inducing a non-zero steady-state error, and limit cycling may occur both destroying high positioning performance. The equilibrium set is a direct consequence of the set-valued modelling of the friction (modelling stiction) and the set-valued design of the friction compensation.

4 Non-exact friction compensation

The case of non-exact friction compensation is studied by introducing a scaled friction compensation rule (with scaling parameter r). It is shown that undercompensation ($r < 1$) leads to the existence of an equilibrium set (non-zero steady-state error) and overcompensation ($r > 1$) induces limit cycling. These results are obtained both numerically and experimentally, see figure 2. Moreover, the equilibrium set in case of undercompensation can be reduced in size by tuning the controller and observer parameters.

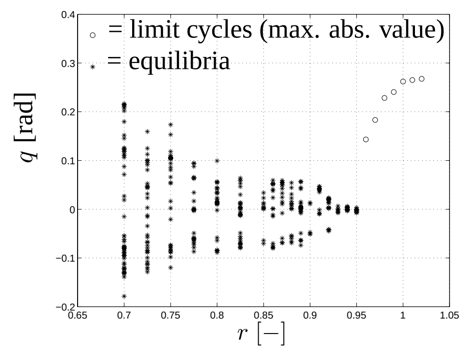

Figure 2: Experimental bifurcation diagram with bifurcation paremeter r.

5 Conclusions

A friction compensation strategy for a controlled one-link robot using a reduced-order observer is proposed. In case of exact friction compensation design rules for the controller and observer parameters ensuring global exponential stability of the set-point are provided. Furthermore, in the case of non-exact friction compensation it is advisable to undercompensate the dry friction in order to avoid limit cycling.

References

[1] Johnson, C.T., Lorenz, R.D., Experimental identification of friction and its compensation in precise, position controlled mechanisms, *Proc. of the Indus. App. Soc. Annual Meeting*, pp. 1400-1406, 1991.

Robust State Estimation Techniques : Application to an Autonomous Underwater Vehicle.

G. Goffaux, A. Vande Wouwer, M. Remy

Service d'Automatique, Faculté Polytechnique de Mons,
Boulevard Dolez, 31, 7000 Mons, Belgium
Fax: 32-65-37.41.36; (E-mail: {Guillaume.Goffaux, Alain.VandeWouwer, Marcel.Remy}@fpms.ac.be)

Abstract

Determining a vehicle position is a crucial task in many environments: maritime, road, railway, aviation, aerospace … Indeed, position is the basic information needed for vehicle guidance and security. Of course, the required accuracy can differ from a few millimetres to about ten metres depending on the aimed objectives.

To get information on the vehicle position, several sensors can be used, such as GPS receivers, INS or radar systems … However, these measurements are subject to errors, noises as well as to faults. For instance, transmission interruption can occur due to obstacles. The availability of several sensors results from a compromise between precision and cost.

To improve accuracy, state estimation techniques have been developed. They use a model of the vehicle behaviour in relation with sensors to get the best position estimates. However, such models are uncertain, as a result from linearization, time-varying parameters, non-modelled phenomena.

State estimation has therefore to be robust with respect to measurement errors and model uncertainties. To address these problems, robust state estimation techniques have been proposed in the literature [1].

In this study, robust state estimation methods are considered in the context of a maritime application. The objective is to estimate the position of an autonomous underwater vehicle (AUV) described in [2]. The assumption of a movement in a horizontal plane is made.

Several data sources are used to calculate the position (x,y) and the heading ψ.

- Acoustic Positioning Systems. They provide distance and angle measurements. Because the acoustic signals are sent from and received by the AUV, noise sources come from the environment. A loss of signal can occur if obstacles are in the acoustic trajectory.

- Inertial Navigation System. By using accelerometers, INS provides distance measurements. Since INS is set in the AUV, it is not subject to signal loss. The existence of bias limits its use to a short-time evaluation.

- Command sensors. They measure the force intensity applied to the AUV by thrusters.

The robust observer is based on a linearized model of the AUV and an uncertainty is taken into account in order to compensate the loss of information.

The performance of the robust observer is illustrated in simulation, for various situations, i.e. various level of measurement noise and model uncertainty.

Acknowledgement

This work is performed in the framework of the PIST project funded by the Walloon Region – DGTRE (Belgium).

References

[1] Mangoubi, R. S. (1998). *Robust Estimation and Failure Detection: A Concise Treatment,* Springer, London.

[2] Flakstad Ihle, I.A., (2003). *Observer design for synchronization of vessels with unreliable position measurements*, Master Thesis, Department of Engineering Cybernetics, NTNU, Trondheim (Norway).

Experimental design of a switching observer strategy to a piece-wise linear beam

A. Doris*, A. Juloski, N. van de Wouw*, H. Nijmeijer***

*Department of Mechanical Engineering
Technische Universiteit Eindhoven
P.O. Box 513, NL 5600 MB Eindhoven
The Netherlands
Email: a.doris@tue.nl

**Department of Electrical Engineering
Technische Universiteit Eindhoven
P.O. Box 513, MB 5600 MB Eindhoven
The Netherlands
Email: a.juloski@tue.nl

Abstract

This project is within the scope of the European SICONOS project on analysis and control of nonsmooth dynamical systems. It involves an experimental study of an observer design strategy for a class of piece-wise linear systems [1] by application to an elastic beam with a one-sided support.

The beam system consists of a steel beam, which is clamped on two sides and is supported at a discrete location by a one-sided linear spring. Due to the one-sided spring the beam has two different dynamics regimes.

Focus is on the implementation of a model-based switching observer on the experimental beam system and on the comparison of the observer predictions with experimental measurements. To achieve that, the observer incorporates a 3DOF model of the experimental system, which is based on a finite element model of the beam and is reduced using the Rubin reduction method [2]. The dynamics of the model is

$$M\ddot{q}+B\dot{q}+Kq+f_{nl}(q)=[-F(t)\ 0\ 0]^T$$

where $q=\left[q_{mid}\ q_{act}\ q_{\xi}\right]^T$, q_{mid} and q_{act} are defined in Figure 1 and q_{ξ} reflects the contribution of the first eigenmode of the beam. M, B and K are the mass, damping and stiffness matrices of the system, respectively. $F(t)$ and f_{nl} are a periodic excitation force applied on the beam and the restoring force of the one-sided spring, respectively.

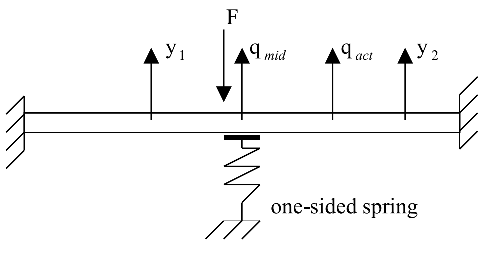

Figure 1: Elastic beam with one-sided support.

The location of the displacement measurement y_1 on the beam is chosen such that the reduced piece-wise linear model is observable in both dynamic regimes of the beam. According to the observer design strategy global asymptotic stability of the state estimation error can be achieved. Furthermore, the designed observer does not require information on the currently active dynamic regime of the piece-wise linear system.

Comparison of the experimental results with observer predictions (see Figure 2) confirms the stability of the implemented observer and indicates a satisfactory observer performance.

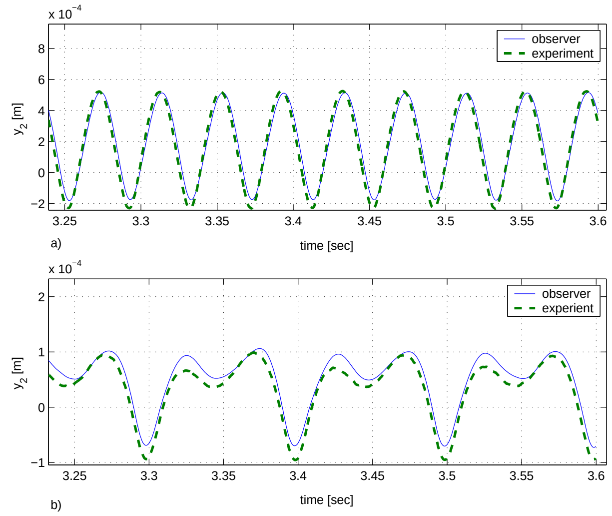

Figure 2: Comparison of the measured y_2 and the predicted displacement $\hat{y}_2$ of the beam (see figure 1) at different excitation frequencies.

Further research in the direction of performance improvement is ongoing.

References

[1] Observer Design for a Class of Piece-wise Affine Systems, A.L.Juloski, M. Heemels, S. Weiland in Proc. 2002 41st IEEE Conf. Decision and Control,Las Vegas, Nevada, USA.

[2] Controlled Stabilization of Long-Term Solutions in a Piece-wise Linear Beam System, PhD thesis, M. F. Heertjes, Eindhoven: Techniche Universiteit Eindhoven, 1999.

A controller-observer combination for a unicycle mobile robot.

Sander Noijen, Paul Lambrechts, Henk Nijmeijer
Department of Mechanical Engineering
Technische Universiteit Eindhoven
P.O. Box 513, 5600 MB Eindhoven, The Netherlands
Email: S.P.M.Noijen@student.tue.nl

We consider the problem of output feedback trajectory tracking with a unicycle mobile robot system. A state-feedback controller for the non-linear error dynamics of the robot is combined with an observer that estimates the orientation error based on available trajectory information and measurement of the position coordinates. The derivation and implementation of the resulting controller is given and tested on an experimental mobile robot.

Global exponential tracking results [3] of a unicycle mobile robot with coordinates, reference coordinates and error coordinates as in figure 1, are obtained by

$$\begin{array}{ll} \omega = \omega_r + c_1 \sin\Theta_e, & c_1 > 0 \\ v = v_r + c_2 x_e - c_3 \omega_r y_e, & c_2 > 0, \quad c_3 > -1 \end{array}$$

In [1] this output-feedback trajectory tracking controller was extended with an observer under the assumption that one of the tracking error coordinates is unknown.

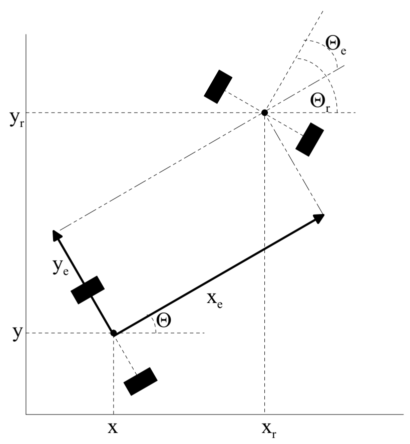

Figure 1: The unicycle coordinates **x**, reference coordinates $\mathbf{x_r}$ and error coordinates $\mathbf{x_e}$.

In this presentation we will consider the situation in which the absolute cartesian coordinates of the mobile robot are measured, but its orientation angle Θ is unknown. Jakubiak [1] solved this problem by estimating $\sin\Theta$. This result will be extended with an estimation of $\cos\Theta$

$$\begin{array}{rcl} \widehat{\phi} & = & \hat{f} - c_4 v_r y_e \\ \widehat{\psi} & = & \hat{g} - c_5 v_r x_e \\ \dot{\hat{f}} & = & (\omega_r - \omega)\hat{g} + (\omega - \omega_r) c_5 v_r x_e + c_4 \dot{v}_r y_e - \dots \\ & & c_4 v_r \omega x_e + c_4 v_r^2 \hat{f} - c_4^2 v_r^3 y_e \\ \dot{\hat{g}} & = & (\omega - \omega_r)\hat{f} + (\omega_r - \omega) c_4 v_r y_e + c_5 \dot{v}_r x_e + \dots \\ & & c_5 v_r \omega y_e - c_5 v_r v + c_5 v_r^2 \hat{g} - c_5^2 v_r^3 x_e \end{array}$$

with $\left[\widehat{\phi}, \widehat{\psi}\right]$ estimates for $[\sin\Theta, \cos\Theta]$, $[v(_r), \omega(_r)]$ the (reference) forward and angular velocity respectively and c_3, c_4, c_5 constants, such that implementation of an orientation error observer is possible [2]. The resulting exponentially stabilizing output-feedback trajectory tracking controller is implemented on an experimental mobile robot system. Figure 2 proves stability of the total system driving a Lissajoux figure.

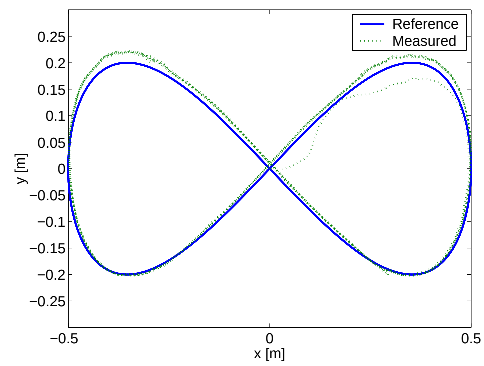

Figure 2: Stability of the total system.

References

[1] Jakubiak, J., Lefeber, E., Tchoń, K., and Nijmeijer, H., Two observer-based tracking algorithms for a unicycle mobile robot. *International Journal of Mathematical Computational Science*, 2002, **12**, No. 4:513-522.

[2] Noijen, S.P.M., Lambrechts, P.F., Nijmeijer, H., A controller-observer combination for a unicycle mobile robot. *Subm. IJC*

[3] Panteley, E., Lefeber, E., Loría, A., and Nijmeijer, H., Exponential tracking control of a mobile car using a cascaded approach. In *Proceedings IFAC Workshop on Motion Control*, 1998, Grenoble, pp. 221–226.

Adaptive control without prior by dynamic programming

Matthias C. M. Troffaes[1]
SYSTeMS Research Group, Universiteit Gent
Technologiepark Zwijnaarde 914, 9052 Zwijnaarde, Belgium
Matthias.Troffaes@UGent.be

1 Introduction

Adaptive control is often subject to serious bias in the learning phase, simply because insufficient information is available in order to motivate the choice of a unique prior, and hence, a unique optimal feedback. Imprecise probability theory may resolve this problem by means of using sets of priors. In doing so, we end up with a set of possibly optimal feedback controls—rather than a single one. This allows us to quantify the lack of information for finding an optimal feedback, and tells us exactly how many transitions must be observed before we can have a unique, robust optimal feedback. Such a result would be especially useful in applications where sampling costs are relatively high compared to the rewards incurred at each transition.

Adaptive control of Markov decision processes with uncertain transition probabilities has already been studied in great detail during the sixties [2]. In the classical approach to this control problem, the uncertainty of the transition probabilities is described by means of a product of Dirichlet priors, which are updated in time as transitions are observed. It is well-known that the optimal solution can be found through a dynamic programming algorithm.

Renewed interest in this problem has been initiated by recent developments in imprecise probability theory. It has been demonstrated how we can learn about the probabilities of a multinomial sampling model without having to give a unique prior, by means of a set of Dirichlet priors [3]. In optimal control, it turns out that the dynamic programming formalism still applies to dynamical systems whose gain is described by a set of probability distributions [1]. These results are our main inspiration for generalising adaptive control of Markov decision processes with uncertain transition probabilities to the framework of imprecise probabilities.

2 Example

Consider the Markov decision process depicted in Figure 1. At each time k we can choose between two actions, u and v. Transition probabilities are denoted as p^v_{yx} (the probability from state y to state x when taking action v), and the reward associated with this transition is denoted by r^v_{yx}. Transition probabilities are unknown, we only know the rewards, *e.g.*

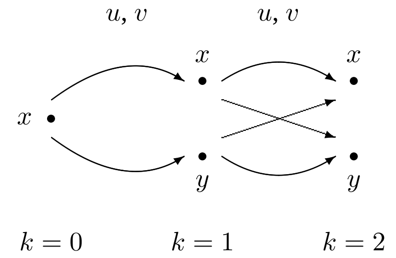

Figure 1: A simple Markov decision process

$$r^u_{xx} = r^u_{yx} = 1 \qquad r^v_{xx} = r^v_{yx} = 2$$
$$r^u_{xy} = r^u_{yy} = 1.5 \qquad r^v_{xy} = r^v_{yy} = 0.75$$

Intuitively, it is clear that insufficient information is available in order to construct a unique optimal feedback. Suppose we are in state x at time $k = 0$, take action v and end up in state x at time $k = 1$. Then it seems reasonable to assume that when we select action v again, the probability that we end up in x again is higher than the probability of ending up in y. In fact, the reward associated with this transition, r^v_{xx}, is the highest possible reward. Even if we do not know precisely the value of p^v_{xx}, after observing the transition from state x at time k to state x at $k + 1$ under action v, we obtain, through the imprecise Dirichlet model (hyperparameter $s = 1$), a sufficiently narrow probability interval for p^v_{xx} in order to ensure that we will end up with the highest possible reward by taking action v from state x at time $k = 1$. Secondly, we have found that this model satisfies the principle of optimality. So, globally optimal feedback controls can be obtained through an efficient dynamic programming algorithm.

[1] This paper presents research results of project G.0139.01 of the Fund for Scientific Research, Flanders (Belgium), and of the Belgian Programme on Interuniversity Poles of Attraction initiated by the Belgian state, Prime Minister's Office for Science, Technology and Culture. The scientific responsibility rests with the author.

References

[1] Gert de Cooman and Matthias C. M. Troffaes. Dynamic programming for discrete-time systems with uncertain gain. In Jean-Marc Bernard et al., editors, *ISIPTA '03 – Proceedings of the Third International Symposium on Imprecise Probabilities and Their Applications*, pages 162–176. Carleton Scientific, July 2003.

[2] J. J. Martin. *Bayesian Decision Theory and Markov Chains*. John Wiley & Sons, New York, 1967.

[3] Peter Walley. Inferences from multinomial data: Learning about a bag of marbles. *Journal of the Royal Statistical Society*, 58(1):3–34, 1996.

Robust Helicopter UAV Control

Gerwin Voorsluijs
Faculty of Aerospace
Delft University of Technology
Kluyverweg 1 2629 HS Delft
The Netherlands
Email: G.M.Voorsluijs@LR.TUDelft.NL

Samir Bennani
Faculty of Aerospace
Delft University of Technology
Kluyverweg 1 2629 HS Delft
The Netherlands
Email: S.Bennani@LR.TUDelft.NL

1 Introduction

The remote operation of an unaugmented mini helicopter requires a skilled and experienced pilot. Its instability and high level op coupling between lateral and longitudinal motion make its operation a high-workload task. Therefore as first part of a joint project of the Delft University of Technology, FlyCam and NLR to build an autonomous helicopter UAV system [4], certain tasks of the operator are taken over by an automatic control and stability augmentation system. This so-called *user-friendly control system* should cancel out the instability and cross-coupling effects and provide control of the vehicle by simple speed commands.

2 Modelling

Starting from a mathematical representation of the mini helicopter developed using theoretical and empirical estimation methods [2], a modular and generic helicopter model was made that links the modules together through data-flows [5]. Since the dynamics of the helicopter change considerably over the flight regime, this behaviour was included in the linear model that is used for analysis and controller design. Numerical linearizations of the longitudinal dynamics of the nonlinear model of the FlyCam helicopter were made for varying forward speed and this set of linear models was used to construct an LFT representation of the system by element-wise interpolation of the stability and control derivatives matrices. On top of this, a mass-variation of 25% is added in the form of another LFT.

3 Synthesis

The LFT model of the longitudinal dynamics of the mini helicopter augmented with an ideal model and performance weights serves as system for which four controllers are designed differing in controller synthesis method. The first technique that is used is H_∞-synthesis [1]. Because it does not take the diagonal structure of the uncertainties into account it leads to a conservative controller which is expected to have good robust stability but poor robust performance. The second technique that is employed is μ-synthesis [1]. In this synthesis, both mass and velocity variations are included as diagonal matrices with scalar complex uncertainty blocks. The resulting μ-controller is expected to have good robust stability and reasonable robust performance.
Finally, two versions of full-block LPV controller synthesis [3] are performed on the LFT model using the velocity variation to schedule the controllers. The socalled LPV-H_∞-controller, like the H_∞-synthesis, doesnot take any uncertainty structure into account whereas the LPV-μ-controller uses scalings for the mass-uncertainty similar to those used in the μ-synthesis to reduce conservatism.

4 Results and conclusion

The resulting four controllers are compared in frequency and time domain with eachother and with locally optimzed H_∞- and μ-controllers. The H_∞-controller gives good robust stability but poor robust performance. The μ controller gives similar robust stability and a reasonable robust performance but time-domain results show a relative high cross-coupling between u and w. The LPV controllers show good robust stability and performance and a significant decrease in cross-coupling and their time-responses are almost as good as the local optimized controllers. As expected, the LPV-μ-controller delivers the best results in both frequency and time domain.

References

[1] G.J. Balas, J.C. Doyle, K. Glover, A. Packard, and R. Smith. *μ-Analysis and synthesis toolbox for use with Matlab*. The MathWorks, Inc., 1998.

[2] C.F. Muller and E.G. IJsselmuiden. Fly Motion Cam Project part I. Master's thesis, Delft University of Technology, Aerospace Department, 2001.

[3] C.W. Scherer, R.G.E. Njio, and S. Bennani. Parametrically varying flight control system design with full block scalings. In *Proceedings of the 36th IEEE Conference on Decision and Control*, 1997.

[4] M. Selier, G. M. Voorsluijs, A. J. de Jong, J.K. Langendoen, C. F. Muller, and E. G. IJsselmuiden. Future surveillance using autonomous unmanned helicopters. In *Proc. of the AIAA/ICAS International Air and Space Symposium and Exposition: The Next 100 Years*, Ohio, 2003.

[5] G.M. Voorsluijs. A modular generic helicopter model. Master's thesis, Delft University of Technology, Aerospace Department, 2002.

Feedback mechanisms for global oscillations

STAN Guy-Bart, SEPULCHRE Rodolphe
Systèmes et Automatique,
Université de Liège
Institut Montefiore B28,
Sart Tilman, B-4000 LIEGE 1, BELGIUM
Email : gb.stan@ulg.ac.be, r.sepulchre@ulg.ac.be

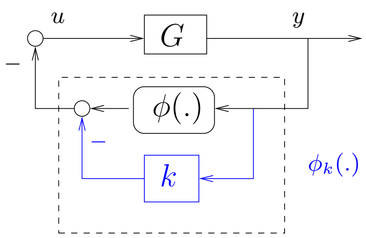

Figure 1: Block diagram for the class of Hopf bifurcation oscillators.

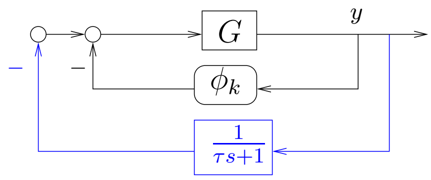

Figure 2: Block diagram for the class of relaxation oscillators.

Abstract

This paper describe two basic mechanisms responsible for the creation of limit cycle oscillations in particular classes of high-dimensional nonlinear systems.

Main results

We consider the feedback system shown in Figure 1 where the SISO system G is described by a linear controllable and detectable state space model

$$(G)\left\{\begin{array}{rcl}\dot{x} & = & Ax+bu\\ y & = & cx\end{array}\right. \tag{1}$$

whereas ϕ_k is the static nonlinearity

$$\phi_k(y) = -ky + \phi(y) \tag{2}$$

and $\phi(\cdot)$ is a smooth sector nonlinearity in the sector $(0,\infty)$, which satisfies $\phi'(0) = \phi''(0) = 0$, $\phi'''(0) > 0$ and $\lim_{|s|\to\infty}\frac{\phi(s)}{s} = \infty$ ("stiffening" nonlinearity). We note G_k the (positive) feedback interconnection of G with the feedback gain k. The feedback system is equally described as the feedback interconnection of G_k and the (strictly passive) nonlinearity $\phi(\cdot)$.

If G is a passive system, the feedback system is absolutely stable for $k = 0$ and the equilibrium $x = 0$ is globally asymptotically stable (GAS). As k increases, a root locus argument shows that the feedback system must loose stability at some critical value k^*. (As the transfer function of a passive system, $G(s)$ has a relative degree equal to one and one branch (at least) of the root locus must enter the right half plane). The following result characterizes the possible bifurcations under a passivity assumption for G_{k^*}.

Theorem 1 *Consider the system shown in Figure 1 and characterized by (1),(2). If G is passive, then a bifurcation occurs for some $k^* \geq 0$ as k increases.*

If $G_{k^*}(s)$ has a unique pole on the imaginary axis and if G_{k^*} is passive, the bifurcation is a supercritical pitchfork bifurcation; for $k \gtrsim k^*$, the system is globally bistable, that is, the equilibrium $x = 0$ is a saddle and its stable manifold separates the state space in two open sets, each of which is the basin of attraction of a stable equilibrium.

If $G_{k^*}(s)$ has a unique pair of conjugated poles on the imaginary axis and if G_{k^*} is passive, the bifurcation is a supercritical Hopf bifurcation; for $k \gtrsim k^*$, the system has a limit cycle which is GAS in $\mathbb{R}^n\backslash\{0\}$.

Theorem 1 is the basis for two different oscillation feedback mechanisms including, as particular low-dimensional cases, the Van der Pol (based on the second part of Theorem 1) and the FitzHugh-Nagumo oscillators (based on the first part of Theorem 1 and on Theorem 2).

Theorem 2 *Under the assumptions of Theorem 1, let $k \gtrsim k^*$ such that the feedback loop of G and ϕ_k is globally bistable. Then there exists a constant $\tau > 0$ such that $\forall\tau \geq \bar{\tau}$, the feedback system shown in Figure 2 has a globally asymptotically stable limit cycle.*

Theorem 1 and Theorem 2 extend the feedback mechanism for oscillations of these two well-known oscillators (Van der Pol and FitzHugh-Nagumo) to higher-dimensional systems.

Exponential Stability Analysis for Uncertain Linear Systems

Sjoerd G. Dietz
Delft Center for Systems and Control Mekelweg 2
2628 CD Delft The Netherlands
s.dietz@dcsc.tudelft.nl

Carsten W. Scherer
Delft Center for Systems and Control Mekelweg 2
2628 CD Delft The Netherlands
c.w.scherer@dcsc.tudelft.nl

1 Abstract

In this presentation, we look at the problem of stability analysis of an uncertain linear system of the form

$$x_{k+1} = A(\Delta_k)\, x_k\,, \quad \Delta_k \in \mathbf{\Delta}, \quad k = 1, 2, \ldots \qquad (1)$$

with

$$\mathbf{\Delta} = \mathrm{co}\{\hat{\Delta}^1, \hat{\Delta}^2, \ldots, \hat{\Delta}^N\}$$

the uncertainty set formed by the N generators $\hat{\Delta}^1, \hat{\Delta}^2, \ldots, \hat{\Delta}^N$. It is well known that the existence of a Lyapunov function for system (1) proves exponentially stability. Conversely, given that the system is exponentially stable a Lyapunov Function is guaranteed to exists. One can prove that in this case one can also find a polyhedral norm Lyapunov function, see refs. [4, 3, 1, 2]. Unfortunately, there are no a priori bounds on the required dimension of this function class. At present, the practical importance of this approach is therefore limited.

An alternative approach to prove exponential stability of the discrete time system (1) is to analyze the set of products of matrices

$$\mathcal{P}_k = \{P \,|\, P = A(\Delta_{k-1})A(\Delta_{k-2})\ldots A(\Delta_0)$$
$$\Delta_i \in \mathrm{co}\{\hat{\Delta}^1, \hat{\Delta}^2, \ldots, \hat{\Delta}^N\} \quad \text{for} \quad i = 0, \ldots, k-1\}$$

If for some $k = k_0$,

$$\|P\| \leq \epsilon \quad \text{for all} \quad P \in \mathcal{P}_{k_0}$$

we have proven exponential stability. Note that $\|P\|$ can be any norm on P.

Again, this 'direct approach' (performed for some k_0) is only a sufficient condition for exponential stability. It has a number of advantages, though. First, it is a convex test so that a number of relaxation schemes (Full-Block S-procedure, Polya-relaxation, sum of squares techniques) can be applied and numerically verified in the LMI framework. Second, it allows to incorporate constraints on the rate of variation in a very natural way, i.e. via norm bound constraints of the form $\|\Delta_k - \Delta_{k-1}\| < \gamma$ for all $k \in \mathbb{N}$, with $\gamma \in \mathbb{R}$.

In this presentation, we present the direct approach to analyze stability of system (1). We show how constraints on the rate of variation can be taken into account. Different relaxation schemes are applied. Finally, we discuss exactness of the relaxation in case the test for exponential stability fails for some chosen k_0. The main goal is then to try to prove instability of the system and construct a destabilizing time-varying perturbation.

References

[1] F. Blanchini. Nonquadratic Lyapunov Functions for Robust Control. *Automatica*, 31(3):451–461, 1995.

[2] F. Blanchini and S. Miani. A New Class of Universal Lyapunov Functions for the Control of Uncertain Linear Systems. *IEEE Transactions on Automatic Control*, 44(3):641–647, 1999.

[3] J. Kiendl, H. Adamy and P. Stelzner. Vector Norms as Lyapunov Functions for Linear Systems. *IEEE Transactions on Automatic Control*, 37(6):839–842, 1992.

[4] A.P. Molchanov and E.S. Pyatnitskii. Lyapunov Functions That Specify Necessary And Sufficient Conditions Of Absolute Stability Of Nonlinear Nonstationary Control Systems I,II,III. *Automation and Remote Control*, 47(3,4,5):344–354,443–451,620–630, 1986.

The output regulation problem: a quadratic stability approach

Alexei Pavlov, Nathan van de Wouw, Henk Hijmeijer
Eindhoven University of Technology, Department of Mechanical Engineering,
P.O. Box 513, 5600 MB Eindhoven, The Netherlands.
e-mail: A.Pavlov@tue.nl, N.v.d.Wouw@tue.nl, H.Nijmeijer@tue.nl

1 Introduction

In this presentation, we consider the problem of asymptotic regulation of the output of a dynamic system, which is subject to disturbances generated by an external system. This problem is known as the *output regulation problem.* In the context of this problem, we consider systems of the form

$$\begin{aligned} \dot{x} &= f(x, \quad, w) \\ e &= h(x, w), \end{aligned} \tag{1}$$

with state $x \in \mathbb{R}^n$, input $\quad \in \mathbb{R}^m$, regulated output $e \in \mathbb{R}^p$ and exogenous disturbance input $w \in \mathbb{R}^r$ generated by the exosystem

$$\dot{w} = s(w). \tag{2}$$

The output-feedback output regulation problem can be formulated as follows: *find a controller of the form*

$$\begin{aligned} \dot{\xi} &= \eta(\xi, e) \\ &= \theta(\xi) \end{aligned} \tag{3}$$

such that **($\star$)** *all solutions of system (1), (2) in closed-loop with (3) are bounded and* $e(t) \to 0$ *as* $t \to \infty$. Many control problems can be put in the framework of the output regulation problem, e.g. disturbance rejection, tracking, controlled synchronization.

For a *linear* system, if the output regulation problem is solvable, then the solution is global, i.e. the control goal **($\star$)** is attained globally. Most of the existing solutions to the output regulation problem for different classes of *nonlinear* systems are either local or semiglobal [1]. This motivates our research to find a class of nonlinear systems for which the output regulation problem can be solved globally in a way similar to the linear case. In this presentation, we propose a method for solving the *global* output regulation problem based on the quadratic incremental stability property [2], which is intrinsic to asymptotically stable linear systems.

2 Assumptions and preliminaries

We assume that
(A) every solution of (2) is defined and bounded for $t \geq 0$;
(B) there exist locally Lipschitz functions $\pi(\cdot) : \mathbb{R}^r \to \mathbb{R}^n$ and $c(\cdot) : \mathbb{R}^r \to \mathbb{R}^m$ such that

$$\begin{aligned} \tfrac{d}{dt} \quad \pi(w(t)) &= f(\pi(w(t)), c(w(t)), w(t)), \\ h(\pi(w(t)), w(t)) &\to 0, \text{ as } t \to +\infty, \end{aligned} \tag{4}$$

for all solutions $w(t)$ of the exosystem (2).

A matrix function $\mathcal{A}(z) \in \mathbb{R}^{n \times n}$ is called quadratically stable over a set $\mathcal{Z}$ if for some $\mathcal{P} = \mathcal{P}^T \quad 0$ and $\mathcal{Q} = \mathcal{Q}^T \quad 0$

$$\mathcal{P}\mathcal{A}(z) + \mathcal{A}(z)^T \mathcal{P} \leq -\mathcal{Q} \quad \forall z \in \mathcal{Z}. \tag{5}$$

A pair of matrix functions $\mathcal{A}(z)$ and $\mathcal{B}(z)$ is said to be quadratically stabilizable over $\mathcal{Z}$ if there exist a matrix K such that $\mathcal{A}(z) + \mathcal{B}(z)K$ is quadratically stable over $\mathcal{Z}$. A pair of matrix functions $\mathcal{A}(z)$ and $\mathcal{C}(z)$ is said to be quadratically detectable over $\mathcal{Z}$ if there exist a matrix L such that $\mathcal{A}(z) + L\mathcal{C}(z)$ is quadratically stable over $\mathcal{Z}$.

3 Main result

Theorem. *Under assumptions* **(A)** *and* **(B)**, *if the pair of matrix functions* $\left[\frac{\partial f}{\partial x}\right], \left[\frac{\partial f}{\partial u}\right]$ *is quadratically stabilizable and the pair*

$$\begin{bmatrix} \frac{\partial f}{\partial x} & \frac{\partial f}{\partial w} \\ 0 & \frac{\partial s}{\partial w} \end{bmatrix}, \quad \begin{bmatrix} \frac{\partial h}{\partial x} & \frac{\partial h}{\partial w} \end{bmatrix}$$

is quadratically detectable over $(x, \quad, w) \in \mathbb{R}^{n+m+r}$ *and* $\frac{\partial f}{\partial u}$ *is uniformly bounded, then the global output regulation problem is solvable by a controller of the form*

$$\begin{aligned} &= c(\hat{w}) + K(\hat{x} - \pi(\hat{w}))) \\ \dot{\hat{x}} &= f(\hat{x}, \quad, \hat{w}) + L_1(h(\hat{x}, \hat{w}) - e) \\ \dot{\hat{w}} &= s(\hat{w}) + L_2(h(\hat{x}, \hat{w}) - e) \end{aligned}$$

where the matrices K *and* $L = [L_1^T, L_2^T]^T$ *are chosen such that the matrix functions* $(\frac{\partial f}{\partial x} + \frac{\partial f}{\partial u}K)$ *and*

$$\begin{bmatrix} \frac{\partial f}{\partial x} & \frac{\partial f}{\partial w} \\ 0 & \frac{\partial s}{\partial w} \end{bmatrix} + L \begin{bmatrix} \frac{\partial h}{\partial x} & \frac{\partial h}{\partial w} \end{bmatrix}$$

are quadratically stable over $(x, \quad, w) \in \mathbb{R}^{n+m+r}$.

4 Conclusions

We have presented a global solution to the output regulation problem for a class of nonlinear systems.

References

[1] C.I. Byrnes, F. Delli Priscoli, A. Isidori. *Output regulation of uncertain nonlinear systems.* Birkhauser, 1997.

[2] B.P. Demidovich. *Lectures on stability theory*. Nauka: Moscow, 1967 (in Russian).

Acknowledgments: this research is supported by the Netherlands Organization for Scientific Research (NWO).

A trajectory-space approach to hybrid systems

Pieter Collins
Centrum voor Wiskunde en Informatica
P.O. Box 94079
1090 GB Amsterdam
The Netherlands
Email: Pieter.Collins@cwi.nl

Abstract

Hybrid systems are usually studied by considering the equations governing the time evolution of the system. We instead give a behavioural approach based on considering the space of all possible trajectories of this system. This approach is similar to the study of discrete event systems by considering the language generated by all possible event sequences. The main advantage is that it facilitates the study of non-deterministic systems and systems for which the evolution does not depend continuously on the initial conditions. We illustrate the method by studying example systems such as a switched arrival system [6] and a heating system.

We consider a trajectory of a hybrid system as a function defined on a collection of disjoint intervals, equivalent to that used in [4]. This yields a framework under which discrete events may cause jumps in the continuous state, and for which more than one event may occur at a given time. The natural topology on this hybrid trajectory space is the *compact-open Skorohod topology* [2], under which trajectories are close if they are uniformly close on finite time intervals after allowing for a small reparameterisation of time. There are two natural types of evolution operators on the hybrid trajectory space, the *return* operators, which are continuous on their domains of definition, and the *time evolution* operators, which need not be.

A hybrid system can be specified abstractly by giving the set of allowed trajectories in the full hybrid trajectory space. The most interesting class of hybrid system is that for which the trajectory space is compact in the compact-open Skorohod topology. We show that such a system is either non-Zeno, or has a trajectory which undergoes infinitely many events at a single time. We also show that the asymptotic behaviour of such systems can be described symbolically by a compact subshift, and probabilistically by an invariant measure [5], either for the time-evolution operator or the return operator.

A sufficient condition for a hybrid system to have compact trajectory space is that the continuous-time evolution is described by a differential inclusion [1] and the discrete-time behaviour by a set-valued map, both of which are upper-semicontinuous. Upper-semicontinuity requires that whenever a tangential or *grazing* incidence of a system trajectory with the guard set of a discrete event occurs, the system evolves non-deterministically, and the discrete event may or may not occur. Upper-semicontinuity may typically be imposed on a system model without significantly changing the behaviour, though some care is sometimes needed in the formulation of the model to avoid chattering [3].

Although we do not consider stochastic systems, there are potentially strong links between the theory developed here, the existence of invariant measures in particular, and stochastic systems, especially when considering zero-noise limits, providing extra motivation and directions for further research.

References

[1] Jean-Pierre Aubin and Arrigo Cellina. *Differential inclusions: Set-valued maps and viability theory*. Number 364 in Grundlehren der Mathematischen Wissenschaften. Springer-Verlag, Berlin, 1984.

[2] Mireille Broucke. Regularity of solutions and homotopic equilibria for hybrid systems. In *Proceedings of the 37th IEEE Conference on Decision and Control*, New York, 1998. IEEE Press.

[3] Alekseĭ F. Filippov. *Differential Equations with Discontinuous Righthand Sides*. Mathematics and Its Applications. Kluwer Academic Publishers, Dordrecht, 1988.

[4] John Lygeros, Karl Henrik Johansson, Shankar Sastry, and M. Egerstedt. On the existence of executions of hybrid automata. In *Proceedings of the 38th IEEE Conference on Decision and Control*, New York, 1999. IEEE Press.

[5] Mark Pollicott and Michiko Yuri. *Dynamical systems and ergodic theory*. Number 40 in London Mathematical Society Student Texts. Cambridge University Press, Cambridge, 1998.

[6] P.J. Ramadge. On the periodicity of symbolic observations of piecewise smooth discrete-time systems. *IEEE Trans. Automatic Control*, 35:807–813, 1990.

Modelling manufacturing systems: a max-plus approach

Joost van Eekelen
Department of Mechanical Engineering, Systems Engineering Group
Eindhoven University of Technology
j.a.w.m.v.eekelen@tue.nl

1 Background

Manufacturing systems are often discrete event systems: the state of these systems changes due to the occurrence of an event instead of a change in time. Typical events are: release of a lot into the system, lots entering or leaving a process and lots leaving the system.
Industrial complexity increases with product complexity and vice versa. A typical example is semiconductor industry, where the multitude of production steps and their reoccurring nature make it very difficult for low level control to meet all production requirements/orders and other targets. The need for more intelligent, higher level control becomes stronger.

2 Max-plus linear systems

Before a manufacturing system can be controlled, a model has to be made. The model describes the behavior of the system and can be used to test and tune a (future) controller. One way of modelling discrete event manufacturing systems is using max-plus algebra. A proper description of the operators used in max-plus algebra and some analysis methods are given in [1].
The basic operations are max-addition and max-multiplication:

$$\begin{aligned} x \oplus y &= \max(x, y) \\ x \otimes y &= x + y \end{aligned} \qquad (1)$$

for $x, y \in \mathbb{R} \cup \{-\infty\}$. The 'zero' element in max-plus algebra is $\varepsilon = -\infty$. A remarkable analogy exists between conventional algebra and max-plus algebra.
A large class of deterministic discrete event manufacturing systems can be described in an exact way with max-plus linear systems of the form: (x, u and y can be vectors)

$$\begin{aligned} x(k+1) &= A \otimes x(k) \oplus B \otimes u(k) \\ y(k) &= C \otimes x(k) \oplus D \otimes u(k). \end{aligned} \qquad (2)$$

3 Modelling: building blocks and interconnection

The basic elements of a manufacturing system (buffers, machines) are denoted as the building blocks of the modelling process. Different building blocks are buffers with finite or infinite capacity, batch machines and single lot machines. All building blocks of processes P are schematically represented as in Figure 1. An interesting observation is that material flow goes downstream whereas process availability information goes upstream.

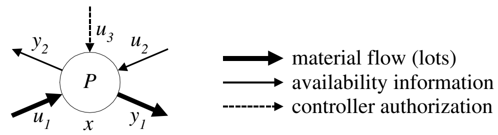

Figure 1: Elementary building block of manufacturing process.

With proper definitions for $u_i(k)$, $y_i(k)$ and $x(k)$, each process can be written in the form of (2). Building blocks can be combined by connecting inputs and outputs. For example, a simple manufacturing system (Figure 2) consisting of an infinite buffer B_{inf}, two parallel machines M that are not necessarily identical, a 3-place buffer B_3 and a batch machine with fixed batch size 2, F_2, can be modelled as in (2) with a state vector $x(k)$ containing 7 elements (minimal order). This is a relatively compact exact model of a manufacturing structure that might be difficult to analyze by hand.
The resulting max-linear state space model can be analyzed to derive properties of the system (e.g. throughput, bottleneck) and to develop a controller. Control techniques exist for this type of systems, model predictive control for example (see [2]).

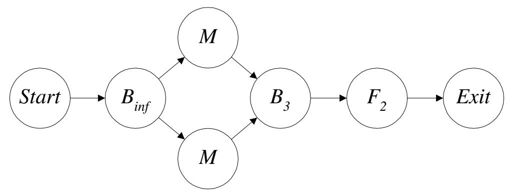

Figure 2: Simple manufacturing system (material flow only): state vector contains 7 elements.

References

[1] B. de Schutter, "Max-Algebraic System Theory for Discrete Event Systems". PhD thesis, Faculty of Applied Sciences, K.U.Leuven, 1996.

[2] B. De Schutter and T. van den Boom, "Model predictive control for max-plus-linear discrete event systems". Automatica, vol. 37, no. 7, pp. 1049-1056, 2001.

A Timed Discrete Event Model for Urban Traffic Control

Ciro Carbone
Università degli Studi di Salerno
84084, Fisciano (Sa), Italy
ccarbone@unisa.it

René Boel
SYSTeMS, Universiteit Gent,
B-9052 Zwijnaarde, Belgium
rene.boel@ugent.be

1 Abstract

In this abstract[1] a new approach to control urban traffic is presented. The main aim is to maximize the throughput of the system by means of real-time actions such as the timing coordination of traffic lights in a urban area. The optimization problem for urban traffic control can be formulated as follows: minimize $\sum_i (t_{departure} - t_{arrive})_i$, where the sum is extended to all the vehicles in the system over the whole optimization horizon.

An urban area, composed of elementary components such as intersections, freeways with on-ramps and off-ramps and traffic light network, can be thought as a very complex *Discrete Event System* (DES). The basic idea is to use a detailed model of urban areas based on *timed Petri nets* (PNs), one of the formalism proposed in literature for DES modelling [1]. PNs have been proved to be a valuable tool for the analysis, state estimation and control of DES. In this abstract a modular approach is proposed, in which urban areas to be controlled are modelled as interconnected timed PN modules. In such a way a microscopic representation of urban traffic as in [2] can be used for some parts of the network while coarser, more aggregated models can be used for other parts.

Figure 1 shows a general scheme for urban traffic control. Each *urban area* to be controlled (e.g. two signalized intersections connected each other with a road link) together with sensor signals, is viewed as a *plant*, according to the classical closed loop scheme in the control theory. Sensor signals about vehicle arrivals and departures plus intermediate information on the controlled urban area are considered as input events for the *observer* subsystem [3]. The observer contains a detailed timed PN model of the controlled urban area. Such a model is modular and with changeable parameters according to the plant state (i.e. the time associated to timed transitions could change according to the traffic conditions). In other words, the model can adapt to the traffic conditions. The modularity is realized by considering as a module each elementary component of a urban area (i.e. a module for the signalized intersection, a module for a road link, etc.) and by interconnecting them with *fusion places*. Each fusion place of a PN is a set of places that are considered to be identical, i.e. they all represent a single conceptual place even though they are drawn as individual places. The control is distributed, that is each *local controller* optimizes a single urban area. A local controller works in real-time: it can read the observer estimated plant state and makes predictions about the future states (e.g. by using *what-if* techniques) if a detailed and reliable model of the plant is provided. It is important to notice that each controller action is sent to the plant as well as to the observer, in order to update the estimated state according to the real plant one. In order to avoid that the optimization of an area is realized at other area's expense an higher level *optimizer* is needed. The optimizer can gain access to the state of each observer; moreover it knows how modules are aggregated each other. Consequently, it can coordinate the local controllers, in real time, in order to improve the overall performance.

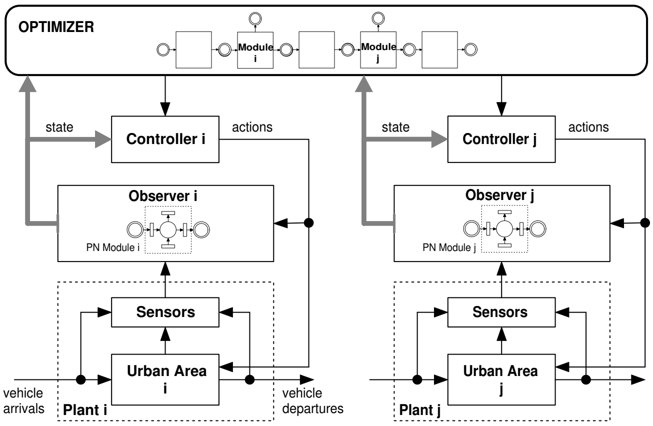

Figure 1: A general scheme for urban traffic control.

[1]This work has been supported by the EC Marie Curie Multi-partner Control Training Site (CTS) contract number HPMT-CT-2001-00278.

References

[1] Tadao Murata, "Petri Nets: Properties, Analysis and Applications", *Proceedings of IEEE*, Vol. 77, No. 4, pp. 541–580, April 1989.

[2] A. Di Febbraro, D. Giglio and N. Sacco, "On applying Petri nets to determine optimal effects for coordinated traffic light timings", *Proc. IEEE Int. Conf. on Intelligent Transportation Systems*, Singapore, September 2002.

[3] Th. Riedel and U. Brunner, "Traffic Control using Graph Theory", *Control Eng. Practice*, Vol. 2, No. 3, pp. 397–404, 1994.

Kernel methods for subspace identification of multivariable LPV and bilinear systems

Vincent Verdult
Delft Center for Systems and Control
Delft University of Technology
Mekelweg 2, 2628 CD Delft
The Netherlands
Email: v.verdult@dcsc.tudelft.nl

Michel Verhaegen
Delft Center for Systems and Control
Delft University of Technology
Mekelweg 2, 2628 CD Delft
The Netherlands
Email: m.verhaegen@dcsc.tudelft.nl

1 Abstract

Subspace identification methods are widely used for the identification of linear time-invariant systems. Unlike the classical identification methods, subspace methods do not require a particular parameterization; this makes them numerically attractive and especially suitable for multivariable systems. In recent years subspace identification methods have also been developed for linear parameter-varying (LPV) and bilinear systems. LPV systems are widely used in control, especially in gain-scheduling and robust control techniques. Bilinear systems form an important class of nonlinear systems for which a considerable body of theoretical results has been obtained over the years [4].

The first subspace methods that were developed for the identification of bilinear systems were based on the assumption that the input to the system is a white-noise sequence [3, 5]. Although white-noise inputs provide a good excitation of the dynamical system, in several applications the input cannot be taken equal to a white-noise sequence; it might be that only sum-of-sine inputs or step signals with a minimum duration are allowable or possible. Therefore, bilinear subspace identification methods that can deal with more general input signals are of interest. Favoreel [2] and Chen and Maciejowski [1] described such bilinear subspace identification methods. We recently described how these subspace methods can be extended to identify LPV systems with affine parameter dependence [5, 6].

A major drawback of the LPV and bilinear subspace identification methods is the enormous dimension of the data matrices involved. The number of columns in the data matrices equals the number of samples, and the number of rows grows exponentially with the order of the system. In addition, the methods require the number of columns to be larger than or equal to the number of rows, thus the number of samples needed can be enormous. Even for relatively low-order systems with only a few inputs and outputs, the amount of memory required to store the data matrices exceeds the limits of what is currently available on the average desktop computer. This limits the applicability of the methods to high-order systems with several inputs and outputs.

We have developed a novel approach to deal with the dimensionality problem in LPV and bilinear subspace identification. We propose a kernel method that only relies on computations with the kernel matrix, which is a square matrix with dimensions equal to the number of samples. The major advantage of such a method is that the computational complexity no longer depends on the exponentially growing number of rows in the data matrices, but on the (usually much smaller) number of samples available. It is well known that estimation of a large number of parameters using a small number of samples can lead to a large variance error in the estimated parameters. In such a case it is reasonable to allow for a small bias to reduce the variance error. To balance the bias and variance errors, we integrate regularization methods in the kernel methods for subspace identification.

References

[1] Huixin Chen and Jan Maciejowski. An improved subspace identification method for bilinear systems. In *Proceedings of the 39th IEEE Conference on Decision and Control*, Sydney, Australia, December 2000.

[2] Wouter Favoreel. *Subspace Methods for Identification and Control of Linear and Bilinear Systems*. PhD thesis, Faculty of Engineering, K. U. Leuven, Leuven, Belgium, November 1999.

[3] Wouter Favoreel, Bart De Moor, and Peter Van Overschee. Subspace identification of bilinear systems subject to white inputs. *IEEE Transactions on Automatic Control*, 44(6):1157–1165, June 1999.

[4] Ronald R. Mohler and W. J. Kolodziej. An overview of bilinear system theory and applications. *IEEE Transactions on Systems, Man and Cybernetics*, 10(10):683–688, October 1980.

[5] Vincent Verdult. *Nonlinear System Identification: A State-Space Approach*. PhD thesis, University of Twente, Faculty of Applied Physics, Enschede, The Netherlands, 2002.

[6] Vincent Verdult and Michel Verhaegen. Subspace identification of multivariable linear parameter-varying systems. *Automatica*, 38(5):805–814, 2002.

Subset based least squares subspace regression in RKHS

L. Hoegaerts, J.A.K. Suykens, J. Vandewalle, B. De Moor
Katholieke Universiteit Leuven, Dept. of El. Engineering, ESAT-SCD-SISTA
Kasteelpark Arenberg 10, B-3001 Leuven (Heverlee), Belgium
Email: {luc.hoegaerts,johan.suykens}@esat.kuleuven.ac.be

1 Abstract

Kernel based methods suffer from exceeding time and memory requirements when applied on large datasets since the involved optimization problems typically scale polynomially in the number of data samples. Next to low-rank approximation, reduced sets appear in recent literature as a viable remedy. Along this line we focus on regression in RKHS with features based on a subset of basis functions. We show that the Nyström based feature approximation fits readily into this framework and investigate several alternative subspaces of the subset to transform features. In the context of subspace regression we discuss kernel PCA, kernel PLS and kernel CCA with regression in the primal space leading to sparse representations as in fixed-size LS-SVMs. The different models are illustrated and compared on artificial and real world benchmark datasets [1].

2 Overview

Over the last years one can see many learning algorithms being transferred to a kernel representation [2]. The benefit lies in the fact that nonlinearity can be allowed, while avoiding to solve a nonlinear optimization problem. In this paper we focus on least squares regression models in the kernel context. By means of a nonlinear map into a Reproducing Kernel Hilbert Space (RKHS) the data are projected to a high-dimensional space.

Kernel methods typically operate in this RKHS. The high-dimensionality which could pose problems for proper parameter estimation is circumvented by the kernel trick, which brings the dimensionality to the number of training instances n and at the same time allows excellent performance in classification and regression tasks. Yet, for large datasets this dimensionality in n means a serious bottleneck, since the corresponding training methods scale polynomially in n. Downsizing the system in dimensions to size $m \ll n$ is therefore needed. On the one hand, low-rank approximations offer reduction to smaller $m \times m$ matrices. On the other hand reduced set methods work with a thin tall $n \times m$ system. This work connects at the latter perspective.

We deal with least squares (LS) regression in the feature space. The estimation of the regression coefficients in the RKHS should be performed in a (potentially) high-dimensional basis. Most kernel LS based methods circumvent this by the kernel trick or a functional formulation. Here, we propose to explicitly restrict the regression coefficients to a subspace, which allows to control the number of regression parameters. The use of kernels is then naturally introduced by expression of the subspace in the basis formed by mapped training data points. This formulation yields a complementary, unifying viewpoint on some kernel methods. We especially focus on the expression in a *subset* $m \ll n$ of features of the RKHS. This scheme of LS subspace regression delivers a linear system that consequently only needs polynomial training times in m.

With such a model formulation we then connect to the Nyström approximation to show that it delivers a direct approximation of features, which, applied in an ordinary least squares model, can be interpreted as a regression with restriction to an eigenspace of, and expression relative to, a basis of the reduced set. As in fixed-size LS-SVMs [2], regression is done in the primal space leading to sparse representations in combination with the Nyström method, unlike estimation in the dual space as done in Gaussian Processes without having a sparse representation [3].

Acknowledgments

Funding agencies and sources: Research Council KU Leuven: Concerted Research Action GOA-Mefisto 666 (Math. Eng.), IDO (IOTA Oncology, Gen. netw.), PhD/postdoc & fellow grants; Flemish Government: Fund for Scientific Research Flanders (several PhD/postdoc grants, projects G.0407.02 (support vector machines), G.0256.97 (subspace), G.0115.01 (bio-i and microarrays), G.0240.99 (multilinear algebra), G.0197.02 (power islands), research communities ICCoS, ANMMM), AWI (Bil. Int. Collaboration Hungary/ Poland), IWT (Soft4s (softsensors), STWW-Genprom (gene promotor prediction), GBOU-McKnow (Knowledge management algorithms), Eureka-Impact (MPC-control), Eureka-FLiTE (flutter modeling), several PhD grants); Belgian Federal Government: DWTC (IUAP IV-02 (1996-2001) and IUAP V-10-29 (2002-2006) (2002-2006): Dynamical Systems and Control: Computation, Identification & Modelling), Program Sustainable Development PODO-II (CP/40: Sustainibility effects of Traffic Management Systems); Direct contract research: Verhaert, Electrabel, Elia, Data4s, IPCOS. LH is a PhD student supported by the Flemish Institute for the Promotion of Scientific and Technological Research in the Industry (IWT). JS is an associate professor at KU Leuven. BDM and JVDW are full professors at KU Leuven, Belgium.

References

[1] L. Hoegaerts, J. Suykens, J. Vandewalle, and B. De Moor. Subset based least squares subspace regression in rkhs. *Neurocomputing (submitted)*, 2004.

[2] J.A.K. Suykens, T. Van Gestel, J. De Brabanter, B. De Moor, and J. Vandewalle. *Least Squares Support Vector Machines*. World Scientific, Singapore, August 2002.

[3] C.K.I. Williams and M. Seeger. Using the nyström method to speed up kernel machines. In *Advances in Neural Information Processing Systems, eds. T. K. Leen, T. G. Diettrich, V. Tresp*, volume 13. MIT Press, 2001.

Robust Vector ARMA estimation from Discrete-Time Frequency Domain Power Spectra Estimates

Karel Hinnen
Delft Center for Systems and Control
Delft University of Technology
Mekelweg 2, 2628 CD Delft
The Netherlands
k.j.g.hinnen@dcsc.tudelft.nl

Michel Verhaegen
Delft Center for Systems and Control
Delft University of Technology
Mekelweg 2, 2628 CD Delft
The Netherlands
m.verhaegen@dcsc.tudelft.nl

1 Abstract

This presentation considers an algorithm for estimating a state space quadruple $[A,B,C,D]$ of the minimum-phase spectral factor, from matrix valued power spectrum data. The key step in the algorithm is the preservation of the positive realness (PR) property in estimating the power spectrum associated with the spectral factor. For a given pair $[A,C]$ with A stable, this PR property is guaranteed via the solution of a conic linear programming problem. In comparison with the classical LMI based solution, this results in a more efficient way to minimise the weighted 2-norm of the error between the estimated and given power spectrum.

2 Problem Description

In several applications such as active vibration suppression, it is important to have an accurate estimate of the spectral factor of a stochastic system. The problem considered in this note is that of identifying such a spectral factor directly from the power spectrum. Given $N+1$ samples of a power spectrum $\{\Phi(\mathrm{e}^{j(2\pi l/2N)})\}_{l=0}^{N}$, the goal is to find a state-space realisation of the minimum-phase linear time invariant filter

$$H : \left\{ \begin{array}{rcl} x_{k+1} & = & Ax_k + Be_k \\ y_k & = & Cx_k + De_k \end{array} \right. , \qquad (1)$$

that minimises the weighted 2-norm of the difference between the spectral samples and the power spectrum of the signal y_k for unit variance white input noise e_k.

3 Outline of approach

The proposed vector ARMA parameter estimation method consists of a subspace identification algorithm supplemented by a prediction error method. The subspace identification algorithm provides an initial estimate of the spectral factor H, while the prediction error method is used to further improve the performance with respect to the cost-function:

$$J = \sum_{l=0}^{N} \|(\Phi(z_l) - H(z_l)H^T(z_l)) \circ W_l\|_F^2, \; z_l = \mathrm{e}^{\frac{j2\pi l}{2N}}, \quad (2)$$

where W_l is a weighting function, $\circ$ the Hadamard product and $\|\cdot\|_F$ the Frobenius norm. In the later step, the spectral factor H is parametrised in output normal form.

The applied subspace identification algorithm differ in several aspects from the subspace identification algorithm for discrete time frequency domain power spectra as described in [1]. We have shown that in estimating the pair $[A,C]$, it is advantageous to use the inverse discrete Fourier transform (IDFT) of the given power spectrum as an approximation of the first N process covariances, rather than using the explicit relation with the state space matrices. In this way there is no need to carry out a cumbersome factorisation, which numerically very sensitive.

Another important issue in the identification of stochastic systems is to ensure that the estimated power spectrum is positive real (PR). Positive realness is needed to ensure that the estimated power spectrum has a spectral factor. The positive realness requirement imposes a constraint on the pair $[B,D]$. For a given pair $[A,C]$ finding the optimal $[B,D]$ can be formulated as a least squares problem with LMI constraint. In the proposed subspace identification algorithm this problem is efficiently solved as a conic linear programming problem. This approach is more efficient than solving the problem as a large scale LMI or by using a non-linear least squares approach [1, 2].

The property that the conic linear programming problem can be solved in a globally optimal sense, is exploited in the prediction error part of the algorithm to derive a separable least squares procedure for the (local) minimisation of cost-function (2). The advantages of the derived subspace algorithm and the iterative local minimisation procedure have been illustrated in a brief simulation study. In this study, the effect of calculating the power spectrum on the basis of a short length data set, has been considered in detail.

References

[1] P. van Overschee, B. de Moor, W. Dehandschutter, J. Swevers. *A subspace algorithm for the identification of discrete time frequency domain power spectra*. Automatica, Vol. 33, p.2147-2157, 1997.

[2] J. Mari, P. Stoica, T. McKelvey. *Vector ARMA estimation: A reliable subspace approach*. IEEE Transactions on Signal Processing, Vol. 47, p.2092-2104, 2000.

Discrete-time sliding mode control of a direct-drive robot

Geert van der Zalm,[1] Dragan Kostić,[2] and Bram de Jager[3]
Department of Mechanical Engineering
Technische Universiteit Eindhoven
P.O. Box 513, 5600 MB Eindhoven, The Netherlands

Email: [1]G.M.v.d.Zalm@student.tue.nl, [2]D.Kostic@tue.nl, and [3]A.G.de.Jager@wfw.wtb.tue.nl

Abstract

Theoretically, a continuous time sliding mode control (SMC) features invariance to disturbances and to modelling errors, closed-loop system order reduction, and predictable transient behavior [1]. In practice, especially with discrete-time (sampled) implementations of SMC algorithms, control chattering occurs due to the £nite duration of controller switching. The chattering is an undesirable high-frequency oscillation of the control input that may excite unmodelled dynamics present in electromechanical systems and decrease control performance.

Some methodological and conceptual solutions have been proposed to deal with problems caused by sampled implementation of SMC algorithms. The methodological solutions are directed towards elimination or reduction of the chattering effects. Typical examples are implementation of the boundary layer concept [1] and SMC design using the power rate reaching law method [2]. The most important conceptual contribution is the development of discrete-time sliding mode control (DSMC) algorithms [2],[3] that directly take into account the effects of discretization.

The DSMC algorithm considered in [3], utilizes both conceptual and methodological advances. It ensures that the sliding mode is reached in £nite time without chattering. Additionally, the characteristics of SMC are preserved, such as ensured closed-loop stability in the presence of disturbance effects and modelling errors, with direct control of the system transient behavior. In the absence of disturbances and modelling uncertainties, the order of the closed-loop system is reduced in the sliding mode. A distinguishing property is the simplicity of the DSMC feedback control law, which can be implemented on-line with minimal computational costs. These appealing merits have motivated us to apply the algorithm in robot motion control, since, so far, the algorithm was experimentally tested only in the control of a simple linear unloaded DC motor [3]. In this work, we adapt the original formulation of the algorithm presented in [3], making it applicable for robot motion control.

The DSMC law is designed based on the rigid-body robot dynamics. With a theoretical analysis, as well as by experimental results, we show that the obtained chattering-free control law can still cause undesirable ampli£cation of noise and parasitic dynamics. This is a consequence of a restriction in the ratio between proportional and derivative feedback gains, which induces high-gain feedback at higher frequencies. It appears that even with very careful tuning, the DSMC law can cause undesirable effects in the robotic system, degrading the performance of motion control. The observed problems are experimentally demonstrated on a benchmark direct-drive robot of spatial kinematics [4]. The excited parasitic dynamics cause undesirable oscillations in the robot motions, as seen from the position errors shown in Fig. 1. Inclusion of robot parasitic dynamics in the DSMC design is the possible improvement to be examined in the future, together with some some structural changes of the algorithm itself.

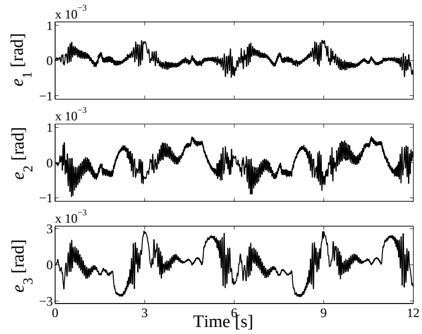

Figure 1: Experimental position errors in the robot joints.

References

[1] V.I. Utkin, “Sliding Modes in Control Optimization,” Springer-Verlag, Berlin, 1992.

[2] W. Gao, Y. Wang, and A. Homaifa, “Discrete-time Variable Structure Control Systems,” IEEE Trans. on Indust. Elect., Vol. 42, No. 2, pp. 117-122, 1995.

[3] G. Golo and C. Milosavljević, “Robust Discrete-time Chattering Free Sliding Mode Control,” Syst. and Control Let., Vol. 41, No. 1, pp. 19-28, 2000.

[4] D. Kostić, R. Hensen, B. de Jager, and M. Steinbuch, “Closed-form Kinematic and Dynamic Models of an Industrial-like RRR Robot,” in Proc. IEEE Conf. Rob. Autom. pp. 1309-1314, Washington D.C., 2002.

Virtual sensors and active vibration control on a six-degrees-of-freedom vibration isolation set-up

H. Super, G. Nijsse, J. van Dijk and J.B. Jonker
University of Twente, Faculty of Engineering Technology (CTW)
Department of Mechanical Engineering, Laboratory of Mechanical Automation (WA)
P.O. Box 217, 7500 AE Enschede, The Netherlands
Email: h.super@ctw.utwente.nl

1 Experimental vibration isolation set-up

This work discusses the use of a virtual sensor strategy for control of the experimental vibration isolation set-up schematically depicted in figure 1. A thick triangular aluminium plate is being excited by an electrodynamic shaker. This vibration source is connected to a receiver structure by three mounts. Each mount is controllable in two degrees-of-freedom due to its two piezoelectric actuators. The goal for this set-up is to minimize the overall vibration or sound radiation from the receiver plate given a certain disturbance shaker force on the source. Without control, relatively large forces are induced on the receiver plate when the source vibrates due to the high stiffness of the piezoelectric actuators. A possible control approach for

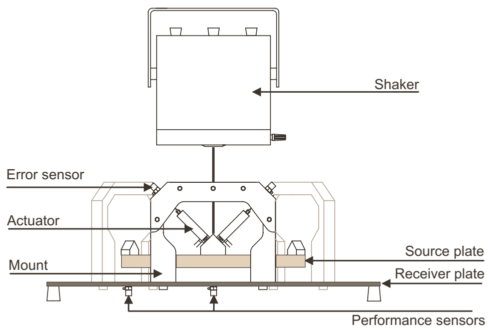

Figure 1: Schematic overview of the 6 degree-of-freedom vibration isolation set-up.

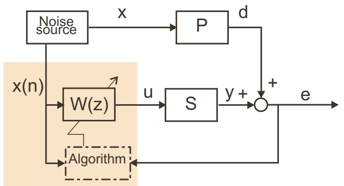

Figure 2: Adaptive feedforward control structure

this problem is given in figure 2. The plant is represented by P and S. The primary path P represents the transfer functions from the shaker input signal to the six error sensors. The secondary path S represents the 6x6 transfer functions from the six actuator inputs **u** to the six error sensors **e**. A reference signal x(n) based on the disturbance is used as the input for a feedforward controller W(z) which output **u** controls the six piezoelectric actuators in the mounts. An adaptive algorithm is used to adapt the filter W(z) based on minimizing a certain costfunction. This costfunction should be related to the overall vibration levels of the receiver. Practically the acceleration levels measured by the six error sensors in line with the actuators on top of the mounts are being used. In order to validate the isolation performance, two additional accelerometers have been placed on the receiver. These are denoted as performance sensors in figure 1. Experiments have shown that at certain disturbance frequencies the controller steering the six actuators based on the six error sensors does not result in the maximum achievable reduction on the two performance sensors. However, the results are different when placing the performance sensors on different locations. Obviously using only two sensors is not sufficient to get a global estimate for the overall vibration level of the receiver. A better estimate could be obtained with a grid of multiple sensors on the receiver plate. However, this approach is too expensive to pursue and therefore the use of 'virtual' sensors comes into view.

2 Virtual sensors

For simulation and control system design statespace models for P and S have been obtained using subspace identification. By collecting appropriate input-output data sets with the performance sensors at different locations it is possible to obtain an extended model of the set-up for a grid of 'virtual' performance sensors. These models can be used to obtain a filter matrix containing information from the transfer functions between the error sensors and the virtual sensors. By filtering the real error sensor signals with this filter and using the resulting virtual sensor signals for adapting the controller, the controller effectively minimizes a costfunction which should be a better representation for the overall vibration level of the receiver. Therefore the global vibration reduction on the reciever can be expected to be higher compared to using the error sensors directly.

Data-based design of high-performance motion controllers

Dragan Kostić,[1] Bram de Jager,[2] and Maarten Steinbuch[3]
Department of Mechanical Engineering
Technische Universiteit Eindhoven
P.O. Box 513, 5600 MB Eindhoven, The Netherlands

Email: [1]D.Kostic@tue.nl, [2]A.G.de.Jager@wfw.wtb.tue.nl, and [3]M.Steinbuch@tue.nl

Abstract

In data-based (DB) control designs, the need for (non) parametric plant models is omitted, since only experimental data are used. In this work, the reasons for using DB control are simpli£ed off-line design of high-performance motion controllers, and direct control of the controller structure and its complexity. Our practice with model-based motion control con£rms that closely accounting for experimental properties of the controlled system can signi£cantly improve the control performance and the robustness against disturbances and parasitic dynamics [1]. However, the problem we commonly experience is the complexity of controllers that result from model-based designs. To make them admissible for online implementation, we must lower their complexity via model reduction.

Here, we investigate if the control performance feasible with model-based motion controllers can also be realized with controllers designed using some DB method. The requirement is that the DB method must allow prescribing the controller structure and the complexity at the very beginning of the design. A starting point we found in the virtual reference feedback tuning approach [2]. Using this, we derive our own DB method for controller design, which enables simultaneous shaping of the closed-loop sensitivity and the complementary sensitivity transfer functions.

The DB design begins with the de£nition of the model-based cost function which imposes the desired shapes of the sensitivity and the complementary sensitivity functions. Then, a DB counterpart of this function is derived, which depends merely on input-output signals that are either experimentally measured on the controlled system, or are synthetically generated using a system model of arbitrary complexity. It is irrelevant if the signals are collected under open-loop or closed-loop operating conditions. However, it is important that these signals are rich around frequencies of interest for control, such as the crossover frequency. For the selected controller class, the designer optimizes the DB cost function in one-shot using a least-squares algorithm. The result of optimization is the optimal controller tuning with respect to the desired shapes of the reference transfer functions.

Feedback motion controllers of a benchmark direct-drive robot of spatial kinematics were designed using the DB method. The design problems experienced when using experimentally collected signal, such as poor coherence at low frequencies and the presence of nonlinear effects, has been circumvented by using data synthetically generated from a relevant high-order plant model. The designed feedback controllers were experimentally implemented to realize reference trajectories that require the full authority of the robot drives. The experimental results shown in Fig. 1 reveal high motion accuracy when performing the reference trajectories, without excitation of the robot parasitic dynamics. These results verify that the DB method is capable of tuning controllers of given structure and complexity such that the motion control of high performance is realized. Our next objective is to overcome the need for synthetically generated data in the DB design of the robot motion controllers. We are also eager to achieve a stability test compatible with our DB method. Finally, we investigate the possibility for online controller tuning using the considered DB method.

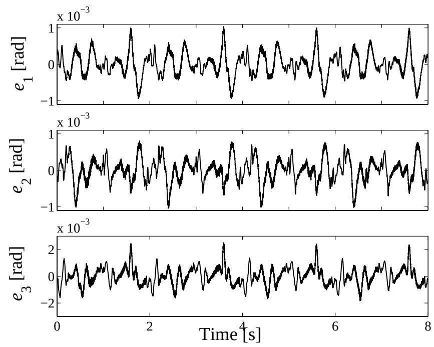

Figure 1: Experimental position errors in the robot joints.

References

[1] D. Kostić, B. de Jager, and M. Steinbuch, "Control Design for Robust Performance of a Direct-drive Robot," in Proc. IEEE Conf. Control Appl., pp. 1448-1453, Istanbul, Turkey, 2003.

[2] A. Lecchini, M.C. Campi, and S.M. Savaresi, "Virtual Reference Feedback Tuning for Two Degree of Freedom Controllers," Int. J. Adapt. Control Sig. Process., Vol. 16, No. 5, pp. 355-371, 2002.

Decentralized control for systems with input saturation

Jasmine Minteer[1]
School of Electrical Engineering and Computer Science
Washington State University
Pullman, WA 99164-2752
U.S.A.
E-mail: jminteer@eecs.wsu.edu

A.A. Stoorvogel
Faculty of Electrical Engineering, Mathematics and Computer Science
Delft University of Technology
P.O. Box 5031
2600 GA Delft
The Netherlands
E-mail. A.A.Stoorvogel@ewi.tudelft.nl

Ali Saberi
School of Electrical Engineering and Computer Science
Washington State University
Pullman, WA 99164-2752
U.S.A.
E-mail: saberi@eecs.wsu.edu

1 Abstract

Decentralized control has been an important research area for a long time. There are many application for instance in power systems where we have several local controllers with their own measurements and actuators but no central controller. A major objective is then to stabilize the system subject to the constraint that each local controller can only act upon the locally available information. In the seminal paper [4] it was established that stabilization was possible as long as the so-called decentralized fixed modes are all in the open left half plane.

On the other hand, many actuators have limitations. Common limitations are rate or amplitude constraints. It is well known that in this case global stabilization is possible if and only if the underlying linear dynamics is stabilizable and all poles of the open loop system are in the closed left half plane, see for instance [3, 2].

This talk will discuss the combination of the two. In other words, we consider linear systems with input saturation and decentralized control. First, we note that input saturation requires in general nonlinear controllers for global stabilization. But the fixed modes established in [4] are intrinsically based on linear controllers. We will show that using nonlinear controllers, we can actually reduce the number of fixed modes. In contrast to the literature, which studied nonlinear, time-varying controllers (see [1]), we will show, by example, that we can find time-invariant nonlinear controllers.

Our conjecture is that when all poles are in the closed left half plane, the system is stabilizable and all fixed modes are in the open left half plane then we can find a decentralized controller for this system which achieves global stability without violating the constraints. We have no full result available at this moment but we will present the results obtained so far.

References

[1] Z. Gong and M. Aldeen, “Stabilization of decentralized control systems”, J. Math. Syst. Estim. Control, 7(1), 1997, pp. 1–16.

[2] A. Saberi, Z. Lin, and A. Teel, “Control of linear systems with saturating actuators”, IEEE Trans. Aut. Contr., 41(3), 1996, pp. 368–378.

[3] E.D. Sontag and H.J. Sussmann, “Nonlinear output feedback design for linear systems with saturating controls”, in Proc. 29th CDC, Honolulu, 1990, pp. 3414–3416.

[4] S.H. Wang and E.J. Davison, “On the stabilization of decentralized control systems”, IEEE Trans. Aut. Contr., 18(5), 1973, pp. 473–478.

[1] Currently visiting the Faculty of Electrical Engineering, Mathematics and Computer Science at Delft University of Technology

Data-based LQG control

Wouter Aangenent,[1] Dragan Kostić,[2] Bram de Jager,[3] and Maarten Steinbuch[4]
Department of Mechanical Engineering
Technische Universiteit Eindhoven
P.O. Box 513, 5600 MB Eindhoven, The Netherlands

Email: [1]W.H.T.M.Aangenent@student.tue.nl, [2]D.Kostic@tue.nl,
[3]A.G.de.Jager@wfw.wtb.tue.nl, and [4]M.Steinbuch@tue.nl

Abstract

In spite of the current state of control theory, a fundamental issue in control remains open: which model is appropriate for control design? Mathematical models of complex systems are not always reliable, while adaptive and robust control methods have not completely overcome the danger of modelling errors. Furthermore, the design of an accurate model from first principles or from system identification, is often a time consuming and not a straightforward task. In this work [1], another approach to design controllers for a system is discussed. The control action that realizes system regulation or tracking control is derived without the use of any model or preliminary information about the system, but is merely based on input-output data observed from the system. This way, the step of modelling or system identification is not required anymore. Such a control strategy is known as data-based control.

Standard model-based discrete-time finite horizon optimal control is obtained using a state-space description of the system. A linear quadratic cost function is optimized resulting in two difference Riccati equations, with which the optimal state feedback and state observer gains can be computed. Since a linear quadratic cost function is used together with Gaussian process and measurement noises, the combination of the optimal control and the state observation is known as Linear Quadratic Gaussian (LQG) control.

Reference [2] presents an algorithm that omits the need for a state-space model of the system, when computing the solution to the discrete-time finite horizon LQG problem. The computation makes use of closed-form solutions to the difference Riccati equations instead of the normally used recursive solutions. This way, the solution no longer requires an explicit system model, but is based on a finite number of Markov parameters of the system that equal the values of the impulse response at discrete sample times. These parameters can be estimated on-line from almost any set of input/output data of the system using ARMarkov representations [3].

The combination of on-line Markov parameter estimation and data-based LQG control can be used to construct a moving horizon controller. A system can then be regulated using only the input and output data, without requiring any model of the system or any parametric representation of the controller. Based on the measured input/output data, the controller can adapt its action to the actual dynamics. Consequently, the data-based controller can also be used to control systems with changing dynamics. Apart from state regulation, the data-based controller can be used for tracking control tasks.

The effectiveness of data-based LQG control is evaluated in simulations and in experiments. Simulations show that, in case of time-invariant plants, a model-based and data-based LQG controller give identical results while in case of time-varying plants, the data-based controller is able to adapt itself to the changing dynamics. Although not yet delivering a high tracking performance, experimental results obtained on a direct-drive robot of spatial kinematics look promising. At this moment, a high computational burden is the most important factor which limits the performance. Reduction of the computational costs, so performance improvement can be obtained with a longer horizon length is under investigation.

References

[1] W.H.T.M. Aangenent, “Data-Based LQG Control”. *Master's thesis*, Technische Universiteit Eindhoven, 2003, DCT 2003.113.

[2] R. E. Skelton and G. Shi, “Markov Data-Based LQG Control”. *J. of Dyn. Systems, Meas., and Control*, Vol. 122, 2000, 551–559.

[3] M. Q. Phan, R. K. Lim, and R.W. Longman, “Unifying Input-Output and State-Space perspectives of Predictive Control”. *Technical report No. 3044*, Princeton University, Princeton, NJ, September 1998.

Synthesis of numerical state feedback laws for singular optimal control

Stefan C. de Graaf, Johannes D. Stigter, Gerrit van Straten

Wageningen University, Department of Agrotechnology and Food Sciences
P.O. Box 43, 6700 AA Wageningen, The Netherlands
Email: stefan.degraaf@wur.nl

Closed-loop optimisation techniques, such as receding horizon optimal control often have the limitation with respect to dealing with measurable disturbances that these techniques reject these disturbances in order to track open-loop defined optimal input control trajectories. Sometimes measurable disturbances can also be exploited to improve the performance of processes. For example, the amount of sunlight, which is a measurable disturbance in greenhouse vegetable cultivation, can be exploited to improve the greenhouse vegetable cultivation. If disturbances in sunlight are rejected in optimal greenhouse climate control, the cultivation will be sub-optimal.

Measurable disturbances can be exploited in closed-loop optimisation by using an iterative optimisation algorithm at each time controls need to be recalculated for adjustment (Rahman and Palanki 1996). Iteration is time consuming, so non-iterative algorithms are needed to recalculate controls.

An interesting non-iterative closed-loop optimisation procedure was developed by Palanki, *et al.* (1993) and Rahman and Palanki (1996). They proposed to develop optimal feedforward/state-feedback laws symbolically for optimal singular regions for this procedure. They also proposed to use minimum or maximum input values for the non-singular regions. To determine switching times between singular and non-singular regions and what values (minimum or maximum) the manipulated inputs take in the non-singular regions, the adjoint equations in addition to the state-equations needed to be integrated in open-loop (off-line).

They recommended using symbolic manipulation software such as MAPLE or MATHEMATICA for the calculation of feedforward/state-feedback laws of large systems, because of the computation of a large number of necessary Lie-derivatives. Symbolic manipulation will lead to difficult-to-handle feedforward-/state-feedback laws for large systems however. Numerical development of optimal feedforward/state-feedback laws is therefore more convenient.

Magana Jimenez (2002) devolped a MATLAB5.3-ADIFOR2.0-FORTRAN^{compaq}6.0-CONTROL (MAFC) software package that is able to synthesize numerical feedforward/state-feedback laws for nonlinear systems. In the synthesis of these laws automatic differentiation is incorporated to compute the necessary Lie-derivatives numerically.

In order to be able to use this software package, the optimisation problem has to be cast in a non-linear system. Rahman and Palanki (1996), and Van der Schaft (1984) showed how to do this.

The development of numerical feedback/state-feedback laws for singular regions, which can be used in non-iterative closed-loop optimisation using the MAFC software package is going to be shown. First the optimal control problem is cast in a non-linear system. Then the development of feedforward/state-feedback laws are presented, that are synthesized by the MAFC software package. Singular trajectories defined by numerical feedforward/state-feedbak laws are validated with singular trajectories calculated by a gradient algorithm in an example.

References

Magana Jimenez, Q. (2002). Nonlinear control via automatic differentiation. Department of chemical engineering. Cleveland, Case western reserve univeristy.

Palanki, S., C. Kravaris, et al. (1993). "Synthesis of state feedback laws for end-point optimization in batch processes." Chemical Engineering Science **48**(1): 135-152.

Rahman, S. and S. Palanki (1996). "On-line optimization of batch processes in the presence of measurable disturbances." American institute of chemical engineering journal **42**(10): 2869-2882.

Schaft, v. d. A. J. (1984). System theoretic description of physical systems. Amsterdam, Centre for mathematics and computer science.

Receding horizon optimal control of a solar greenhouse

R. J. C. van Ooteghem
Mansholtlaan 10, 6708 PA, Wageningen
Rachel.vanOoteghem@wur.nl

J. D. Stigter
Mansholtlaan 10, 6708 PA, Wageningen
Hans.Stigter@wur.nl

L. G. van Willigenburg
Mansholtlaan 10, 6708 PA, Wageningen
Gerard.vanWilligenburg@wur.nl

G. van Straten
Mansholtlaan 10, 6708 PA, Wageningen
Gerrit.vanStraten@wur.nl

Keywords: solar greenhouse, receding horizon optimal control, temperature integration

1 Scope and objective

To reduce the fossil energy use in greenhouse horticulture a new greenhouse has been designed, which is called the solar greenhouse. In combination with model based optimal control we intend to maximize solar energy use, minimize fossil energy consumption and obtain optimal crop growth conditions.

2 Methodology

2.1 Solar greenhouse

The heat insulation and the transmission of solar radiation of the greenhouse are maximized. An aquifer consisting of a warm- and a cold-water basin is used to store the solar energy. The greenhouse can be heated with little energy input with a heat pump and warm aquifer water. The greenhouse can be cooled with a heat exchanger and cold aquifer water, while energy is harvested to use at times of heat demand. CO_2 supply is independent of boiler operation, thus avoiding the need to use the boiler at times of CO_2 demand. Ventilation with heat recovery is used to dehumidify the greenhouse at times of heat demand. A dynamic model of the solar greenhouse with crop is developed to accurately describe the process.

2.2 Receding Horizon Optimal Control

The aim is to minimize fossil energy consumption, while maximizing crop dry weight and keeping temperature and humidity within certain limits. Long-term effects of temperature are incorporated in a temperature integral. These requirements are defined in a goal function, which is minimized by optimal control. An indirect gradient method is used to calculate the optimal control trajectories. The control solution consists of actuator trajectories, which result in temperature, humidity and CO_2 concentration that optimize the goal function.

3 Results and Conclusions

The receding horizon optimal control has been tested with year-round weather data. From the results, it can be concluded that

- Receding horizon optimal control of the solar greenhouse is feasible. Although the model is non-linear and complex, rational optimal control solutions can be found.
- The results of the optimal control strongly depend on the weather conditions; therefore reliable predictions are needed.
- The heat pump and the heat exchanger are valuable additions to the greenhouse control system. In all months, except in winter, the greenhouse is mainly heated by the heat pump. The heat exchanger is used to cool the greenhouse in spring and summer, thus harvesting energy for the aquifer.
- Temperature and relative humidity stay well within their bounds, and the temperature integral requirements are well met.
- The energy use of the solar greenhouse is much lower than a conventional greenhouse.

Stabilizing receding horizon control of constrained PWA systems

M. Lazar*, W.P.M.H. Heemels*, S. Weiland*, A. Bemporad**

*Department of Electrical Engineering, Control Systems Group
Eindhoven University of Technology, P.O. Box 513, 5600 MB Eindhoven, The Netherlands
E-mail addresses: {m.lazar, w.p.m.h.heemels, s.weiland}@tue.nl
**Dipartimento di Ingegneria dell'Informazione
Universitá di Siena, Via Roma 56, 53100 Siena, Italy
E-mail address: bemporad@dii.unisi.it

Abstract

Recently researchers have become gradually more interested in the optimal control and stabilization of hybrid systems in general and Piecewise Affine (PWA) systems in particular, mainly due to the fact that the PWA framework can describe a broad class of hybrid models [4, 7]. Extension of receding horizon control, also known as Model Predictive Control (MPC), to PWA systems came as a natural opportunity and successful implementations have been carried out, including [2, 5]. The main drawbacks encountered consist in the on-line computational load and in guaranteeing closed-loop stability. Efficient solutions for reducing the on-line computational burden in hybrid MPC have already been developed, such as the Piecewise Linear (PWL) explicit approach [2] or the discrete events controllable sets based approach [5], while the stability aspects have been addressed only marginally, e.g. see [1, 2].

In this paper we develop sufficient stabilization conditions for quadratic cost based receding horizon control of constrained PWA systems. Stability is ensured using the terminal cost and constraint set method [6] for guaranteeing stability in linear or nonlinear MPC. Lyapunov arguments are employed to obtain the stabilization conditions that yield after suitable novel transformations a set of Linear Matrix Inequalities (LMI). If the resulting LMI is feasible, then the value function of the MPC cost is a Lyapunov function of the PWA system in closed-loop with the MPC controller. A different terminal weight matrix can be used in the MPC cost for each sub-model of the PWA system to reduce conservativeness. The terminal weight matrix (or matrices) and feedback gains are easily obtained from the solution of the developed LMI, and the terminal state has to be constrained to a positively invariant set [3] containing the origin to ensure closed-loop stability. A procedure for computing a polyhedral positively invariant set for a PWL system is also presented. Therefore, the finite horizon open-loop optimal control problem that has to be solved at each sampling instant remains a Mixed Integer Quadratic Programming (MIQP) problem while stability is guaranteed. The implementation of the whole procedure has been tested on several examples with good results.

The proposed method can be used to achieve stability for other relevant classes of hybrid systems equivalent to PWA systems [4], when a quadratic cost MPC scheme is used, and it does not depend on the algorithm employed to solve the corresponding MIQP problem (e.g. the results would also hold for a PWL approach).

References

[1] Bemporad, A. and Morari, M., "Control of systems integrating logic, dynamics, and constraints", *Automatica*, *35*, 1999, pp. 407-427.

[2] Bemporad, A., Borrelli, F. and Morari, M., "Optimal controllers for hybrid systems: Stability and piecewise linear explicit form", *Proceedings of the 39th IEEE Conference on Decision and Control*, Sydney, Australia, 2000, pp. 1810-1815.

[3] Blanchini, F., "Set invariance in control", *Automatica*, *35*, 1999, pp. 1747-1767.

[4] Heemels, W.P.M.H., De Schutter, B., and Bemporad, A., "Equivalence of hybrid dynamical models" *Automatica*, *37*, 2001, pp. 1085-1091.

[5] Lazar, M. and Heemels, W.P.M.H., "A semi-explicit MPC set-up for constrained piecewise affine systems", *Proceedings of the European Control Conference*, Cambridge, UK, 2003.

[6] Mayne, D.Q., Rawlings, J.B., Rao, C.V. and Scokaert, P.O.M., "Constrained model predictive control: Stability and optimality", *Automatica*, *36*, 2000, pp. 789-814.

[7] Sontag, E.D., "Interconnected automata and linear systems: A theoretical framework in discrete-time", *Hybrid systems III: Verification and Control*, (R. Alur, T.A. Henzinger, and E.D. Sontag, Ed. NY: Springer), 1996, pp. 436-448.

Model predictive control for perturbed continuous PWA systems

Ion Necoara
Delft Center for Systems and Control
Delft University of Technology
Mekelweg 2, 2628 CD Delft, The Netherlands
email: i.necoara@dcsc.tudelft.nl

Bart De Schutter
Delft Center for System and Control
Delft University of Technology
Mekelweg 2, 2628 CD Delft, The Netherlands
email: b.deschutter@dcsc.tudelft.nl

Ton van den Boom
Delft Center for System and Control
Delft University of Technology
Mekelweg 2, 2628 CD Delft, The Netherlands
email:t.j.j.vandenboom@dcsc.tudelft.nl

Hans Hellendoorn
Delft Center for Systems and Control
Delft University of Technology
Mekelweg 2, 2628 CD Delft, The Netherlands
email:j.hellendoorn@dcsc.tudelft.nl

Abstract

Hybrid systems have recently attracted the interest of both academia and industry due to their ability to model the interaction between continuous and logic components. In particular, several authors have studied a subclass of hybrid systems, viz. piecewise affine (PWA) systems, since they represent a powerful tool for approximating nonlinear systems with arbitrary accuracy and since a rich class of hybrid systems can be described by PWA systems. Another subclass of hybrid systems is the class of the max-min-plus-scaling (MMPS) systems, the evolution equations of which can be described using the operations maximization, minimization, additions, and scalar multiplication. Recently, a link between *continuous* PWA and MMPS systems has been demonstrated. In this presentation we consider MMPS systems, and thus also continuous PWA systems.

Several authors have considered Model Predictive Control (MPC) for classes of hybrid systems, and, in particular, several approaches and efficient algorithms have been developed for MPC for PWA systems. We extend the approach of [1], in which MPC for MMPS systems (and equivalently — for continuous PWA systems) has been proposed. In [1] the deterministic noise-free case without modeling errors is considered, and in this presentation we extend these results to the cases with noise and modeling errors.

An important difference between MPC and some other control methods is the explicit use of a prediction model. Because the models play such an important role in MPC, we must also take into account noise and error modeling when we implement MPC. Indeed, ignoring the noise can lead to a bad tracking or even to unstable closed-loop behavior. Both modeling errors and noise and disturbance perturb the system by introducing uncertainty in the equations of the system. We model the noise and disturbances by including extra additive terms in the max-min canonical forms of the system equations for MMPS systems.

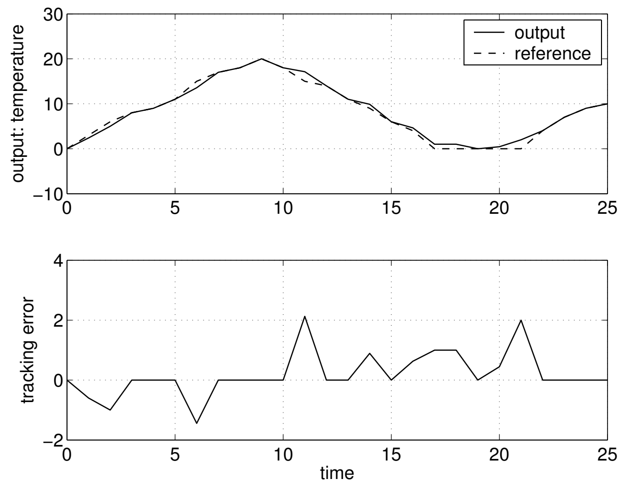

Figure 1: Illustration of the worst-case MPC for a perturbed MMPS system.

By adapting and extending the MPC approach for perturbed max-plus discrete event systems developed in [2] to perturbed MMPS systems, we obtain an efficient MPC approach which is based on minimizing the worst-case cost criterion. More specifically, we prove that the optimization problem at each step of the MPC algorithm can be transformed into a sequence of linear programming problems, for which efficient solution methods exist. We also illustrate the new approach for a simple case study (see Figure 1).

Acknowledgments

Research supported by the STW projects "Model predictive control for hybrid systems" and "Multi-agent control of large-scale hybrid systems".

References

[1] B. De Schutter and T.J.J. van den Boom. MPC for Continuous Piecewise-Affine Systems To appear in *Systems and Control Letters*, 2004.

[2] T.J.J. van den Boom and B. De Schutter. Model Predictive Control for Perturbed Max-Plus-Linear Systems In *Systems & Control Letters*, vol. 45, no. 1, Jan. 2002, p. 21–33.

Model selection for state estimation

Robert Bos, Xavier Bombois, Paul Van den Hof
Delft Center for Systems and Control
Delft University of Technology
Mekelweg 2, 2628 CD Delft
The Netherlands
Email: r.bos@dcsc.tudelft.nl

Abstract

In monitoring the goal is to accurately estimate the state of a true system. For estimating the state a single model of the true process is usually available. In some situations multiple candidate models are available for describing the current behavior of the true system. An example of such a situation is in model based fault detection and isolation (FDI). In model based FDI, at least one model is given to describe to nominal process behavior, while a second set of models describe the behavior of the process after corresponding faults have occurred. These fault models could be the same as the nominal models, but with time varying parameters. In this abstract we will focus on the problem of selecting the best possible model for state estimation.

Model selection for filtering problems is often described using Bayes conditional probability theory [1]. Suppose n models are available, denote these models as $\mathscr{M}_i$, with $i = 1, 2, \ldots, n$. Then the filtering procedure is carried out for each model, on measurement data y. Afterwards, using Bayes conditional probability theory, the conditional probability $p(\mathscr{M}_i|y)$ is computed. The model with the highest conditional probability is then selected, and the state estimates based on this model are used. The conditional probability $p(\mathscr{M}_i|y)$ can be computed via: $p(\mathscr{M}_i|y) = p(y|\mathscr{M}_i)p(\mathscr{M}_i)/p(y)$. Using this equation in practice for complex process models is generally difficult, because the term $p(y|\mathscr{M}_i)$ is not trivial to compute for non-linear systems and knowledge of the priori probability of each model $p(\mathscr{M}_i)$ is rarely available.

An alternative approach to the model selection problem is given in [2]. If a moving horizon state estimator (MHE) is used for state estimation, the state estimation problem is written as a weighted and regularized least squares problem. The problem of model selection is therefore approximately similar to model selection in system identification theory. Given this similarity, the model selection is done using the Akaike Information Criterion (AIC). Advantages of this approach are that exact probability distributions are no longer required, and the technique can also be easily adapted for non-linear models. Drawbacks of this approach are that the technique can only be used in conjunction with moving horizon estimators. Another drawback is that the AIC criterion may not be the best criterion, since it was derived only for least squares problems without weighting and regularization, while states are estimated with weighting and regularization.

In the remainder we consider a model selection procedure closely related to [2] will be considered. We propose to use the expected asymptotic prediction error $\mathscr{V}(k)$ as a selection criterion:

$$\mathscr{V}(k) = E_{\hat{x}_k}\overline{V}(\hat{x}_k, k). \quad (1)$$

$$\text{with } \overline{V}(x,k) = E_{y_k}\|y_k - \hat{y}(x)\|_R^2 \quad (2)$$

in which $\hat{x}_k$ is the estimated state using all measurement data up to (and including) y_k, $\hat{y}(x)$ is the best one step ahead prediction of y_k given x, and R is a chosen positive semi definite weighting matrix. Since this criterion is a prediction error, models with a lower $\mathscr{V}(k)$ are considered to be better. A practical problem with using this criterion is that exactly computing the asymptotic fit requires an infinite number of measurements. Since this is impossible, an estimate of the expected asymptotic fit is required. Our derived estimator is a generalized version of the FPE criterion [3] used in system identification. The generalized version can also compute the expected asymptotic fit if model parameters have been estimated using regularized least squares problems. The new criterion is similar to the AIC criterion used in [2], but is better suited for monitoring problems because it also incorporates knowledge on how the states are estimated.

Acknowledgement

The work of Robert Bos is supported by Dutch research organization TNO/TPD.

References

[1] F. Gustafsson, *Adaptive Filtering and Change Detection*, Wiley & Sons, Chichester, United Kingdom, 2000.

[2] M. L. Tyler, K. Asano and M. Morari, “Application of moving horizon estimation based fault detection to cold tandem steel mill,” *Int. J. Control*, vol. 73, no. 5, pp. 427-438, 2000.

[3] L. Ljung, *System Identification: Theory for the user*, Prentice-Hall, Upper Saddle River, N.J., 1999

Performance evaluation for fault detection and isolation algorithms

C. Parloir [1], M. Kinnaert
Control Engineering Department
Université Libre de Bruxelles
Av.F.D. Roosevelt, 50 (CP 165/55)
1050 Bruxelles, Belgium
e-mails: [cedric.parloir, michel.kinnaert]@ulb.ac.be

1 Abstract

Model based fault detection systems are made of two parts: a residual generator and a decision module. The first is a filter notch which takes as inputs the actuator commands and the measured plant outputs and generates signals called residuals. The residuals are signals that, in the absence of faults, deviate from zero only due to modelling uncertainties, with nominal value being zero, or close to zero under actual working conditions. If a fault should occur, the residuals deviate from zero with a magnitude such that the new condition can be distinguished from the fault free working mode. The role of the decision module is to determine whether the residuals differ significantly from zero and, from which residuals are different from zero, to analyse the pattern of zero and non zero residuals and to deduce which is the most likely fault.

The performance of such systems are characterized by their false detection (isolation) rate, their missed detection (isolation) rate and their mean detection (isolation) delay [1].

Yet such criteria are very difficult to evaluate analytically once modelling uncertainties are considered.

The aim of this contribution is to study the use of Monte Carlo simulation to estimate the above mentioned performance criteria. The uncertain model parameters are described by their probability density function. Three methods are considered to obtain realizations of these random variables [2,3] :

- The random sampling method
- The stratified sampling method
- The Latin hypercube sampling method

The random sampling method is the most obvious one: a value of each parameter is simply generated on the basis of its probability density function. This method requires an important number of simulations to cover appropriately the entire domain of each probability density function, especially if the number of parameters is large.

In order to alleviate this problem, alternatives have been developed like the stratified and the Latin Hypercube sampling methods. The latter amounts to divide the domain of each probability density function into subsets and to generate realizations of the random variable from each of those subsets. This allows covering the domain of each probability density function more suitably.

After presenting the methodology in a general context, it is illustrated on a simple system. The different sampling methods are compared and the effect of the choice of the distribution of the uncertain parameters is studied.

References

[1] M.Basseville and I. Nikiforov, Detection of abrupt changes, theory and application, Prentice Hall, 1993

[2] McKay MD, Beckman RJ and Conover WJ, A comparison of three methods for selecting values of the input variables in the analysis of output from a computer code, Technometrics 21(2): 239-45, 1979

[3] J.C. Helton and F.J. Davis, Latin hypercube sampling and the propagation of uncertainty in analyses of complex systems, Reliability engineering and system safety 81 23-69, 2003

[1] The work of Cédric Parloir is supported by project EU-IST-2001-32122 IFATIS

Detection and Identification of Two Classes of Actuator Faults in Aircraft using Augmented Kalman Filters

R. Hallouzi, V. Verdult, R. Babuška and M. Verhaegen
Delft Center for Systems and Control
Delft University of Technology
Mekelweg 2, 2628 CD Delft, The Netherlands
{R.Hallouzi, V.Verdult, R.Babuska, M.Verhaegen}@dcsc.tudelft.nl

1 Introduction

Fault Detection and Identification (FDI) is a topic that has grown with the increasing demand of fault-tolerant control systems. Especially in safety-critical systems such as aircraft, the demand of reliable FDI is large. For this reason an important element of the European ADFCS-II (Affordable Digital fly-by-wire Flight Control Systems) project, of which this research is part, consists of sensor and actuator FDI. In this project methods are studied for cost-efficient implementation of FDI in small commercial aircraft. Therefore "hardware redundancy", which is very common in aircraft should be replaced by "analytical redundancy". This research will focus on actuator FDI because the sensor FDI part has already been extensively studied [3].

2 Actuator FDI in aircraft

There are two types of common actuator faults in aircraft [1]. These two types are partial faults and total faults. A total fault is characterized by the fact that the concerning actuator does not react at all on the commanded inputs. When a partial fault has occurred the actuator still reacts on the input, but with reduced efficiency. Furthermore there are different types of total faults [1]. The goal of this research is to firstly detect the fault and then find out to which class it belongs. Subsequently the size of the fault should be estimated.

3 FDI method

Previous research has been conducted on actuator FDI in aircraft using the parameter estimation method based on subspace identification [4]. A recommendation from this research was to investigate a recursive identification method instead of the used batch-wise method in order to improve the speed of detection. Therefore an augmented Kalman filter has been implemented that does not only estimate the states but also an extra fault parameter [2]. Such an augmented filter in the case of additive faults is given by:

$$\hat{x}_a(k+1) = \begin{bmatrix} A & B \\ 0 & I \end{bmatrix} \hat{x}_a(k) + \begin{bmatrix} B \\ 0 \end{bmatrix} u(k) + w(k) \qquad (1)$$

$$y(k) = \begin{bmatrix} C & 0 \end{bmatrix} \hat{x}_a(k) + D\big(u(k) + \hat{\alpha}(k)\big) + v(k) \qquad (2)$$

where $\hat{x}_a(k) = [\hat{x}(k) \;\; \hat{\alpha}(k)]^T$, with $\hat{x}_a(k) \in \mathbb{R}^n$, is the estimated augmented state, $u(k) \in \mathbb{R}^m$ is the input, $y(k) \in \mathbb{R}^l$ is the output and $w(k)$ and $v(k)$ are respectively the process noise and the measurement noise. $\hat{\alpha}(k)$ is the parameter that represents additive faults on the input.

The augmented filters by themselves are not sufficient for FDI. Some additional FDI logic has to be added to determine what type of fault has occurred after the detection of the fault. The detection of a fault is performed by applying the cumulative-sum (CUSUM) algorithm on the fault parameter. The logic is based on the fault characteristics of the two fault types.

4 Evaluation

The proposed method is evaluated with data from the non-linear simulation of an aircraft as used in the ADFCS-II project. The system matrices are based on a linearization of the non-linear aircraft in a certain working point. Realistic flight maneuvers with insertion of faults in the primary control surfaces are simulated.

References

[1] J. D. Bošković and R. K. Mehra, "Stable Multiple Model Adaptive Flight Control for Accomodation of a Large Class of Control Effector Failures", *Proc. of the American Control Conference 1999*, pp. 1920-1924, San Diego, June 1999.

[2] S. Mešić, V. Verdult, M. Verhaegen and S. Kanev, "Estimation and Robustness Analysis of Actuator Faults based on Kalman Filtering", *Proc. of the IFAC SAFEPROCESS 2003*, pp. 241-246, Washington DC, USA, June 2003.

[3] M. Oosterom, R. Babuška and H. B. Verbruggen, "Soft Computing Applications in Aircraft Sensor Management and Flight Control Law Reconfiguration", *IEEE Transactions on Systems, Man and Cybernetics*, vol. 32, no.2, pp. 125-139, May 2002.

[4] V. Verdult, S. Kanev, J. Breeman and M. Verhaegen, "Estimating multiple sensor and actuator faults using subspace identification", *Proc. of the IFAC SAFEPROCESS 2003*, pp. 387-392, Washington DC, USA, June 2003.

Bias tuning of the G-estimate in the multivariable case

M. Leskens[a], P.M.J. Van den Hof[b] and O.H. Bosgra[c]
[a]TNO Environment, Energy and Process Innovation, Apeldoorn, The Netherlands
[b, c]Delft Center for Systems and Control, Delft University of Technology, Delft, The Netherlands
[a]m.leskens@mep.tno.nl, [b]p.m.j.vandenhof@dcsc.tudelft.nl and [c]o.h.bosgra@dcsc.tudelft.nl

Abstract

In the system identification literature one distinguishes two possible assumptions when performing analytic investigations on the asymptotic characteristics of the obtained estimates: (i) the true system can exactly be disclosed and (ii) the true system can at best only be approximated. Focussing on the G-estimate obtained with the prediction error method of identification [1], this distinction translates to the distinction in (i) the assumption that the true system G is contained in the model set ($G_o \in \mathcal{G}/\mathcal{S} \in \mathcal{M}$) and (ii) the assumption that the true G is not contained in the model set ($G_o \notin \mathcal{G}/\mathcal{S} \notin \mathcal{M}$). This distinction reflects itself also in the nature of the convergence analyses for both these approaches. In the (*exact* modelling) case of (at least) $G_o \in \mathcal{G}$ the convergence analysis focuses on finding conditions for which a consistent G-estimate is obtained. Well-known results in this respect are that

- in the case of (completely) closed-loop data the noise model has to be estimated consistently in order to obtain also a consistent G-estimate
- in the case of open-loop data a consistent G-estimate is obtained irrespective of whether a consistent noise model is obtained or not

A less well-known result in this respect is that in the case of partial closed-loop data, i.e. when part of the inputs is being manipulated and a remaining part is not, under general conditions the complete noise model has to be estimated consistently in order to obtain a completely unbiased G-estimate; when it comes to consistency it thus resembles a completely closed-loop situation. When the output additive disturbances are uncorrelated and the noise model is parameterized accordingly or when certain channels in the real G are absent, only part of the noise model needs to be estimated consistently in order to obtain a completely unbiased G-estimate. See [2].

In contrast, in the (*approximate* modelling) case of $G_o \notin \mathcal{G}$, the convergence analysis focuses on maintaining the possibility of tuning the inevitable bias in such a way that its distribution over the dynamical c.q. frequency range is optimal with respect to the intended use of the model. When this intended use is control design, the presence of the possibility of tuning the bias allows for *identification for control* or *control relevant identification*, which is currently one of the main reseach directions in the identification community. The idea of using a control-relevant bias tuning filter to improve the incorporation of the control-relevant dynamics in the estimated model is used in e.g. [3].

One characteristic of the *identification for control*- c.q. bias tuning literature is that it generally considers only SISO systems. Tuning the bias of the G-estimate for these systems is easily performed using a prefilter consisting of the input spectrum, noise model and/or data filters. The particular issues and possible problems related to tuning the bias of a *multivariable* G-estimate have not been considered to this date, not even for the open-loop case, (at least not to the knowledge of the authors) while many real-life systems to be identified are multivariable, in particular in the process industries. The aim of this presentation is to fill in this gap: the question that will be addressed is how to tune the biases of part or all of the SISO transfer functions of a multivariable G-estimate. This will be done only for the open-loop case.

The results discussed during the presentation are summarized in [4].

References

[1] L. Ljung (1999). *System Identification: Theory for the User*, Second Edition, Prentice-Hall, Upper Saddle River, NJ.

[2] M. Leskens and P.M.J. Van den Hof (2004). Closed-loop identification of multivariable processes with part of the inputs controlled. *Accepted for the 2004 American Control Conference, Boston*.

[3] D.E. Rivera, J.F. Pollard and C.E. Garcia (1992). Control-Relevant Prefiltering: A Systematic Design and Case Study. *IEEE Trans. Aut. Contr.* , **37**, pp. 964-974.

[4] M. Leskens and P.M.J. Van den Hof (2004). Bias tuning of a multivariable G-estimate.*To be discussed and perhaps submitted*.

Identification of Local Linear Models with Separable Least Squares

José Borges
DCSC
Mekelweg 2
2628 CD Delft
The Netherlands
j.borges@dcsc.tudelft.nl

Vincent Verdult
DCSC
Mekelweg 2
2628 CD Delft
The Netherlands
v.verdult@dcsc.tudelft.nl

1 Abstract

This paper presents a new approach towards the identification of Local Linear Models (LLM) from input-output data. The main feature of this approach is to estimate the LLM parameters based on the Separable Least Squares (SLS) optimization technique. Additionally, this approach also considers the use of a dynamic parametrization for the state space matrices.

2 Local linear Models

The motivations to approximate nonlinear dynamical systems via LLM is widely discussed e.g. in [1]. The LLM can be described as a weighted combination of several local linear models, which are designed to approximate the dynamical behavior of nonlinear systems. In the work of Verdult [1] a new approach for the identification of LLM was proposed, consisting of the identification of several linear state-space models and their combination based on radial basis functions:

$$\begin{aligned} x_{k+1} &= \sum_{i=1}^{s} p_i\left(\phi_k, c_i, w_i\right)\left(A_i x_k + B_i u_k + O_i\right) \\ y_k &= C x_k + v_k \end{aligned}$$

where s is the number of LLM, $x_k \in \mathbb{R}^n$ is the state vector, $u_k \in \mathbb{R}^m$ is the input, $y_k \in \mathbb{R}^l$, s is the output, $v_k \in \mathbb{R}^l$ is a white noise sequence and $p_i\left(\phi_k, c_i, w_i\right)$ is the scheduling vector, defined as normalized radial basis functions with center c_i and width w_i. Therefore, the identification problem resumes to the estimation of A_i, B_i, O_i, C and of the parameters for the weights c_i and w_i.

3 Separable Least Squares

This identification of LLM is based on a gradient-type optimization process, therefore, a nonlinear cost function has to be minimized over the available input-output data. This type of procedure normally implies a large number of parameters to be manipulated at a time, with consequences both in the numerical stability and conditioning of the problem and also in the computational burden. Therefore, to handle these problems, the viability of performing a Separable Least Squares (SLS) optimization is currently under research. The SLS is a method developed by Golub and Pereyra [2] to solve nonlinear optimization problems, based in a reduction of the number of parameters to be optimized. This reduction is accomplished by the separation of these parameters accordingly to the way they enter in the output equation, i.e., linearly, θ_l, or nonlinearly, θ_n. The optimization is then performed independently, first for the nonlinear part and then for the linear part. This procedure demands the manipulation of the LLM equations into a suitable structure, resulting in the following problem:

$$\min_{\theta_n,\theta_l} \left\| Y - \Phi\left(\theta_n\right)\theta_l \right\|_2^2$$

$$\downarrow_{\text{SLS}}$$

$$\begin{cases} \min\limits_{\theta_n} \left\| Y - \Phi\left(\theta_n\right)\Phi\left(\theta_n\right)^{\dagger} Y \right\|_2^2 \\ \theta_l = \Phi\left(\theta_n\right)^{\dagger} Y \end{cases}$$

Regarding an efficient implementation of these algorithms, the use of mathematical tools, e.g. the *QR-decomposition*, is also under research.

4 Parametrization

The performance of the optimization algorithms, used for system identification, is highly influenced by the nonuniqueness of the input-output state-space representation. This feature normally results in an ill-conditioned optimization problem. To handle this problem an adequate parametrization for the system matrices has to be used. This parametrization needs to take into account the requirements of the SLS optimization. Here, the use of an approach similar to that used by Ribarits [3] is under research.

References

[1] V. Verdult, L. Ljung and M. Verhaegen. Identification of composite local linear state-space models using a projected gradient search. *INT. J. CONTROL*, 75(16/17):1385 – 1398, 2002.

[2] G. H. Golub and V. Pereyra. The differentiation of pseudo-inverse and nonlinear least squares problems whose variables separate. *SIAM J. Numer. Anal*, 10(2):413 – 432, April 1973.

[3] T. Ribartis, M. Deistler and B. Hanzon. Separable least squares data driven local coordinates. *13th IFAC Symposium on System Identification*, pages 1922–1927, 2003.

Computation of LTI system responses directly from input/output data

Ivan Markovsky, Jan C. Willems, Bart De Moor
Departement Elektrotechniek, Katholieke Universiteit Leuven
{ivan.markovsky, jan.willems, bart.demoor}@esat.kuleuven.ac.be

Paolo Rapisarda
Departement Mathematics, Universiteit Maastricht
p.rapisarda@math.unimaas.nl

Abstract

Let $w = (u, y)$ be an exact input/output trajectory of an LTI system $\mathcal{S}$. We give conditions under which an arbitrary response of $\mathcal{S}$ can be constructed directly from w and an iterative algorithm that does this. In particular, the impulse response can be obtained from w. Followed by a realization algorithm, this gives a new exact identification procedure.

Let $\mathcal{H}_l(\cdot)$ be a block-Hankel matrix with l block-rows, *e.g.*, with $u(1),\dots,u(T)$,

$$\mathcal{H}_l(u) = \begin{bmatrix} u(1) & u(2) & \cdots & u(T-l+1) \\ u(2) & u(3) & \cdots & u(T-l+2) \\ \vdots & \vdots & & \vdots \\ u(l) & u(l+1) & \cdots & u(T) \end{bmatrix}.$$

Let $\mathtt{n}_{\max}$ be an upper bound on the system order $\mathtt{n}$ and define $U_\mathrm{p} \in \mathbb{R}^{\mathtt{n}_{\max}\mathtt{m}\times\cdot}$ $U_\mathrm{f} \in \mathbb{R}^{l\mathtt{m}\times\cdot}$, $Y_\mathrm{p} \in \mathbb{R}^{\mathtt{n}_{\max}\mathtt{p}\times\cdot}$, $Y_\mathrm{f} \in \mathbb{R}^{l\mathtt{p}\times\cdot}$, by

$$\mathcal{H}_{\mathtt{n}_{\max}+l}(u) =: \begin{bmatrix} U_\mathrm{p} \\ U_\mathrm{f} \end{bmatrix}, \qquad \mathcal{H}_{\mathtt{n}_{\max}+l}(y) =: \begin{bmatrix} Y_\mathrm{p} \\ Y_\mathrm{f} \end{bmatrix}.$$

Theorem 1 (Response from data). *Let (u, y) be a trajectory of a controllable LTI system $\mathcal{S}$ of order $\mathtt{n} \le \mathtt{n}_{\max}$ and let u be persistently exciting of order $l + 2\mathtt{n}_{\max}$. Then the system of equations*

$$\begin{bmatrix} U_p \\ U_f \\ Y_p \end{bmatrix} g = \begin{bmatrix} \bar{0} \\ \bar{u}_f \\ 0 \end{bmatrix}, \tag{1}$$

is solvable for any u_f and any particular solution $\bar{g}$ allows the computation of the response $\bar{y}_f$ of $\mathcal{S}$ due to the input $\bar{u}_f$ and zero initial conditions as $\bar{y}_f = Y_f\bar{g}$.

The persistency of excitation assumption implies that

$$l \le \frac{T+1}{\mathtt{m}+1} - 2\mathtt{n}_{\max}, \tag{2}$$

so using (1), we are limited in the length of the response $\bar{y}_\mathrm{f}$ that can be computed from a finite w. It is possible, however, to find an arbitrary many sample of the response. Algorithm 1 does this by computing iteratively blocks of l consecutive samples.

Algorithm 1 (Iterative computation of response from data).

Input: u, y, $\bar{u}_\mathrm{f}$, and $\mathtt{n}_{\max}$.

1. *Initialization:* choose l according to (2), set $k := 0$,
$$f_\mathrm{u}^{(0)} := \begin{bmatrix} 0 \\ \bar{u}_\mathrm{f}(1{:}l) \end{bmatrix}, \quad \text{and} \quad f_\mathrm{y}^{(0)} := \begin{bmatrix} \bar{0} \\ * \end{bmatrix}.$$
2. *Repeat*
   - 2.1. Solve
$$\begin{bmatrix} U_\mathrm{p} \\ U_\mathrm{f} \\ Y_\mathrm{p} \end{bmatrix} g^{(k)} = \begin{bmatrix} f_\mathrm{u}^{(k)} \\ f_\mathrm{y,p}^{(k)} \end{bmatrix}, \text{ where } \begin{bmatrix} f_\mathrm{y,p}^{(k)} \\ f_\mathrm{y,f}^{(k)} \end{bmatrix} := f_\mathrm{y}^{(k)}.$$
     Let $\bar{g}^{(k)}$ be the particular solution found.
   - 2.2. Define $\bar{y}_\mathrm{f}^{(k)} := Y_\mathrm{f}\,\bar{g}^{(k)}$.
   - 2.3. Set $f_\mathrm{y,f}^{(k)} := \bar{y}_\mathrm{f}^{(k)}$ and shift $f_\mathrm{u}, f_\mathrm{y}$
$$f_\mathrm{u}^{(k+1)} := \begin{bmatrix} \sigma^l f_\mathrm{u}^{(k)} \\ \bar{u}(kl+1:(k+1)l) \end{bmatrix}, \; f_\mathrm{y}^{(k+1)} := \begin{bmatrix} \sigma^l f_\mathrm{y}^{(k)} \\ * \end{bmatrix}.$$
   - 2.4. $k := k+1$

   Until $t < kl$ $\qquad$ ($t :=$ # of samples in $\bar{u}_\mathrm{f}$)

Output: $\bar{y}_\mathrm{f} := \begin{bmatrix} \bar{y}_\mathrm{f}^{(0)\top} & \cdots & \bar{y}_\mathrm{f}^{(k-1)\top} \end{bmatrix}^\top.$

Acknowledgments

Research supported by: Research Council KUL: GOA-Mefisto 666, several PhD/postdoc & fellow grants; Flemish Government: FWO: PhD/postdoc grants, projects, G.0240.99 (multilinear algebra), G.0407.02 (support vector machines), G.0197.02 (power islands), G.0141.03 (Identification and cryptography), G.0491.03 (control for intensive care glycemia), G.0120.03 (QIT), G.0800.01 (collective intelligence), research communities (ICCoS, ANMMM); AWI: Bil. Int. Collaboration Hungary/ Poland; IWT: PhD Grants, Soft4s (softsensors), Belgian Federal Government: DWTC (IUAP IV-02 (1996-2001) and IUAP V-22 (2002-2006), PODO-II (CP/40: TMS and Sustainability); EU: CAGE; ERNSI; Eureka 2063-IMPACT; Eureka 2419-FliTE; Contract Research/agreements: Data4s, Electrabel, Elia, LMS, IPCOS, VIB;

Broad-band Active Vibration Suppression

Arjen den Hamer[1] Georgo Angelis[2] N.B. Roozen[1,2] René v.d. Molengraft[1]

[1] Eindhoven University of Technology
a.j.d.hamer@student.tue.nl
m.j.g.v.d.molengraft@tue.nl

[2] PHILIPS Centre for Industrial Technology
georgo.angelis@philips.com
n.b.roozen@philips.com

1 Introduction

Due to the demand of higher accuracy and lower acoustic noise levels, there is a growing interest for active vibration suppression in industrial application. Noise and vibration problems often occur in mechanical distributed parameter systems which are badly damped and typically suffer from high modal density [3].

In literature, control concepts have been proposed in the field of active vibration suppression using multiple siso-feedback filters with collocated sensor/actuator pairs [2]. These concepts are suited to introduce damping in systems with a large number of modes and overcome the problems of high authority controllers such as $\mathcal{H}_2$ and $\mathcal{H}_\infty$ which suffer from spill-over effects resulting from either model- or controller-order reduction.

Due to good experiences reported in literature, Positive Position Feedback (PPF) is chosen to implement. However tuning such controllers is often focussed on reduction of one dominant mode. Other approaches are needed for broad-banded reduction of vibration levels.

2 Approach

Using negative feedback, the transfer-function of a PPF controller can be written as a summation of k modal components

$$\frac{Y_c(s)}{U_c(s)} = \sum_{n=1}^{n=k} G_n \frac{-1}{s^2 + 2\xi_{c_n}\omega_{c_n}s + \omega_{c_n}^2}$$

where Y_c and U_C are the controller output and input whereas ξ_{c_n}, ω_{c_n} and G_n are respectively the modal damping, eigenfrequency and gain of mode n.

The idea behind PPF is to create damped auxiliary degrees of freedom which participate in certain modes. (see analogy of Tuned Mass Damper [1]). A combined loop-shaping and root-locus approach is proposed to tune PPF controllers for broad-band vibration suppression.

Local performance, as can be derived from open-loop information, does not imply global performance as shown by [4]. This makes loop-shaping less suited to tune for vibration suppression. Nevertheless, open-loop information is still valuable for stability analysis.

Since every input-output transfer of a mechanical distributed system can be written as a sum of modal components, each transfer has the same pole locations. So shifting poles locally into the left half-plane (LHV), i.e. increasing modal damping, will result in vibration suppression in a global way. This is used as a root-locus tuning criterium.

The poles of the PPF controller are placed such that the attraction of root-loci of dominant modes into the LHP is maximized. By doing so, a trade-off occurs for the damping of the controller poles. Less damping results in a shift of one particular pole into the LHP whereas more damping in the controller spreads the interaction of root-loci over more modes but reduces effectiveness. As an alternative, a summation of several PPF modes can be used to create a broader frequency range for vibration suppression.

3 Results

The tuning approach is experimentally evaluated on a vibrating plate using PZT piezo's for collocated sensing and actuating. Laser vibrometer measurements show that besides local performance, reduction of vibration levels over the entire plate is achieved.

Additional aspects such as time-delay, spill-over and digital as well as analogue implementation will be discussed and verified by means of experiments.

References

[1] J. Bell and R. Kashani. Structure-borne noise reduction by active damping of a radiating panel. Proceedings of the SAE Noise and Vibration Conf., May 15-18 1995.

[2] J. L. Fanson and T. K. Caughey. Positive position feedback control for large space structures. *AIAA Journal*, 28(4), 1990.

[3] M. P. Koster. *Design Principles for Accurate Motion and Positioning (in Dutch)*. Twente University Press, Enschede.

[4] A. Preumont. *Vibration Control of Active Structures*. Kluwer Academic Publishers, Université Libré de Bruxelles, 2002.

Feedback control of broadband disturbances on a one-degree-of-freedom experimental vibration isolation set-up

G. Nijsse, H. Super, J. van Dijk and J.B. Jonker
University of Twente, Faculty of Engineering Technology
Department of Mechanical Engineering, Laboratory of Mechanical Automation
P.O. Box 217, 7500 AE Enschede, The Netherlands
Email: G.Nijsse@CTW.UTwente.NL

1 Background on vibration isolation

Vibration isolation aims at reducing the transmission of vibration from one body or structure to another [2], to prevent undesirable phenomena such as sound radiation. A well-known method for vibration isolation is the technique of passive vibration isolation, such as the use of springs and dampers. By carefully designing the stiffness properties of the material, it is possible to provide a certain level of vibration isolation. However, often it is not possible to decrease the stiffness to such a degree that proper vibration isolation is being accomplished. Especially vibrations in the lower frequencies are difficult to isolate [2]. A more promising method for vibration isolation is hybrid isolation techniques. In addition to passive isolation, an active isolation control system is being used with sensors, actuators and a controller, which compensates for those lower frequency vibrations [1].

2 Experimental set-up used for validation

For research and development, a one-degree-of-freedom (1DOF) experimental vibration isolation setup has been built at the laboratory. The setup is depicted in Figure 1. An electro-dynamic shaker serving as a vibration source excites a mass with an unknown disturbance. The mass is mounted on a clamped metal plate by a ceramic piezo-electric actuator which operates as a hybrid isolation mount. The goal of the set-up is to minimize the acceleration sensor output by properly steering the ceramic piezo-electric actuator input on the basis of an adaptive controller. The set-up is sampled at a sample frequency of 4 kHz. For control hardware the dSPACE DS1103 single board ISA controller is used.

3 Contribution of our work

First, for control of the set-up, a model of the transfer path between the ceramic piezo-electric actuator input to the error sensor output is required (i.e. a model of the secondary path **S**). This problem is solved by making use of the PO-MOESP class of subspace identification routines [5, 6]. It is demonstrated that an accurate 28^{th} order state space based black-box model can be identified of the secondary path **S**. Second, it is shown that by making use of an adaptive feedback controller which is parameterized as a finite impulse response filter and which is updated on the basis of the post-conditioned filtered-x least mean square algorithm [1, 3, 4], broadband isolation control is achieved with reductions of 9 dB, 5 dB, 12 dB and 3 dB on the four main resonance peaks of the set-up.

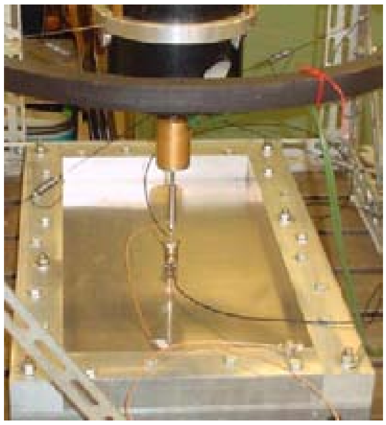

Figure 1: The one-degree-of-freedom vibration isolation set-up

References

[1] Stephen Elliott. *Signal Processing for Active Control*. Academic Press, 2000.

[2] Colin H. Hansen and Scott D. Snyder. *Active Control of Noise and Vibration*. E & FN Spon, 1997.

[3] Simon Haykin and Bernard Widrow. *Least-Mean-Square Adaptive Filters*. Wiley-Interscience, 2003.

[4] G. Nijsse, M. Verhaegen, B. De Schutter, D. Westwick, and N. Doelman. State space modeling in multichannel active control systems. In *ACTIVE 99*, pages 909–920, Fort Lauderdale, Florida, USA, December 1999.

[5] Peter van Overschee and Bart de Moor. *Subspace identification for linear systems*. Kluwer Academic Publishers, 1996.

[6] M. Verhaegen. Identification of the deterministic part of MIMO state space models given in innovations form from input-output data. *Automatica*, 30(1):61–74, 1994.

Self-Excited Vibrations of Drag Bits

Christophe Germay, Rodolphe Sepulchre
Department of Electrical Engineering and Computer Science
Université de Liège, Belgium
germay@montefiore.ulg.ac.be, R.Sepulchre@ulg.ac.be

1 Abstract

This research is concerned about the study of self-excited vibrations that occur when drilling with rotary system equiped with PDC bits. In this novel approach [5], the discrete model takes into consideration the axial and the torsional modes of vibration. This simple mechanical model consists in a torsional spring, a punctual mass and inertia. The coupling between these two modes through rate-independent bit-rock interaction laws that account for the cutting and the frictional process are based on the phenomenological DD model [3].

Because of the helical motion of the bit, the cutting forces depend on a varying delayed axial position of the bit. This delay dependance is ultimately responsible for the existence of self-excited vibrations. Numerical simulations showed that they may degenerate into stick-slip oscillations or bit bouncing for sets of parameters in accordance with quantities used in real field operations. Such extrem types of vibrations are at the origin of important bit or drillstring failures.

It was found that the key quantity governing the mean response of the system is a parameter κ, which is an indirect measure of the level of the axial vibrations. Indeed, the mean rate of penetration and the mean torque depend on this quantity, as well as on the rate independant parameters characterizing the system.

Commonly assumed to be an intrinsic property of the bit-rock interaction laws [1, 4, 2], the velocity weakening law (decrease of the friction coefficient with respect to the prescribed angular velocity) is not a cause but a consequence of the self-excited vibrations. It is directly related to the variation of κ (level of axial vibrations).

The importance played by the axial vibrations on the mean system response emphasizes the necessity to increase the number of degrees of freedom to model the drillstring in a more realistic way. Current research is focused on the integration of finite elements in the mechanical model to see the influence on the system response when a softer mechanical system is placed above the bit .

References

[1] J. F. Brett, *The genesis of torsional drillstring vibrations*, SPE Drilling Engineering (1992), 168–174.

[2] N. Challamel, *Rock destruction effect on the stability of a drilling structure*, Journal of Sound and Vibration **233** (2000), no. 2, 235–254.

[3] E. Detournay and P. Defourny, *A phenomenological model of the drilling action of drag bits*, Int. J. Rock Mech. Min. Sci. & Geomech. Abstr. **29** (1992), no. 1, 13–23.

[4] D. R. Pavone and J. P. Desplans, *Application of high sampling rate downhole measurements for analysis and cure of stick-slip in drilling*, SPE 28324 (1994).

[5] T. Richard, *Self-excited stick-slip oscillations of drag bits*, Ph.D. thesis, University of Minnesota, December 2001.

$\mathscr{H}_2$-Optimal Controller Synthesis - A MIMO Frequency-Domain Solution

J.A. Villegas
Department of Applied Mathematics
Twente University
P.O. Box 217, 7500 AE Enschede
The Netherlands
Email: j.a.villegas@math.utwente.nl

1 Introduction

This article develops a frequency domain solution to the $\mathscr{H}_2$ control problem. This is a two-block optimal controller synthesis problem, with standard solutions in the time domain. This paper presents a frequency domain solution to this problem. The advantages of such an approach are discussed. Also some examples are given, which illustrate the computational solution.

2 Approach

In the optimal 2-norm controller synthesis, one seeks a controller which stabilizes the control system and minimizes a given quadratic cost function. The first important contributions to this problem uses the Kalman filter and its extension to Linear Quadratic Gaussian control (LQG). This was further extended by robust control theorists, who generalized the problem, leading to the four block $\mathscr{H}_2$ problem. The best known solution of this problem is described by Doyle et al. [1].

A nice feature of the present approach is that the solution is closed form. Being in the frequency domain, it is more transparent than a pair of coupled time domain Riccati equations. This method also gives insight into many issues, such as where the controller poles go as weights varies.

The approach taken here uses the sensitivity and complementary sensitivity function as a measure of robustness. Here we solve the two-block problem, which is to minimize the two-norm of the square of the magnitude of the sensitivity and the complementary sensitivity function. This amounts to the minimization of

$$\left\| \begin{array}{c} W_s S \\ W_t T \end{array} \right\|_2^2 , \qquad (1)$$

where W_s and W_t are weighting functions used to shape S and T, respectively. The sensitivity function, S, determines the effect of disturbances on the closed-loop system. The complementary sensitivity function, T, is important for the closed-loop response, the effect of measurement noise, and robust stability.

Typically, control system design amounts to shaping these functions aiming for the following objectives

- Make the sensitivity S small at low frequencies.
- Make the complementary sensitivity T small at high frequencies.
- Prevent both S and T from peaking at crossover frequencies.

The approach taken here is based on the Youla parameterization (see Maciejowski [2, §6]), which is a useful tool that facilitates the solution of the $\mathscr{H}_2$ problem, since it allows the cost function (1) to be written in terms of a single parameter, Q. That is, the optimal Q is calculated and then using the Youla parameterization the corresponding optimal controller K is found. In this way, closed loop stability is equivalent to the stability of Q.

3 Presentation

First the general idea of the approach is introduced. Next the Youla parameterization is briefly stated. It is also shown how to reduce the two-block problem (1) into a one-block problem. The solution to the one-block problem is given next. Ideas of how to choose the weights are presented and some examples are shown which give more details on the selection of weights. Finally, some concluding remarks are presented.

References

[1] J. Doyle, K. Glover, P. P. Khargonekar and B. A. Francis, “State-space solutions to the standard $\mathscr{H}_2$ and $\mathscr{H}_\infty$ control problems,” IEEE Trans. Automat. Contr., Vol. 34, No. 8, pp. 831–846, 1989.

[2] J. M. Maciejowski, “Multivariable Feedback Design,” Addison Wesley, 1989.

H_2-optimal control of systems with multiple i/o delays: time domain approach

Agoes A. Moelja and Gjerrit Meinsma
Department of Applied Mathematics, University of Twente
P.O. Box 217, 7500 AE Enschede, The Netherlands
Email: {a.a.moelja, g.meinsma}@math.utwente.nl

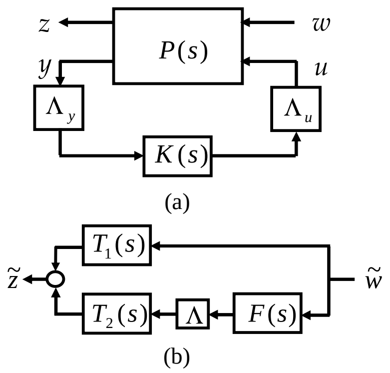

Figure 1: The H_2 control problem with multiple i/o delays and its equivalent filtering problem.

Abstract

We consider the control system configuration of Figure 1(a) where the plant $P(s)$ is a rational transfer matrix and the multiple-delay operators $\Lambda_u(s)$ and $\Lambda_y(s)$ represent different delays in each channel of the input and output of the plant, respectively. The H_2-optimal control problem is to find a stabilizing LTI causal controller such that the H_2-norm of the overall transfer function from w to z is minimized:

$$\min_{K(s)} \|F_\ell\left(P(s), \Lambda_u(s)K(s)\Lambda_y(s)\right)\|_2. \tag{1}$$

In [2], partly using techniques developed in [1], it is shown that if the delays are present only either in the input or in the output, i.e. if either $\Lambda_u(s) = I$ or $\Lambda_y(s) = I$, then the control problem (1) is equivalent to a (transposed) filtering problem of the form

$$\min_{F(s)} \|T_1(s) + T_2(s)\Lambda(s)F(s)\|_2 \tag{2}$$

where $T_1(s)$ and $T_2(s)$ are rational transfer matrices that can be determined from the plant $P(s)$. The delay operator $\Lambda(s)$ is equal to either $\Lambda_u(s)$ or $\Lambda_y(s)$, whichever not equal to the identity. It is also shown that the connection between the filter $F(s)$ and the controller $K(s)$ is established through a causal bijection. Once the optimal filter F_{opt} is known, it is trivial to compute the optimal controller.

In [2], the (transposed) filtering problem (2) is solved using frequency domain techniques. However, the method works well only for open-loop stable plants. For unstable plants pre-multiplication of the filtering equation (2) by a certain all-pass transfer function, which makes the formulas unnecessarily complicated, is needed. In addition, the resulting optimal filter has a considerably larger dimension than the plant.

In this work, an alternative time-domain approach for solving the filtering problem (2) is developed. In time domain, the objective (2) is

$$\min_{F(t)} \|T_1(t) + T_2(t) * \Lambda(t) * F(t)\|_2 \tag{3}$$

where $F(t)$, $T_1(t)$, $T_2(t)$, and $\Lambda(t)$ are the impulse responses of F, T_1, T_2, and Λ. Since in (2) we may optimize each column of $F(t)$ independently, without loss of generality we may assume that $F(t)$ is a single-column impulse response. By this assumption, we may view the quantity $(T_1(t) + T_2(t) * \Lambda(t) * F(t))$ as the output of the system $\begin{bmatrix} T_1 & T_2 \end{bmatrix}$ with $\text{col}(\delta(t), \Lambda(t) * F(t))$ as its input. The objective (3) becomes finding the optimal input $(\Lambda(t) * F(t))$ for the system $\begin{bmatrix} T_1 & T_2 \end{bmatrix}$ such that the H_2-norm of the output is minimized. This is actually a linear quadratic regulator (LQR) problem with multiple input delays.

By employing the fundamental principle of optimal control theory, namely the principle of optimality, it may be shown that the resulting LQR problem with multiple input delays may be reduced to N standard finite-horizon LQR problems plus a standard infinite-horizon LQR problem, the solutions to which are readily available. Here N is the number of distinct delays in Λ. The resulting controller consists of a rational transfer matrix block, a finite impulse response block, and delay components. The rational part of the controller has the same dimension as the plant and the method does not have any problem in handling unstable plants.

References

[1] L. Mirkin, "On the extraction of dead-time controllers and estimators from delay-free parametrization", *IEEE Trans. Automatic Control*, vol. 48, pp. 543-553, 2003.

[2] A.A, Moelja, G. Meinsma, and J. Kuipers, "H_2-optimal control of systems with multiple i/o delays", *Preprints of the IFAC workshop on time-delay sytems*, Rocquencourt, France, 2003.

Shape change of tensegrity structures: design and control

Jeroen van de Wijdeven
Department of Mechanical Engineering
Technische Universiteit Eindhoven
P.O. Box 513, 5600 MB Eindhoven
The Netherlands
Email: J.J.M.v.d.Wijdeven@tue.nl

Bram de Jager
Department of Mechanical Engineering
Technische Universiteit Eindhoven
P.O. Box 513, 5600 MB Eindhoven
The Netherlands
Email: A.G.de.Jager@wfw.wtb.tue.nl

1 Introduction

Tensegrity structures are built up from bars and tendons, where bars are placed discontinuously in a continuous network of tendons [1]. While tendons can only handle tensile forces, bars can be subjected to both tensile and compressive forces. Integrity (stability) of the tensegrity structure is obtained through pre-stress of the tendons. The word *tensegrity* is obtained by coining *tens*ion and int*egrity*.

Changes in the shape of a tensegrity structure are possible by altering the unstressed length of tendons [2]. Methods for generating reference trajectories for shape control of tensegrity structures and for designing a feedback controller that suppresses structural vibrations, while maintaining integrity of the structure, have been developed.

2 Shape changes

Design of the reference trajectory for changing shape is accomplished using an optimization algorithm. The objective for the optimization problem is selected to represent the control effort, the changes in tendon length. Several constraints must be met:

- *Collision avoidance*: if elements collide during the shape change, the shape change may not be feasible or elements can be damaged.
- *Geometry related constraints*: desired shape and/or desired nodal positions, fixed bar lengths, minimum allowed tendon lengths, and fixed nodal positions by, e.g., joints.
- *Force related constraints*: tension in all tendons, minimum and maximum allowed element forces related to pre-stress and buckling or yield respectively, and maximum allowed change in element forces to avoid possible damage to the elements.

When the optimization problem is feasible, a reference trajectory for the shape change is generated.

3 Dynamics and control

The reference trajectory is used as a feedforward signal for the shape change of the tensegrity structure. To suppress vibrations in the system, an $\mathcal{H}_2$ controller is introduced. However, other control strategies can also be used [3]. Since the control strategy is based on a linear model, the non-linear dynamics of the structure is linearized.

With de design of the $\mathcal{H}_2$ controller, attention is paid to external disturbances, control inputs, and weighting filters. Since integrity of the structure throughout the shape change is desired, a minimal tension requirement is included in the control objectives.

4 Example

The methods developed are applied to a two dimensional tensegrity structure:

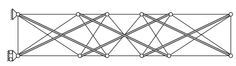

When only the feedforward signals are used for the shape change, structural vibrations are clearly visible and integrity cannot be guaranteed throughout the shape change. With the $\mathcal{H}_2$ controller in the feedback loop, tension in tendons is preserved and vibrations are suppressed:

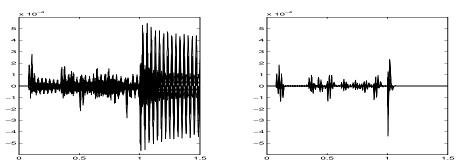

References

[1] R.E. Skelton et al., An introduction to the mechanics of tensegrity structures, www.mae.ucsd.edu/research/reskelton/tbook41.pdf, University of California, San Diego USA, 2001

[2] C. Sultan, R.E. Skelton, Deployment of tensegrity structures, *Int. Journal of Solids and Structures*, (40):4637-4657, 2003

[3] N. Kanchanasaratool, Control of flexible structure, PhD thesis, The Australian National University, March 2003

Structured Interior-Point Method based MPC for Nonlinear Processes

Andrei Tiagounov
Department of Electrical Engineering
Eindhoven University of Technology,
P.O. Box 513, 5600 MB Eindhoven
The Netherlands
a.tiagounov@tue.nl

Jeroen Buijs
Department of Energy
Leuven Engineering School, Group T
Vesaliusstraat 13,
3000 Leuven, Belgium
jeroen.buijs@groept.be

Siep Weiland
Department of Electrical Engineering
Eindhoven University of Technology,
P.O. Box 513, 5600 MB Eindhoven
The Netherlands
s.weiland@tue.nl

Ton Backx
IPCOS Technology Netherlands
Bosscheweg 145a,
5282 WV Boxtel
The Netherlands
ton.backx@ipcos.com

1 Introduction

Process industry requires now more accurate, efficient and flexible operation of the plants. Nonlinear MPC optimizations become computationally expensive to be solved in real-time. This presentation considers MPC algorithm for nonlinear plants using successive linearization. The prediction equation is computed via nonlinear integration. Local linear approximation of the state equation is used to develop an optimal prediction of the future states. The output prediction is made linear with respect to the undecided control input moves, which allows to reduce the MPC optimization to a quadratic programming problem (QP). A structured interior-point method (IPM) has been proposed to solve the MPC problem for large-scale nonlinear systems. The cost of this approach is linear with the horizon length, compared with the cubic growth for the standard optimizers.

2 Structured IPM based MPC

The constrained optimization programs tend to become too large to be solved in real-time when standard QP solvers are used. To reduce computational complexity we solve the QP problem using a structured interior-point method [1, 2, 3, 4]. Many industrial examples show that large-scale, usually stiff, nonlinear systems may require long horizons to fulfill performance requirements. Naive implementations of standard QP solvers could be inefficient for such MPC problems. The proposed optimization algorithm explicitly takes the structure of the given problem into account such that the computational cost varies linearly with the number of optimization variables. The algorithm also easily allows to introduce multiple linear models. The state elimination was not carried out and the structure given by the dynamics of the plant reflected in the Karush-Kuhn-Tucker (KKT) equations that were used to solve the QP using an interior-point method. The structured IPM is implemented using primal-dual Mehrortra's algorithm including prediction, correction and centering steps. The optimization variables consist of the inputs and the states over the horizon, but the optimization problem becomes sparse to allow computational time reduction, which is an important issue for on-line implementations of MPC for nonlinear stiff systems. In this paper the effectiveness of the structured IPM based model predictive controller is demonstrated on two industrial chemical processes, namely a continuous stirred tank reactor and a stiff nonlinear batch reactor.

References

[1] A. Tiagounov, J. Buijs, S. Weiland, and B. De Moor. Long horizon model predictive control for nonlinear industrial processes. In Proc. European Control Conference, Cambridge, UK, 2003.

[2] A. Tiagounov and S. Weiland. Model predictive control algorithm for nonlinear chemical processes. In Proc. Physics and Control Conference, St.Petersburg, Russia, 2003.

[3] C.V. Rao, S.J. Wright, and J.B. Rawlings. Application of interior-point methods to model predictive control. Journal of Optimization Theory and Applications 99:723–757, 1998.

[4] J. Buijs, J. Ludlage, W. van Brempt, B. De Moor. Quadratic programming in model predictive control for large scale systems. Proc. IFAC World Congress 2002. Barselona, Spain.

Model predictive control for mixed urban and freeway networks

M. van den Berg
Delft Center for Systems and Control
Delft University of Technology
Mekelweg 2, 2628 CD Delft
The Netherlands
m.vandenberg@dcsc.tudelft.nl

B. De Schutter
Delft Center for Systems and Control
Delft University of Technology
Mekelweg 2, 2628 CD Delft
The Netherlands
b.deschutter@dcsc.tudelft.nl

J. Hellendoorn
Delft Center for Systems and Control
Delft University of Technology
Mekelweg 2, 2628 CD Delft
The Netherlands
j.hellendoorn@dcsc.tudelft.nl

Abstract

We consider coordinated traffic control for networks consisting of both urban roads and freeways. One of the main problems that has to be addressed when designing traffic control strategies for such networks is that we should prevent a shift of problems from the urban network to the freeway network (or vice versa) due to the applied control strategy.

We develop an integrated model to describe the evolution of the traffic situation in mixed urban and freeway networks. For the freeways we use the METANET [3] macroscopic traffic flow model, that describes the evolution of the state variables density, the speed, and the flow for each segment of a freeway.

For the urban traffic a new model is developed that is based on an earlier model by Kashani [1]. We have added the following extensions:

- blocking effect: horizontal queues are used to describe the effect that a full link can block an upstream link.
- turning-dependent queues: the queue dynamics if one direction is blocked are modeled by turning-dependent queues.
- shorter simulation time step: a shorter time step makes it possible to give a more accurate description, and especially to detect a blockage earlier.

To complete the model for mixed urban and freeway networks we provide model equations that describe the connection between the two models via on-ramps and off-ramps.

We present a model predictive control (MPC) framework [2] for mixed urban and freeway networks. The control objective used is the total time spent by all vehicles in the network, and the control measures are the urban traffic signals (but the method can easily be extended to include other objectives, control measures and/or constraints).
The model and the control approach are illustrated via a simple case study, for which MPC control results in a reduction with about 8 % of the total time spent with respect to fixed-time control.

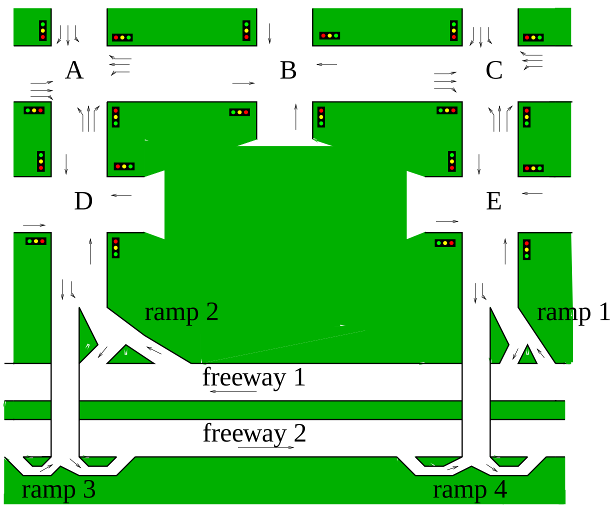

Figure 1: Network used for the case study

References

[1] G.N Saridis H.R. Kashani. Intelligent control for urban traffic systems. *Automatica*, 19(2):191–197, 1983.
[2] J.M. Maciejowski. *Predictive Control with Constraints*. Prentice Hall, Harlow, England, 2002.
[3] A. Messmer and M. Papageorgiou. METANET: A macroscopic simulation program for motorway networks. 31:466–470, 1990.

Efficient MPC with time-varying terminal cost using convex combinations

Bert Pluymers, Johan Suykens, Bart De Moor
K.U. Leuven, ESAT-SCD-SISTA
Kasteelpark 10, B-3001 Heverlee-Leuven, Belgium
{bert.pluymers,johan.suykens,bart.demoor}@esat.kuleuven.ac.be

Abstract

In this presentation an efficient implementation of MPC using a time-varying terminal cost is explained. The implementation uses online computed convex combinations of a precalculated set of terminal costs and constraints. The new method is shown to have better scaling properties than other MPC-schemes using time-varying terminal cost, while retaining the performance and feasibility. A generalized stability proof is given, unifying MPC with fixed terminal cost, time-varying terminal cost and the newly introduced scheme.

1 Introduction

Stability is an aspect of MPC that has been studied intensively in the last decade. The main ingredients for imposing stability are **a)** a locally stabilizing feedback controller (terminal controller) that is appended at the end of the horizon, **b)** a terminal cost, corresponding to the Lyapunov function of the terminal controller, which is imposed on the last state of the horizon (terminal state) and **c)** a terminal constraint, corresponding to a region of attraction of the terminal controller inside which the latter doesn't violate the state and input constraints, which is also imposed on the terminal state.

These ingredients guarantee that the subsequent optimization problems are feasible (if initially feasible) and that the MPC cost function acts as a Lyapunov function, implying assymptotic stability for those initial states that result in feasible MPC optimization problems. However, a trade-off has to be made between a large terminal constraint (resulting in good feasibility) and a small terminal cost (resulting in good performance in terms of total control cost).

2 Time-varying terminal cost

Several MPC-schemes using a time-varying terminal cost have been introduced in recent years to tackle the trade-off between feasibility and optimality. They all have the common property that one or several additional variables, parametrizing the considered set of terminal costs and constraints, are added to the optimization problem, resulting in the most optimal feasible choice of terminal cost at each time step. In general, several LMI-constraints that express the dependence of the terminal cost and constraint on the parameters, also have to be added to the optimization problem. Generally, this results in a significant increase in computational complexity compared to MPC with fixed terminal cost.

3 Convex combinations

A significant amount of online computations can be avoided, by calculating a discrete set of terminal costs and constraints beforehand. Online, convex combinations can then be used to achieve a time-varying terminal cost and constraint. In this way, only a very limited number of variables and LMI constraints have to be added to the online optimization problem, restoring the scalability of the more classical MPC scheme with fixed terminal cost and constraint. Almost no concessions have to be made, however, in terms of feasibility and performance. A further refinement can be made by using a time-varying subset of the discrete set of precalculated terminal costs and constraints, to further reduce the computational complexity. Finally, stability is proven by means of a unifying stability theorem and illustrated by examples.

Acknowledgements Bert Pluymers is a research assistant with the KUL. Johan Suykens is an associate professor with KU Leuven Dr. Bart De Moor is a full professor at the KU Leuven, Belgium. Research supported by Research Council KUL: GOA-Mefisto 666, several PhD/postdoc & fellow grants; Flemish Government: FWO: PhD/postdoc grants, projects, G.0240.99 (multilinear algebra), G.0407.02 (support vector machines), G.0197.02 (power islands), G.0141.03 (Identification and cryptography), G.0491.03 (control for intensive care glycemia), G.0120.03 (QIT), G.0800.01 (collective intelligence), research communities (ICCoS, ANMMM); AWI: Bil. Int. Collaboration Hungary/ Poland; IWT: PhD Grants, Soft4s (softsensors), Belgian Federal Government: DWTC (IUAP IV-02 (1996-2001) and IUAP V-22 (2002-2006), PODO-II (CP/40: TMS and Sustainability); EU: CAGE; ERNSI; Eureka 2063-IMPACT; Eureka 2419-FliTE; Contract Research/agreements: Data4s, Electrabel, Elia, LMS, IPCOS, VIB;

References

[1] Marko Bacic, Mark Cannon, Young Il. Lee, and Basil Kouvaritakis. General interpolation in MPC and its advantages. *IEEE Transactions on Automatic Control*, 48(6):1092–1096, June 2003.

[2] Hayco H.J. Bloemen, Ton J.J. van den Boom, and Henk B. Verbruggen. Optimizing the end-point state-weighting matrix in model-based predictive control. *Automatica*, 38:1061–1068, 2002.

[3] S. Boyd, L. El Ghaoui, E. Feron, and V. Balakrishnan. *Linear Matrix Inequalities in System and Control Theory*. SIAM Publications, 1994.

[4] M. V. Kothare, V. Balakrishnan, and M. Morari. Robust constrained model predictive control using linear matrix inequalities. *Automatica*, 32:1361–1379, 1996.

[5] Young Il Lee and Basil Kouvaritakis. Superposition in efficient robust constrained predictive control. *Automatica*, 38:875–878, 2002.

[6] D. Q. Mayne, J. B. Rawlings, C. V. Rao, and P. O. M. Scokaert. Constrained model predictive control: Stability and optimality. *Automatica*, 36:789–814, 2000.

[7] Z. Wan and M. V. Kothare. Efficient robust constrained model predictive control with a time varying terminal constraint set. *Systems and Control Letters*, 39:375–383, 2003.

Experiment design and realization for the identification of a six-degree of freedom Stewart Platform

Maria Isabel Parra Calvache
Delft Center for Systems and Control
Delft University of Technology
Mekelweg 2, 2628 CD Delft, The Netherlands
Email: m.i.parra@dcsc.tudelft.nl

1 Abstract

Non-linear mechanical systems with several degrees of freedom that require high dynamical performance over their whole operating envelope must be based on dynamic models that carefully represent both the global non-linear behavior, the representation of dominant structural flexible dynamics and the inclusion of relevant other parasitic phenomena.

The SIMONA research simulator project (SIMONA stands for the Institute for research in Simulation, Motion and Navigation) has as one objective the study in the field of simulation with an advanced flight-simulator. This simulator is composed by a light-weight cockpit mounted over a six degree of freedom motion platform. It is desired that this simulator works on a wider bandwidth than conventional simulators, in order to simulate special conditions; therefore the simulator is lighter and more flexible which would introduce important flexible dynamics to be considered for high performance control. The wide bandwidth makes necessary the high dynamical performance over the flight simulator limited workspace, which is to be achieved by a model based controller that takes into account uncertainties and non-linearities of the system over the operating envelope.

At present, an approximation of the real system considering only the motion platform dynamics has been used for an initial control design [1]. Better approximations of the dynamics of the whole system are necessary for increasing the performance in the entire working envelope and fulfill bandwidth requirements.

In order to obtain an adequate model with system identification procedures attention should be given to the experiment design. The proper excitation of the system is crucial in order to obtain measurements with enough information over the relevant dynamics for the subsequent use of identification routines. Due to the system magnitude (6 inputs, 6 outputs), a choice has been made to use frequency domain measurements that properly designed prove to be adequate and informative. Moreover, frequency domain measurements can be superposed and adapted to particular frequency spectra resulting in good signal to noise ratios on the frequencies of interest [4].

Having a representation prior to model fitting would give us more freedom on the experiments and the frequency spectrum used. Additionally we would have the possibility to reduce or eliminate error sources prior to fitting. The errors due to model structure selection and order can be isolated from errors in excitation and measurement.

References

[1] S.H. Koekebakker, “Model based control of a flight simulator motion system, Delft University of Technology, 2001.

[2] M.R. Schroeder, “Synthesis of Low-Peak-Factor signals and binary sequences with low autocorrelation, IEEE Transactions on Information Theory, January 1970.

[3] P. Guillaume, J. Schoukens, R. Pintelon, I. Kollar, “ Crest-Factor minimization using non-linear chebyshev approximation methods, IEEE Transactions on Instrumentation and measurement, Vol. 40, No. 6, Dec, 1991.

[4] R. Pintelon, J. Schoukens. “ System Identification: A Frequency Domain approach, John Wiley and Sons, 2001.

Measuring the transfer function and characteristic impedance of transmission lines

Wim De Block
Vrije Universiteit Brussel (Dept. TW - ELEC), Pleinlaan 2, B-1050 Brussels
Phone: +32 2 6292844, Fax: +32 2 6292850, Email: wdeblock@vub.ac.be

Abstract

Measurements of transmission lines are usually done using network analyzers. To remove the systematic errors of these measurement devices, several calibration techniques have been developed (SOLT, TRL, ...). All these techniques introduce a plane of reference to which the measurements are referred. This is due to the calibration elements and for a TRL-calibration it is the characteristic impedance of the line used in the calibration method, in SOLT-calibration this is the value of the load element. When the value of the load is different from the characteristic impedance of the transmission line reflection effects will appear in the measurement data as an unwanted side-effect of calibration. In this paper it will be shown that it is possible to extract both the undistorted transfer function and the characteristic impedance of the measured transmission line.

1 INTRODUCTION

Many modeling techniques are measurement based, so accurate network measurement need to be available. These measurements are done using vectorial network analyzers (VNA) and these devices are calibrated to eliminate systematic errors by means of well known calibration techniques (SOLT, TRL,...) [1],[2].
These calibration techniques introduce a plane of reference to which the measurements are referred to. For a TRL-calibration approach this plane of reference is the characteristic impedance of the transmission line used in the calibration. For a SOLT-calibration this is typically 50Ω.
If the plane of reference does nor coincide with the characteristic impedance of the measured transmission line, reflection effects will remain in the calibrated measurements. These can be very annoying when it comes to using the measurements for modeling purposes.
It will be shown that the real transfer function and the unknown characteristic impedance of the measured transmission line can be extracted from measurements by means of an eigenvalue decomposition.

2 PROBLEM STATEMENT

The vectorial network analyzer allows the measurement of the scattering parameters S_{ij} (1). As mentioned before, this setup has to be calibrated in order to minimize systematic measurement errors [3]. Common to all methods is the introduction of a plane of reference that indicates the reference impedance in which the measurements are done.
In practice the impedance of the reference plane Z_R and the characteristic impedance Z_0 differ and reflection effects remain. As long as these effects remain, the value of the measured scattering matrix (1) is not equal to the theoretical value (2).

$$\begin{aligned} S_{11} = S_{22} &= \frac{(\bar{Z}_0^2 - 1)\sinh(\gamma l)}{2\bar{Z}_0\cosh(\gamma l) + (\bar{Z}_0^2+1)\sinh(\gamma l)} \\ S_{12} = S_{21} &= \frac{2\bar{Z}_0}{2\bar{Z}_0\cosh(\gamma l) + (\bar{Z}_0^2+1)\sinh(\gamma l)} \end{aligned} \tag{1}$$

When $Z_0 = Z_R$ (1) falls back to the theoretical scattering matrix of a transmission line (2)

$$\begin{aligned} S_{11} = S_{22} &= 0 \\ S_{12} = S_{21} &= e^{-\gamma l} \end{aligned} \tag{2}$$

3 SOLUTION

It can be shown that the eigenvalues of the transmission matrix of the transmission line are identical to the transfer function and its inverse as they would be measured in the characteristic impedance of the transmission line.

Using these eigenvalues for the transfer function and its inverse, the hyperbolic sine and cosine in (1) can be written as the sum and difference of the eigenvalues. Using these values, the system (1) has only one unknown remaining, the normalized characteristic impedance $\bar{Z}_0$. This unknown can be found using a LS-approach.

References

[1] Doug Rytting. An analysis of vector measurement accuracy enhancement techniques. *RF & Microwave Measurement Symposium and Exhibition*, March 1982.

[2] Applying error correction to network analyzer measurements. *Agilent AN 1287-3 Application Note*.

[3] Wim De Block and Yves Rolain. The influence of connector repeatability on the identification of transmission lines. *IMTC Conference Proceedings*, May 2003.

[4] Peter A. Rizzi. *Microwave Engineering: Passive Circuits*. Prentice Hall, Englewood Cliffs, 1988.

Multi-modelling of activated sludge wastewater treatment plants using data-driven techniques

G. Gins, I.Y. Smets, A.H. Geeraerd, and J.F. Van Impe
BioTeC, Bioprocess Technology and Control, Department of Chemical Engineering
Katholieke Universiteit Leuven
W. de Croylaan 46, B-3001 Heverlee, Belgium
geert.gins@cit.kuleuven.ac.be – jan.vanimpe@cit.kuleuven.ac.be

1 Introduction

Due to the decreasing availability of fresh water, there is a large need for well performing wastewater treatment plants (WWTPs). Since the common trial-and-error approach is insufficient for adequate (re)design or control, a model-based approach is adopted.

2 Model type

When selecting a model, the choice must be made whether to use a *white-box* or a *black-box* model. The knowledge-driven *white-box* model (or *first principles* model) incorporates all available mechanistic knowledge into the model structure. This type of model is very accurate in describing the observed phenomena, but the high degree of complexity and non-linearity makes it very difficult to incorporate in a design or control strategy. Examples of *white-box* models are the Activated Sludge Models proposed by Henze and co-authors for the biodegradation process and the 1D-settling model introduced by Takács and co-authors for the sedimentation process, characterizing important dynamics in an activated sludge WWTP [2, 4].

A *black box* model, like, e.g., a neural network, is data-driven, and identifies a relationship between measured values of the different in- and output variables. While this type of model often has a very low computational complexity, largely facilitating its implementation in (re)design and control schemes, it does not incorporate any available mechanistic knowledge. Furthermore, the validity of the *black-box* model is mostly limited to the range of in- and outputs that was used during the identification process.

This research will aim at combining the advantages of these two model types in a *grey-box* model: by exploiting the available mechanistic knowledge and combining it with a data-driven approach, a realistic, yet practical, model is obtained.

3 Multi-modelling of WWTPs

To model the global activated sludge WWTP, a *fuzzy* multi-model is used because this multi-model can accurately describe complex system behaviour [5]. To identify this model, the two main operations, biology and sedimentation, are modelled separately. For each unit operation (*i*) data are generated through simulations, (*ii*) the dimensionality of the dataset is reduced by means of *Principal Component Analysis*, (*iii*) the area of operation is divided into different operational regimes using a *fuzzy* clustering technique, and (*iv*) a linear model, the so-called corner model, is identified on each cluster [1, 3]. Combination of the different corner-models and appropriate control actions for the various operational regimes, using the *fuzzy* rules obtained during the clustering step, results in a global multi-model which can be exploited in control schemes for activated sludge WWTPs.

Acknowledgements

Work supported in part by Project OT/03/30 of the Research Council of the Katholieke Universiteit Leuven and the Belgian Program on Interuniversity Poles of Attraction, initiated by the Belgian Federal Science Policy Office. IS and AG are postdoctoral fellows with the Fund for Scientific Research Flanders-Belgium (FWO-Vlaanderen). The scientific responsibility is assumed by its authors.

References

[1] D.E. Gustafson, and W.C. Kessel. Fuzzy clustering with a fuzzy covariance matrix. *IEEE CDC*, 2:761-770, 1979.

[2] M. Henze, C. Grady, W. Gujer, G.V.R. Marais, and T. Matsuo. Activated sludge model no. 1. *IAWQ Scientific and Technical Report No. 1*, 1987. IAWQ, London.

[3] H. Hotelling. Analysis of a complex of statistical variables into principal components. *Journal of Educational Psychology*, 24:417-441,498-520, 1933.

[4] I. Takács, G.G. Patry, and D. Nolasco. A dynamic model of the clarification-thickening process. *Water Research*, 25(10):1263-1271, 1991.

[5] T. Takagi, and M. Sugeno. Fuzzy identification of systems and its applications to modelling and control. *IEEE transactions on Systems, Man, and Cybernetics*, 15(1):116-132, 1985.

A computational procedure for the predetermination of parameters in bioprocess models

Jürgen Fritz
Service d'Automatique
Faculté Polytechnique de Mons
Boulevard Dolez 31
B-7000 Mons
mail@fritzjuergen.de

Jens Haag
Service d'Automatique
Faculté Polytechnique de Mons
Boulevard Dolez 31
B-7000 Mons
jens.haag@fpms.ac.be

Alain Vande Wouwer
Service d'Automatique
Faculté Polytechnique de Mons
Boulevard Dolez 31
B-7000 Mons
alain.vandewouwer@fpms.ac.be

1 Abstract

Modeling and parameter identification of bioprocesses are notoriously difficult tasks, due to the following issues:

- the lack of experimental data, i.e. the number of samples and measurements is often restricted by time- and money-consuming laboratory analysis;
- the difficulty to perform experiments in a reproducible way, due to the large number of phenomena influencing cell growth;
- the lack of a priori knowledge on the biological reaction scheme, in terms of yield coefficients and kinetics;
- the model complexity, i.e. the potentially large number of involved components and number of reactions, and nonlinearities (mostly involved in the kinetics).

Once a model structure and parametrisation have been selected, it is required to infer the numerical values of the model parameters from experimental data. Recently, a systematic identification procedure has been proposed in [1], which is based on the state transformation originally introduced in [2], and which allows the yield coefficients to be estimated independently from the kinetic parameters. This procedure takes all the measurement errors into account through the formulation of maximum-likelihood criteria. Even though very efficient, this procedure can sometimes be time-consuming, and there is still a need for fast data evaluation and modeling procedure.

In this connection, this study aims at developing a semi-analytical procedure which allows a fast predetermination of model parameters. To allow analytical developments to be performed, some simplifying assumptions are required, which makes the problem solution approximate. However, a first evaluation of the model parameters can be very useful to check basic modeling assumptions, and to investigate the qualitative behavior of the key components of interest. In addition, the estimated parameter values can serve as starting points for more rigorous identification methods.

The proposed computational procedure is implemented in a Matlab tool, and illustrated with a few application examples.

References

[1] Bogaerts, Ph. and R. Hanus (2000). Macroscopic modelling of bioprocesses with a view to engineering applications. In: Focus on Biotechnology, vol. IV (Engineering and Manufacturing for Biotechnology) (Ph. Thonart and M. Hofman, Eds.), Kluwer Academic Publishers.

[2] Bastin, G. and D. Dochain (1990). On-line estimation and adaptive control of bioreactors, Elsevier, Amsterdam.

Model Reduction for Model Predictive Control of a NO_x Trap Catalyst

Maarten Nauta
Department of Electronic Engineering
Technische Universiteit Eindhoven
P.O. Box 513, 5600 MB Eindhoven
The Netherlands
Email: k.m.nauta@tue.nl

Ton Backx
Department of Electronic Engineering
Technische Universiteit Eindhoven
P.O. Box 513, 5600 MB Eindhoven
The Netherlands

1 Introduction

A NO_x trap catalyst can be used to reduce harmful NO_x emissions from vehicles that use a combustion mixture with a high amount of oxygen (lean-burn). This is done by storing NO_x on the catalyst surface during the time the engine runs lean and subsequently switching the engine to rich operation (high amount of fuel in the combustion mixture) to reduce the stored NO_x. As a fuel efficiency penalty is incurred by running the engine using a rich mixture, there is a trade-off between NO_x emission levels and fuel efficiency. A control algorithm can be used to determine how and at what moment to conduct this switch in order to obtain the best compromise between emission levels and fuel efficiency.

2 Goal

In the automotive industry simple, lumped-parameter type models are currently used as a basis for control design. The models are formulated based on practical experience and the parameters are obtained by identification. This identification process has to be repeated for different catalyst specifications and in case the catalyst ages. To approach this control problem in a more systematic manner we intend to use a model-based design approach, which starts from a first-principle model of the catalyst. The first-principle model of the catalyst that has been developed is based om a 1D model of a single catalyst channel. It contains a reaction system of 51 elementary chemical reactions and 21 species to describe storage and conversion at the catalyst surface. Limited heat and mass transfer equations are also included in the model. We aim to reduce the complexity of this type of model to obtain a control-oriented model. This model can be used for online model predictive control. This approach has the advantage that different catalyst specifications or catalyst ageing effects can easily be incorporated into the control design.

3 Model Reduction

The PDE model can be discretized along the channel axis to obtain an ODE model. The ODE model is both stiff and nonlinear due to the nature of reaction system. First, a sensitivity-based method has been used to trim the number of reactions involved and chemical species at different operating points. Subsequently singular perturbation methods have been used to identify the time-scales associated with the different reactions and species. By relating these time-scales to heat and mass transfer dynamics, steady-state approximations can be derived for parts of the model.

4 First Results

When considering a typical operating trajectory at different temperatures, around 12-17 elementary reactions and 1 chemical species on the catalyst surface can be removed from the model without affecting the response for this trajectory. Singular perturbation analysis indicated that 12-14 species can be considered to be in steady-state. This currently leaves a 7th order ODE reaction system model with a coupled AE model for the steady-state part of the model. It was also found that diffusion to the surface can be neglected for most species in a large part of the temperature range.

5 Further Work

After potential further reduction we intend to use function approximation to determine the solution of the AE system for each relevant value of the dynamic states. This will allow online integration of the dynamic model. After focusing on the reaction system it is also necessary to apply reduction methods to heat- and mass-transfer dynamics. As these dynamics are coupled to the reaction system an integrated approach will be taken. Finally, a nonlinear Model Predictive Control problem will have to be formulated based on the reduced model. In conjunction with online state and parameter estimation it should then be possible to control the NO_x trap, taking into account ageing effects.

References

[1] T. Lu, Y. Ju "Complex CSP for Chemistry Reduction and Analysis," Combust. Flame 126:1445-1455, 2001.

[2] A. Ketfi-Cherif, D. von Wissel, S. Beurthey, M. Sorin "Modeling and Control of a NOx Trap Catalyst," SAE Paper 2000011199, 2001.

Control of a spray process characterized by a dead zone and a time delay

Jan Anthonis, Herman Ramon
Department of Agro-Engineering and -Economics
K.U.Leuven
Kasteelpark Arenberg 30 3001 Heverlee
Belgium
Email: jan.anthonis@agr.kuleuven.ac.be

1 Introduction

Spraying is the most used method in agriculture to apply pesticides to the crop. Nowadays, a field is sprayed completely and farmers try to distribute the liquid as homogeneously as possible. However from an economic and ecologic viewpoint this is not the optimal way of working. Studies pointed out that weeds occur in patches on the field [1], such that it is more effective to spray only these patches. Optical sensors have been developed which can discriminate between crop and weed [1]. Once a weed is detected, a nozzle can be opened to spray the weed. The continuously opening and closing of the nozzles imposes different requirements to the hydraulics. By opening and closing of nozzles, the pressure in the systems changes abruptly. To ensure the correct dose and the desired droplet spectrum, the pressure should be maintained constant. This paper designs a control system to maintain the pressure in the conduct of the nozzles as constant as possible.

2 Description of the spray system and model for control

The pressure in the system is controlled by changing the opening to the return which lowers or increases the resistance to the return for the fluid. An electrical motor accomplishes this through a gear box, manipulating a ball valve. By the construction of the valve and friction of the ball, the valve contains a dead zone and a variable time delay. A long flexible laminated thread reenforced rubber conduct connects the valve to a steel conduct to which 6 nozzles are attached. A linear second order system approximates sufficiently accurate the behaviour of the flexible conduct. The dynamics of the steel conduct are negligible. The nozzles behave like hydraulic resistances. By opening and closing of the nozzles, their resistance changes from a certain value when opened to infinity when closed. The objective is to control the pressure after the flexible conduct, just before the spray nozzles.

For control, the considered model consists of a simple integrator, representing the action of the electrical motor (1), with a dead zone (2). The output of the model y is the square root of the pressure. This output depends through a non-linear function on the delayed motor angle x. The latter delay h can change abruptly between a minimum h_{min} and maximum h_{max} value.

$$\begin{array}{l} \dot{x} = K_m f_d(u) \\ y = \frac{\alpha x(t-h)+\beta}{x(t-h)+\gamma} \quad 0 \leq h_{min} \leq h \leq h_{max} \end{array} \tag{1}$$

$$\begin{array}{lll} f_d(u) = u & if & c_1 \leq |u| \\ f_d(u) = 0 & if & c_1 > |u| \end{array} \tag{2}$$

in which K_m, c_1, α, β, γ are constants of the system.

3 Design of the control law

Control is based on a prediction of the motor angle $\hat{x(t)}$ by making use of a Kalman filter. The control law u is as follows and is rather natural when some assumptions are made.

$$u = -a(\hat{x(t)} - x_d(t)) - u_d sign(\hat{x(t)} - x_d(t)) \tag{3}$$

in which a and u_d are design parameters. In case the prediction $\hat{x(t)}$ equals the true value $x(t)$, abstraction is made of the discontinuous term in equation (3) and $|u|$ is larger than c_1, the pole of the closed loop system is located at a.

Deeper investigation of this control law reveals that equation (3) corresponds to sliding mode control and that the speed of response is almost not governed by constant a but by the Kalman gain of the predictor. It is proven that the sliding manifold is in all cases attractive and that the closed loop system is stable for varying delay h, not exceeding a certain maximum value h_{max}. The variations of the delay h, don't need to be continuous.

References

[1] E. Vrindts, J. De Baerdemaeker, H. Ramon, 2002, "Weed detection using canopy reflection," Precision Agriculture, 3 (1): 63-80.

On open- and closed-loop control of an MMA polymerization reactor

Renato Lepore, Alain Vande Wouwer, Marcel Remy
Laboratoire d'Automatique, Faculté Polytechnique de Mons, Belgium
Renato.Lepore@fpms.ac.be

Rolf Findeisen, Frank Allgöwer
Institute for Systems Theory in Engineering, University of Stuttgart, Germany

1 Abstract

Methyl-methacrylate (MMA) polymers are used in a very wide range of applications, e.g., packaging, construction, so that their production is of notoriously high interest. Recent studies witness the challenges associated with the control of this bulk, free-radical polymerization process (see [1]). These challenges are essentially due to the following factors: stringent quality requirements on the final product, severe perturbations (reactor fouling, gel effect), model uncertainties, scarse on-line measurements of the product properties (only temperature measurements are reliable).

In this work, the control of a pilot-scale batch process, located in the C.P.E.R.I. laboratories (Prof. C. Kiparissides), Thessaloniki (Greece), is considered. In this plant, the solution temperature of the reaction liquid, hence the reaction kinetics, is adjusted by continuous heating/cooling of the reactor jacket. This is achieved by two independent valves acting on the hot and cold water flows. For control and supervisory purposes, the solution and jacket temperatures are measured on line. For simulation purposes as well as model-based control, a nonlinear state space model (see [2]) is used, which describes the mass and thermodynamic balances. The model has twelve states and the so-called gel effect is represented by a deterministic, nonlinear function of the conversion factor. The state variables are the conversion factor, three moments of the polymer distribution (quasi-steady state assumption holds for the free-radical phenomena) and the temperatures of the solution, the metal wall and the jacket.
For the control, it is assumed that all states can be measured. A two-level control strategy is employed: first, an optimal trajectory is computed off line, this trajectory is then tracked by adjusting the jacket temperature. The off line-calculated, tracked trajectory is obtained such that a cost criterion that weights a certain final molecular weight, final mass conversion and batch time is minimized.

In the frame of this paper, different controllers for tracking the optimal trajectory are examined. These controllers do actually not directly act onto the hot and cold water valves. Rather they provide the temperature setpoint for two PID controllers operating in so-called split range mode (this mode allows only one valve to be active at each time instant). As controllers providing the temperature setpoint a classical PI controller, a standard nonlinear model-based predictive (NMPC) controller (in which the jacket temperature is optimized) and an NMPC parameterized as a PI controller (in which the two PI parameters are optimized) are considered.
The performances of the controllers are compared with respect to certain, practically relevant disturbances and model-plant mismatches. In practice, most of the control problems arise due to the accumulation of impurities in the reactor, causing variations in the heat exchanges and/or the efficiency of the initiator, and to modelling uncertainties (particularly, associated to the gel effect). Hence, disturbance rejection is of particular importance. Here, as a test-example, an unknown disturbance in the heat exchange between the metal wall and the solution is considered. In this case, all three schemes exhibit satisfactory performance with respect to disturbance rejection, NMPC being more agressive with regards to the control moves. Interestingly, the NMPC schemes allow for some energy management by appropriate penalization of the system inputs.

As shown in the work, for the considered problem setup, NMPC parameterizing low-level controllers for immediate disturbance rejection does lead to satisfying control performance and disturbance rejection. More effort is currently dedicated to robustness with respect to model-plant mismatch as well as to output feedback (that is, when the state vector is estimated).

References

[1] Kiparissides, C. (1996). Polymerization reactor modeling: a review of recent developments and future directions, *Chemical Engineering Science* **51**(10), 1637-1659.

[2] Mourikas, G. (1998). Modelling, estimation and optimisation of polymerisation processes, *Ph.D. thesis*.

Datamining in the process industry: performance assessment of PID controllers

Ing. Steven Bex and Prof. Dr. Ir. Bart De Moor
K.U.Leuven ESAT – SCD / SISTA
Arenbergpark 10, 3001 Heverlee (Leuven), Belgium
{steven.bex; bart.demoor}@esat.kuleuven.ac.be
http://www.esat.kuleuven.ac.be/sista-cosic-docarch/

Introduction
In the (Chemical) Process Industry, there is a growing need to monitor the performance of actuators and the associated control loops. Small drops in performance because of bad tuning, or deteriorating mechanical characteristics of the actuator can lead to significant economical losses.

Since a few years, the availability of large databases ensures that novel techniques can be applied, using large amounts of data to assess the performance of local loops. Typically, the data will be used to model a part of the process, after which changes in the model or in the residual after simulation are being monitored to check for deterioration.

However, a few problems arise using this data-driven approach. The amount of data available can lead to problems with classical identification techniques, especially as the systems are typically non-linear, and the occurring faults will change exactly these non-linearities. Further, a major issue is to detect quality data; the systems are not persistently excited when running in steady state.

In order to address these issues, an approach based on LS-SVM [3] is proposed, using an entropy based sub-sampling technique.

Example: Simulation of level controlled tank
Description: A valve controls the flow to a tank, the level of which is being controlled by a PID controller. Over time, the valve's performance drops, due to wear.

Method: After a simple linear identification using recursive ARX, the data (e.g. 10^6 points) is being arranged into a Hankel structure where beside the delayed output and inputs, the delayed residuals after linear identification are included. This extended Hankel ensures a focus on the non-linearities, not using a non-linear algorithm to identify the linear part.

It is not possible to use this Hankel matrix in an LS-SVM non-linear regression (neither in any other non-linear technique known to us) because of the size of the matrix (typically > 1 GB). Using an entropy based criterion, a subsample can be selected with which the identification can be achieved without too much risk of running into problems with persistency of excitation.

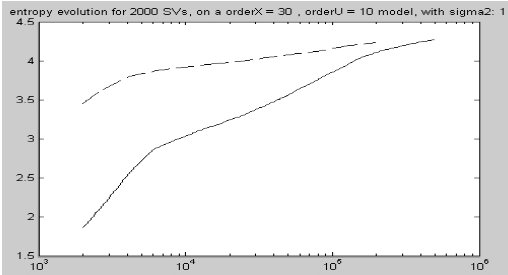

By using a heuristic algorithm, the entropy selection can be stopped considerably faster, without losing much accuracy.

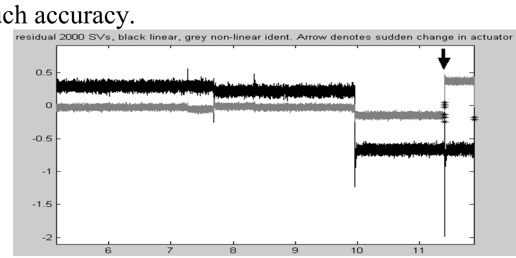

The residual clearly shows a change in the local loop, after which more detailed assessment can pinpoint the wear of the valve. Linear identification doesn't detect the problem.

[1] K. Åström & T. Hägglund. *PID Controllers: Theory, Design, and Tuning.* Second edition, 1995, ISA.

[2] J. Chen & C-M. Liao. *Dynamic process fault monitoring based on neural network and PCA*. Journal of Process Control 12 (2002) 277-289

[3] Suykens J.A.K., Van Gestel T., De Brabanter J., De Moor B., Vandewalle J., *Least Squares Support Vector Machines*, World Scientific Publishing Co., Pte, Ltd. (2002)

Ing. Steven Bex is a PhD student at the Katholieke Universiteit Leuven, Belgium.
Dr. Bart De Moor is a full professor at the Katholieke Universiteit Leuven, Belgium. Research supported by **Research Council KUL**: GOA-Mefisto 666, several PhD/postdoc & fellow grants; **Flemish Government**: **FWO**: PhD/postdoc grants, projects, G.0240.99 (multilinear algebra), G.0407.02 (support vector machines), G.0197.02 (power islands), G.0141.03 (Identification and cryptography), G.0491.03 (control for intensive care glycemia), G.0120.03 (QIT), G.0800.01 (collective intelligence), research communities (ICCoS, ANMMM); **AWI**: Bil. Int. Collaboration Hungary/ Poland; **IWT**: PhD Grants, Soft4s (softsensors), **Belgian Federal Government**: DWTC (IUAP IV-02 (1996-2001) and IUAP V-22 (2002-2006), PODO-II (CP/40: TMS and Sustainability); **EU**: CAGE; ERNSI; Eureka 2063-IMPACT; Eureka 2419-FliTE; **Contract Research/agreements**: Data4s, Electrabel, Elia, LMS, IPCOS, VIB;

Sparse LS-SVMs using Additive Regularization with a Penalized Validation Criterion

Pelckmans K., Suykens J.A.K., De Moor B.
K.U. Leuven, ESAT-SCD-SISTA
Kasteelpark Arenberg 10, B-3001 Leuven (Heverlee), Belgium
{kristiaan.pelckmans,johan.suykens}@esat.kuleuven.ac.be

Abstract

This research focusses on a new way for determining the regularization trade-off in least squares support vector machines (LS-SVMs) via a mechanism of additive regularization which has been recently introduced in [2]. This framework enables computational fusion of training and validation levels and allows to train the model together with finding the regularization constants by solving a single linear system at once. In this paper we show that this framework allows to consider a penalized validation criterion that leads to sparse LS-SVMs. The model, regularization constants and sparseness follow from a convex quadratic program in this case.

Summary

Regularization has a rich history which dates back to the theory of inverse ill-posed and ill-conditioned problems [5]. Regularized cost functions have been considered e.g. in splines, multilayer perceptrons, regularization networks, support vector machines (SVM) and related methods (see e.g. [1]). SVM [6] is a powerful methodology for solving problems in nonlinear classification, function estimation and density estimation which has also led to many other recent developments in kernel based learning methods in general [3]. SVMs have been introduced within the context of statistical learning theory and structural risk minimization. In the methods one solves convex optimization problems, typically quadratic programs. Least Squares Support Vector Machines (LS-SVMs) [4] are reformulations to standard SVMs which lead to solving linear KKT systems for classification tasks as well as regression and primal-dual LS-SVM formulations have been given for kFDA, kPCA, kCCA, kPLS, recurrent networks and control [4] [1].

The relative importance between the smoothness of the solution and the norm of the residuals in the cost function involves a tuning parameter, usually called the regularization constant. If the relative importance is given by a single parameter in the classical sense, we refer to this trade-off scheme as a Tikhonov regularization scheme [5]. The determination of regularization constants is important in order to achieve good generalization performance with the trained model and is an important problem in statistics and learning theory [1, 3]. Several model selection criteria have been proposed in literature to tune the model to the data. In this paper, the performance on an independent validation dataset is considered. The optimization of the regularization constant in LS-SVMs with respect to this criterion proves to be non-convex in general. In order to overcome this difficulty, a reparameterization of the regularization trade-off has been recently introduced in [2] referred to as *additive regularization* (AReg). The combination of model training equations of the AReg LS-SVM and the validation minimization leads to one convex system of linear equations from which the model parameters and the regularization constants follow at once. In order to explicitly restrict the degrees of freedom of the additive regularization constants (to avoid data snooping), a penalizing term is introduced here at the validation level leading to sparse solutions of AReg LS-SVMs with parameter tuning by solving a convex quadratic program. **Acknowledgements**. Research Council KU Leuven: Concerted Research Action GOA-Mefisto 666, IDO,several PhD/postdoc & fellow grants; FWO (projects G.0407.02, G.0256.97, G.0115.01, G.0240.99, G.0197.02, research communities ICCoS, ANMMM), AWI (Bil. Int. Collaboration Hungary/ Poland), IWT (Soft4s, STWW-Genprom, GBOU-McKnow, Eureka-Impact, Eureka-FLiTE, several PhD grants); Belgian Federal Government: DWTC (IUAP IV-02 (1996-2001) and IUAP V-10-29 (2002-2006)); Program Sustainable Development PODO-II (CP/40); Direct contract research: Verhaert, Electrabel, Elia, Data4s, IPCOS. JS and BDM are an associate and full professor with K.U.Leuven Belgium, respectively.

[1] http://www.esat.kuleuven.ac.be/sista/lssvmlab

References

[1] T. Hastie, R. Tibshirani and J. Friedman. The Elements of Statistical Learning: Data Mining, Inference, and Prediction. Springer-Verlag, 2001.

[2] K. Pelckmans, J.A.K. Suykens, and B. De Moor. Additive regularization: fusion of training and validation levels in kernel methods. *Internal Report 03-184, ESAT-SCD-SISTA, K.U.Leuven (Leuven, Belgium)*, 2003, submitted for publication.

[3] B. Schölkopf and A. Smola. *Learning with Kernels*. MIT Press, Cambridge, MA, 2002.

[4] J.A.K. Suykens, T. Van Gestel, J. De Brabanter, B. De Moor, and J. Vandewalle. *Least Squares Support Vector Machines*. World Scientific, 2002.

[5] A.N. Tikhonov and V.Y. Arsenin. *Solution of Ill-Posed Problems*. Winston, Washington DC, 1977.

[6] V.N. Vapnik. *Statistical Learning Theory*. Wiley and Sons, 1998.

Open questions about similarity search in high-dimensional spaces

Damien Francois(1), Vincent Wertz(1), Michel Verleysen(2)
Université catholique de Louvain
(1)CESAME Research Center
Av. G. Lemaitre, 4
B-1348 Louvain la Neuve
{francois,wertz}@auto.ucl.ac.be
(2)DICE - Machine Learning Group
Place du Levant, 3
B-1348 Louvain la Neuve
verleysen@dice.ucl.ac.be

1 Similarity search

Many data analysis methods (classification tools, clustering algorithms, ...) make use of a *similarity measure* on data. For example the well-known k-NN classifier determines the class of a new data element according to its 'similarity' with other elements for which the class label is known.

In many cases, those data are embedded (described) in a metric space (often a Euclidean space) and the similarity between two data elements is measured by the distance between their respective vector representations in the space.

A growing number of applications now involve complex data that require a high number of numerical components to be completely described. Those data have to be embedded in high-dimensional spaces (from tens to thousands dimensions). Examples are spectrophotometric data, gene expression data, texts, pictures, etc.

2 The concentration of measure phenomenon

It is well known that the Euclidean norm is subject to the *concentration phenomenon*, which expresses that the respective norms of two randomly chosen vectors in a high-dimensional space will be very similar, with a high probability. That leads to question the relevance of the Euclidean distance as a measure of similarity for complex data.

It can indeed be shown that, if $x = [x_1, \cdots, x_d]$ is a random variable in $\Re^d$,

$$\lim_{d\to\infty} \frac{\text{Std}\,(\|x\|)}{\text{E}\,(\|x\|)} = 0. \tag{1}$$

The equation says that when dimensionality grows, the standard deviation of the norm (or Euclidean distance to origin) of a random vector gets small compared to the expected value of the norm. This means that the norm of a high dimensional vector becomes nearly a constant independant on the coordinates of the vector !

Furthermore, Beyer [1] have proved that for any random $x = [x_1, \cdots, x_d] \in \Re^d$ surrounded by other points $y_i \in \Re^d$,

$$\lim_{d\to\infty} \frac{\max_i(d(x, y_i)) - \min_i(d(x, y_i))}{\min_i(d(x, y_i))} = 0. \tag{2}$$

In other words, the distances from a point to its nearest and farthest neighbours respectively, tend to be quite similar when dimension is high...

3 Practical considerations

The above-mentioned results were obtained from a theoretical viewpoint. We need to further investigate whether the intuition of irrelevance of the Euclidean norm as a similarity measure in high-dimensional spaces does have an impact in practical cases. The following questions are thus of interest.

Has the concentration phenomenon an impact on the stability of a nearest neighbour search ? Indeed we would like that if a data element x is similar to y, then y would be similar to x. In other words, if x is the nearest neighbour of y, y should be among the closest neighbours of x.

Will the use of some other metric less subject to concentration help ? It can be shown that Minkowski metrics

$$\|x\|_p = \left(\sum_i (x_i)^p\right)^{\frac{1}{p}}$$

have slower convergence rates to concentration when p is small. Will a nearest neighbour search be more stable if the value of p is well chosen ?

What impact has concentration on robustness to noise ? If two ideal elements are similar, we would like the corresponding observed data to be similar too. Are all Minkowski norms equally robust to noise ?

How influent is the intrinsic dimensionality of the data? Results (1) and (2) rely on the independance of the components x_i. Is concentration observed when there are dependences ?

Answering those questions will help improving the global performances of data analysis methods that rely on data similarity estimation.

References

[1] K.S. Beyer, J. Goldstein, R. Ramakrishnan and U. Shaft: "When Is 'Nearest Neighbor' Meaningful?", Proc. 7th International Conference on Database Theory (ICDT'99), pp.217-235

Command line completion: learning and decision making using the imprecise Dirichlet model

Erik Quaeghebeur
SYSTeMS research group
Universiteit Gent
Technologiepark 914, 9052 Zwijnaarde
Belgium
Email: Erik.Quaeghebeur@UGent.be

Gert de Cooman
SYSTeMS research group
Universiteit Gent
Technologiepark 914, 9052 Zwijnaarde
Belgium
Email: Gert.deCooman@UGent.be

1 Introduction

Our purpose is to to illustrate how models using *imprecise probabilities* [1] can be used in a practical application such as command line completion.

The central model is the imprecise Dirichlet model (IDM) [2]. It is a model for representing probabilistic information about multinomial processes, combined with an updating scheme. The updating scheme allows for learning from observations. An IDM, together with utility specifications for completion actions, can be used in decision making.

Our research, using the IDM for learning in Markov models, is incorporated in the current illustration to allow the completion method to take preceding commands into account.

2 Concepts and models

Command line completion is a feature that operating systems (OS's) provide for users working in text-mode. The user invokes the feature by pressing a predefined key after having typed part of a command. The user is then either presented with a list of n possible completions i, or, if there is only one, this completion is given on the command line.

Our objective is to add supplementary functionality to command line completion when multiple completions are possible. By modelling (making assumptions about) the behavior of the user, the OS can order the completion actions.

We assume that the user chooses an i according to an unknown, but fixed, multinomial distribution $\boldsymbol{c}$ over all possible completions. A component c_i gives the chance that the user chooses i. The set of all possible distributions $\boldsymbol{c}$ is C_n.

Practically, we only have partial, probabilistic, information about $\boldsymbol{c}$. The *imprecise Dirichlet model*, used by the OS to represent this probabilistic information, consists of a convex set of Dirichlet distributions over C_n. The expectation of $\boldsymbol{c}$ under this model consists of a subset M_t of C_n.

Every time the user enters a command, the OS updates the IDM. This results in a new IDM with a more precise expectation M_{t+1}. We take M_0 to be the whole interior of C_n.

We can make the assumptions about the user's behavior more complex by allowing the multinomial distribution $\boldsymbol{c}$ over all possible completions to depend on the command typed on the preceding command line. This behavior corresponds to a *Markov model* with an unknown transition matrix T. Each row of T will correspond to a multinomial distribution, conditional on the preceding command.

The OS then uses a modified version of the IDM, consisting of one set of Dirichlet distributions per row, to represent the probabilistic information available about T. This IDM can be updated after observing two successive commands.

3 Actions, utility and decision making

Completion actions can consist of actions a_i (presenting completion i on the command line) and a default action (giving a specially ordered list of n completions).

Whatever action the OS takes, there is only one completion that the user is looking for. Each action the OS takes thus has a certain *utility* for the user. For example, action a_i gives a utility of $+1$ if i is the correct completion and -1 if it isn't.

The OS now has a model both for what completion the user is looking for, the IDM, and for the utility of his actions. By combining these two models, the OS can calculate the *expected utility* for each of the completion actions.

The expected utility for the a_i's can then be used for *decision making*, i.e., a partial ordering of these actions can be constructed. If this ordering has one maximal element, the OS decides to present the corresponding completion. If there are multiple maximal elements, the default action is taken: showing the partial ordering to the user, such that the maximal elements are the most conspicuous ones.

References

[1] Peter Walley, *Statistical reasoning with imprecise probabilities*, Chapman and Hall, London, 1991.

[2] Peter Walley, "Inferences from multinomial data: learning about a bag of marbles," *Journal of the Royal Statistical Society* B, vol. 58, no. 1, pp. 3–57, 1996.

Identification of isotherm parameters and mass transfer coefficient in batch and SMB chromatography

V. Grosfils, M. Kinnaert,
Service d'Automatique et d'Analyse des Systèmes,
Université Libre de Bruxelles,
CP 165/55, 50, Av. F. D. Roosevelt,
B-1050 Brussels,
Belgium
Email : valerie.grosfils@ulb.ac.be

C. Levrie, A. Vande Wouwer
Service d'Automatique,
Faculté Polytechnique de Mons,
Boulevard Dolez, 31, 7000 Mons,
Belgium
Email : Caroline.Levrie@fpms.ac.be

Chromatographic separation processes are based on the differential adsorption of the components of a mixture. The Simulated Moving Bed (SMB) process, made of a series of chromatographic columns, allows a counter-current movement of the solid phase and the liquid phase, which contains the mixture to be separated, by periodically switching inlet and outlet valves in the direction of the liquid flow. The Simulated Moving Bed technology is important in various fields, from sugar to enantiomer separation. But the transfer of the SMB technology, used industrially for hydrocarbons and sugars separation, to the separation of fine chemicals is not immediate. The main issues are the selection of optimal operating conditions and the process control, problems which require the development of a model of the process and the estimation of the model parameters.

SMB models are based on the differential fluid and solid mass balances in the columns. The following equation is obtained for the component i in one column in the SMB process:

$$\frac{\partial c_i}{\partial t} = -v\frac{\partial c_i}{\partial z} + D\frac{\partial^2 c_i}{\partial z^2} - \frac{1-\varepsilon}{\varepsilon}\frac{\partial q_i}{\partial t} \qquad (1)$$

with c_i, the fluid concentration, q_i, the solid concentration, v, the fluid velocity, D, the diffusion coefficient, ε, the porosity. t denotes the time and z, the axial coordinate. The last term of the equation characterizes the mass transfer between the solid and the liquid phase. It is a function of the difference between the adsorbed concentration and the adsorbed equilibrium concentration. The latter is, in our case, a non-linear function of the fluid concentration. This function is called isotherm.

The model complexity can be modified by neglecting diffusion or by modifying the shape of transfer term. In this study, three models have been taken into account:
- the linear driving force model, that considers linear driving force for the mass transfer:

$$\frac{\partial q_i}{\partial t} = k({q^{eq}}_i - q_i) \qquad (2)$$

with q_i^{eq} the adsorbed equilibrium concentration and k the mass transfer resistance.
- the equilibrium dispersive model, which considers equilibrium between solid and fluid phase:

$$q_i = {q^{eq}}_i \qquad (3)$$

- the kinetic model that considers linear driving force for the mass transfer (Eq. 2) but neglects axial diffusion (D =0 in Eq.1).

The parameters to be estimated are the isotherm parameters, the mass transfer resistance and/or the diffusion coefficient. The parameters are estimated from experimental data (batch or SMB) by minimizing the differences between measured and simulated concentration profiles with an optimization procedure.

The parameters identifiability is checked by sensitivity analysis and by studying the identification from fictitious measurements resulting from simulations performed with a model with known parameters. These results combined with a study of the computational load for integration of the model equations show that the kinetic model offers significant advantages in comparison with the other two models.

A systematic procedure for the estimation of isotherm parameters and mass transfer resistance of a kinetic SMB model from batch and SMB measurements is presented. The contribution of this study is to propose an approach that, contrary to the techniques previously described in the literature, uses few assumptions and gives a confidence interval on the parameters.

Asymptotic Stability of a Nonisothermal Plug Flow Reactor Model

Ilyasse Aksikas, Denis Dochain
CESAME, Université Catholique de Louvain
4-6 avenue G. Lemaître, B-1348 Louvain-la-Neuve, Belgium
aksikas@auto.ucl.ac.be
dochain@auto.ucl.ac.be

Joseph J. Winkin
University of Namur (FUNDP), Department of Mathematics
8 Rempart de la vierge, B-5000 Namur, Belgium
joseph.winkin@fundp.ac.be

Key Words

Asymptotic stability, nonisothermal plug flow reactor, nonlinear contraction semigroup, nonlinear infinite dimensional system, dissipativity.

Abstract

Tubular reactors cover a large class of processes in chemical and biochemical engineering, they are typically reactors in which the medium is not homogeneous (like fixed-bed reactors, packed-bed reactors, fluidized-bed reactors,...) and possibly involve different phases (liquid/solid/gas). Such systems are sometimes called "Diffusion-Convection-Reaction" systems since their dynamical model typically includes these three terms.

The dynamics of nonisothermal plug flow reactors are described by semi-linear partial differential equations (PDE's) derived from mass and energy balances. The main source of nonlinearities in the dynamics is concentrated in the kinetics terms of the model equations.

Here we consider a nonisothermal reactor with the chemical reaction : $A \to bB$, where $b > 0$ denotes the stoichiometric coefficient of the reaction. If the kinetics of the above reaction are characterized by first order kinetics with respect to the reactant concentration $C_A(mol/l)$ and by an Arrhenius-type dependence with respect to the temperature $T(K)$, the dynamics of the process in a plug flow reactor are described by the following energy and mass balance PDE's, where $C_B(mol/l)$ denotes the product concentration :

$$\frac{\partial T}{\partial t} = -v\frac{\partial T}{\partial z} - \frac{\Delta H}{\rho C_p} k_0 C_A exp(-\frac{E}{RT}) - \frac{4h}{\rho C_p d}(T - T_c) \quad (1)$$

$$\frac{\partial C_A}{\partial t} = -v\frac{\partial C_A}{\partial z} - k_0 C_A exp(-\frac{E}{RT}) \quad (2)$$

$$\frac{\partial C_B}{\partial t} = -v\frac{\partial C_B}{\partial z} + bk_0 C_A exp(-\frac{E}{RT}) \quad (3)$$

with the boundary conditions given, for $t \geq 0$, by :

$$\begin{array}{rcl} T(0,t) & = & T_{in} \\ C_A(0,t) & = & C_{A,in} \\ C_B(0,t) & = & 0\ , \end{array} \quad (4)$$

where T_{in} and $C_{A,in}$ denote the inlet temperature and reactant concentration respectively. The initial conditions are assumed to be given, for $0 \leq z \leq L$, by

$$\begin{array}{rcl} T(z,0) & = & T_0(z) \\ C_A(z,0) & = & C_{A,0}(z) \\ C_B(z,0) & = & 0\ . \end{array} \quad (5)$$

The objective of this work is basically two-fold : (a) to develop a theory of asymptotic stability for semi-linear infinite-dimensional systems [1], by using tools of infinite-dimensional nonlinear system theory [2], (b) to implement this theory for studying the asymptotic stability of the reactor model above. More precisely, it is shown that the constant temperature equilibrium profile (T_{in}) is an asymptotically stable equilibrium profile [1]. The motivation for choosing such an equilibrium profile is the fact that it minimizes the reactant concentration at the reactor outlet and the energy consumption along the reactor (see [3]).

References

[1] I. Aksikas, J.J. Winkin, D. Dochain, Asymptotic stability of infinite-dimensional semi-linear systems : application to a nonisothermal reactor, in preparation.

[2] Z. Luo, B. Guo, O. Morgül, Stability and stabilization of infinite dimensional systems with applications, *Springer Verlag*, London, 1999.

[3] I. Y. Smets, D. Dochain, J. F. Van Impe, Optimal temperature control of a steady-state exothermic plug flow reactor, *AIChE J.* 48(2), 2002, pp. 279-286.

Nonlinear distributed parameter observers applied to chromatographic separation processes

C. Levrie[a], V. Grosfils[b], M. Kinnaert[b], A. Vande Wouwer[a]

[a] *Service d'Automatique, Faculté Polytechnique de Mons, Boulevard Dolez, 31, 7000 Mons, Belgium Fax: 32-65-37.41.36; (E-mail: {Caroline.Levrie, Alain.VandeWouwer}@fpms.ac.be)*

[b] *Service d'Automatique et d'Analyse des Systèmes, Université Libre de Bruxelles, CP 165/55, 50, Av. F. D. Roosevelt, B-1050 Brussels, Belgium Fax: 32-2-650.26.77; (E-mail:{Valerie.Grosfils, Michel.Kinnaert}@ulb.ac.be)*

Chromatographic separation is based on the difference in the adsorption affinities of the components of a mixture. Simulated Moving Bed (SMB) is a continuous chromatographic separation process in which a counter-current movement of the liquid phase and the solid bed of particles is "simulated" by periodically switching the inlet and outlet ports [1]. This technology is used in various fields, from sugar to enantiomer separation.

SMB processes are distributed parameter systems, i.e. systems in which the state variables (the component concentrations) vary both in time and space. On-line point-wise measurements of the component concentrations can be performed using HPLC or UV sensors, but there is a need for state observers (software sensors) to reconstruct the complete spatial concentration profiles. In turn, this information can be used for process supervision and/or control.

The keystone of the software sensors is a dynamic model, which, based on the assumption of a continuous counter-current movement, takes the form of a True Moving Bed (TMB) model. The partial differential equations of the model can be solved using an approach based on a method of lines [2].

In this study, two different nonlinear distributed parameter observers are considered and compared:

- an extended Luenberger observer [3],
- a receding-horizon observer.

In the first observer, a correction term based on the deviation between the measured output and the estimated output is introduced in the model equations. One or several parameters allow the convergence of the estimated state to the real state to be adjusted. More specifically, the correction terms can be written

$$\alpha \cdot \sum_{k=1}^{m} (c_i(z_k,t) - \hat{c}_i(z_k,t)) \cdot w_k(z)$$

where α is a gain factor, z_k is the sensor location ($k = 1,\cdots,m$), $c_i(z_k,t)$ is the measured concentration, $\hat{c}_i(z_k,t)$ is the estimated concentration, and $w_k(z)$ is a weighting function.

The function $w_k(z)$ can be chosen in several ways, e.g. exponentials, triangularly shaped functions, and weights the output error correction term in space.

In the second observer, the most-likely initial conditions of the TMB model are estimated based on the available on-line measurements on a receding time window. To this end, an output-error criterion is minimized using a modified Levenberg-Marquardt algorithm. In order to limit the number of unknowns, the initial concentration profiles are represented by shape functions, whose parameters are estimated.

Both observers are compared in terms of performance, i.e. speed of convergence, sensitivity to measurement noise, sensitivity to model errors and computational load. The influence of the sensor number and location is also highlighted.

Acknowledgement

This work is performed in the framework of the MOVIDA project (contracts n°0114843 and 0114961) funded by the Walloon Region (Belgium).

References

[1] Ruthven, D.M. and Ching, C.B. (1989), *Counter-current and simulated counter-current chromatographic adsorption separation processes*, Chemical Engineering, vol.44, n°5, pp. 1011-1038.

[2] J. Haag, A. Vande Wouwer, S. Lehoucq, P. Saucez (2001), *Modeling and Simulation of a Chromatographic Process designed for Enantioseparation*, Control Engineering Practice **9**, pp. 921-928.

[3] Mangold, M., Lauschke, G., Schaffner, J., Zeitz, M. and Gilles, E.-D. (1994), *State and parameter estimation for adsorption columns by nonlinear distributed parameter state observers*, Journal of Process Control, vol.4, n°3, pp. 163-172.

Optimal control of a tubular reactor with axial dispersion

F. Logist, I. Smets, and J. Van Impe
BioTeC, Bioprocess Technology and Control, Department of Chemical Engineering
Katholieke Universiteit Leuven
W. de Croylaan 46, B-3001 Heverlee, Belgium
filip.logist@cit.kuleuven.ac.be – jan.vanimpe@cit.kuleuven.ac.be

1 Introduction

In the chemical industry most of the reactors are still operated by trial and error procedures based on the experience of the operators. Opposed to this heuristic approach, model based process control allows a more efficient operation.

2 Optimal control of a tubular reactor: a case study

In order to find an optimal model based control strategy, three essential components are needed, i.e, *(i)* a mathematical model describing the reaction process quantitatively, *(ii)* constraints imposed on the states and/or controls and *(iii)* a cost criterion that has to be minimized [2].

The reactor under study is a classical tubular reactor in which an irreversible, exothermic, first-order reaction takes place. A surrounding heating/cooling jacket is used to control the reactor temperature. Describing the reactor under steady-state conditions by a 1D-model with axial mass and heat dispersion, results in a system of two second-order differential equations with respect to the spatial coordinate z and four Danckwerts boundary conditions [1]. Next to physical constraints on the states, e.g., temperature and concentration have to be positive, a lower and an upper limit are imposed on the control input, i.e., the temperature T_w of the jacket fluid. Two different cost criteria are proposed in order to measure the control performance. Both penalize a low conversion and a high reactor temperature or hot spot. The first criterion only consists of a terminal cost, depending on the reactor outlet values. The second criterion however, combines a terminal cost for the concentration with an integral cost for the temperature, meaning that the temperature profile along the reactor is taken into account.

3 Results and discussion

After the transformation of the two second-order differential equations into a system of four first-order differential equations, optimal control theory is applied [2]. According to the minimum principle of Pontryagin a Hamiltonian $\mathcal{H}$ has to be minimized with respect to the control input. Minimization of the Hamiltonian usually involves the solution of a two point boundary value problem (TPBVP), which can become very tedious. For this case study however, the Hamiltonian $\mathcal{H}$ is affine in the control input T_w:

$$\mathcal{H} = \phi + \psi \cdot T_w.$$

As a result, the optimal control T_w^* depends on the value of ψ. If ψ is positive or negative, then the optimal control T_w^* is equal to $T_{w,min}$ or $T_{w,max}$ respectively. If ψ equals zero over an interval $[z_i, z_{i+1}]$, then the optimal control T_w^* is a singular control $T_{w,sing}^*$, obtained by repeatedly differentiating ψ with respect to z until the control input T_w appears explicitly.

For the first (terminal cost) criterion no singular phase exists and the optimal control sequence is of the *bang-bang* type, i.e., the optimal temperature profile T_w^* is a step profile that switches between the maximum value $T_{w,max}$ and the minimum value $T_{w,min}$. The switching position has to be determined numerically. For the combined terminal and integral cost, a *bang-singular-bang* profile is obtained, i.e., the profile starts with $T_{w,max}$, then switches to $T_{w,sing}$ and ends with $T_{w,min}$. Again, both switching positions have to be determined by numerical optimization.

4 Future research

The obtained open loop control laws can be assessed under transient conditions, in order to check *(i)* whether the reactor profiles evolve to the same steady-state when the control law is applied from the start of the reactor operation and *(ii)* whether the reactor variables do not pass inadmissible regions during the transition phase.

Acknowledgments

Work supported in part by Project OT/03/30 of the Research Council of the Katholieke Universiteit Leuven and the Belgian Program on Interuniversity Poles of Attraction, initiated by the Belgian Federal Science Policy Office. The scientific responsibility is assumed by its authors. IS is a postdoctoral fellow with the Fund for Scientific Research Flanders-Belgium (FWO-Vlaanderen).

References

[1] P.V. Danckwerts. Continuous flow systems. *Chemical Engineering Science*, 2(1):1-13, 1953

[2] D.E. Kirk. *Optimal Control Theory: an Introduction*. Prentice Hall, Englewood Cliffs, New Jersey, 1970

Complexity of control on automata

Jean-Charles Delvenne
Research fellow FNRS
CESAME, UCL, Bâtiment Euler,
Avenue Georges Lemaître, 4-6
B-1348 Louvain-la-Neuve, Belgium
delvenne@inma.ucl.ac.be

Vincent Blondel
CESAME, UCL, Bâtiment Euler,
Avenue Georges Lemaître, 4-6
B-1348 Louvain-la-Neuve, Belgium
blondel@inma.ucl.ac.be

Abstract

We consider control questions about finite automata, viewed as input/output systems. In particular we find estimations of the minimal size needed to control a given automaton. We show that on average feedback is not much simpler than open-loop.

1 Motivation

It is common sense that feedback, when available, is better than open-loop to control an input/output system. Several theoretical approaches may be followed to formalize this intuition. Many of them rely on robustness (feedback can cope with errors and noise). Here we would like, following [1], to explore a complexity argument: Is feedback easier to implement than open-loop? Does feedback lead to simpler, shorter algorithms than open-loop?

2 Model

To treat this question, we study systems in discrete time, with finite input, finite output and finite state space. These systems are called 'finite automata'.

We consider the problem of driving an automaton from a state to another state by giving a correct sequence of inputs.

The open-loop strategy consists in directly giving a correct input sequence, regardless of the output. This input may be seen, in a quite trivial way, as produced by an automaton.

The feedback strategy consists in computing at each step of time the next input from the output, with the help of a finite automaton. In other words, we control an automaton with another automaton.

For every strategy, we would like to achieve the goal with the simplest possible strategy, i.e. the smallest possible controller automaton. We would like to know whether this optimal controller is smaller in the feedback strategy or in the open-loop strategy.

Of course, feedback cannot be more complex than open-loop. We can exhibit particular examples where it is much simpler. But what about a typical case? What if the automaton we would like to control is taken at random?

3 Results and conclusions

We prove that the average complexity needed to drive a n-state automaton from one state to another is, up to a constant factor, close to $\log n$ —regardless of the chosen strategy, feedback or control. This means that feedback is not particularly better from the point of view of complexity on a random finite system. Coupled with the existence of examples on which feedback is efficient, we are lead to the following conclusion: ***Measuring the output of a system is useful only if the system is structured***.

Further work could be devoted to investigating on what particular structured automaton feedback is potentially efficient, for instance automata derived from the quantization of a linear system. Is feedback useful for a (discrete approximation of) a typical linear system?

References

[1] Egerstedt, M., Brockett, R., Feedback can reduce the specification complexity of motor programs. *IEEE Transactions on Automatic Control*, 48(2):213–223, 2003.

Structure preserving model reduction of second order systems

Y. Chahlaoui[1]
Florida State University
chahlaou@csit.fsu.edu

D. Lemonnier[1]
Université catholique de Louvain
lemonnier@anma.ucl.ac.be

A. Vandendorpe[1,2]
Université catholique de Louvain
vandendorpe@anma.ucl.ac.be

P. Van Dooren[1]
Université catholique de Louvain
vdooren@anma.ucl.ac.be

1 Abstract

Balanced truncation is probably the most widely used model reduction technique for linear systems. The objective of this talk is to generalize it to systems with particular structure in such a way that the resulting reduced order system preserves some properties of the original system. We focus our attention on second order systems and present our *Second Order Balanced Truncation* technique.

2 Introduction

Second-order linear time-invariant systems are of the type :

$$\left\{ \begin{array}{rcl} M\ddot{q}(t) + D\dot{q}(t) + Kq(t) & = & Bu(t) \\ y(t) & = & Cq(t) \end{array} \right. , \quad (1)$$

where $u(t) \in \mathbb{R}^{\mathrm{m}}$, $y(t) \in \mathbb{R}^{\mathrm{p}}$, $q(t) \in \mathbb{R}^{\mathrm{n}}$, $B \in \mathbb{R}^{\mathrm{n}\times\mathrm{m}}$, $C \in \mathbb{R}^{\mathrm{p}\times\mathrm{n}}$, $M,\ D,\ K \in \mathbb{R}^{\mathrm{n}\times\mathrm{n}}$ with M assumed to be invertible. It is often advisable to construct a reduced model of size $k \ll n$ that nevertheless keeps the "second-order structure" of the system. We thus need to build a reduced model,

$$\left\{ \begin{array}{rcl} \hat{M}\ddot{\hat{q}}(t) + \hat{D}\dot{\hat{q}}(t) + \hat{K}\hat{q}(t) & = & \hat{B}u(t) \\ \hat{y}(t) & = & \hat{C}\hat{q}(t) \end{array} \right. \quad (2)$$

where $\hat{q}(t) \in \mathbb{R}^{\mathrm{k}}$, $\hat{M},\ \hat{D},\ \hat{K} \in \mathbb{R}^{\mathrm{k}\times\mathrm{k}}$, $\hat{B} \in \mathbb{R}^{\mathrm{k}\times\mathrm{m}}$, $\hat{C} \in \mathbb{R}^{\mathrm{p}\times\mathrm{k}}$, such that its transfer function is "close" to the original transfer function. Since (1) is a particular case of a linear time-invariant system, one may consider its corresponding state-space model and apply the techniques of model reduction known for state-space models. In doing so, the reduced system is generally not of the same type anymore. Since from a physical point of view it makes sense to impose the reduced system to be of the same type, we propose in this paper a new method of model reduction that preserves the second-order form. Our technique is inspired from [2].

The idea of our balance and truncate technique for second-order systems (called SOBT for Second-Order Balanced Truncation) is the following. First, we need to define *two* pairs of $n \times n$ gramians ("second-order gramians") that change according to contragradient transformations, and that do have an energetic interpretation. The first pair $(\mathcal{P}_{pos}, \mathcal{Q}_{pos})$ correspond to an energy optimization problem depending only on the *positions* $q(t)$ and not on the *velocities* $\dot{q}(t)$. Reciprocally, the second pair $(\mathcal{P}_{vel}, \mathcal{Q}_{vel})$ is associated to an optimization problem depending only on the velocities $\dot{q}(t)$ and not the on the positions $q(t)$. By analogy to the first order case, the gramians $\mathcal{Q}_{pos}$ and $\mathcal{Q}_{vel}$ are defined from the dual systems. After these definitions we then come to the balancing part of the method. For this we transform to a balanced coordinate system in which the second-order gramians are equal and diagonal : $\bar{\mathcal{P}}_{pos} = \bar{\mathcal{Q}}_{pos} = \Sigma_{pos}$, $\bar{\mathcal{P}}_{vel} = \bar{\mathcal{Q}}_{vel} = \Sigma_{vel}$. Their diagonal values will enable us to point out what the *important* positions and the *important* velocities are, i.e. those with (hopefully) large effect on the I/O map. Hence to get a reduced second-order model we keep only the part of the system that depends on these variables. This is the truncation part of the method. Numerical examples and possible extensions will be given during the talk. A deeper study of the Second-Order Balanced truncation technique and a comparaison with other techniques can be found in [1].

References

[1] Y. Chahlaoui, D. Lemonnier, A. Vandendorpe, and P. Van Dooren. Second-Order Balanced Truncation. *Linear Algebra Appl., Special Issue*, 2003. accepted.

[2] D. G. Meyer and S. Srinivasan. Balancing and model reduction for second-order form linear systems. *IEEE Trans. Automat. Control*, 41(11):1632–1644, 1996.

[1]This paper presents research supported by the Belgian Programme on Inter-university Poles of Attraction, initiated by the Belgian State, Prime Minister's Office for Science, Technology and Culture.

[2]A research fellowship from the Belgian National Fund for Scientific Research is gratefully acknowledged by the author.

Computing the joint spectral radius of a set of matrices

Vincent D. Blondel
CESAME/UCL
blondel@inma.ucl.ac.be

Yurii Nesterov
CORE/UCL
nesterov@core.ucl.ac.be

Jacques Theys
CESAME/UCL
theys@inma.ucl.ac.be

The *joint spectral radius* of a set of matrices measures the maximal asymptotic growth rate that can be obtained by forming long products of matrices taken from the set; see [4]. More formally, it is defined by:

$$\rho(M) := \limsup_{k\to\infty} \rho_k(M),$$

$$\text{where}\quad \rho_k(M) = \sup_{A_1,\ldots,A_k\in M} \|A_k \cdots A_1\|^{1/k}.$$

When the set M consists of only one matrix A, the joint spectral radius coincides with the usual notion of spectral radius of a single matrix which is equal to the maximum magnitude of the eigenvalues of the matrix.

Questions related to the computability of the joint spectral radius of sets of matrices have been posed in [5] and [2]. The joint spectral radius can easily be approximated to any desired accuracy. Indeed, bounds proved in [2] can be evaluated and lead to arbitrarily close approximations of ρ. These are expensive calculations. Moreover, it is proved in [6] that, unless $P = NP$, there is in fact no polynomial-time approximation algorithm for the joint spectral radius of two matrices.

We provide two easily computable approximations of the joint spectral radius for finite sets of matrices. The first approximation, $\hat{\rho}$, is based on the computation of a common quadratic Lyapunov function, or, equivalently, on the computation of an ellipsoid norm. This approximation has the advantage that it can be expressed as a convex optimization problem for which efficient algorithms exist. This first approximation satisfies

$$\frac{1}{\sqrt{n}}\,\hat{\rho} \le \rho \le \hat{\rho}$$

where n is the dimension of the matrices. For the special case of symmetric matrices or triangular matrices , we prove equality between the joint spectral radius and its approximation, $\rho = \hat{\rho}$.

Also, we prove a simple bound for the joint spectral radius of sets of matrices that have *non-negative entries*. The spectral radius of the matrix S whose entries are the componentwise maximum of the entries of the matrices in M satisfies

$$\frac{\rho(S)}{m} \le \rho(M) \le \rho(S)$$

where m is the number of matrices in the set.

The problem of computing approximations of the joint spectral radius is raised and analyzed in a number of recent contributions. In [3], the exponential number of products that appear in the computation of ρ'_k based on its definition is reduced by avoiding duplicate computation of cyclic permutations; the total number of product to consider remains however exponential. In [1], an algorithm based on the above idea is presented. The algorithm gives arbitrarily small intervals for the joint spectral radius, but no rate of convergence is proved.

The approximations we provide allow us to define algorithms for which the complexity can be determined and for which the precision of the approximation can be evaluated a priori.

References

[1] G. Gripenberg, Computing the Joint Spectral Radius, Linear Algebra and its Applications, 234, pp.43-60, 1996.

[2] J.C. Lagarias and Y. Wang, The finiteness conjecture for the generalized spectral radius of a set of matrices, Linear Algebra Appl., 214, 17-42, 1995.

[3] M. Maesumi, An Efficient Lower Bound for the Generalized Spectral Radius, Linear Algebra and its Applications, 240, pp.1-7, 1996.

[4] G.-C. Rota and G. Strang, A note on the joint spectral radius, Indag. Math., 22, pp.379-381, 1960.

[5] J.N. Tsitsiklis, The Stability of the Products of a Finite Set of Matrices, Open Problems in Communication and Computation, T.M. Cover and B. Gopinath (Eds.), Springer–Verlag, New York, 161–163, 1987.

[6] J. Tsitsiklis, V. Blondel, The Lyapunov exponent and joint spectral radius of pairs of matrices are hard – when not impossible – to compute and to approximate, Mathematics of Control, Signals, and Systems, 10, pp. 31-40, 1997. (Correction in 10, pp. 381, 1997)

Convergence of graph similarity algorithms

Vincent Blondel, Laure Ninove, Paul Van Dooren
Division of Applied Mathematics
Université catholique de Louvain
Avenue G. Lemaître, 4
B-1348 Louvain-la-Neuve, Belgium
Email: {blondel, ninove, vandooren}@inma.ucl.ac.be

Recently, different notions of similarity in graphs have been introduced [1, 2, 3]. Given two graphs G_A and G_B, possibly identical, we want to measure the similarity between nodes of G_A and G_B.

The similarity between pairs of nodes, described by a nonnegative vector, is computed iteratively until convergence to a fixed point, or until convergence of a the iterates to a periodic point.

In [1], the similarity score vector is computed by the power method

$$s_{k+1} = \frac{Ms_k}{\|Ms_k\|},$$

where $M \geq 0$ is the adjacency matrix of a graph constructed from G_A and G_B. Depending on the eigenvalues of A, several convergence cases can occur. The similarity score is chosen among the set of subsequences limits according to an extremal condition.

In [2], only similarity for a graph G_A with itself is studied. The iteration considered there can be written

$$s_{k+1} = Ms_k + b,$$

where $M \geq 0$ is a weighted adjacency matrix of the product graph $G_A \times G_A$ and $b \geq 0$ is a vector taken such that the similarity between a node and itself equals 1. This affine map admits only one fixed point and the convergence is global on the nonnegative quadrant.

The different variants of iterations in [3] may be formulated in a unified expression

$$s_{k+1} = \frac{Ms_k + b}{\|Ms_k + b\|},$$

where $M \geq 0$ is a weighted adjacency matrix of a graph constructed from G_A and G_B, b is a positive vector supposed to speed up the convergence without too much changing the fixed point, and the norm is the uniform norm. In this presentation, we will use the notion of projective distance [4] to prove the existence of a unique fixed point and the global convergence towards this point on the positive quadrant.

After the convergence of these algorithms is established, other questions arise about their convergence properties. How can one characterize the speed of convergence? What is the sensitivity of the solution towards a perturbation of the initial value or towards a perturbation of the adjacency matrix of the product graph? Is the algorithm accelerated by a variant of the iteration formula? We will briefly report our most recent results on these questions.

Acknowledgements

This paper presents research supported by the Belgian Programme on Inter-university Poles of Attraction, initiated by the Belgian State, Prime Minister's Office for Science, Technology and Culture. The scientific responsibility rests with its author.
The second author was supported by the Fonds National de la Recherche Scientifique.

References

[1] V. Blondel, A. Gajardo, M. Heymans, P. Senellart, P. Van Dooren, *A measure of similarity between graph vertices: Applications to synonym extraction and web searching*, SIAM Review, to appear.

[2] G. Jeh, J. Widom, *SimRank: A measure of structural-context similarity*, Proceedings of the Eighth International Conference on Knowledge Discovery and Data Mining (KDD), Edmonton (2002).

[3] S. Melnik, H. Garcia-Molina and A. Rahm, *Similarity Flooding: A Versatile Graph Matching Algorithm and its Application to Schema Matching*, Proceedings of the 18th International Conference on Data Engineering (ICDE), San Jose (2002).

[4] E. Seneta, *Nonnegative matrices and Markov chains*, second ed., Springer Series in Statistics, Springer-Verlag, New York, 1981.

Part 2

Plenary Lectures

control & communication@liu

Model-based filtering for automotive safety systems

Outline

- Existing and future safety systems – sensors and actuators
- Sensor fusion and virtual sensors
- Examples from Volvo collaboration
- Examples from spin-off company NIRA Dynamics AB

Fredrik Gustafsson
Prof in Communication Systems
Department of Electrical Engineering
Linköping University
fredrik@isy.liu.se

Model-based filtering for automotive safety systems — Fredrik Gustafsson

Automotive control systems

control & communication@liu

Some background facts:

- Consumers want many functions (long check box list), performance of safety critical systems still not important.
- Consumers are very price sensitive.
- Current controllers still quite simple. It is more important to feedback accurate information.
- Electronic actuators and many sensors available today in high-end cars.
- New safety functions can be added by clever model-based filtering in only software, or with cheap extra sensors.

Model-based filtering for automotive safety systems — Fredrik Gustafsson

Automotive control systems

control & communication@liu

- Main actuators already in use
  - Electronic brakes, steering and accelerator (by-wire in the future)
  - Electronic suspension still uncommon
- Sensor information from the CAN bus
  - Wheel speeds, engine torque, brake pressure, steering angle, etc
- Specific application dependent sensors
  - Inertial: Yaw and roll gyros, longitudinal and lateral accelerometers, vertical accelerometers and level sensors at each wheel
  - Vision: camera, microwave radar, IR, LIDAR
- Driver information sensors
  - Temperature, ultrasound parking aid, tire pressure, friction,

Model-based filtering for automotive safety systems — Fredrik Gustafsson

Automotive control systems

control & communication@liu

Examples of recent new control systems.

- Active suspension systems
- Multistep and adaptive airbags
- Adaptive light control
- Traction and anti-spin control
- Dynamic stability control
- Roll stability control
- Brake assistance systems

Model-based filtering for automotive safety systems — Fredrik Gustafsson

Active suspension systems

control & communication@liu

- Sensors:
  - Accelerometers
  - Level sensors
- Actuators:
  - Spring or damper

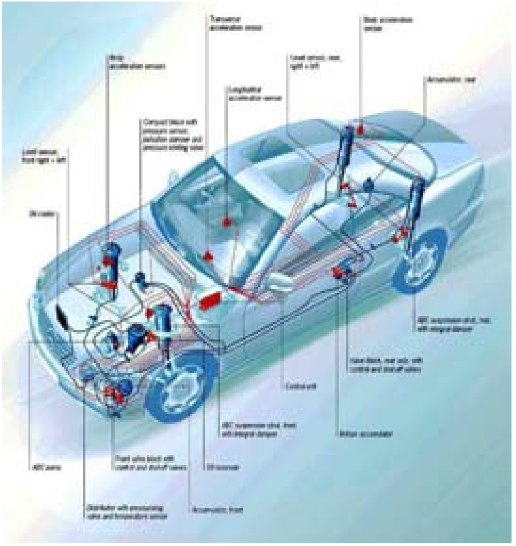

Model-based filtering for automotive safety systems
Fredrik Gustafsson

Airbags

control & communication@liu

- Sensors:
  - Accelerometer for front airbag
  - Roll gyro for curtains
  - Weight and position sensors for multi-step airbags
  - Sensors for pedestrian airbags

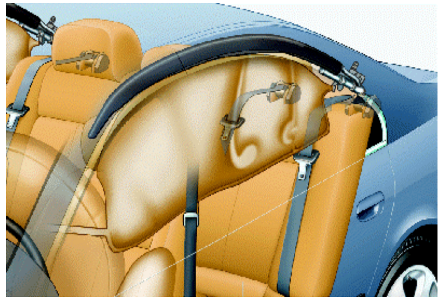

Model-based filtering for automotive safety systems
Fredrik Gustafsson

Adaptive light control (ALC)

control & communication@liu

- Vision systems for road recognition
- Roll angle estimator for motor-cycles
- Headlight actuator

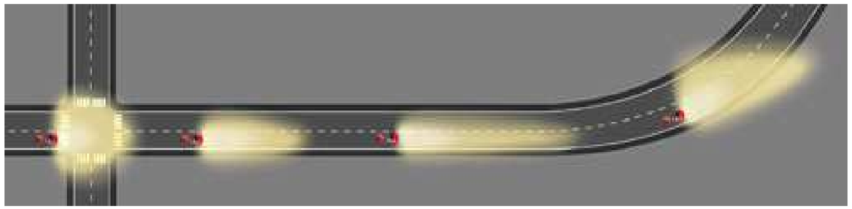

Model-based filtering for automotive safety systems
Fredrik Gustafsson

Anti-spin and traction control

control & communication@liu

- Anti-spin is a start help to avoid wheel spin (<20km/h)
  - ABS sensor for wheel speed
  - ABS brakes for decreasing spin
  - Product name example: ASR (anti-spin regulation)
- Traction control works during normal driving (>20km/h)
  - ABS sensor for wheel speed
  - Engine control for decreasing engine torque
  - Product name example: DSTC (Volvo and Nira), TRACS, TCS

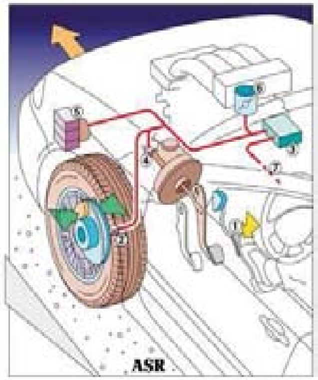

Model-based filtering for automotive safety systems
Fredrik Gustafsson

Electronic stability program (ESP, DSTC)

control & communication@liu

- Uses brakes as actuators to avoid under- and over-steering
- Sensors:
  - Yaw rate gyro
  - Steering angle for yaw rate support
  - ABS for yaw rate support and absolute velocity and wheel slip control

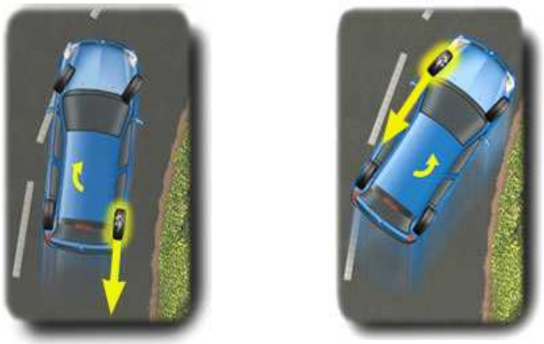

Model-based filtering for automotive safety systems — Fredrik Gustafsson

DSTC in action

control & communication@liu

DSTC off

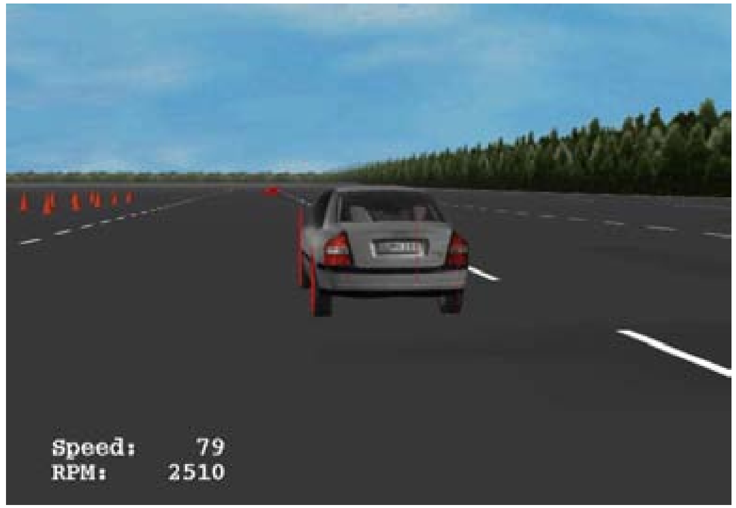

Model-based filtering for automotive safety systems — Fredrik Gustafsson

DSTC in action

control & communication@liu

DSTC on

Model-based filtering for automotive safety systems — Fredrik Gustafsson

Roll stability control

control & communication@liu

NHTSA - Static Stability Factor

$$SSF = \frac{B/2}{h}$$

- XC 90 1,21
- Ford Explorer 1,09
- Honda CRV 1,23
- Lexus RX300 1,23
- MB M-Klasse 1,29
- Passenger Car 1,30-1,50

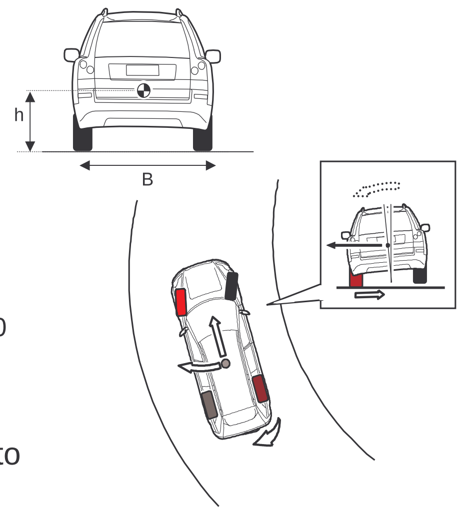

- Roll gyro and PIDDD controller
- Uses the ESP principles to generate forces and yaw torques

Model-based filtering for automotive safety systems — Fredrik Gustafsson

Brake assistance system (BAS)

control & communication@liu

- Brake servo increases brake torque when pedal effort is high or quickly increases (PD control)

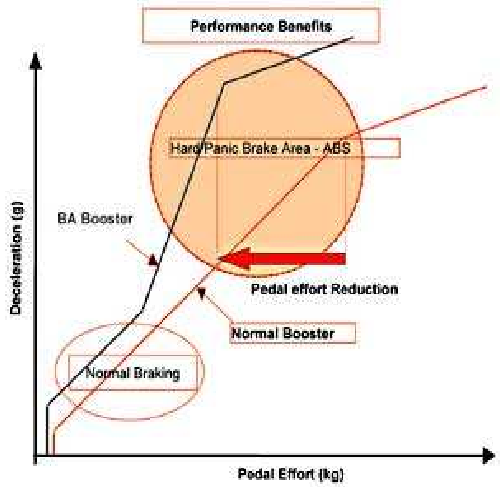

Model-based filtering for automotive safety systems — Fredrik Gustafsson

System architecture

control & communication@liu

- It is clear from the examples that many systems use the same set of actuators and sensors: “buy five, get five for free”
- Today the car manufacturers are forced to buy software from the actuator suppliers
- But they would like to be more independent and separate sensor, actuator and software suppliers
- System architecture becomes critical
- How to open up the system when…

Model-based filtering for automotive safety systems — Fredrik Gustafsson

Sensors

control & communication@liu

… there is a multitude of distributed sensors for drivetrain, convenience, safety

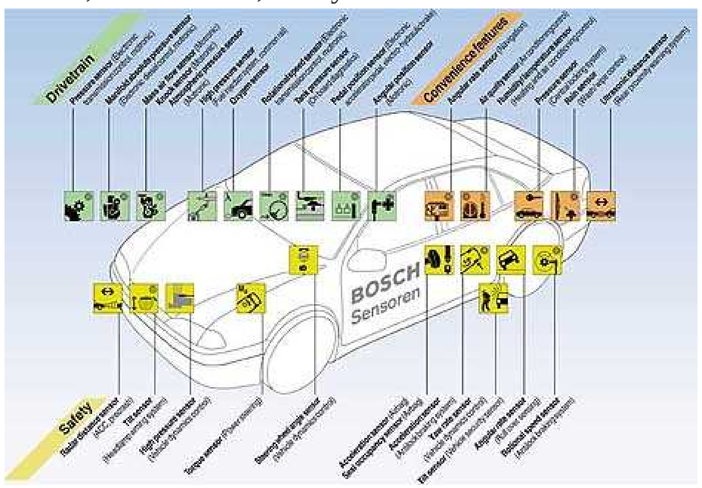

Model-based filtering for automotive safety systems — Fredrik Gustafsson

On-board computers

control & communication@liu

…and many computation nodes…

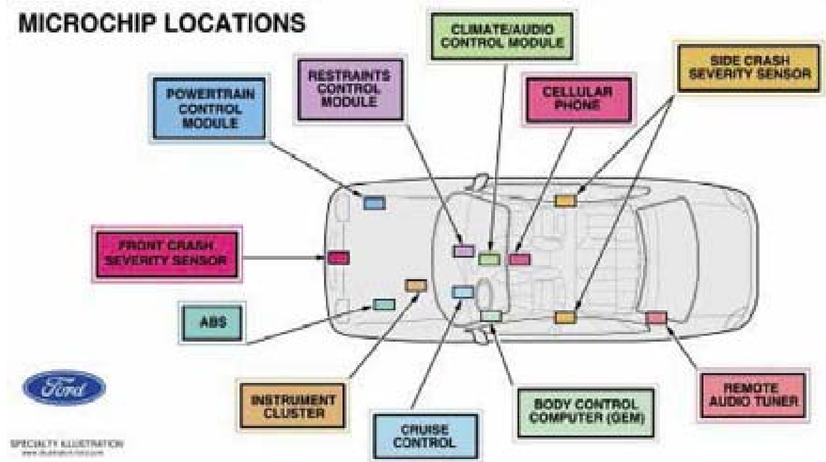

Model-based filtering for automotive safety systems — Fredrik Gustafsson

Sensor cluster and software modules

control & communication@liu

…so it would be clever to separate sensors, actuators and algorithms

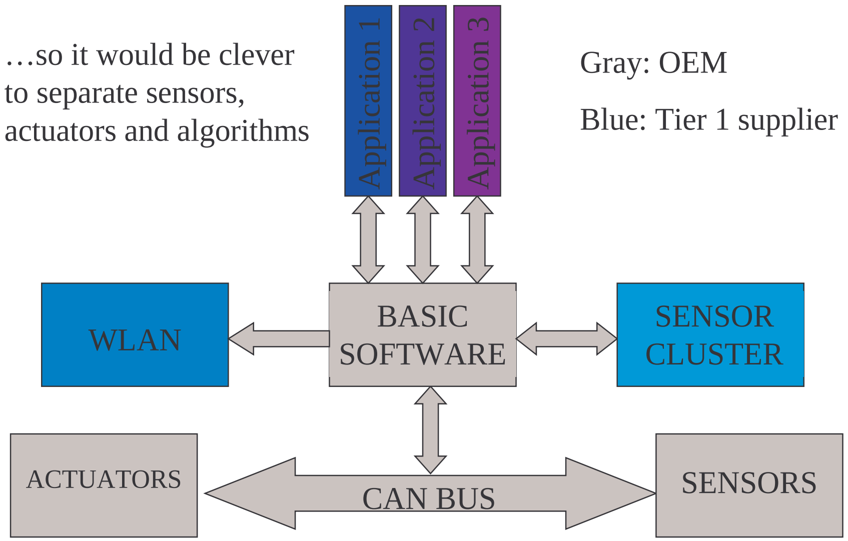

Gray: OEM

Blue: Tier 1 supplier

Model-based filtering for automotive safety systems — Fredrik Gustafsson

Inter-vehicle communication

control & communication@liu

For instance, a hardware platform with

- Sensor cluster
- Sensor fusion algorithms
- Virtual sensor algorithms
- WLAN ad-hoc communication

Could compute and exchange safety critical information

Examples and animation:

- Braking info
- Friction information

Model-based filtering for automotive safety systems — Fredrik Gustafsson

2003 initiative: Autosar.org

control & communication@liu

German OEM and pier 1 supplier partnership (now also including Ford): **automotive open system architecture**

“To achieve the technical goals modularity, scalability, transferability and re-usability of functions AUTOSAR will provide a common software infrastructure for automotive systems of all vehicle domains based on standardized interfaces for the different layers shown” [in the figure].

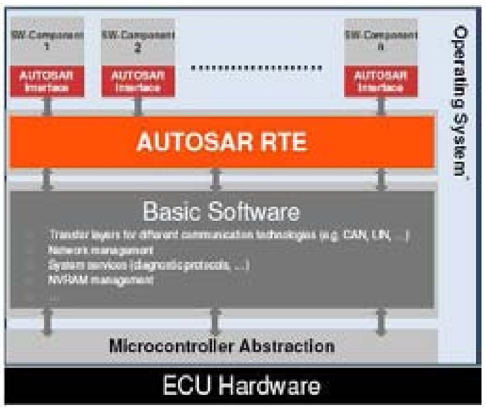

Model-based filtering for automotive safety systems — Fredrik Gustafsson

Sensor fusion

control & communication@liu

Linköping University background

- Started with sensor fusion and related diagnosis algorithms 1995 with SAAB Aircraft and the JAS fighter project.
- Developed a new terrain navigation algorithm based on sensor fusion and particle filters. This is today the main position sensor in this aircraft!
- Contributed to its new 2G integrated navigation system.

2000: a spinn-off company NIRA Dynamics was founded, established formarly 2002, with focus on transfering aircraft technology in sensor fusion to the automotive industry.

Model-based filtering for automotive safety systems — Fredrik Gustafsson

Sensor fusion

control & communication@liu

- What is needed?
- A dynamic model of longitudinal, lateral, vertical, yaw, roll… dynamics with suitable accuracy (simple models often work well, so try simple things first)
- Sufficiently many relevant sensors
- Sensor error model!
  - Drifts for gyros
  - Offsets for accelerometers
  - Wheel radius variations for wheel speeds, etc
- A filter
  - Kalman filter for linear models
  - EKF for almost linear models
  - Particle filter for non-linear or non-Gaussian shaped noise distributions

Model-based filtering for automotive safety systems Fredrik Gustafsson

Virtual sensors

control & communication@liu

A virtual sensor measures variables that are not readily available from sensors. Examples:

- The sensor offsets, drifts and noise are reduced by sensor fusion
- The dynamic model may contain states that are
  - Expensive to measure with sensors (tire pressure)
  - Technically difficult to measure (road friction)

Model-based filtering for automotive safety systems Fredrik Gustafsson

Applications

control & communication@liu

Applications will be used to illustrate these principles

- Volvo collaborations with sensor fusion for decision making
- NIRA collaborations with sensor fusion for virtual sensors

Model-based filtering for automotive safety systems Fredrik Gustafsson

Volvo collaboration: Driver assistance systems

control & communication@liu

•Sensor fusion of radar, lidar, IR, forward and rear mirror vision systems, inertial sensors and wheel speeds

•Demonstrator cars

•Two Volvo PhD students: collision mitigation by braking and lane keeping aid systems.

Model-based filtering for automotive safety systems Fredrik Gustafsson

Overview of related functions

control & communication@liu

- Systems using forward looking sensors as
  - Radar
  - IR radar
  - Lidar
  - Vision
- Adaptive cruise controller (ACC) keeps constant distance
- Stop-and-go functions
- Lane Keeping Aid Systems (LKA)
- Forward Collision Warning (FCW)
- Forward Collision Mitigation by Braking (CMbB)
- Forward Collision Avoidance by Steering (CAbS)

Model-based filtering for automotive safety systems Fredrik Gustafsson

Sensors - Millimetre wavelength Radar

control & communication@liu

- Range 150 m
- Field of view 10 degrees
- Wavelength 3.9 mm (77 GHz)

- Range accuracy 1 m
- Range rate accuracy 0.3 m/s
- Azimuth accuracy 1 degree

Model-based filtering for automotive safety systems Fredrik Gustafsson

Sensors - Lidar

control & communication@liu

- Range 150 m
- Field of View 10 degrees
- Wavelength 850 nm (352 THz)

- Range accuracy 1 m
- Range rate accuracy 1 m/s
- Azimuth accuracy 1 degree

Model-based filtering for automotive safety systems Fredrik Gustafsson

Sensors - Infrared vision

control & communication@liu

- Similar to vision systems in many aspects

- Already installed in some cars to enhance the drivers perception at night

Model-based filtering for automotive safety systems Fredrik Gustafsson

Sensors- Vision

control & communication@liu

- 'Web' camera with image processing feature extraction algorithms
- Measure other vehicles and road curvature (from lane markers)

Model-based filtering for automotive safety systems — Fredrik Gustafsson

Dynamic navigation models

control & communication@liu

- Model when velocity is measured (own vehicle):

$$x_t = (X_t, X_t, \Psi_t)^T$$
$$X_{t+1} = X_t + Tv_t \cos(\Psi_t) + w_{X,t}$$
$$Y_{t+1} = Y_t + Tv_t \sin(\Psi_t) + w_{Y,t}$$
$$\Psi_{t+1} = \Psi_t + T\dot{\Psi}_t$$
$$y_t = h(X_t, Y_t) + e_t$$

- Model when velocity is <u>not</u> measured (other vehicles):

$$x_t = (X_t, \dot{X}_t, Y_{,t} \dot{Y}_t)$$
$$x_{t+1} = \begin{pmatrix} 1 & T & 0 & 0 \\ 0 & 1 & 0 & 0 \\ 0 & 0 & 1 & T \\ 0 & 0 & 0 & 1 \end{pmatrix} x_t + \begin{pmatrix} T^2/2 & 0 \\ T & 0 \\ 0 & T^2/2 \\ 0 & T \end{pmatrix} w_t$$
$$y_t = h(X_t, Y_t) + e_t$$

Model-based filtering for automotive safety systems — Fredrik Gustafsson

Sensor examples

control & communication@liu

- Generic measurement depends only on the current position (X,Y)

$$y_t = h(X_t, Y_t) + e_t$$

- Examples of relative position sensors:
  - Radar measures range and bearing to (X,Y)
  - IR measures bearing to (X,Y)
- Examples of own position sensors:
  - INS measures acceleration and rotations of coordinates (X,Y)
  - GPS

Model-based filtering for automotive safety systems — Fredrik Gustafsson

Collision mitigation by braking

control & communication@liu

- Dynamic model of relative position using radar measurements

$$x_{t+1} = f(x_t) + w_t$$
$$y_t = h(x_t) + e_t = \begin{pmatrix} R \\ \dot{R} \\ \psi \end{pmatrix} + e_t$$

- Extended Kalman filter for tracking relative position

$$\hat{x}_{t+1|t} = A_t \hat{x}_t$$
$$P_{t+1|t} = A_t P_{t|t} A_t^T + Q_t$$
$$\hat{x}_{t|t} = \hat{x}_{t|t-1} + P_{t|t-1} C_t^T (C_t P_{t|t-1} + R_t)^{-1} (y_t - C_t \hat{x}_{t|t-1})$$
$$P_{t|t} = P_{t|t-1} - P_{t|t-1} C_t^T (C_t P_{t|t-1} C_t^T + R_t)^{-1} C_t P_{t|t-1}$$

Model-based filtering for automotive safety systems — Fredrik Gustafsson

Collision mitigation by braking

control & communication@liu

- Statistical decision making (approximate or simulation based)

$$P_{t+1}(\text{collision}) = P_{t+1}(\tilde{p}_x, \tilde{p}_y, \tilde{\psi} \in D) =$$
$$= \iiint_{\tilde{p}_x, \tilde{p}_y, \tilde{\psi} \in D} p_{t+1}(\tilde{p}_x, \tilde{p}_y, \tilde{\psi} \mid Y_t) dx dy d\psi$$

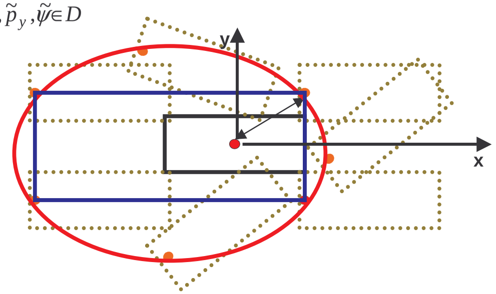

Model-based filtering for automotive safety systems Fredrik Gustafsson

Tracking filters for CA and LKA

control & communication@liu

- Vision system provides very noisy curvature
- Cars ahead can stabilize the curvature
- Tracking other vehicles can be improved by using road model

That is, solve the joint problem of tracking road geometry and other vehicles in one filter!

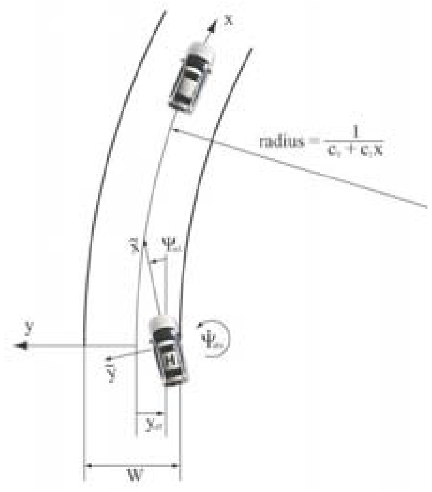

Model-based filtering for automotive safety systems Fredrik Gustafsson

Tracking filters for CA and LKA

control & communication@liu

- State model for each car i, lane width W, lateral offset, relative yaw and curvature/clothoid
- Measurements from vision (lane position), yaw gyro, lane markers (curvature) and radar (relative position)

$$\begin{aligned}
x^i_{t+1} &= x^i_t + T_s \dot{x}^i_t + a_{host,t} \cos \Psi_{rel,t} T_s 2/2 + w_{1,t} \\
\dot{x}^i_{t+1} &= \dot{x}^i_t + a_{host,t} \cos \Psi_{rel,t} T_s + w_{2,t} \\
y^i_{t+1} &= y^i_t + w_{3,t} \\
W_{t+1} &= W_t + w_{4,t} \\
y_{off,t+1} &= y_{off,t} + v T_s \Psi_{rel,t} + w_{5,t} \\
\Psi_{rel,t+1} &= \Psi_{rel,t} + v T_s c_{0,t} + T_s \dot{\Psi}_{abs,t} + w_{6,t} \\
c_{0,t+1} &= c_{0,t} + v T_s c_{1,t} + w_{7,t} \\
c_{1,t+1} &= c_{1,t} + w_{8,t}
\end{aligned}$$

$$\begin{aligned}
m_{left,t} &= -W_t/2 - y_{off,t} + e_{1,t} \\
m_{right,t} &= W_t/2 - y_{off,t} + e_{2,t} \\
\Psi^m_{rel,t} &= \Psi_{rel,t} + e_{3,t} \\
c^m_{0,t} &= c_{0,t} + e_{4,t} \\
\tilde{p}^m_{i,t} &= T(x_{i,t}, y_{i,t}) + e_{5,6,t}
\end{aligned}$$

Model-based filtering for automotive safety systems Fredrik Gustafsson

The key sensor: Wheel speeds!

control & communication@liu

The ABS wheel speed sensors contain a lot of information:

- Temporal information (Fourier transformed velocity) reveals friction, tire pressure, tire condition and wheel balance information.
- Spatial information (correlation of velocities) reveals road condition and absolute velocity (different axles) and curvature/yaw rate (same axle).
- Model-based approaches to friction estimation (longitudinal and lateral slip models), dynamic state estimation and navigation.

Linköpings Universitet and NIRA Dynamics AB have developed some very efficient algorithms and products (*virtual sensors*) based on these general ideas and the principles of sensor fusion and information fusion.

Model-based filtering for automotive safety systems Fredrik Gustafsson

Research results with NIRA Dynamics

control & communication@liu

Virtual sensors:

- Offset-free yaw angle and drift-free yaw rate (lateral dynamics)
- Offset-free velocity and acceleration (longitudinal dynamics)
- Roll angle estimation for MC's (roll dynamics)
- Map based positioning (GPS complement or replacement) based on particle filters.
- Road friction indication algorithms (originates from Prometheus)
- Tire pressure indication algorithms
- Detection of aqua-planning, rough road and tire imbalance

Model-based filtering for automotive safety systems — Fredrik Gustafsson

Tire-road friction estimation

control & communication@liu

- Model of wheel slip s(t) as a function of wheel torque T(t) and normal force N(t) at driven wheel as a function of slip slope k(t) and slip offset $\delta(t)$
- Kalman filter with change detector
- 2001 movie with
  - transition from asphalt to ice to asphalt
  - ABS brake for verification

$$s(t) = \frac{T(t)}{N(t)k(t)} + \delta(t) + e(t)$$

Model-based filtering for automotive safety systems — Fredrik Gustafsson

Roll angle estimation

control & communication@liu

- Dynamic model of roll dynamics
- Sensors: one vertical and one lateral accelerometer (cheap on the chip component)
- Roll angle estimation for:
  - ABS
  - Anti-spin systems
  - Head-light control

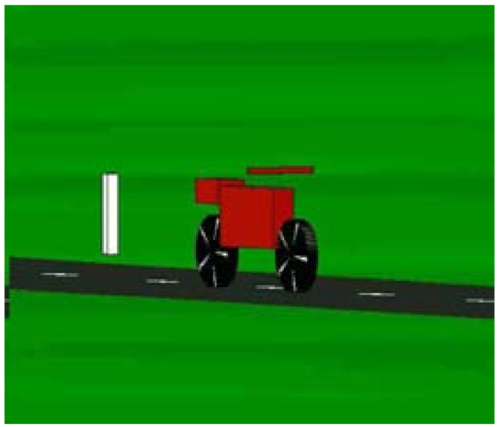

Model-based filtering for automotive safety systems — Fredrik Gustafsson

Yaw rate estimation

control & communication@liu

- Dynamic yaw model with geometric wheel speed transformation, using wheel speeds and yaw gyro as only sensors (steering angle and lateral accelerometer are useful but not necessary)
- Simulation with animation and real-time implementation shows dead reckoned yaw rate and speed with and without sensor fusion

Model-based filtering for automotive safety systems — Fredrik Gustafsson

Conclusions

control & communication@liu

- The automotive industry will move focus from the platform approach of today to modules and standardized interfaces.
- All actuators are electronic (by-wire in the end) and all sensor information available at the CAN bus
- These facts open up possibility for new actors to improve existing control systems and include new ones.
- More effort will be spent on software development including control design and sensor management, and a considerable part of the car price is predicted to be software license, relative to hardware costs.
- The consumers will get a multitude of safety and comfort related functions, using the same set of sensors and actuators.

Model-based filtering for automotive safety systems Fredrik Gustafsson control & communication@liu

The particle filter and its application to positioning

Fredrik Gustafsson
Prof in Communication Systems
Department of Electrical Engineering
Linköping University
fredrik@isy.liu.se

The particle filter and its application to positioning — Fredrik Gustafsson

Background and acknowledgement

control & communication@liu

Presentation based on

- Work in competence center ISIS with
  - SAAB Aircraft: aircraft terrain aided positioning and navigation
  - SAAB Dynamics: missile tracking and torpedo positioning
  - NIRA Dynamics: Map-Aided Positioning (MAP) for cars
  - Ericsson: wireless networks
- F. Gustafsson, F. Gunnarsson, N. Bergman, U.Forssell, J. Jansson, R. Karlsson and P-J. Nordlund: *Particle filters for positioning, navigation and tracking*. IEEE Trans. On Signal Processing, 2002. Survey in special issue.

The particle filter and its application to positioning — Fredrik Gustafsson

Literature

control & communication@liu

- Robert and Casella, Monte Carlo Statistical Methods, Springer, 1999
- Gilks, Ricardson and Spiegelhalter, Markov Chain Monte Carlo in Practice, 1996
- Doucet, Freitas and Gordon (editors), Sequential Monte Carlo Methods in Practice, Springer, 2001.

The particle filter and its application to positioning — Fredrik Gustafsson

Random number generation

control & communication@liu

- Uniform distribution $U \in [0,1]$ – integer multiplication with truncation – shift registers
- General PDF f(x), compute distribution function F(x), take

$$X = F^{-1}(U)$$

- This inverse may be complicated to compute, resort to numerical methods

The particle filter and its application to positioning — Fredrik Gustafsson

Monte Carlo based estimation

control & communication@liu

- Goal: estimate $I = E(g(X)) = \int g(x)p(x)dx$
- Given: function g(x), pdf p(x), random number generator with pdf q(x)

The Monte Carlo method. Generate N samples of X and take

$$\hat{I} = \frac{1}{N}\sum_{i=1}^{N} g(x^{(i)})$$

The law of large numbers assures convergence and the central limit theorem assures asymptotic Gaussian distribution.

Problem if p(x) can be evaluated but not sampled (F(x) hard to compute and invert analytically), so we cannot generate samples of X

The particle filter and its application to positioning — Fredrik Gustafsson

Accept-reject methods

control & communication@liu

1. Let U be uniform and generate X from arbitrary pdf q(x)
2. Accept Y=X if

$$U \le \frac{p(X)}{Mq(X)}$$

otherwise return to 1

Proof: $P(Y \le y) = P(X \le y \,|\, U \le \frac{p(X)}{Mq(X)})$

$$= \left(\frac{P\left(X \le y, U \le \frac{p(X)}{Mq(X)} \right)}{P\left(U \le \frac{p(X)}{Mq(X)} \right)} \right) = \int_{-\infty}^{y} p(x)dx$$

The particle filter and its application to positioning — Fredrik Gustafsson

Accept-reject example

control & communication@liu

- p(x) truncated Gaussian, q(x) uniform, both defined on the interval [-4,4], and M=4.
- Left figure shows true and estimated distributions, the right one the chain of random numbers
- The larger M, the more rejections and the slower convergence

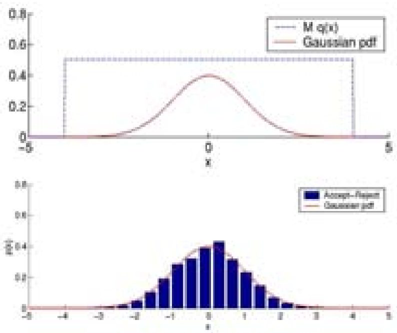

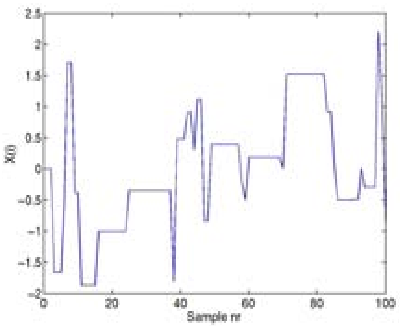

The particle filter and its application to positioning — Fredrik Gustafsson

Accept-reject example

control & communication@liu

- Convergence in distribution

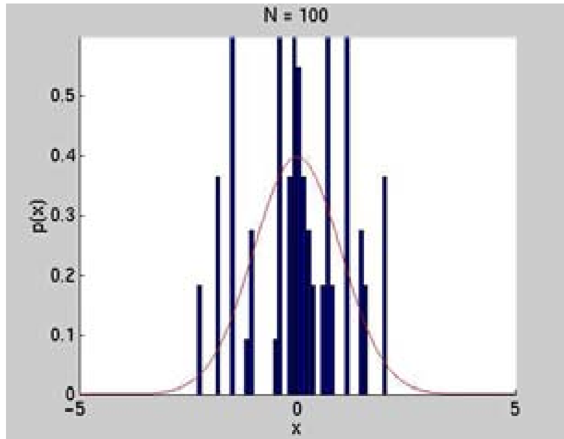

The particle filter and its application to positioning — Fredrik Gustafsson

Example: Matlab's `randn`

control & communication@liu

- Ancient versions: `randn(1,1)=sum(rand(12,1))-6`
- Prior ver. 5: Made use of polar transformation

$$(X_1, X_2) = F^{-1}(U_1, U_2)$$

where U and V are uniformly distributed on the unit disc. Matlab code:

```
r=2;
while r>1
  U=2*rand(2,1)-1;
  r=U'*U;
end
X=sqrt(sqrt(-2*log(r)/r*U;
```

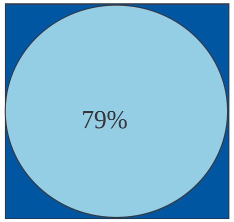

The particle filter and its application to positioning — Fredrik Gustafsson

Example: Matlab's `randn`

control & communication@liu

- After ver. 5.3: the Ziggurat algorithm (Marsaglia, Knuth).
- Accept-reject idea: accept uniform 2D numbers in the upper half plane that fall below p(x)
- Compute once in each session a rectangle approximation of p(x)

$$x_k : (f(x_k) - f(x_{k+1}))x_k = c, k = 1,...,n-1$$

$$\sigma_k = x_{k-1} / x_k$$

Accept rule (97% accepted) code:

```
K=ceil(128*rand);
U=2*rand-1;
if abs(U)<sigma(k)
  X=U*x(k);
  return
end
```

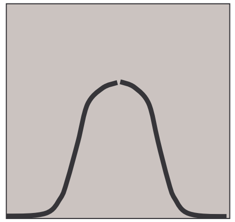

The particle filter and its application to positioning — Fredrik Gustafsson

Importance sampling

control & communication@liu

Generate N samples X from proposal pdf q(x) (support of q(x) includes support of p(x)) and take

$$\hat{I} = \frac{1}{N}\sum_{i=1}^{N} \frac{p(x^{(i)})}{q(x^{(i)})} g(x^{(i)}) \approx \int \frac{p(x)g(x)}{q(x)} q(x)dx = I$$

Example: Mean of (g(x)=x)
p(x)=0.5N(x;0,1)+0.5N(x;3,0.5)
using q(x) uniform on [-5,5].

Histogram of importance weights $\frac{p(x^{(i)})}{q(x^{(i)})}$

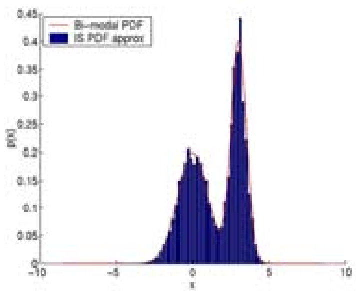

The particle filter and its application to positioning — Fredrik Gustafsson

Markov Chain Monte Carlo (MCMC)

control & communication@liu

This is a combination of

1. Monte Carlo methods,
2. Accept-reject
3. Importance sampling,

with the difference that the proposal distribution depends on the previous sample,

$$Z \propto q(z \mid x^{(i)})$$

and thus forms a Markov Chain. The idea is that the sequence of samples will converge to p(x)

The particle filter and its application to positioning — Fredrik Gustafsson

Metropolis (1970)-Hastings (1953) I

control & communication@liu

1. Let U be uniform and generate $Z \propto q(z \mid x^{(i)})$
2. Accept $x^{(i+1)} = Z$ if

$$U \le \min\left(1, \frac{p(Z)q(x^{(i)} \mid Z)}{p(x^{(i)})q(Z \mid x^{(i)})}\right)$$

Otherwise $x^{(i+1)} = x^{(i)}$

The independent M-H algorithm is very similar to the accept-reject method. Take

$$Z \propto q(z) \qquad U \le \min\left(1, \frac{p(Z)q(x^{(i)})}{p(x^{(i)})q(Z)}\right)$$

The particle filter and its application to positioning   Fredrik Gustafsson

Metropolis (1970)-Hastings (1953) II

control & communication@liu

Algorithm in special case:

- Use Bayes rule $p(x \mid y) \propto p(y \mid x)p(x)$
- Random walk Markov chain where Z from q(z) $x^{(i+1)} = x^{(i)} + Z$
- Acceptance rule

$$U \le \min\left(1, \frac{p(y \mid x^{(i)} + Z)p(x^{(i)} + Z)q(Z)}{p(y \mid x^{(i)})p(x^{(i)})q(-Z)}\right)$$

In the symmetric case p(Z)=p(-Z) (Gaussian random walk for instance) with non-informative prior (p(x)=c), then we always accept the new state if the likelihood increases. The smaller likelihood, the lower acceptance probability.

The case when using the prior as proposal distribution gives a similar rule and interpretation.

The particle filter and its application to positioning   Fredrik Gustafsson

Gibbs sampling

control & communication@liu

- For high-dimensional pdf's p(x), the marginals may be much simpler to describe than the multivariate distribution. Then sample from one marginal at the time.

Example: Generate samples X from

$$X \mid \sigma^2 \propto N(0, \sigma^2)$$
$$\sigma^2 \mid X \propto Exp(1)$$

Theoretical distribution is Laplace

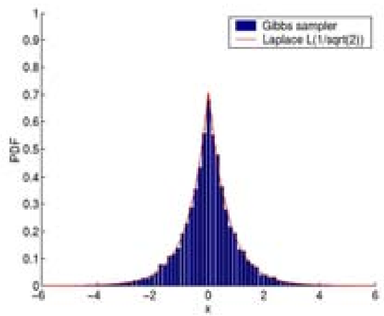

The particle filter and its application to positioning   Fredrik Gustafsson

Bootstrap

control & communication@liu

- Idea: given a sequence of iid random variables X(i) from p(x), generate a new sequence by randomly resampling N samples from this set, with replacement.
- Motivation:

$$I = \int g(x)p(x)dx \approx \frac{1}{N}\sum_{i=1}^{N} g(x^{(i)}) \approx \sum_{i=1}^{N} \frac{N(i)}{N} g(x^{(i)})$$

if E(N(i))=1

The point is that many data sets of N samples can be generated from just one, and one can get an idea of variability in the estimates (that are non-linear transformation of the samples).

The particle filter and its application to positioning   Fredrik Gustafsson

Transition to particle filter

control & communication@liu

- The particle filter contains ideas from accept-reject, Metropolis-Hastings, Gibbs, MCMC and Bootstrap!
- MCMC-interpretation: (x(1),…x(t)) -> (x(1),…,x(t+1)) forms a Markov chain. Since the state space is increasing, the standard results do not apply automatically.

The particle filter and its application to positioning — Fredrik Gustafsson

Filtering model

control & communication@liu

Model:

$$x_{t+1} = f(x_t, w_t), \quad y_t = h(x_t, e_t).$$

$$\Longleftrightarrow$$

$$x_{t+1} \sim p(x_{t+1}|x_t), \quad y_t \sim p(y_t|x_t)$$

Goal: Transform the information in the measurements $Y_t = \{y_i\}_{i=1}^{t}$ to x_t

$\downarrow$

Compute $p(x_t|Y_t)$

The particle filter and its application to positioning — Fredrik Gustafsson

Bayes

control & communication@liu

Thomas Bayes theorem is instrumental in all derivations

$$p(x|y) = \frac{p(y|x)p(x)}{p(y)}$$

The particle filter and its application to positioning — Fredrik Gustafsson

General Solution

control & communication@liu

$$p(x_t|Y_t) = \frac{p(y_t|x_t)p(x_t|Y_{t-1})}{p(y_t|Y_{t-1})}$$

$$p(y_t|Y_{t-1}) = \int_{\mathbb{R}^{n_x}} p(y_t|x_t)p(x_t|Y_{t-1})dx_t$$

$$p(x_{t+1}|Y_t) = \int_{\mathbb{R}^{n_x}} p(x_{t+1}|x_t)p(x_t|Y_t)dx_t$$

Approximate solution

PF: Approximate optimal filter on correct model
EKF: Optimal filter on approximate model

The particle filter and its application to positioning — Fredrik Gustafsson

Numerical alternatives

control & communication@liu

- Point-mass filter: Design a grid for the state space, compute

$$p(x_{t+1}|Y_t)=\int p(x_{t+1}|x_t)p(x_t|Y_t)dx_t=\int p_w(x_{t+1}-f(x_t))p(x_t|Y_t)dx_t$$

$$p(x_t|Y_t)=\frac{p(y_t|x_t)p(x_t|Y_{t-1})}{p(y_t|Y_{t-1})}=Cp_e(y_t-h(x_t))p(x_t|Y_{t-1})$$

for each grid point!
  - Simple to implement.
  - Adaptive translation and scaling of state grid required.
  - State space soon becomes very sparse, that is, a large number of grid points are required.
- Variants with Gaussian sums, splines, rectangles.

The particle filter and its application to positioning — Fredrik Gustafsson

Numerical alternatives

control & communication@liu

- The Monte Carlo idea: Simulate a large number of trajectories of the system

$$x_{t+1}=f(x_t)+w_t$$
$$y_t=h(x_t)+e_t$$

Compute the likelihood of each trajectory, and compute the weighted state mean.
  - Simple to implement.
  - Does not work at all! The state space grows with time and becomes very large.

The particle filter and its application to positioning — Fredrik Gustafsson

Particle filter algorithm

control & communication@liu

Generic Particle Filter

1. Generate random states $x_0^{(i)}\in p(x_0)$
2. Compute likelihood

$$\omega_t^{(i)}=p_e(y_t-h(x_t^{(i)}))$$

3. Resampling: $x_t^{(i)}\propto\omega_t^{(i)},\omega_t^{(i)}=\frac{1}{N}$
4. Prediction: $x_{t+1}^{(i)}=f(x_t^{(i)})+w_t^{(i)},w_t^{(i)}\in p_w$

Example: x(t+1)=x(t)+v(t)+w(t),

y(t)=h(x(t))+e(t)

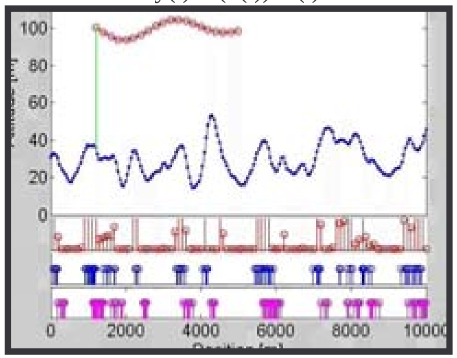

The particle filter and its application to positioning — Fredrik Gustafsson

EKF versus PF

control & communication@liu

Example: x(t+1)=x(t)+v(t)+w(t),

y(t)=h(x(t))+e(t)

EKF: linearize h(x) around current estimate.

This works well for good initialization and small noise

EKF linearizing around true trajectory gives Cramer-Rao lower bound as P(t)!

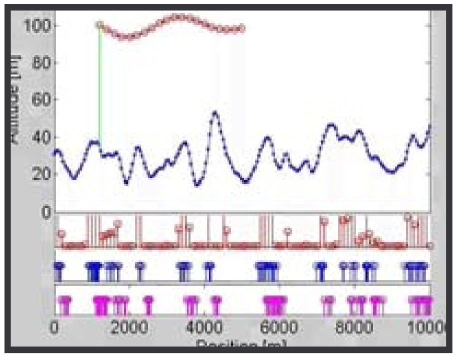

The particle filter and its application to positioning — Fredrik Gustafsson

Particle filter interpretation

control & communication@liu

1. Point-mass filter with stochastic and adaptive grid
2. Monte-Carlo method with recursive cut and branch of state trajectories
3. Approximate MCMC method
4. Genetic algorithm with probability based rules

The main difference to pure numerical methods is that certain variants of the law of large numbers and the central limit theorem exist.
Basically, these say the estimation error is bounded as

$$Var(\hat{I}) \propto \frac{p(t)}{N}$$

where p(t) is a polynomial and N is the number of particles.
At least in theory, the accuracy is independent of the state dimension.

The particle filter and its application to positioning Fredrik Gustafsson

Particle filter patches

control & communication@liu

1. Basic algorithm bootstrap inspired. One alternative is to resample only when needed, compute the effective number of samples Neff is smaller than some threshold (Sampling Importance Resampling SIR)
$$1 \leq N_{eff} = \frac{1}{\sum_{i=1}^{N} (\bar{q}_t^{(i)})^2} \leq N$$
2. Preview the next measurement in the time update (prior editing)
3. Add roughening noise to state equation to help the particles explore a larger surrounding.
4. Large number of particles needed in the transient, use clever initialization procedures or an adaptive number N(t) of particles (and perhaps also sample time!).
5. Feasability: is the required number of particles possible to implement (memory and real-time constraints)? If not, try to marginalize linear states and exclude these in the particle filter. This gives a smaller state space, saving particles.

The particle filter and its application to positioning Fredrik Gustafsson

Marginalization I (The basic idea)

control & communication@liu

- A.k.a. Rao-Blackwellization
- The case when the same Riccati equation can be used for all KF's
- General idea, exploit linear sub-structures

$$x_t = \begin{bmatrix} x_t^l \\ x_t^n \end{bmatrix}$$

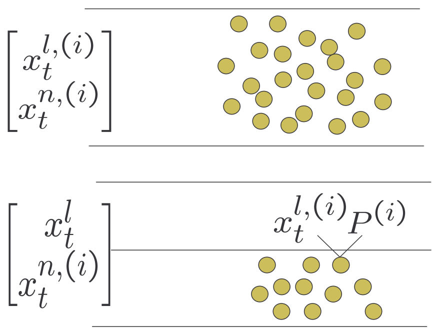

The particle filter and its application to positioning Fredrik Gustafsson

Marginalization II

control & communication@liu

Basically it is all about using Bayes' theorem:

$$p(x_t^l, X_t^n | Y_t) = \underbrace{p(x_t^l | X_t^n, Y_t)}_{Optimal KF} \underbrace{p(X_t^n | Y_t)}_{Appr. PF}$$

It is instructive to think about information flow when it comes to understanding marginalization.

The particle filter and its application to positioning Fredrik Gustafsson

Marginalization III

control & communication@liu

General model structure:

$$x^n_{t+1} = f^n_t(x^n_t) + A^n_t(x^n_t)x^l_t + G^n_t(x^n_t)w^n_t,$$
$$x^l_{t+1} = f^l_t(x^n_t) + A^l_t(x^n_t)x^l_t + G^l_t(x^n_t)w^l_t,$$
$$y_t = h_t(x^n_t) + C_t(x^n_t)x^l_t + e_t.$$

Nonlinear states x^n_t,

Linear states x^l_t

The particle filter and its application to positioning Fredrik Gustafsson

Marginalization IV

control & communication@liu

The marginalized particle filter algorithm:

1. Initialize the particles.
2. Evaluate weights.
3. Particle filter measurement update, i.e., resample.
4. Particle filter time update.
   - 4.a Kalman filter measurement update.
   - 4.b Predict new particles.
   - 4.c Kalman filter "measurement" and time update.
5. Iterate from step 2.

Difference from the standard particle filter

The particle filter and its application to positioning Fredrik Gustafsson

Marginalization V

control & communication@liu

A very important model class in applications:

$$x^n_{t+1} = A^n_{n,t}x^n_t + A^n_{l,t}x^l_t + G^n_t w^n_t,$$
$$x^l_{t+1} = A^l_{n,t}x^n_t + A^l_{l,t}x^l_t + G^l_t w^l_t,$$
$$y_t = h_t(x^n_t) + e_t.$$

Many positioning applications fall into this class, where only the position measured.

The same Ricatti equation for all Kalman filters, thus the same Kalman gain!

The particle filter and its application to positioning Fredrik Gustafsson

Positioning: Dynamic model examples

control & communication@liu

- Model when velocity is measured:

$$x_t = (X_t, X_t, \Psi_t)^T$$
$$X_{t+1} = X_t + Tv_t\cos(\Psi_t) + w_{X,t}$$
$$Y_{t+1} = Y_t + Tv_t\sin(\Psi_t) + w_{Y,t}$$
$$\Psi_{t+1} = \Psi_t + T\dot{\Psi}_t$$
$$y_t = h(X_t, Y_t) + e_t$$

- Model when velocity is <u>not</u> measured (then estimate it!):

$$x_t = (X_t, \dot{X}_t, Y_t, \dot{Y}_t)$$
$$x_{t+1} = \begin{pmatrix} 1 & T & 0 & 0 \\ 0 & 1 & 0 & 0 \\ 0 & 0 & 1 & T \\ 0 & 0 & 0 & 1 \end{pmatrix} x_t + \begin{pmatrix} T^2/2 & 0 \\ T & 0 \\ 0 & T^2/2 \\ 0 & T \end{pmatrix} w_t$$
$$y_t = h(X_t, Y_t) + e_t$$

The particle filter and its application to positioning Fredrik Gustafsson

Positioning: Sensor examples

control & communication@liu

- Generic measurement depends only on the current position (X,Y)

$$y_t = h(X_t, Y_t) + e_t$$

- Examples of target tracking standard sensors:
  - Radar measures range and bearing to (X,Y)
  - IR and radar warning systems measure bearing to (X,Y)
- Examples of navigation standard sensors:
  - INS measures acceleration and rotations of coordinates (X,Y)
  - GPS
  - Wireless network measurements: Loran-C, GSM (cell ID, timing advance, time difference of arrival
  - Maps!!

The particle filter and its application to positioning Fredrik Gustafsson

Positioning: Sensor examples in com.

control & communication@liu

- Cell-Identifier (CI)
- Sector information or Angle of Arrival (AOA) (requires adaptive antennas)
- Timing Advance (TA) d_{TA} = ½ • 3.69µs symbol period • 3e8 m/s = 554m
- Enhancement: usage of received signal levels (RXLEV), see operator's power attenuation map below.

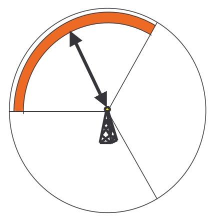

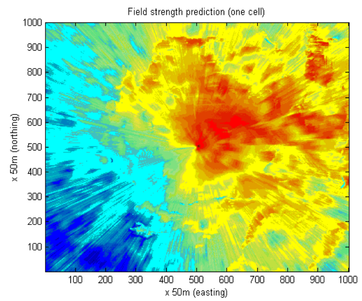

The particle filter and its application to positioning Fredrik Gustafsson

Positioning: GIS as a sensor

control & communication@liu

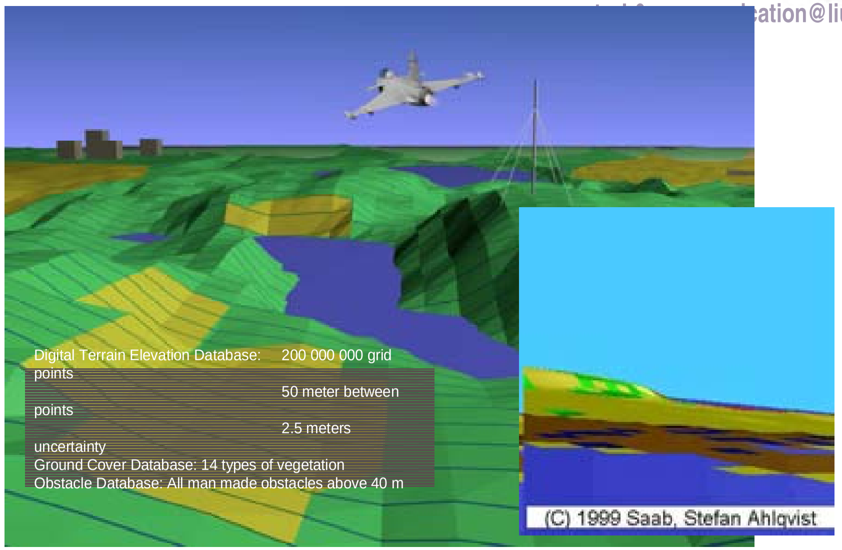

The particle filter and its application to positioning Fredrik Gustafsson

Aircraft navigation

control & communication@liu

New (2G) integrated navigation and landing system for JAS is based on particle filter for terrain navigation

Next generation may be based on marginalized particle filter for sensor fusion (27 state EKF today)

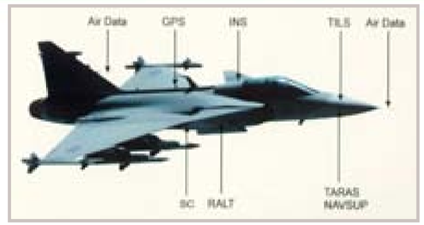

The particle filter and its application to positioning Fredrik Gustafsson

Terrain-aided navigation I

control & communication@liu

Two-dimensional version of example:

x(t+1)=x(t)+v(t)+w(t),
y(t)=h(x(t))+e(t)

Two applications:

1. h(x) terrain map and
   y(t)=barometric altitude - height radar
   v(t) from INS
2. h(x) under-water depth map and
   y(t)=echo sound
   v(t) from rudder and propeller speed

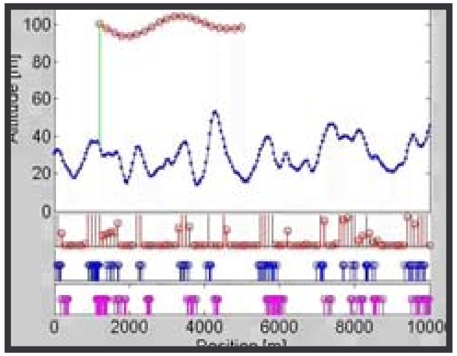

Note:

1. **Cramer-Rao: position error > sqrt (altitude error * velocity error / terrain variation)**
2. **The particle filter normally attains the Cramer-Rao bound!**

The particle filter and its application to positioning — Fredrik Gustafsson

Terrain-aided navigation II

control & communication@liu

2D Example

- Simulated flight trajectory on GIS
- Snapshots at t=0, 20 and 31 seconds
- Red: true   Green: estimate

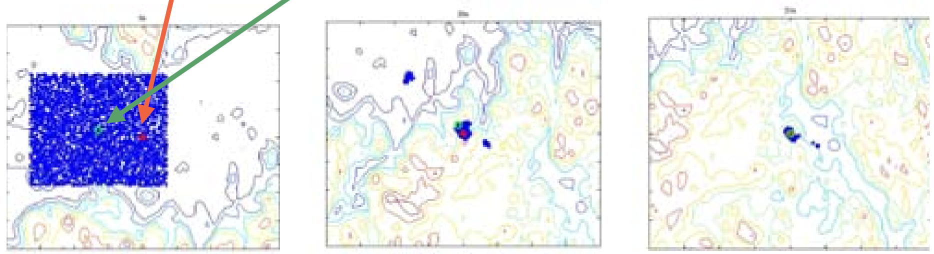

The particle filter and its application to positioning — Fredrik Gustafsson

Terrain-aided navigation III

control & communication@liu

Animation of terrain navigation in 2D using real GIS

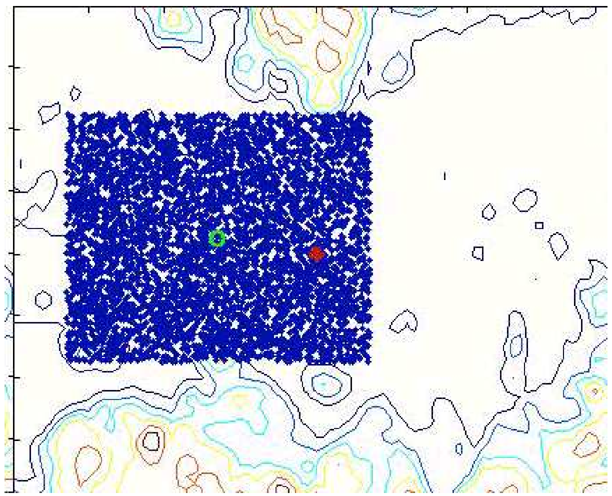

The particle filter and its application to positioning — Fredrik Gustafsson

Underwater terrain navigation

control & communication@liu

- Underwater navigation using sonar sensors with aid from rudder and log (propeller speed) for motion model.
- Underwater map built in swedish lake, using surface ship with GPS for validation.
- Particle filter satisfies Cramer-Rao lower bound (depends on the map)

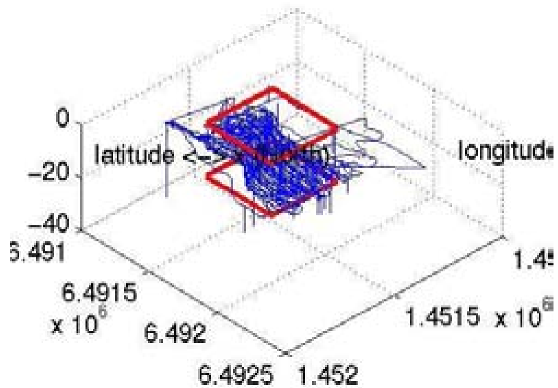

The particle filter and its application to positioning — Fredrik Gustafsson

Car positioning I

control & communication@liu

- Initizalization using manual marking or GSM positioning

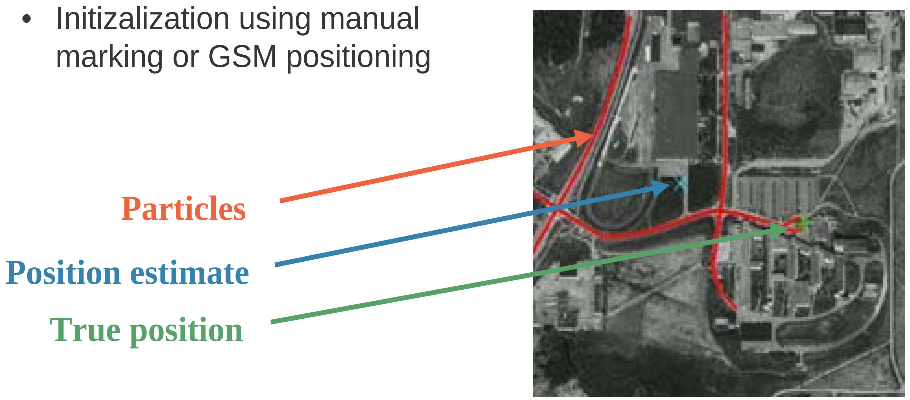

The particle filter and its application to positioning — Fredrik Gustafsson

Car positioning II

control & communication@liu

- Initizalization using manual marking or GSM positioning
- After slight bend, four particle clusters left

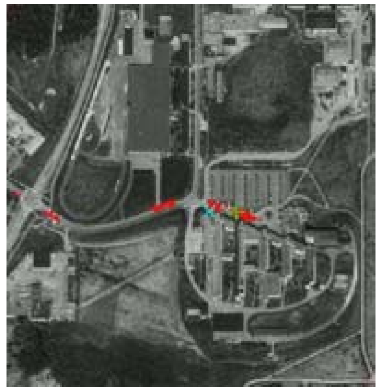

The particle filter and its application to positioning — Fredrik Gustafsson

Car positioning III

control & communication@liu

- Initizalization using manual marking or GSM positioning
- After slight bend, four particle clusters left
- Convergence after turn

The particle filter and its application to positioning — Fredrik Gustafsson

Car positioning IV

control & communication@liu

- Initizalization using manual marking or GSM positioning
- After slight bend, four particle clusters left
- Convergence after turn
- Spread along the road

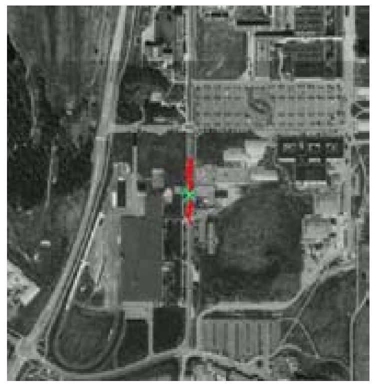

The particle filter and its application to positioning — Fredrik Gustafsson

Car positioning V

control & communication@liu

- Particle filter using street map and v(t),$\dot{\Psi}(t)$ from car's ABS sensors.
- Green - true position
- Blue – estimate
- Red - particles

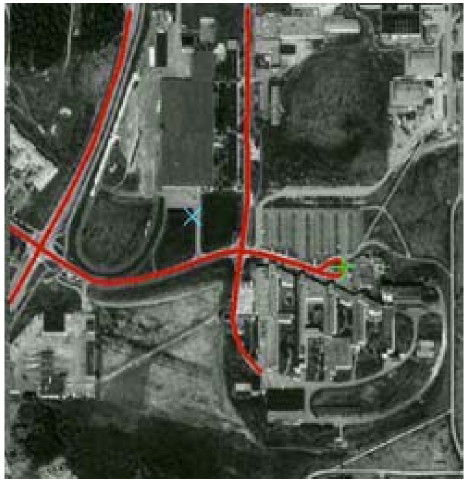

The particle filter and its application to positioning Fredrik Gustafsson

Car positioning VI

control & communication@liu

- Particle filter using street map and v(t),$\dot{\Psi}(t)$ from car's ABS sensors and GSM cell ID and sector for initialization
- Purple: GPS
- Blue: particles
- Light blue: estimate
- Photo background

The particle filter and its application to positioning Fredrik Gustafsson

Car positioning VII

control & communication@liu

- Red – GPS
- Light green: particles
- Blue: estimate (after convergence)
- Real-time implementation on Compac iPAQ
- Works without or with GPS
- Map database background

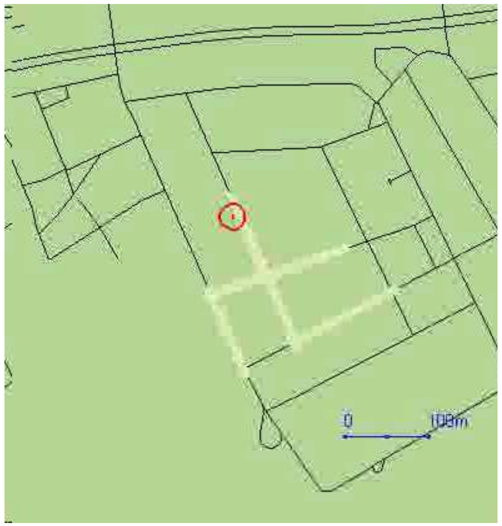

The particle filter and its application to positioning Fredrik Gustafsson

Car positioning VIII

- Complete navigator with voice guidance!
- Integer implementation of the particle filter (ISIS project)
- PF in simulation mode off-road
- # particles up to 15000 (without GPS) or as small as 50 (with GPS)
- On-going R&D work at NIRA Dynamics AB and ISIS

The particle filter and its application to positioning Fredrik Gustafsson

Network measurements I

control & communication@liu

1. Cell ID and Received signal strength:
- Sector information (usually 60 degrees)
- One or more sectors:
  - Connected antenna (yellow pages service)
  - Power measurements from 5 (GSM) or 6 (WCDMA) antennas
- Power attenuation: Hata's formula or map-based

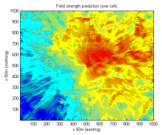

The particle filter and its application to positioning Fredrik Gustafsson

TDOA static positioning

control & communication@liu

- Particle filter with decaying roughening noise

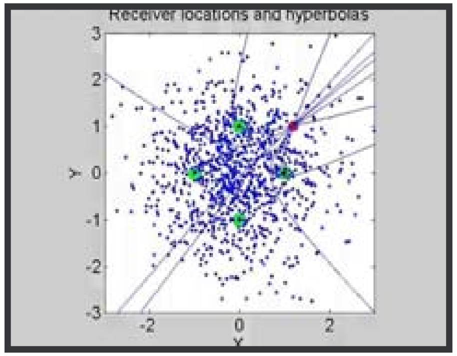

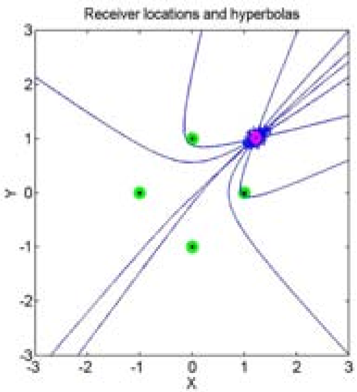

The particle filter and its application to positioning Fredrik Gustafsson

Network positioning

control & communication@liu

- Positioning of cellular phones using network measurements
- Focus on dynamic estimation and automotive application
- Flexible framework configurable with an asynchronous mixture of information sources:
  1. Map: street, altitude, attenuation
  2. Angle and range to fix-point: AOA, TOA, TDOA, GPS
  3. Velocity and turn rate: $v(t), \dot{\Psi}(t)$
- Particle filter suitable because of its ability to include:
  1. Non-linear constraints (map)
  2. Non-Gaussian noise (Rice and Rayleigh fading, operator's power attenuation map, etc.)

The particle filter and its application to positioning Fredrik Gustafsson

Conclusions

control & communication@liu

- Flexible framework for **positioning** configurable with an asynchronous mixture of information sources:
  1. Map: street, altitude, attenuation
  2. Wireless measurements as angle and range to fix-point: AOA, TOA, TDOA, GPS
  3. Inertial measurements like velocity and turn rate: $v(t), \dot{\Psi}(t)$
  4. Distance and range measurements from radar, IR, etc.
- **Particle filter** suitable because of its ability to include:
  1. Non-linear dynamic models
  2. Non-linear constraints (map)
  3. Non-Gaussian noise (radar loob, geometric transformation, Rice and Rayleigh fading, operator's power attenuation map, etc.)

The particle filter and its application to positioning Fredrik Gustafsson

Distributed Control in Large Actuator/Sensor Arrays

Bassam Bamieh

http://www.engineering.ucsb.edu/~bamieh

DEPARTMENT OF MECHANICAL ENGINEERING
UNIVERSITY OF CALIFORNIA, SANTA BARBARA

23rd Benelux Meeting on Systems and Controls, March '04I

0

LARGE ARRAYED SYSTEMS OF SENSORS AND ACTUATORS

- **New (and old) technologies**
  - Micro-Electro-Mechanical-Systems (MEMS) ⟶ Large Arrays
  - Vehicular Platoons
  - Cross Directional (CD) control in pulp and paper processes
- **Modeling and control issues**
  - Complexity (Control-Oriented Modeling)
  - Overall *System Design* (vs. individual device design)
  - Controller architecture
- **Distributed Systems Theory**
  - Infinite-dimensional systems with special structure
  - Controller architecture

1

EXAMPLE: MASSIVELY PARALLEL DATA STORAGE

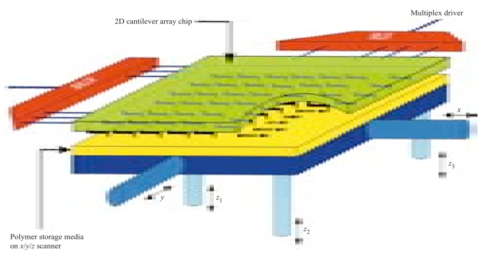

Figure 1: The IBM Millipede system (from Vettiger et. al.)

- Atomic level resolution using Atomic Force Microscopy (AFM) and Scanning Tunneling Microscopy (STM) techniques

  $100 \sim 1000\ Tb/in^2$ density possible!

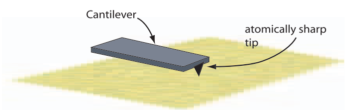

- **Problem:** slow scans = low throughput
  Solution: go massively parallel

2

ARRAYS OF MICRO-ELECTRO-MECHANICAL-SYSTEMS (MEMS)

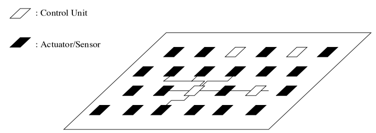

Figure 2: Device array with integrated controls

CURRENTLY FEASIBLE: Very large arrays of MEMS with integrated control circuitry

Issues:

- **Tightly coupled dynamics** ⟶ Spatio-temporal instabilities *(e.g. string instability)*
  Current designs avoid this with large spacing
- **Controller architecture**
  - Layout of sensors/actuators
  - Communication between actuators/sensors
    how to decentralize or localize

3

Micro-cantilever Array Control

Capacitively actuated micro-cantilevers: *Combined* actuator and sensor

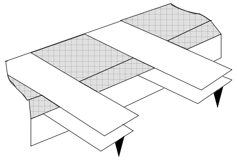

Important Considerations:

- Higher throughput, faster "access time" ⟶ Tightly packed cantilevers
- For tightly packed cantilevers, significant dynamical coupling due to
  - Mechanical coupling
  - Fringe fields
    (Napoli & Bamieh, '01)

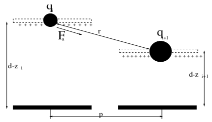

- Large arrays ≈ 10,000 devices
  ⇒ must use localized control

4

Distributed Systems with Special Structure

- General Infinite-dimensional Systems Theory
  - Well posedness issues (semi-group theory)
  - Constructive (convergent) approximation techniques

THEME: *Make infinite-dimensional problems look like finite-dimensional ones*

- Special Structure
  - Distributed control and measurement *(now more feasible)*
  - Regular (lattice) arrangement of devices

Together ⟹ *Spatial Invariance*

- Control of "Vehicular Strings", (Melzer & Kuo, 71)
- Discretized PDEs, (Brockett, Willems, Krishnaprasd, El-Sayed, '74, '81)
- "Systems over rings", (Kamen, Khargonekar, Sontag, Tannenbaum, ...)
- Systems with "Dynamical Symmetry", (Fagniani & Willems)

More recently:

- Controller architecture and localization, (Bamieh, Paganini, Dahleh)
- LMI techniques, localization, (D'Andrea, Dullerud, Lall)

5

Example: Distributed Control of the Heat Equation

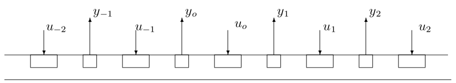

u_i: input to heating elements. y_i: signal from temperature sensor.
Dynamics are given by:

$$\begin{bmatrix} \vdots \\ y_{-1} \\ y_o \\ y_1 \\ \vdots \end{bmatrix} = \begin{bmatrix} & \vdots & & \vdots & \\ \cdots & & H_{-1,0} & & \cdots \\ & H_{0,-1} & H_{0,0} & H_{0,1} & \\ \cdots & & H_{1,0} & & \cdots \\ & \vdots & & \vdots & \end{bmatrix} \begin{bmatrix} \vdots \\ u_{-1} \\ u_o \\ u_1 \\ \vdots \end{bmatrix}$$

Each $H_{i,j}$ is an infinite-dimensional SISO system.

Fact: Dynamics are spatially invariant ⇒ H is Toeplitz

The input-output relation can be written as a *convolution over the actuator/sensor index*:

$$y_i = \sum_{j=-\infty}^{\infty} \bar{H}_{(i-j)}\, u_j,$$

The limit of large actuator sensor array:

$$\frac{\partial \psi}{\partial t}(x,t) = c\frac{\partial^2 \psi}{\partial x^2}(x,t) + u(x,t) \qquad \psi_x = \int_{-\infty}^{\infty} H_{x-\zeta}\, u_\zeta d\zeta,$$

6

Vehicular Platoons

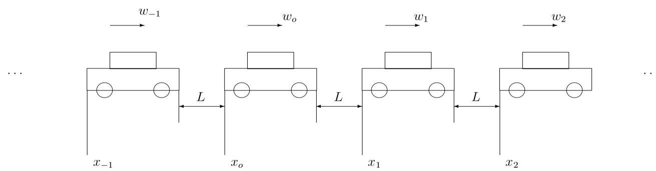

Figure 3: Longitudinal control of a vehicular platoon

Objective: Design a controller for each vehicle to:

- Maintain constant small slot length L.
- Reject the effect of disturbances $\{w_i\}$ (wind gusts, road conditions, etc...)

Warning: Designs based on two vehicle models may lack "string stability", i.e. disturbances get amplified as they propagate through the platoon.

Problem Structure:

- Actuators: each vehicle's throttle input.
- Sensors: position and velocity of each vehicle.

7

Vehicular Platoons Set-up

x_i: i'th vehicle's position.

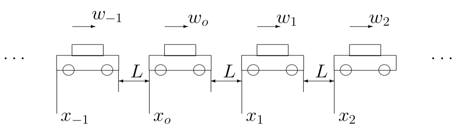

$$\tilde{x}_i := x_i - x_{i-1} - L - C$$
$$\tilde{x}_{1,i} := \tilde{x}_i$$
$$\tilde{x}_{2,i} := \dot{\tilde{x}}_i$$

State space model of the platoon (identical vehicles):

$$\dot{\tilde{x}}_i = \begin{bmatrix} 0 & 1 \\ 0 & 0 \end{bmatrix} \tilde{x}_i + \begin{bmatrix} 0 \\ \alpha \end{bmatrix} w_i + \begin{bmatrix} 0 \\ -\alpha \end{bmatrix} w_{i-1} + \begin{bmatrix} 0 \\ \beta \end{bmatrix} u_i + \begin{bmatrix} 0 \\ -\beta \end{bmatrix} u_{i-1}$$
$$z_i = C_1 \tilde{x}_i + D_{12} u_i$$
$$y_i = C_2 \tilde{x}_i$$

Structure of generalized plant:

$$H = \begin{bmatrix} H_{11} & H_{12} \\ H_{21} & H_{22} \end{bmatrix} = \begin{bmatrix} \times & & \times & \\ & & & 0 \\ & & h_o & \\ \times & & h_1 & \\ & 0 & & \end{bmatrix}$$

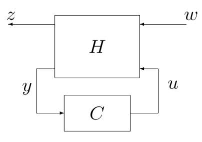

The generalized plant has a Toeplitz structure!

$$z = \mathcal{F}(H, C)\, w$$

8

Optimal Controller for Vehicular Platoon

Example: Centralized $\mathcal{H}^2$ optimal controller gains for a 50 vehicle platoon (From: Shu and Bamieh '96)

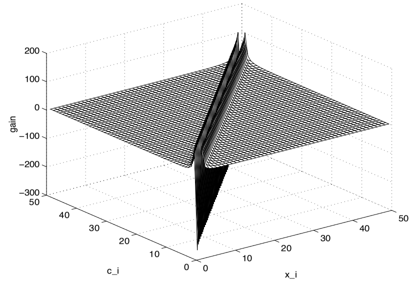

Figure 4: Position error feedback gains for a 50 vehicle platoon

Remarks:

- For large platoons, optimal controller is Toeplitz $\Rightarrow$ *Controller* is spatially invariant
- Optimal centralized controller has some inherent decentralization *Controller gains decay away from the diagonal*

Question: Are the above two results peculiar to this problem, or do they occur in all spatially-invariant problems?

9

Spatial Invariance of Dynamics

Indexing of actuator and sensor signals:

Let

$$u_i(t) := u_{(i_1,\ldots,i_n)}(t), \qquad y_i(t) := y_{(i_1,\ldots,i_n)}(t).$$

$i := (i_1, \ldots, i_n)$ is a spatial multi-index, $\quad i \in \mathbb{G} := \mathbb{G}_1 \times \ldots \times \mathbb{G}_n$.

Linear input-output relations:

A general linear system from u to y can be written as:

$$y_i = \sum_{j \in \mathbb{G}} H_{i,j}\, u_j, \quad \Leftrightarrow \quad y_{(i_1,\ldots,i_n)} = \sum_{j_1 \in \mathbb{G}_1} \cdots \sum_{j_n \in \mathbb{G}_n} H_{(i_1,\ldots,i_n),(j_1,\ldots,j_n)}\, u_{(j_1,\ldots,j_n)},$$

Spatial Invariance:

Assumption 1 *The set of indices of all signals forms a commutative group. Specifically,*

$$\mathbb{G} := \mathbb{G}_1 \times \ldots \times \mathbb{G}_n, \qquad \textit{where each } \mathbb{G}_i \textit{ is a group.}$$

Remark: A "shifting" of a signal's indices can be represented as an action:

$(S_\sigma u)_i := u_{i-\sigma}$ Compare with: *Time shift by* τ $(S_\tau u)(t) := u(t-\tau)$

Assumption 2 *The input-output mapping of the plant is spatially invariant with respect to the signal index. That is:*

$$\forall \sigma \in \mathbb{G}, \qquad H\, S_\sigma = S_\sigma\, H \quad \Leftrightarrow \quad S_\sigma^{-1} H S_\sigma = H$$

10

Examples of Spatial Invariance

Generally: Spatial invariance can be easily ascertained from basic physical symmetry in the problem!

H spatially invariant $\Leftrightarrow$ $S_\sigma^{-1} H S_\sigma = H$ $\Leftrightarrow$ $H S_\sigma = S_\sigma H$

- Vehicular platoons and array of heating elements: signals index over $\mathbb{Z}$.
- Channel flow: Signals indexed over $\{0,1\} \times \mathbb{Z}$:

$$y_{(l,i)} = \sum_{j=-\infty}^{\infty} H_{(l-0,i-j)}\, u_{(0,j)} + \sum_{j=-\infty}^{\infty} H_{(l-1,i-j)}\, u_{(1,j)}, \qquad l = 0, 1.$$

$H_{(0,i-j)}$: Transfer function from j'th actuator to i'th sensor on same side of channel.
$H_{(1,i-j)}$: Transfer function from j'th actuator to i'th sensor on opposite side of channel.

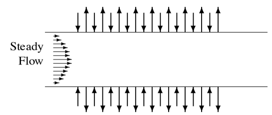

- Pipe flow: Signals indexed over $\mathbb{Z}_N \times \mathbb{Z}$

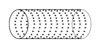

Remark: The input-output mapping of a spatially invariant system can be rewritten:

$$y_i = \sum_{j \in \mathbb{G}} \bar{G}_{i-j}\, u_j, \quad \Leftrightarrow \quad y_{(i_1,\ldots,i_n)} = \sum_{j_1 \in \mathbb{G}_1} \cdots \sum_{j_n \in \mathbb{G}_n} \bar{G}_{(i_1-j_1,\ldots,i_n-j_n)}\, u_{(j_1,\ldots,j_n)}.$$

$$\boxed{y_i = \int_{\mathbb{G}} G_{i-j} u_j\, dj}$$

11

Symmetry in Dynamical Systems and Control Design

- Many-body systems always have some inherent dynamical symmetries: e.g. equations of motion are invariant to certain coordinate transformations
- **Question:** Given an unstable dynamical system with a certain symmetry, is it possible to stabilize it with a controller that has the same symmetry? (i.e. without "breaking the symmetry")
- **Answer:** Yes! (Fagnani & Willems '93)

Remark: Spatial invariance is a dynamical symmetry
we will answer this question with regard to optimal design as well

12

The Standard Problem of Optimal and Robust Control

The standard problem:
H: Generalized plant
C: Controller
w: Exogenous signals (disturbances, noise)
z: regulated variables
u: controls
y: measurements

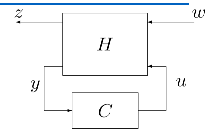

$z = \mathcal{F}(H, C)\, w$

Norms:

Signal norms:

$$\|w\|_p := \left(\sum_{i \in \mathbb{G}} \int_{\mathbb{R}} |w_i(t)|^p dt \right)^{\frac{1}{p}} = \left(\sum_{i \in \mathbb{G}} \|w\|_p^p \right)^{\frac{1}{p}}$$

Induced system norms:

$$\|\mathcal{F}(G, C)\|_{p-i} := \sup_{w \in L^P} \frac{\|z\|_p}{\|w\|_p}.$$

The $\mathcal{H}^2$ norm:

$$\|\mathcal{F}(G, C)\|_{\mathcal{H}^2} = \|z\|_2 = \left(\sum_{i \in \mathbb{G}} \|z_i\|_{L^2}^2 \right)^{\frac{1}{2}},$$

with impulsive disturbance input $w_i(t) = \delta(i)\delta(t)$.

Note: In the platoon problem: finite system norm $\Rightarrow$ string stability.

13

Spatially-Invariant vs. Spatially-Varying Controllers

Question: Can one do better with spatially-varying controllers than with spatially-invariant ones?
Answer: Depends on whether the generalized plant is spatially invariant.

Define:
$LSI :=$ The class of Linear Spatially-Invariant systems.
$LSV :=$ The class of Linear Spatially-Varying systems.

Compare the two problems:

$$\gamma_{si} := \inf_{\substack{\text{stabilizing } C \\ C \in LSI}} \|\mathcal{F}(G, C)\|_{p-i} \qquad \gamma_{sv} := \inf_{\substack{\text{stabilizing } C \\ C \in LSV}} \|\mathcal{F}(G, C)\|_{p-i}$$

The best achievable performance with spatially-invariant controllers — The best achievable performance with spatially-varying controllers

Theorem 1 *If the plant and performance objectives are spatially invariant, i.e. if the generalized plant G is spatially invariant, then the best achievable performance can be approached with a spatially invariant controller. More precisely*

$$\gamma_{si} = \gamma_{sv}.$$

14

Spatially-Invariant vs. Spatially-Varying Controllers (Cont.)

Related Problem: *Time-Varying vs. Time-Invariant Controllers*

Fact: For norm minimization problems and time-invariant plants, time-varying controllers offer no advantage over time-invariant ones!

Proofs are based on the use of the YJBK parameterization to reduce the problem to that of:

$$\gamma_{ti} := \inf_{\substack{\text{stable } Q \\ Q \in LTI}} \|T_1 - T_2QT_3\| \qquad \gamma_{tv} := \inf_{\substack{\text{stable } Q \\ Q \in LTV}} \|T_1 - T_2QT_3\|,$$

where T_1, T_2, T_3 are determined by the plant, and are therefore time invariant.

- The $\mathcal{H}^\infty$ case: (Feintuch & Francis, '85), (Khargonekar, Poolla, & Tannenbaum, '85). *A consequence of Nehari's theorem*
- The ℓ^1 case: (Shamma & Dahleh, '91). *Using an averaging technique*
- Any induced ℓ^p norm: (Chapellat & Dahleh, '92). *Generalization of the averaging technique*

15

Spatially-Invariant vs. Spatially-Varying Controllers (Cont.)

Idea of proof:
After YJBK parameterization Problem becomes:

$$\gamma_{si} := \inf_{\substack{\text{stable } Q \\ Q \in LSI}} \|T_1 - T_2 Q T_3\| \quad \geq \quad \gamma_{sv} := \inf_{\substack{\text{stable } Q \\ Q \in LSV}} \|T_1 - T_2 Q T_3\| ,$$

Let $\bar{Q}$ achieve a performance level $\bar{\gamma} = \|T_1 - T_2 \bar{Q} T_3\|$.

Averaging $\bar{Q}$:

- If $\mathbb{G}$ is finite: define

$Q_{av} := \frac{1}{|\mathbb{G}|} \sum_{\sigma \in \mathbb{G}} \sigma^{-1} \bar{Q} \sigma.$ *Note that Q_{av} is spatially invariant, i.e.* $\forall \sigma \in \mathbb{G}, \quad \sigma^{-1} Q_{av}\, \sigma = Q_{av}.$

Then

$$\|T_1 - T_2 Q_{av} T_3\| = \left\|T_1 - T_2 \left(\frac{1}{|\mathbb{G}|} \sum_{\sigma \in \mathbb{G}} \sigma^{-1} \bar{Q} \sigma\right) T_3\right\| = \left\|\frac{1}{|\mathbb{G}|} \sum_{\sigma \in \mathbb{G}} \sigma^{-1} \left(T_1 - T_2 \bar{Q} T_3\right) \sigma\right\|$$

$$\leq \frac{1}{|\mathbb{G}|} \sum_{\sigma \in \mathbb{G}} \left\|\sigma^{-1} \left(T_1 - T_2 \bar{Q} T_3\right) \sigma\right\| = \|T_1 - T_2 \bar{Q} T_3\|$$

- If $\mathbb{G}$ is infinite, take a sequence of finite subsets $M_1 \subset M_2 \subset \cdots$, with $\bigcup_n M_n = \mathbb{G}$,

Then define: $Q_n := \frac{1}{|M_n|} \sum_{\sigma \in M_n} \sigma^{-1} \bar{Q} \sigma.$

Q_n converges weak $*$ to a spatially-invariant Q_{av} with the required norm bound.

16

Implications of the Structure of Spatial Invariance

Poiseuille flow stabilization:

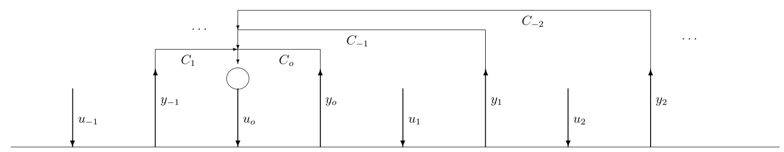

Channel

$$u_i = \sum_j C_{i-j}\, y_j$$

17

Implications of the Structure of Spatial Invariance

Poiseuille flow stabilization:

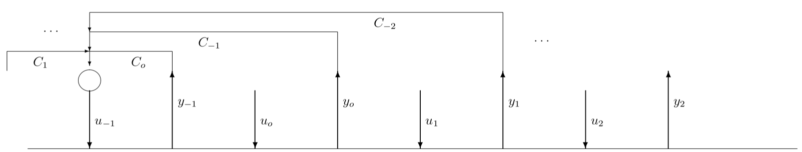

Channel

$$u_i = \sum_j C_{i-j}\, y_j$$

18

Implications of the Structure of Spatial Invariance (Cont.)

Uneven distribution of sensors and actuators

Consider the following geometry of sensors and actuators:

- • Sensor
- ■ Actuator

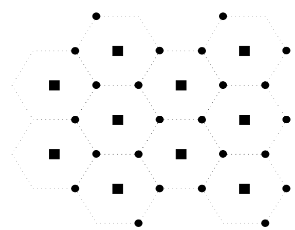

What kind of spatial invariance do optimal controllers have?

19

Implications of the Structure of Spatial Invariance (Cont.)

Uneven distribution of sensors and actuators (Cont.)

Consider the following geometry of sensors and actuators:

- • Sensor
- ■ Actuator

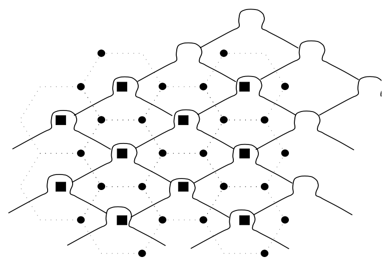

Each "cell" is a 1-input, 2-output system. **underlying group is $\mathbb{Z} \times \mathbb{Z}$**

20

Transform Methods

Consider the following PDE with distributed control:

$$\frac{\partial \psi}{\partial t}(x_1,\dots,x_n,t) = \mathcal{A}\left(\frac{\partial}{\partial x_1},\dots,\frac{\partial}{\partial x_n}\right)\psi(x_1,\dots,x_n,t) + \mathcal{B}\left(\frac{\partial}{\partial x_1},\dots,\frac{\partial}{\partial x_n}\right)u(x_1,\dots,x_n,t)$$
$$y(x_1,\dots,x_n,t) = \mathcal{C}\left(\frac{\partial}{\partial x_1},\dots,\frac{\partial}{\partial x_n}\right)\psi(x_1,\dots,x_n,t),$$

where $\mathcal{A},\mathcal{B},\mathcal{C}$ are matrices of polynomials in $\frac{\partial}{\partial x_i}$.
Consider also combined PDE difference equations such as:

$$\frac{\partial \psi}{\partial t}(x_1,\dots,x_m,k_1,\dots,k_n,t) = \mathcal{A}\left(\frac{\partial}{\partial x_1},\dots,\frac{\partial}{\partial x_n},z_1^{-1},\dots,z_n^{-1}\right)\psi(x_1,\dots,x_n,k_1,\dots,k_n,t)$$
$$+\mathcal{B}\left(\frac{\partial}{\partial x_1},\dots,\frac{\partial}{\partial x_n},z_1^{-1},\dots,z_n^{-1}\right)u(x_1,\dots,x_n,k_1,\dots,k_n,t)$$

We only require that the spatial variables x, k, belong to a commutative group
Taking the Fourier transform:

$$\hat{\psi}(\lambda,t) := \int_{\mathbb{G}} e^{-j<\lambda,x>}\psi(x,t)\,dx,$$

The above system equations become:

$$\frac{d\hat{\psi}}{dt}(\lambda,t) = \mathcal{A}(\lambda)\,\hat{\psi}(\lambda,t) + \mathcal{B}(\lambda)\,\hat{u}(\lambda,t)$$
$$\hat{y}(\lambda,t) = \mathcal{C}(\lambda)\,\hat{\psi}(\lambda,t),$$

where $\lambda \in \hat{\mathbb{G}}$, the dual group to $\mathbb{G}$.
Remark: This can be thought of as a parameterized family of finite-dimensional systems.

21

Transform Methods (Cont.)

For L^2 signals, we have a Parseval's relation:

$$\int_{\mathbb{G}} |w(x,t)|^2 dx = \int_{\hat{\mathbb{G}}} |\hat{w}(\lambda,t)|^2 d\lambda.$$

An isometric isomorphism between spatial domain and spatial frequency domain.

Therefore: *In the L^2 sense, the distributed parameter system is* STABLE, CONTROLLABLE, OBSERVABLE, STABILIZABLE, DETECTABLE *if and only if the system*

$$\frac{d\hat{\psi}}{dt}(\lambda,t) = \mathcal{A}(\lambda)\,\hat{\psi}(\lambda,t) + \mathcal{B}(\lambda)\,\hat{u}(\lambda,t)$$
$$\hat{y}(\lambda,t) = \mathcal{C}(\lambda)\,\hat{\psi}(\lambda,t),$$

is STABLE, CONTROLLABLE, OBSERVABLE, STABILIZABLE, DETECTABLE, *respectively for every $\lambda \in \hat{\mathbb{G}}$.*

Remark: Similar to results in the "systems over rings" literature. (Kamen, Sontag, Khargonekar, Delchamps, early '80's) (For $\mathbb{G} = \mathbb{Z}$, and over the algebra $\ell^1(\mathbb{Z})$).

Furthermore: *For quadratic problems such as $\mathcal{H}^2$ and $\mathcal{H}^\infty$, optimal designs can be performed "frequency by frequency". That is, for each $\lambda \in \hat{\mathbb{G}}$ we design a finite dimensional controller $\mathcal{K}(\lambda)$.*

Remark: The LQR case for $\mathbb{G} = \mathbb{Z}$ appears in Melzer & Kuo, '70, and for $\mathbb{G} = \mathbb{Z}_n$ in Brockett & Willems, '74.

22

Optimal $\mathcal{H}_2$ and $\mathcal{H}_\infty$ Problems (Cont.)

The standard problem:

$$\frac{\partial}{\partial t}\psi(x,t) = A\psi(x,t) + B_1 w(x,t) + B_2 u(x,t)$$
$$z(x,t) = C_1\psi(x,t) + D_{12}u(x,t)$$
$$y(x,t) = C_2\psi(x,t) + D_{21}w(x,t),$$

Solution method:

1. Transform problem to obtain family of finite-dimensional problems parameterized by $\lambda \in \hat{\mathbb{G}}$.
2. For each $\lambda \in \hat{\mathbb{G}}$, solve corresponding matrix ARE's. Get family of solutions $\{X(\lambda)\}$, $\{Y(\lambda)\}$. (*these are the Fourier representation of the translation-invariant solutions to the operator Ricatti equations of the infinite dimensional problem*)
3. For each $\lambda \in \hat{\mathbb{G}}$, construct finite dimensional controller
$$\frac{d}{dt}\hat{\psi}_K(\lambda,t) = \hat{A}_K(\lambda)\psi_K(\lambda,t) + \hat{B}_K(\lambda)y(\lambda,t)$$
$$u(\lambda,t) = \hat{C}_K(\lambda)\psi_K(\lambda,t) + \hat{D}_K(\lambda)y(\lambda,t)$$
4. Invert Fourier transform the matrix-valued functions $\hat{A}_K, \hat{B}_K, \hat{C}_K, \hat{D}_K$ to get convolution representation of controller:
$$\frac{\partial}{\partial t}\psi_K(x,t) = A_K\psi_K(x,t) + B_K y(x,t)$$
$$u(x,t) = C_K\psi_K(x,t) + D_K y(x,t),$$
where A_K, B_K, C_K, D_K are spatial convolution operators.

23

Simple Example; Distributed LQR Control of Heat Equation

$$\frac{\partial}{\partial t}\psi(x,t) \;=\; c\frac{\partial^2}{\partial x^2}\psi(x,t) + u(x,t) \qquad \longrightarrow \qquad \frac{d}{dt}\hat{\psi}(\lambda,t) = -c\lambda^2\hat{\psi}(\lambda,t) + \hat{u}(\lambda,t)$$

Solve the LQR problem with $Q = qI$, $R = I$. The corresponding ARE family:

$$-2c\lambda^2\,\hat{p}(\lambda) - \hat{p}(\lambda)^2 + q = 0,$$

and the positive solution is:

$$\hat{p}(\lambda) = -c\lambda^2 + \sqrt{c^2\lambda^4 + q}.$$

Remark: In general $\hat{P}(\lambda)$ will be an irrational function of λ, even if the original $\hat{A}(\lambda), \hat{B}(\lambda)$ are rational.
i.e. PDE systems have optimal feedbacks which are *not* PDE operators.

Let $\{k(x)\}$ be the inverse Fourier transform of the function $\{-\hat{p}(\lambda)\}$.
Then

$$u(x,t) \;=\; \int_{\mathbb{R}} k(x-\xi)\;\psi(\xi,t)\;d\xi$$

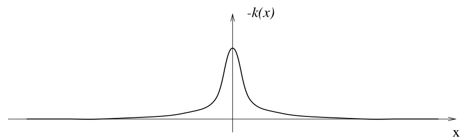

Remark: The "spread" of $\{k(x)\}$ indicates information required from distant sensors.

24

Distributed LQR Control of Heat Equation (Cont.)

Important Observation: $\{k(x)\}$ is "localized". It decays exponentially!!

Recall:

$$\hat{k}(\lambda) = c\lambda^2 - \sqrt{c^2\lambda^4 + q}.$$

This can be analytically extended by:

$$\hat{k}_e(s) = cs^2 - \sqrt{c^2 s^4 + q},$$

which is analytic in the strip

$$\left\{ s \in \mathbb{C}\;;\; Im\{s\} < \frac{\sqrt{2}}{2}\left(\frac{q}{c^2}\right)^{\frac{1}{4}} \right\}.$$

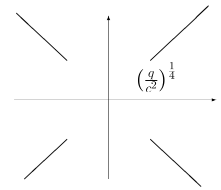

Therefore: $\exists M$ such that

$$|k(x)| \;\leq\; Me^{-\alpha|x|}, \quad \text{for any } \alpha < \frac{\sqrt{2}}{2}\left(\frac{q}{c^2}\right)^{\frac{1}{4}}.$$

This results is true in general: under mild conditions
Solutions of AREs always inverse transform to exponentially decaying convolution kernels

25

Parameterized ARE solutions yield "localized" operators!

Consider unbounded domains, i.e. $\mathbb{G} \;=\; \mathbb{R}$ (or $\mathbb{Z}$).

Theorem 2 *Consider the parameterized family of Riccati equations:*

$$A^*(\lambda)P(\lambda) \;+\; P(\lambda)A(\lambda) \;-\; P(\lambda)B(\lambda)R(\lambda)B^*(\lambda)P(\lambda) \;+\; Q(\lambda) \;=\; 0, \qquad \lambda \in \hat{\mathbb{G}}.$$

Under mild conditions:
there exists an analytic continuation $P(s)$ of $P(\lambda)$ in a region

$$\{|Im(s)| < \alpha\}, \quad \alpha > 0.$$

Remark: The convolution kernel resulting from the solution of a Parameterized ARE has exponential rates of decay.
That is, they have some degree of inherent decentralization (*"localization"*)!

Comparison:

- **Modal truncation:** In the transform domain, ARE solutions decay algebraically.
- **Spatial truncation:** In the spatial domain, convolution kernel of ARE solution decays exponentially.

Therefore: Use transform domain to design $\forall\lambda$. Approximate in the spatial domain!

26

Distributed Architecture of Quadratically Optimal Controllers

Example: Consider a one dimensional arrays of systems indexed in $\mathbb{Z}$.

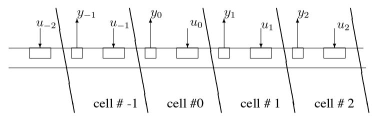

ψ_n: a finite-dimensional approximation of the state of the system in the n'th cell

$$\frac{d}{dt}\psi_n \;=\; \sum_m A_{n-m}\,\psi_m \;+\; \sum_m B_{n-m}\,u_m$$
$$y_n \;=\; C\,\psi_n$$

Note: Need not approximate the state of the *overall* system

27

Distributed Architecture of Quadratically Optimal Controllers

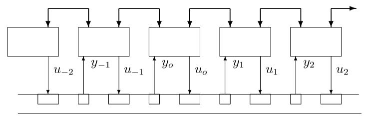

An observer based controller for the overall system would have the following structure:

Plant

$$\begin{aligned} \tfrac{d}{dt}\psi_n &= \textstyle\sum_m A_{n-m}\,\psi_m \;+\; \sum_m B_{n-m}\,u_m \\ y_n &= C\,\psi_n \end{aligned}$$

Controller

$$\begin{aligned} u_i &= \textstyle\sum_j K_{i-j}\,\hat{\psi}_j \\ \tfrac{d}{dt}\hat{\psi}_n &= \textstyle\sum_m A_{n-m}\,\hat{\psi}_m \;+\; \sum_m B_{n-m}\,u_m \\ &\quad + \textstyle\sum_m L_{n-m}\,(y_m - \hat{y}_m) \end{aligned}$$

Remarks:

- Optimal Controller is “locally” finite dimensional.
- The gains $\{K_i\}$, $\{L_i\}$ are localized, therefore can be truncated.
- After truncation, local controller need only receive information (measurements and local state estimates) from neighboring subsystems.
- Quadratically optimal controllers are inherently distributed and semi-decentralized.

28

The many remaining issues

- Various heterogeneities
  - Spatial variance
  - Irregular arrangements of sensors and actuators
- How to specify “localization” apriori
- The complexities of “high order”

29

Understanding and Controlling Turbulent Shear Flows

Bassam Bamieh

http://www.engineering.ucsb.edu/~bamieh

DEPARTMENT OF MECHANICAL ENGINEERING
UNIVERSITY OF CALIFORNIA, SANTA BARBARA

23rd Benelux Meeting on Systems and Controls, March '04I

HYDRODYNAMIC STABILITY (MATHEMATICAL FORMULATION)

The incompressible Navier-Stokes equations

$$\begin{aligned} \partial_t \mathbf{u} &= -\nabla_{\mathbf{u}} \mathbf{u} - \text{grad } p + \tfrac{1}{R}\Delta \mathbf{u} \\ 0 &= \text{div } \mathbf{u} \end{aligned}$$

$\mathbf{u} \leftrightarrow \begin{bmatrix} u(x,y,z,t) \\ v(x,y,z,t) \\ w(x,y,z,t) \end{bmatrix}$ 3D velocity fields

$p(x,y,z,t)$ pressure field

The central question: **Given a laminar flow, is it stable?**

- **laminar flow** $:=$ a stationary solution of the Navier-Stokes equations

- Decompose the fields as

$$\mathbf{u} = \underset{\text{laminar}}{\underset{\uparrow}{\bar{\mathbf{u}}}} + \underset{\text{fluctuations}}{\underset{\uparrow}{\tilde{\mathbf{u}}}}$$

- Fluctuation dynamics:

$$\begin{aligned} \partial_t \tilde{\mathbf{u}} &= -\nabla_{\bar{\mathbf{u}}} \tilde{\mathbf{u}} - \nabla_{\tilde{\mathbf{u}}} \bar{\mathbf{u}} - \text{grad } \tilde{p} + \Delta \tilde{\mathbf{u}} - \nabla_{\tilde{u}} \tilde{u} \\ 0 &= \text{div } \tilde{\mathbf{u}} \end{aligned}$$

In *linear* hydrodynamic stability, $- \nabla_{\tilde{u}} \tilde{u}$ is ignored

PHENOMENA AND MATHEMATICAL THEORIES

The natural phenomena

- As parameters change (e.g. velocity)
  fluid flows "transition" from simple (*laminar*) to very complex (*turbulent*)
- Depending on the flow geometry
  transition can occur abruptly, gradually, or in several stages

The mathematical models

- Transition from one stage to the next $\leftrightarrow$ dynamical instability
  successful in many cases, e.g. Benard convection, Taylor-Coutte flow, etc..
- In important cases, e.g. shear flows in streamlined geometries
  ... instability is too narrow a concept to capture the notion of transition
- Transition in general involves questions of robustness, sensitivity and stability

Examples:

- Poiseuille Flow

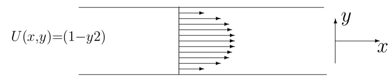

- Couette Flow

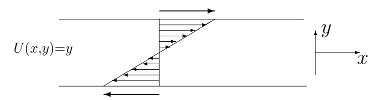

- Pipe Flow

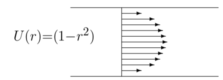

- Blasius boundary layer

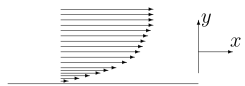

- Others:
  - Benard Convection (Between two horizontal plates)
  - Taylor-Couette (Flow between two concentric rotating cylinders)

The Evolution Model

Can rewrite linearized fluctuation equations using only two fields

v := wall-normal velocity

ω := wall-normal vorticity $:= \dfrac{\partial u}{\partial z} - \dfrac{\partial w}{\partial x}$.

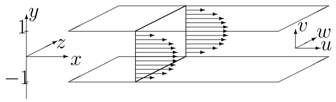

Equivalent equations:

$$\partial_t \begin{bmatrix} v \\ \omega \end{bmatrix} = \begin{bmatrix} (-\Delta^{-1}U\partial_x\Delta + \Delta^{-1}U''\partial_x + \frac{1}{R}\Delta^{-1}\Delta^2) & 0 \\ (-U'\partial_z) & (-U\partial_x + \frac{1}{R}\Delta) \end{bmatrix} \begin{bmatrix} v \\ \omega \end{bmatrix}$$

$$\partial_t \begin{bmatrix} v \\ \omega \end{bmatrix} = \begin{bmatrix} \mathcal{L} & 0 \\ \mathcal{C} & \mathcal{S} \end{bmatrix} \begin{bmatrix} v \\ \omega \end{bmatrix} =: \mathcal{A} \begin{bmatrix} v \\ \omega \end{bmatrix}$$

Abstractly,

$$\partial_t \Psi = \mathcal{A}\,\Psi$$

Classical linear hydrodynamic stability:

Transition $\longleftrightarrow$ instability $\equiv$ $\mathcal{A}$ has spectrum in right half plane

existence of exponentially growing normal modes a modal instability

Tollmien-Schlichting Instability

Example: **Poiseuille** flow at $R = 6000$, $k_x = 1$, $k_z = 0$ has the following eigenvalues:

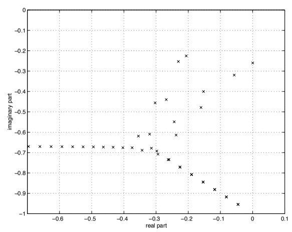

Typical stability regions in K, R space: (for **Poiseuille** and **Blasius** boundary layer flows)

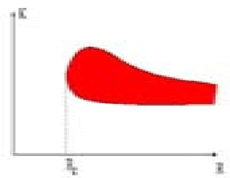

Unstable eigenvalue corresponds to a slowly growing travelling wave: the *Tollmien-Schlichting* wave
Tollmien '29, Schlichting '33. (also occurs in boundary layer flows)
First seen in experiments by Skramstad & Schubauer, 1940.

The Eigenvalue Problem

$$\frac{\partial}{\partial t} \begin{bmatrix} v \\ \omega \end{bmatrix} = \begin{bmatrix} (-\Delta^{-1}U\frac{\partial}{\partial x}\Delta + \Delta^{-1}U''\frac{\partial}{\partial x} + \frac{1}{R}\Delta^{-1}\Delta^2) & 0 \\ (-U'\frac{\partial}{\partial z}) & (-U\frac{\partial}{\partial x} + \frac{1}{R}\Delta) \end{bmatrix} \begin{bmatrix} v \\ \omega \end{bmatrix}$$

$$\frac{\partial}{\partial t} \begin{bmatrix} v \\ \omega \end{bmatrix} = \begin{bmatrix} \mathcal{L} & 0 \\ \mathcal{C} & \mathcal{S} \end{bmatrix} \begin{bmatrix} v \\ \omega \end{bmatrix} = \mathcal{A} \begin{bmatrix} v \\ \omega \end{bmatrix}$$

Remark: $\mathcal{A}$ is translation invariant in x, z (but not in y!). Fourier transform in x and z:

$$\frac{\partial}{\partial t} \begin{bmatrix} \hat{v} \\ \hat{\omega} \end{bmatrix} = \begin{bmatrix} (-ik_x\Delta^{-1}U\Delta + ik_x\Delta^{-1}U'' + \frac{1}{R}\Delta^{-1}\Delta^2) & 0 \\ (-ik_zU') & (-ik_xU + \frac{1}{R}\Delta) \end{bmatrix} \begin{bmatrix} \hat{v} \\ \hat{\omega} \end{bmatrix}$$

k_x, k_z: spatial frequencies in x, z directions (wave-numbers).

$$\frac{\partial}{\partial t} \begin{bmatrix} \hat{v}(t,k_z,k_x) \\ \hat{\omega}(t,k_z,k_x) \end{bmatrix} = \hat{\mathcal{A}}(k_x,k_z) \begin{bmatrix} \hat{v}(t,k_z,k_x) \\ \hat{\omega}(t,k_z,k_x) \end{bmatrix}, \qquad \hat{v}(t,k_z,k_x), \hat{\omega}(t,k_z,k_x) \in L^2[-1,1]$$

Essentially:

$$\text{spectrum}\,(\mathcal{A}) = \bigcup_{k_x,k_z} \text{spectrum}\left(\hat{\mathcal{A}}(k_x,k_z)\right)$$

Problems with the Theory (1st Difficulty)

R_c: The critical Reynolds number at which instability occurs

$R \geq R_c$ $\Rightarrow$ $\exists$ unstable eigenvalues of $\mathcal{A}$

corresponding eigenfunctions are flow structures that grow exponentialy at transition

- Classical linear hydrodynamic stability is successful in many problems, e.g.
  - Benard Convection
  - Taylor-Couette Flow (*Flow between two rotating concentric cylinders*)

- Classical linear hydrodynamic stability fails badly in a very important special case
  Shear flows: (*e.g. flows in channels, pipes, and boundary layers*)

Flow type	Classical linear theory R_c	Experimental R_c
Poiseuille	5772	$\approx$ 1000
Couette	∞	$\approx$ 350
Pipe	∞	$\approx$ 2200

Experimental R_c is highly dependent on conditions such as wall roughness, external disturbances, etc...

Problems with the theory (2nd difficulty)

Second failure: Incorrect prediction of "natural transition" flow structures

- Classical theory predicts *Tollmien-Schlichting waves* in Poiseuille and boundary layer flows:

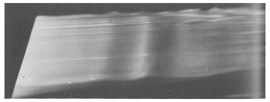

- Except in very noise-free and controlled experiments, flow structures in transition are more like turbulent spots and streaky boundary layers:

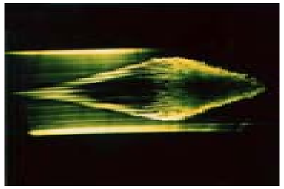

Boundary layer with free-stream disturbances

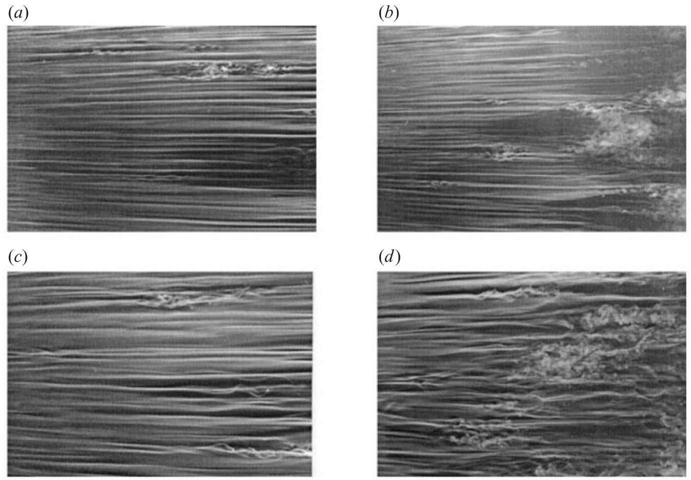

From Matsubara & Alfredsson, 2001

Transition Scenarios

1. Infinitesimal disturbances ⟹ TS-wave ⟹ 3D Secondary instabilities ⟹ Transition

Demonstrable in "clean" experiments

2. Infinitesimal disturbances ⟹ Stream-wise vortices and streaks ⟹ Transition

Occurs when small amounts of noise is present

Possible explanation:
noisy environments ⟶ big disturbances ⟶ "non-linear effects" dominate

The emerging new theory

- Since '89, a new mathematical approach to linear hydrodynamic stability emerged
  (Farrell, Ioannou, Butler, Henningson, Reddy, Trefethen, Driscoll, Gustavsson,...)
  Recent book: Schmidt & Henningson
  - Transient growth
  - Pseudo-spectrum
  - Noise amplification

- Amazing similarity to notions from Robust Control
  Even though systems are stable (subcritical), they have
  - Large transient growth
  - Large input-output norms
  - Small stability margins

BASICALLY: Use *robustness analysis*, rather than eigenvalues to quantify transition
IMPLICATIONS:

- Transition is no longer on/off
- Significant implications for control-oriented modelling

The Evolution Model

$$\frac{\partial}{\partial t}\begin{bmatrix} v \\ \omega \end{bmatrix} = \begin{bmatrix} \left(-\Delta^{-1}U\frac{\partial}{\partial x}\Delta + \Delta^{-1}U''\frac{\partial}{\partial x} + \frac{1}{R}\Delta^{-1}\Delta^2\right) & 0 \\ \left(-U'\frac{\partial}{\partial z}\right) & \left(-U\frac{\partial}{\partial x} + \frac{1}{R}\Delta\right) \end{bmatrix}\begin{bmatrix} v \\ \omega \end{bmatrix}$$

$$\frac{\partial}{\partial t}\begin{bmatrix} v \\ \omega \end{bmatrix} = \begin{bmatrix} \mathcal{L} & 0 \\ \mathcal{C} & \mathcal{S} \end{bmatrix}\begin{bmatrix} v \\ \omega \end{bmatrix} = \mathcal{A}\begin{bmatrix} v \\ \omega \end{bmatrix}$$

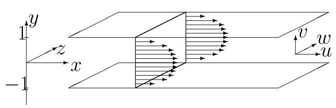

After Fourier transform:

$$\frac{\partial}{\partial t}\begin{bmatrix} \hat{v} \\ \hat{\omega} \end{bmatrix} = \begin{bmatrix} \left(-ik_x\Delta^{-1}U\Delta + ik_x\Delta^{-1}U'' + \frac{1}{R}\Delta^{-1}\Delta^2\right) & 0 \\ (-ik_zU') & \left(-ik_xU + \frac{1}{R}\Delta\right) \end{bmatrix}\begin{bmatrix} \hat{v} \\ \hat{\omega} \end{bmatrix}$$

k_x, k_z: spatial frequencies in x, z directions *(wave-numbers)*.

Linearized Navier-Stokes equations with forcing

- Add body forces to the LNSE

$$\partial_t\tilde{\mathbf{u}} = -\nabla_{\bar{\mathbf{u}}}\tilde{\mathbf{u}} - \nabla_{\tilde{\mathbf{u}}}\bar{\mathbf{u}} - \nabla\tilde{p} + \frac{1}{R}\Delta\tilde{\mathbf{u}} + \mathbf{d}$$
$$0 = \nabla\cdot\tilde{\mathbf{u}}$$

- In new coordinates

$$\partial_t\psi = \underbrace{\begin{bmatrix} \mathcal{L} & 0 \\ \mathcal{C} & \mathcal{S} \end{bmatrix}}_{\mathcal{A}}\psi + \underbrace{\begin{bmatrix} \Delta^{-1} & 0 \\ 0 & I \end{bmatrix}\begin{bmatrix} -\partial^2_{xy} & \partial^2_{xx}+\partial^2_{zz} & -\partial^2_{yz} \\ \partial_z & 0 & -\partial_x \end{bmatrix}}_{\mathcal{B}}\mathbf{d}$$

Transient energy growth of perturbed flow fields

The *energy density* of a perturbation for a given k_x, k_z is

$$E = \frac{k_xk_z}{16\pi^2}\int_{-1}^{1}\int_0^{2\pi/k_x}\int_0^{2\pi/k_z}(u^2+v^2+w^2)\,dz\,dx\,dy$$

which can be rewritten as a quadratic form on the normal velocity and vorticity fields as:

$$E = \left\langle \begin{bmatrix} \hat{v} \\ \hat{\omega} \end{bmatrix}, \begin{bmatrix} I - \frac{1}{k_x^2+k_z^2}\frac{\partial^2}{\partial y^2} & 0 \\ 0 & \frac{1}{k_x^2+k_z^2}I \end{bmatrix}\begin{bmatrix} \hat{v} \\ \hat{\omega} \end{bmatrix}\right\rangle =: \langle \Psi, \mathcal{Q}\,\Psi\rangle .$$

The evolution of the disturbance's energy

$$\|\Psi(t)\|^2 = \|e^{\mathcal{A}t}\Psi(0)\|^2 = \left\langle \Psi(0)\,,\ \left\{e^{\mathcal{A}^*t}\mathcal{Q}e^{\mathcal{A}t}\right\}\Psi(0)\right\rangle$$

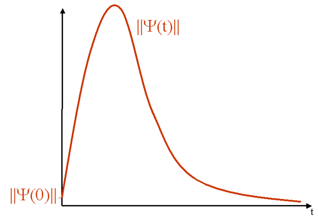

Recently, research in this field has been motivated by the following distinction:

- If $\mathcal{A}$ is stable and normal (w.r.t. Q), then $\|e^{\mathcal{A}t}\Psi(0)\|$ decays monotonically for $t > 0$.
- If $\mathcal{A}$ is non-normal, then large transient energy growth is possible.
  (Farrell, Butler, Trefethen, Driscoll, Henningson, Reddy, et.al.... '89-present)

The Input-Output View

Allow for external excitation into the dynamics:

$$\frac{\partial}{\partial t}\begin{bmatrix} v \\ \omega \end{bmatrix} = \begin{bmatrix} \left(-\Delta^{-1}U\frac{\partial}{\partial x}\Delta + \Delta^{-1}U''\frac{\partial}{\partial x} + \frac{1}{R}\Delta^{-1}\Delta^2\right) & 0 \\ \left(-U'\frac{\partial}{\partial z}\right) & \left(-U\frac{\partial}{\partial x} + \frac{1}{R}\Delta\right) \end{bmatrix}\begin{bmatrix} v \\ \omega \end{bmatrix} + \mathcal{B}\begin{bmatrix} d_v \\ d_\omega \end{bmatrix}$$

Sources of external disturbance d:

- Disturbance body forces (free stream disturbances, thermal fluctuations, etc.)
- Non-smooth geometries (rough walls, uncertain laminar flow profiles)
- Neglected nonlinearity
- Unmodeled dynamics (a "small gain"-type robust stability analysis)

Question: Investigate the system mapping $d \longmapsto \Psi$

Surprises:

- Even when $\mathcal{A}$ is stable, the mapping $d \longmapsto \Psi$ has large norms (and scales badly with R)
- The input-output resonances are very different from the least damped modes of $\mathcal{A}$
  (as spatio-temporal patterns)

Input-Output vs. Modal Analysis

A simple example: given a finite-dimensional Single-Input Single-Output system

$$\begin{aligned} \dot{x} &= Ax + Bu \\ y &= Cx \end{aligned} \qquad \Longleftrightarrow \qquad H(s) = C(sI - A)^{-1}B$$

Theorem: *Let $z_1, \ \ldots, \ z_n$ be any locations in the left half of the complex plane. Any stable frequency response function in $\mathcal{H}^2$ can be arbitrarily closely approximated by a transfer function of the following form:*

$$H(s) = \sum_{i=1}^{N_1} \frac{\alpha_{1,i}}{(s - z_1)^i} + \cdots + \sum_{i=1}^{N_n} \frac{\alpha_{n,i}}{(s - z_n)^i}$$

by choosing any of the N_k's large enough

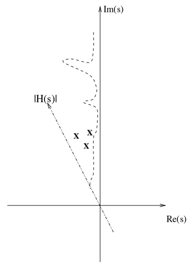

i.e.: *No connection between underdamped modes of A and peaks of frequency response $H(j\omega)$*

Dominance of Stream-wise Constant Flow Structures

$$\lambda_{\max}\left(\int_{-\infty}^{\infty} H(\omega, k_x, k_z) H^*(\omega, k_x, k_z)\, d\omega\right) = \textit{a scalar function of } (k_x, k_z)$$

averaging out time, and taking $\sigma_{\max}$ in y direction

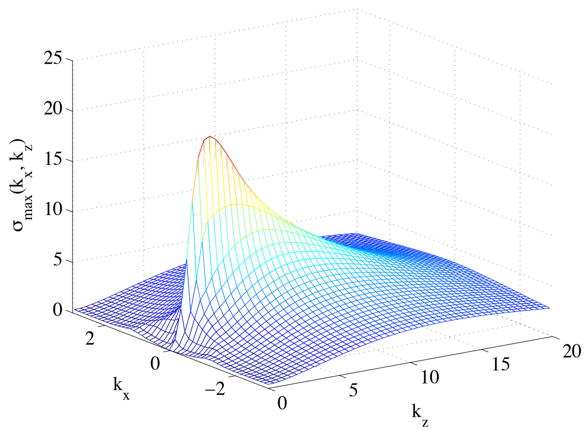

Poiseuille flow at R=2000.

Spatio-temporal Frequency Response

$$\frac{\partial}{\partial t}\Psi(t, k_x, k_z) = \mathcal{A}(k_x, k_z)\, \Psi(k_x, k_z) + \mathcal{B}(k_x, k_z)\, d(t, k_x, k_z)$$

Fourier transform in time

$$\Psi(\omega, k_x, k_z) = \left((j\omega\mathcal{I} - \mathcal{A}(k_x, k_z))^{-1}\mathcal{B}\right) d(\omega, k_x, k_z) =: H(\omega, k_x, k_z)\, d(\omega, k_x, k_z)$$

The operator-valued spatio-temporal frequency response

$$H(\omega, k_x, k_z)$$

is a MIMO (in y) frequency response of several frequency variables

- *Not allways straight forward to visualize, has* ***lots*** *of information*

Dominance of Stream-wise Constant Flow Structures (cont.)

$$\sup_{-\infty<\omega<\infty} \lambda_{\max}\left(H(\omega, k_x, k_z) H^*(\omega, k_x, k_z)\right)$$

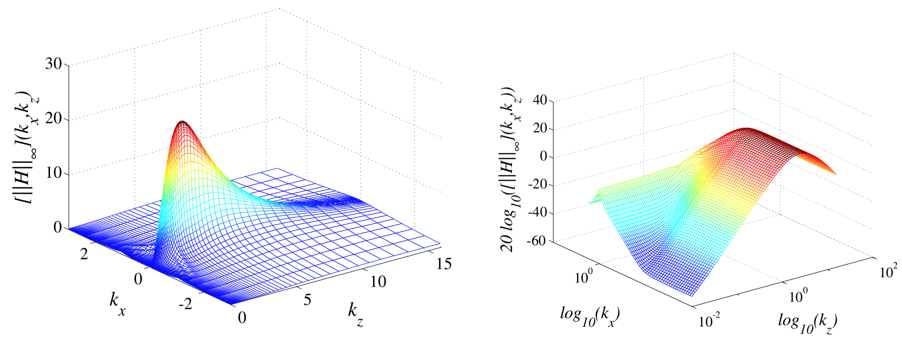

A log-log plot

- Poiseuille flow at R=2000.

DOMINANCE OF STREAM-WISE CONSTANT FLOW STRUCTURES (CONT.)

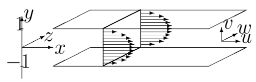

Peak of freq. response corresponds to stream-wise vortices and streaks

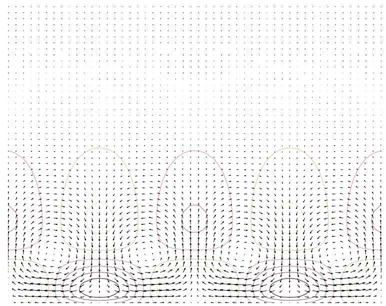

channel cross section view:

arrows are (w, v) velocities (parallel to cross section)

level sets are for stream-wise velocity u

MECHANISM OF GENERATION OF STREAM-WISE VORTICES AND STREAKS

$$\frac{\partial}{\partial t}\begin{bmatrix}\hat v\\ \hat\omega\end{bmatrix} = \begin{bmatrix}(\frac{1}{R}\Delta^{-1}\Delta^2) & 0\\ (-ik_zU') & (\frac{1}{R}\Delta)\end{bmatrix}\begin{bmatrix}\hat v\\ \hat\omega\end{bmatrix} + \begin{bmatrix}d_v\\ d_\omega\end{bmatrix} =: \begin{bmatrix}\frac{1}{R}\mathcal{L} & 0\\ \mathcal{C} & \frac{1}{R}\mathcal{S}\end{bmatrix}\begin{bmatrix}\hat v\\ \hat\omega\end{bmatrix} + \begin{bmatrix}d_v\\ d_\omega\end{bmatrix}$$

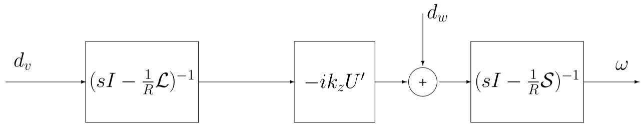

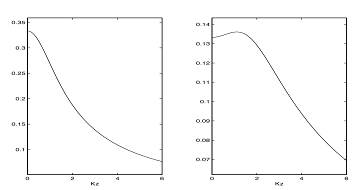

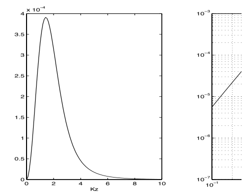

STREAM-WISE VORTICES AND STREAKS

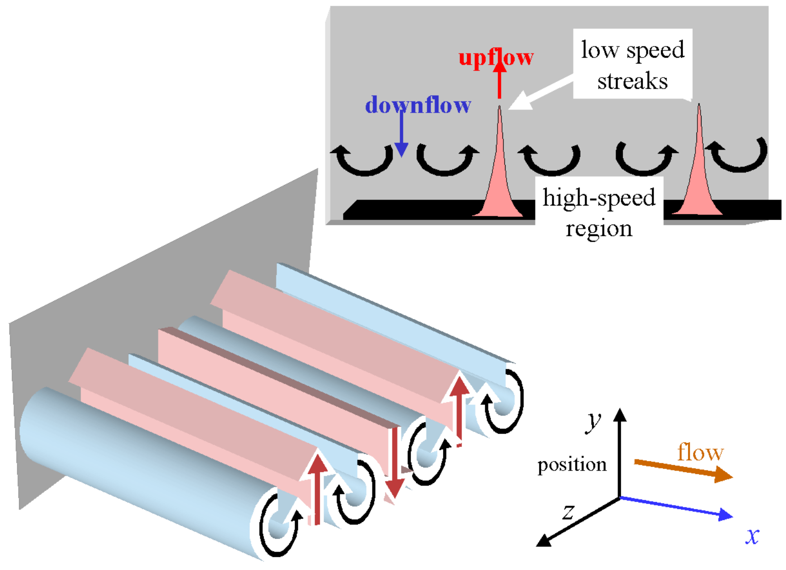

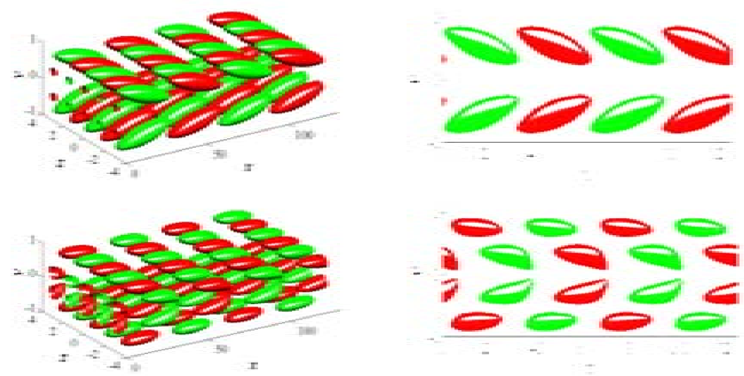

Figure 3: Streamwise velocity perturbation development for largest singular value (first row) and second largest singular value (second row) of operator $\hat{\mathcal{H}}$ at $\{k_x = 0.1,\ k_z = 2.12,\ \omega = -0.066\}$, in Poiseuille flow with $R = 2000$. High speed streaks are represented by red color, and low speed streaks are represented by green color. Isosurfaces are taken at ± 0.5.

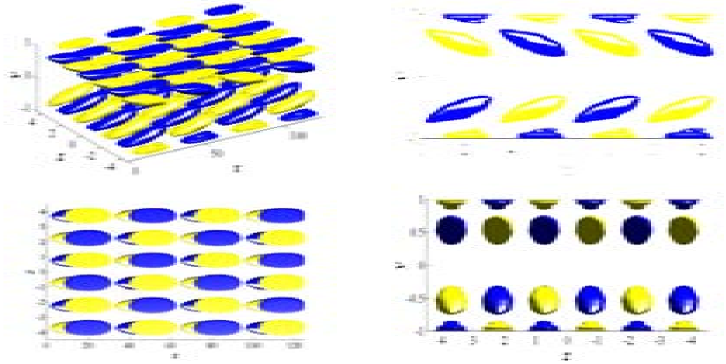

Figure 8: Streamwise vorticity perturbation development for largest singular value of operator $\hat{\mathcal{H}}$ at $\{k_x = 0.1,\ k_z = 2.12,\ \omega = -0.066\}$, in Poiseuille flow with $R = 2000$. High vorticity regions are represented by yellow color, and low vorticity regions are represented by blue color. Isosurfaces are taken at ± 0.4.

Frequency response (more detailed analysis)

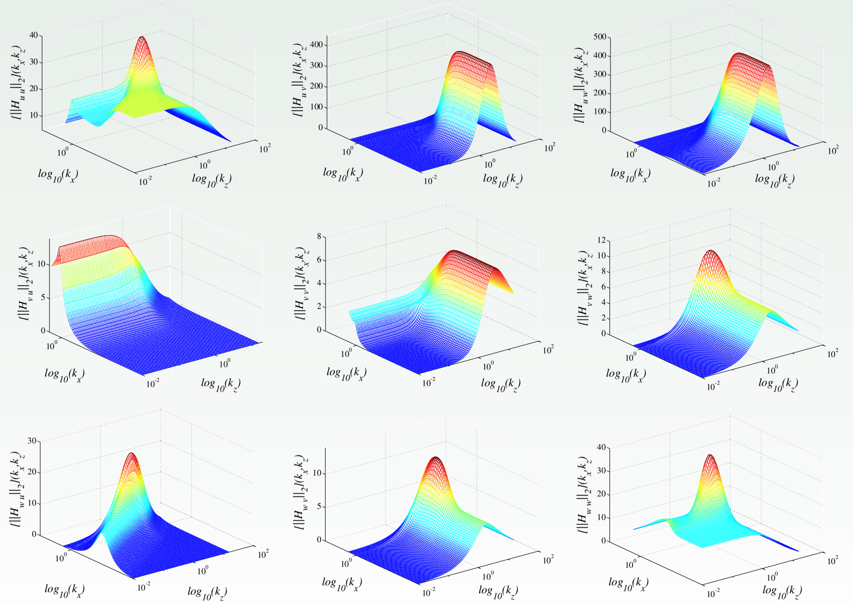

Frequency response (more detailed analysis)

$$\hat{\mathbf{u}}(k_x, k_z, \omega) \;=\; \hat{\mathcal{H}}(k_x, k_z, \omega)\, \hat{\mathbf{d}}(k_x, k_z, \omega)$$

Effect of forcing in different directions on different velocity fields

$$\begin{bmatrix} \hat{u}(k_x,k_z,\omega) \\ \hat{v}(k_x,k_z,\omega) \\ \hat{w}(k_x,k_z,\omega) \end{bmatrix} = \begin{bmatrix} \hat{\mathcal{H}}_{uu}(k_x,k_z,\omega) & \hat{\mathcal{H}}_{uv}(k_x,k_z,\omega) & \hat{\mathcal{H}}_{uw}(k_x,k_z,\omega) \\ \hat{\mathcal{H}}_{vu}(k_x,k_z,\omega) & \hat{\mathcal{H}}_{vv}(k_x,k_z,\omega) & \hat{\mathcal{H}}_{vw}(k_x,k_z,\omega) \\ \hat{\mathcal{H}}_{wu}(k_x,k_z,\omega) & \hat{\mathcal{H}}_{wv}(k_x,k_z,\omega) & \hat{\mathcal{H}}_{ww}(k_x,k_z,\omega) \end{bmatrix} \begin{bmatrix} \hat{d}_u(k_x,k_z,\omega) \\ \hat{d}_v(k_x,k_z,\omega) \\ \hat{d}_w(k_x,k_z,\omega) \end{bmatrix}$$

M. Jovanović & B. Bamieh, UCSB 1

Reynolds Number Dependence (cont.)

☞ **Theorem:** For any parallel channel flow, ‘componentwise’ energy amplification of streamwise constant disturbances is given by

$$\mathrm{trace}(\hat{\mathcal{V}}_s) \;=\; \begin{cases} f_{u1}(k_z)\ R & s = u \\ f_{v1}(k_z)\ R \;+\; f_{v2}(k_z)\ R^3 & s = v \\ f_{w1}(k_z)\ R \;+\; f_{w2}(k_z)\ R^3 & s = w \end{cases}$$

The overall energy amplification at $k_x = 0$ is given by

$$\mathrm{trace}(\hat{\mathcal{V}}) \;=\; \{f_{u1}(k_z) + f_{v1}(k_z) + f_{w1}(k_z)\}\ R \;+\; \{f_{v2}(k_z) + f_{w2}(k_z)\}\ R^3 . \;\blacksquare$$

M. Jovanović & B. Bamieh, UCSB

Reynolds Number Dependence (cont.)

Theorem: For any parallel channel flow, 'componentwise' energy amplification of streamwise constant disturbances is given by

$$\mathrm{trace}(\hat{\mathcal{V}}_s) = \begin{cases} f_{u1}(k_z)\,R & s = u \\ f_{v1}(k_z)\,R + f_{v2}(k_z)\,R^3 & s = v \\ f_{w1}(k_z)\,R + f_{w2}(k_z)\,R^3 & s = w \end{cases}$$

The overall energy amplification at $k_x = 0$ is given by

$$\mathrm{trace}(\hat{\mathcal{V}}) = \{f_{u1}(k_z) + f_{v1}(k_z) + f_{w1}(k_z)\}\,R + \{f_{v2}(k_z) + f_{w2}(k_z)\}\,R^3.$$

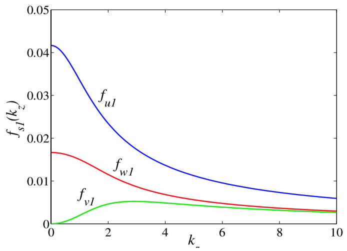

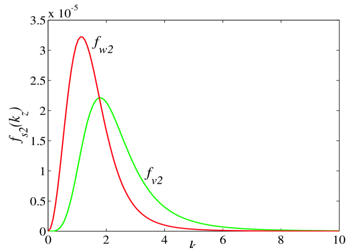

Basic Issue

- Uncertainty and robustness in the Navier-Stokes (NS) equations
  - Streamlined geometries $\Longrightarrow$ Extreme sensitivity of the NS equations

- Transition $\not\Leftrightarrow$ instability (linear or non-linear)
- Transition $\approx$ (instability, fragility, sensitivity)

Linearized NS (LNS) Equations

1

- With stochastic forcing
  - $\mathcal{H}^2$ norm of LNS scales like R^3
  - Amplification mechanism is 3D, streak spacing mathematically related to dynamical coupling (Bamieh & Dahleh, '99)
- "Spatio-temporal Impulse response" of LNS has features of *Turbulent spots* (Jovanovic & Bamieh, '01)
- Wall blowing/suction control in simulations of channel flow
  - Cortelezi, Speyer, Kim, et.al. (UCLA)
  - Bewley, Hogberg, et.al. (UCSD)

  Using $\mathcal{H}^2$ as a problem formulation
  Achieved re-laminarization at low Reynolds numbers

Fluid dynamics community gradually warming up to model-based control

- Matching channel flow statistics by input noise shaping in LNS (Jovanovic & Bamieh, '01)
- Corrugated surfaces (Riblets) effect on drag reduction (current work)

Uncertainty in a Dynamical System

Lyapunov stability
$\dot{x} = f(x)$
uncertain initial conditions

dynamical uncertainty
$\dot{x} = F(x) + \Delta(x)$

exogenous disturbances
$\dot{x}(t) = F(x(t), d(t))$

combinations
$\dot{x}(t) = F(x(t), d(t)) + \Delta(x(t), d(t))$

$\Longrightarrow$ **More uncertainty**

Linearized version:

eigenvalue stability
$\dot{x} = Ax$

umodelled dynamics
$\dot{x} = (A + \Delta)x$
Psuedo-spectrum

exogenous disturbances
$\dot{x}(t) = Ax(t) + Bd(t)$
input-output analysis

combinations
$\dot{x}(t) = (A + B\Delta C)x(t) + (F + G\Delta H)d(t)$

The Nature of Turbulence

Common view of Turbulence

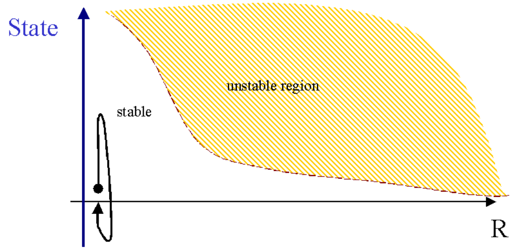

At low Reynolds numbers, all initial perturbations decay

The Nature of Turbulence (cont.)

Common view of Turbulence

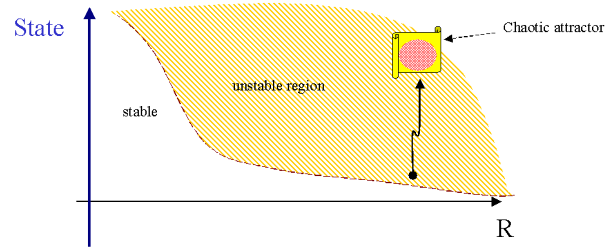

At high Reynolds numbers, move away from laminar flow,
Then flow looks turbulent because it evolves on a chaotic attractor

Intuitive reasoning:

Complex, statistical looking behavior ←→ System with chaotic dynamics

The Nature of Turbulence (cont.)

Alternative view

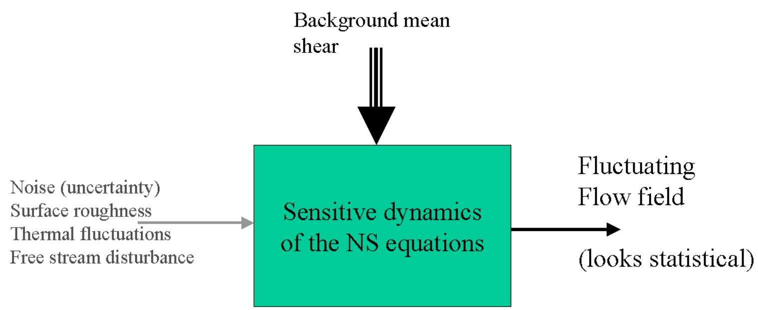

Amplification vs. Instability

2D/3C model: NS equations for stream-wise constant structures

most commonly observed structures in turbulent boundary layers

$$\frac{\partial}{\partial x} = 0$$

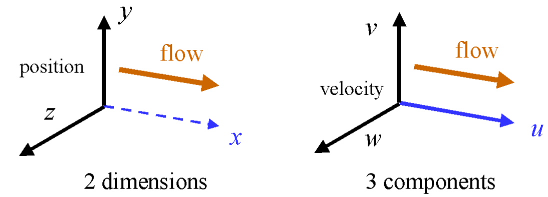

$$\Psi(y,z,t)$$
$$v = \frac{\partial \Psi}{\partial z},\; w = -\frac{\partial \Psi}{\partial y}$$

2d-3c model

$$\frac{\partial u}{\partial t} + \frac{\partial \Psi}{\partial z}\frac{\partial u}{\partial y} - \frac{\partial \Psi}{\partial y}\frac{\partial u}{\partial z} = \frac{1}{R}\Delta u$$
$$\frac{\partial \Delta\Psi}{\partial t} + \frac{\partial \Psi}{\partial z}\frac{\partial \Delta\Psi}{\partial y} - \frac{\partial \Psi}{\partial y}\frac{\partial \Delta\Psi}{\partial z} = \frac{1}{R}\Delta^2\Psi$$

For plane Couette flow

THESE EQUATIONS ARE GLOBALLY STABLE!

ENERGY AMPLIFICATION SCALES LIKE R^3

(Bobba, Bamieh, Doyle, '01)

Amplification vs. Instability

- Most turbulent flows probably have both
  - instabilities (leading to spatio-temporal patterns)
  - and high noise amplification

- The statistical nature of turbulence may be due to ambient noise amplification, not chaos

Realization of Dynamic Systems: Theory and (Many) Applications

Bart De Moor[1]

ESAT-SCD, Katholieke Universiteit Leuven
Kasteelpark Arenberg 10 B-3001 Leuven Belgium
T: +32-(0)16321709 M: +32-(0)475287052 F: +32-(0)16321970
E: bart.demoor@esat.kuleuven.ac.be W:www.esat.kuleuven.ac.be/~demoor

Part 1. Realization from exact observations.

Classically, 'realization' refers to the problem on how to obtain ('to realize') an electrical circuit in terms of electrical components (such as resistors, inductors and capacitors) starting from a given transfer function. More generally, we could state that 'realization' refers to the problem on how to go from an 'external description' of a dynamical system (observations, transfer matrices, input-output equations, impulse response samples, …) to an 'internal' one. By 'internal', we mean a set of equations that explicitly reveals the interaction between external observations (e.g. inputs and/or outputs) and 'internal' states of the dynamical system. Typically, such a representation describes the dynamic behavior of the state as driven by the input, by a set of difference (differential) equations, and the output as a memoryless map from states and inputs to outputs. Reasons to 'realize' a given system into a state space representation are manyfold: analyse inherent properties such as stability, finding eigenfrequencies and – modes, designing observers and control strategies, quantify the distance between systems and/or behaviors in order to cluster and classify them, 'clean up' data (denoising), and obtain reduced order models.
A classical example of a realization problem is given by the path that leads from Kepler's laws to Newton's. A modern example is given by applications in systems biology, such as trying to unravel the mechanisms that lead to chemotaxis.

In the first part, we will concentrate on the realization problem for linear deterministic systems, which is to obtain a state space model from impulse response observations.
We consider its (long) history and will survey the contributions of many, culminating in the realization theory of Ho-Kalman, with its many variations and possible numerical implementations, typically via the singular value decomposition. We will also discuss many linear algebraic and system theoretic properties that are useful in or have been derived from the study of realization problems, such as balancing linear systems, properties of block Hankel matrices, etc…
As an illustration of this, we will treat the so-called modal analysis of a bridge, starting from impulse response experiments. We will show how to do realization theory in the

[1] Acknowledgements
Dr. Bart De Moor is a full professor at the Katholieke Universiteit Leuven, Belgium. Research supported by **Research Council KUL:** GOA-Mefisto 666, GOA-Ambiorics, IDO (IOTA Oncology, Genetic networks), several PhD/postdoc & fellow grants; **Flemish Government:** **FWO:** PhD/postdoc grants, projects, G.0240.99 (multilinear algebra), G.0115.01 (microarrays/oncology), G.0407.02 (support vector machines), G.0197.02 (power islands), G.0141.03 (Identification and cryptography), G.0491.03 (control for intensive care glycemia), G.0120.03 (QIT), G.0413.03 (inference in bioi), G.0388.03 (microarrays for clinical use), G.0229.03 (ontologies in bioi), G.0241.04 ((Functional Genomics), G.0452.04 (QC), G.0499.04 (robust SVM), research communities (ICCoS, ANMMM, MLDM); **AWI:** Bil. Int. Collaboration Hungary/ Poland; **IWT:** PhD Grants, STWW-Genprom (gene promotor prediction), GBOU-McKnow (Knowledge management algorithms), GBOU-SQUAD (quorum sensing), GBOU-ANA (biosensors); **Belgian Federal Government:** DWTC: IUAP V-22 (2002-2006), PODO-II (CP/01/40: TMS and Sustainibility); **EU:** FP5 CAGE (Compendium of Arabidopsis Gene Expression); ERNSI: European Research Network on System Identification; NoE Biopattern; NoE E-tumours; Eureka 2063-IMPACT; Eureka 2419-FliTE; **Contract Research/agreements:** ISMC/IPCOS, Data4s, TML, Elia, LMS, IPCOS, Mastercard;

frequency domain. In yet another illustration we will show how to obtain a realization theory for bilinear systems.

Next we discuss the linear stochastic realization problem, which is the problem of obtaining a state space model starting from a covariance sequence and which has a deep and rich system theoretic history. Here, we discuss the property of positive realness of a realization, which historically was introduced in order to determine whether one could realize a given transfer function by an electrical circuit (details to be explained !), but surprisingly also plays a crucial role in stochastic realization. We will also discuss the notion of stochastic balancing. Again, we will illustrate our findings with some engineering examples, such as state space modeling of civil structures excited by ambient disturbances, compression of movies that are highly correlated in space and time, and calculating distances between behaviors observed from gene expression levels on microarrays.

Part II. Examples and applications

The basics as established in Part I, form a very rich backbone that allows to study and analyse many problems in many different areas. The objective of this Part is to illustrate this with many engineering applications, and to analyse in some detail what additional constraints are necessary in these applications and how they complicate the realization problem. We will treat examples related to mechanical engineering (modal analysis, eigenfrequencies), medicine (nuclear magnetic resonance, denoising), telecommunications (modelling of ATM traffic, buffer modelling), bioinformatics (realization of Hidden Markov Models, DNA sequence modelling), biological systems (nonnegative realization, compartmental systems), image processing (texture analysis), multidimensional realization theory (direction-of-arrival in signal processing, uncertainty modeling in robust control) and geometry (computer tomography, 'shape from moments').
Links with other domains (such as e.g. the very old problem of the moments in probability theory, finding the zeros of sets of multivariate polynomials with Sylvester's elimination theory, cepstral realization and the occurrence of realization problems in coding theory) will also be explored.

Part III. The 'noisy' realization problem and model reduction

In Part III, we show how to tackle the realization problem when our observations are corrupted by noise, as it always happens in every day practice. One heuristic way is to apply the algorithms that were designed for the noiseless problem, and then try to analyse the resulting realization. We will however also analyse the maximum likelihood formulation of the realization problem and show, among other things, how this relates to the so-called structured total least squares problem. We will show how sometimes a priori information can be incorporated in the realization problem.
Then we discuss how to obtain a reduced order model from a given one. This can be done via balanced model truncation, or minimizing some L2-norm. We will also briefly touch on Hankel norm model reduction.

Finally, we will conclude by presenting a list with open research problems.

Part 4

List of Participants

Ir. W.H.T.M. Aangenent
Dept. of Mechanical Engineering
Technische Universiteit Eindhoven
PO Box 513
5600 MB Eindhoven
The Netherlands
w.h.t.m.aangenent@stud.tue.nl

Ilyasse Aksikas
Dept. of Mathematics Engineering
Université Catholique de Louvain
Av Georges Lemaître 4-6
B-1348 Louvain-la-neuve
Belgium
aksikas@csam.ucl.ac.be

Georgo Angelis
Mechatronics Research
PHILIPS CFT
P.O. Box 218, SAQ-2122
5600MB Eindhoven
The Netherlands
georgo.angelis@philips.com

Dr. Ir. J. Anthonis
Departement Agro-Techniek en Economie
K.U.Leuven
Kasteelpark Arenberg 30
3001 Heverlee
Belgium
jan.anthonis@agr.kuleuven.ac.be

Ir. Avram
Dept. of Automation
Tehnical University of Cluj Napoca
str. Ghe. Baritiu, 26-28, Cluj Napoca
240000 Cluj Napoca
Romania
aclaudia1@yahoo.com

Bassam Bamieh
Department of Mechanical & Environmental Engineering
University of California at Santa Barbara
-
- Santa Barbara, CA 93106
USA
bamieh@engineering.ucsb.edu

Prof. G. Bastin BASTIN
Depat. INMA/CESAME
Université catholique de Louvain (UCL)
Avenue Georges Lemaître, 4
B-1348 Louvain-la-Neuve
BELGIUM
bastin@auto.ucl.ac.be

Sophie Beguin
CESAME - AUTO
Université catholique de Louvain
4 avenue Georges Lemaître
1348 Louvain-la-Neuve
Belgium
beguin@auto.ucl.ac.be

Ing. Steven Bex
ESAT / SCD (SISTA)
K.U.Leuven
Kasteelpark Arenberg 10
B-3001 Heverlee (Leuven)
Belgium
steven.bex@esat.kuleuven.ac.be

Prof. V. Blondel BLONDEL
dept. INMA / CESAME
Université catholique de Louvain (UCL)
Avenue Georges Lemaître, 4
B-1348 LOUVAIN-LA-NEUVE
BELGIUM
blondel@inma.ucl.ac.be

Prof. R. K. Boel
SYSTeMS
Universiteit Gent
Technologiepark-Zwijnaarde 914
B-9052 Gent
Belgium
rene.boel@UGent.be

Matthijs Boerlage
Mechatronics Research
TU/e, PHILIPS CFT
P.O. Box 218, SAQ-2114
5600MB Eindhoven
The Netherlands
matthijs@boerlage.net

Jeroen Boets
Dept. Electrical Engineering - SCD/SISTA
Katholieke Universiteit Leuven
Kasteelpark Arenberg 10
3001 Leuven
Belgium
jeroen.boets@esat.kuleuven.ac.be

Prof. Ph. Bogaerts
General Chemistry and Biosystem Dept.
Université Libre de Bruxelles
Av. F.-D. Roosevelt 50 C.P. 165/61
B-1050 Brussels
Belgium
Philippe.Bogaerts@ulb.ac.be

Dr ir X.J.A. Bombois
Delft Center for Systems and Control
Delft University of Technology
Mekelweg 2
2628 CD Delft
The Netherlands
n.vandenberg@dcsc.tudelft.nl

Ir J.H. Bonsel
Dept. of Mechanical Engineering
Technische Universiteit Eindhoven
PO Box 513
5600 MB Eindhoven
The Netherlands
j.h.bonsel@tue.nl

ir B. Bonsen
Dept. of Mechanical Engineering
Technische Universiteit Eindhoven
PO Box 513
5600MB Eindhoven
The Netherlands
b.bonsen@tue.nl

Eng. J. Borges
Delft Center for Systems and Control
Delft University of Technology
Mekelweg 2
2628 CD Delft Delft
The Netherlands
j.borges@dcsc.tudelft.nl

Prof. Dr. Ir. P.P.J. Bosch, van den
Dept. Electrical Engineering
Technische Universiteit Eindhoven
P.O. Box 513
5600 MB Eindhoven
The Netherlands
p.p.j.v.d.Bosch@tue.nl

Prof. ir. O.H. Bosgra
Delft Center for Systems and Control
Technische Universiteit Delft
Mekelweg 2
2623 JR Delft
The Netherlands
o.h.bosgra@dcsc.tudelft.nl

Clément Boussard
CESAME
Université catholique de Louvain
Avenue Georges Lemaître, 4
1348 Louvain-la-Neuve
Belgique
boussard@ensmp.fr

ir. Dennis Bruijnen
Dept. of Mechanical Engineering
Technische Universiteit Eindhoven
PO Box 513
5600 MB Eindhoven
The Netherlands
d.j.h.bruijnen@tue.nl

ir. B.H.M. Bukkems
Dept. of Mechanical Engineering
Technische Universiteit Eindhoven
P.O. Box 513
5600 MB Eindhoven
The Netherlands
b.h.m.bukkems@tue.nl

Ir A. Cappuyns
Dept. Chemical Engineering / BioTeC
Katholieke Universiteit Leuven
W. de Croylaan 46
3001 Leuven
Belgium
astrid.cappuyns@cit.kuleuven.ac.be

ing. C. Carbone
D.I.I.I.E.
Università degli Studi di Salerno
Via Ponte don Melillo
80084 Fisciano Salerno
Italy
ccarbone@unisa.it

Ir L. Catoire
SAAS
ULB
50 av. F.D. Roosevelt - CP 165/55
1050 Brussels
Belgium
laurent.catoire@ulb.ac.be

Dr. P. Collins
Modelling, Analysis, Simulation
Centrum voor Wiskunde en Informatica
PO Box 94079
1090 GB Amsterdam
The Netherlands
Pieter.Collins@cwi.nl

prof. R.F. curtain
wiskunde
Rijksuniversiteit Groningen
PO Box 800
9700 AV Groningen
The Netherlands
r.f.curtain@math.rug.nl

T. D'haene
ELEC
Vrije Universiteit Brussel
Pleinlaan 2
1050 Brussel
Belgium
tdhaene@vub.ac.be

Ir. S.C. de Graaf
Agrotechnology and Food Sciences
Wageningen University
P.O. Box 43
6700 AA Wageningen
The Netherlands
stefan.degraaf@wur.nl

Bram de Jager
Dept. of Mechanical Engineering
Technische Universiteit Eindhoven
PO Box 513
5600 MB Eindhoven
The Netherlands
A.G.de.Jager@wfw.wtb.tue.nl

Ir. Bas de Kruif
Dept. of Control
Universiteit Twente
PO Box 217
7500 AE Enschede
The Netherlands
b.j.dekruif@utwente.nl

Prof. Dr. Ir. Bart De Moor
Elektrotechniek, ESAT/SCD (SISTA)
K.U.Leuven
Kasteelpark Arenberg 10
3001 Leuven
Belgium
ida.tassens@esat.kuleuven.ac.be

Filip De Smet
Dept. of Electrical Energy, Systems and Automation
Universiteit Gent
Trieststraat 119
9960 Assenede
Belgium
filip.desmet@ugent.be

Nico Deblauwe
Dept. ELEC
Vrije Universiteit Brussel
Pleinlaan 2
1050 Brussel
Belgie
ndeblauw@vub.ac.be

Jean-Charles Delvenne
Applied Mathematics
Université Catholique de Louvain
4, Avenue Lemaître
1348 Louvain-la-Neuve
Belgium
delvenne@inma.ucl.ac.be

Dr ir A.J. Den Dekker
Delft Center for Systems and Control
Delft University of Technology
Mekelweg 2
2628 CD Delft
The Netherlands
n.vandenberg@dcsc.tudelft.nl

Arjen den Hamer
Mechatronics Research
TU/e, PHILIPS CFT
P.O. Box 218, SAQ-1139
5600MB Eindhoven
The Netherlands
a.j.d.hamer@student.tue.nl

ir. S.G. Dietz
Delft Center for Systems and Control
Technische Universiteit Delft
Mekelweg 2
2628 CD Delft
The Netherlands
s.dietz@dcsc.tudelft.nl

Dr Ir J. Dijk van
Contructieve Technische Wetenschappen
Universiteit Twente
PO Box 217
7500 AE Enschede
Netherlands
j.vandijk@utwente.nl

Timo Doeswijk
Systems & Control
Wageningen Universiteit
P.O. Box 43
6700 AA Wageningen
The Netherlands
timo.doeswijk@wur.nl

Ir Doris
Dept. of Mechanical Engineering
Technische Universiteit Eindhoven
PO Box 513
5600 MB Eindhoven
The Netherlands
a.doris@tue.nl

Ir R. M. L. Ellenbroek
Dept. of Mechanical Engineering
Technische Universiteit Eindhoven
PO Box 513
5600 MB Eindhoven
The Netherlands
r.m.l.ellenbroek@tue.nl

Dr. J.C. Engwerda
Dept. of Econometrics and Operations Research
Tilburg University
PO Box 90153
5000 LE Tilburg
The Netherlands
engwerda@uvt.nl

Marcelo Espinoza
ESAT/SCD
Katholieke Universiteit Leuven
Kasteelpark Arenberg 10
B-3000 Leuven
Belgium
marcelo.espinoza@esat.kuleuven.ac.be

Ir. R.P.H. Faassen
Dept. of Mech
Technische Universiteit Eindhoven
P.O. Box 513
5600 MB Eindhoven
The Netherlands
r.p.h.faassen@tue.nl

Damien Francois
CESAME
Université catholique de Louvain
av. G. Lemaitre, 4
B-1348 Louvain-la-Neuve
Belgium
francois@auto.ucl.ac.be

Jürgen Fritz
Automatic Control Laboratory
Faculté Polytechnique de Mons
Boulevard Dolez, 31
7000 Mons
Belgium
mail@fritzjuergen.de

Manuel Gerard
Electrical engineering and Computer Science
Université de Liège
Grande Traverse 10
4000 Liège
Belgium
manuel.gerard@ulg.ac.be

Christophe Germay
Dept of Electrical Engineering and Computer Science
University of Liege
30, rue M.Moutschen
4020 Jupille
Belgium
germay@montefiore.ulg.ac.be

Ir. O.J. Gietelink
Delft Center for Systems and Control
Delft University of Technology
Mekelweg 2
2628 CD Delft
The Netherlands
gietelink@wt.tno.nl

Ir S. Gillijns
Dept. Elektrotechniek - SISTA - SCD
Katholieke Universiteit Leuven
Kasteelpark Arenberg 10
3001 Heverlee
Belgium
Steven.Gillijns@esat.kuleuven.ac.be

Ir. G. Gins
Chemical Engineering / BioTeC
Katholieke Universiteit Leuven
De Croylaan 46
3001 Leuven
Belgium
Geert.Gins@cit.kuleuven.ac.be

Ir G. Goffaux
Automatic Control Laboratory
Faculté Polytechnique de Mons
31, Boulevard Dolez
7000 Mons
Belgium
Guillaume.Goffaux@fpms.ac.be

Ir M.B. Groot Wassink
Delft Center for Systems and Control
Delft University of Technology
Mekelweg 2
2628 CD Delft
The Netherlands
n.vandenberg@dcsc.tudelft.nl

Ir V. Grosfils
Control Engineering and System Analysis Department
Université Libre de Bruxelles
CP 165/55, 50, Av. F.D. Roosevelt,
1050 Brussels
Belgium
valerie.grosfils@ulb.ac.be

Ir A. Grosfils
Dept. of General Chemistry and Biosystems
Université Libre de Bruxelles
av. F. D. Roosevelt, 50, CP 165/61
1050 Brussels
Belgium
aline.grosfils@ulb.ac.be

Vincent Guffens
CESAME
University Catholique Louvain-la-Neuve
BATIMENT EULER, AV. G. LEMAITRE 4
1348 Louvain-la-Neuve
Belgium
guffens@auto.ucl.ac.be

Fredrik Gustafsson
Department of Electrical Engineering
Linköping University
Campus Valla
SE-581 83 Linköping
Sweden
fredrik@isy.liu.se

Dr.ir. L.C.G.J.M. Habets
Dept. of Mathematics and Computer Science
Technische Universiteit Eindhoven
P.O. Box 513
5600 MB Eindhoven
The Netherlands
luch@win.tue.nl

Ir R Hallouzi
Delft Center for Systems and Control
Delft University of Technology
Mekelweg 2
2628 CD Delft
The Netherlands
n.vandenberg@dcsc.tudelft.nl

Bertrand Haut
CESAME
Université Catholique de Louvain
Batiment Euler, A017 4, Avenue G. Lemaitre Avenue G. Lemaitre, 4
1348 Louvain-la-Neuve
Belgium
haut@auto.ucl.ac.be

ir A. Hegyi
Delft Center for Systems and Control
Delft University of Technology
Mekelweg 2
2628 CD Delft
The Netherlands
n.vandenberg@dcsc.tudelft.nl

Ir J. van Helvoirt
Dept. of Mechanical Engineering
Technische Universiteit Eindhoven
P.O. Box 513
5600 MB Eindhoven
The Netherlands
J.v.Helvoirt@tue.nl

Ir. J.J.M. van Helvoort
Dept. of Mechanical Engineering
Technische Universiteit Eindhoven
PO Box 513
5600 MB Eindhoven
The Netherlands
j.j.m.v.helvoort@tue.nl

Dr. P.S.C. Heuberger Heuberger
Delft Center for Systems and Control
Delft University of Technology
Mekelweg 2
2628 CD Delft
The Netherlands
p.s.c.heuberger@dcsc.tudelft.nl

Ir. K.J.G. Hinnen
Delft Center for Systems and Control
Delft University of Technology
Mekelweg 2
2628 CD Delft
The Netherlands
k.j.g.hinnen@dcsc.tudelft.nl

Diep HO NGOC Diep
CESAME
Université catholique de Louvain
Avenue G. Lemaitre, 4
B-1348 LOUVAIN-LA-NEUVE
BELGIUM
ho@auto.ucl.ac.be

Luc hoegaerts
Electrical engineering
Katholieke universiteit Leuven
Kasteelpark arenberg 10
3001 heverlee (leuven)
belgium
luc.hoegaerts@esat.kuleuven.ac.be

Dr O.V. IFTIME
Department of Mathematics
University of Groningen
P.O. Box 800
9700 AV Groningen
The Netherlands
iftime@math.rug.nl

Schoukens Johan
ELEC
Vrije Universiteit Brussel
Pleinlaan 2
1050 Brussel
Belgie
johan.schoukens@vub.ac.be

Dipl.ing. A. Jokic
Dept. of Electrical Engineering
Technische Universiteit Eindhoven
PO Box 513
5600 MB Eindhoven
The Netherlands
a.jokic@tue.nl

Prof.dr.ir. J.B. Jonker
Dept. CTW, faculty Mechanical Engineering
Universiteit Twente
PO Box 217
7500 AE Enschede
The Netherlands
j.b.jonker@ctw.utwente.nl

Jens Jordan
Systems and Control
University of Liege (resp. Wuerzburg)
Institut Montefiore B28
B-4000 Liege Sart-Tilman
Belgium
jordan@mathematik.uni-wuerzburg.de

Agung Julius
Dept. Applied Mathematics
Universiteit Twente
PO Box 217
7500 AE Enschede
The Netherlands
a.a.julius@math.utwente.nl

A. Juloski
Dept. of Electrical Engineering
Technische Universiteit Eindhoven
PO Box 513
5600 MB Eindhoven
The Netherlands
a.juloski@tue.nl

Rajasekhar Kakumani
Faculty of EEMCS
University of Twente
PO Box 217
7500 AE Enschede
The Netherlands
kakumanir@cs.utwente.nl

KAREL Keesman
Systems & Control Group
Wageningen University
P.O. Box 43
6700 AA Wageningen
The Netherlands
karel.keesman@wur.nl

Ir. J.T.B.A. Kessels
Dept. of Electrical Engineering
Technische Universiteit Eindhoven
PO Box 513
5600 MB Eindhoven
The Netherlands
j.t.b.a.kessels@tue.nl

Prof Dr Ir M. Kinnaert
Dept. of Control Engineering and System Analysis
Université Libre de Bruxelles
CP 165/55, 50 Av. F.D. Roosevelt
B-1050 Brussels
Belgium
michel.kinnaert@ulb.ac.be

M. Sc. Klaassen
Mechanical Engineering
University of Technology, Eindhoven
PO Box 513
5600 MB Eindhoven
The Netherlands
t.w.g.l.klaassen@tue.nl

Dr.Ir. S.H. Koekebakker
DV2/3G08
Océ-Technologies B.V.
PO box 101
5900 MA Venlo
TheNetherlands
koek@oce.nl

M.W.T. Koot
Dept. of Mechanical Engineering
Technische Universiteit Eindhoven
PO Box 513
5600 MB Eindhoven
The Netherlands
m.w.t.koot@tue.nl

Dragan Kostic
Dept. of Mechanical Engineering
Technische Universiteit Eindhoven
PO Box 513
5600 MB Eindhoven
The Netherlands
d.kostic@tue.nl

Dr. Ir. P. F. Lambrechts
Dept. of Mechanical Engineering
Technische Universiteit Eindhoven
PO Box 513
5600 MB Eindhoven
The Netherlands
p.f.lambrechts@tue.nl

Mircea Lazar
Dept. of Electrical Engineering
Technische Universiteit Eindhoven
PO Box 513
5600 MB Eindhoven
The Netherlands
m.lazar@tue.nl

Ir Renato LEPORE
Service d'Automatique
Faculté Polytechnique de Mons
Boulevard Dolez 31
7500 Mons
Belgium
Renato.Lepore@fpms.ac.be

ir M. Leskens
Delft Center for Systems and Control
Delft University of Technology
Mekelweg 2
2628 CD Delft
The Netherlands
n.vandenberg@dcsc.tudelft.nl

Ir C. LEVRIE
Laboratoire d'Automatique
Faculté Polytechnique de Mons (F.P.Ms)
31, Boulevard Dolez
7000 Mons
Belgium
Caroline.Levrie@fpms.ac.be

Prof. Dr. Ir. M. Loccufier
Dept. of Electrical Energy, Systems and Automation
Ghent University
Technologiepark - Zwijnaarde 913
B-9052 Gent
Belgium
Mia.Loccufier@Ugent.be

Ir F., Logist
Dept. Chemical Engineering / BioTeC
Katholieke Universiteit Leuven
W. de Croylaan 46
3001 Leuven
Belgium
Filip.Logist@CIT.kuleuven.ac.be

Sven Maerivoet
Department of Electrical Engineering ESAT-SCD (SISTA)
Katholieke Universiteit Leuven
Kasteelpark Arenberg 10
3001 Leuven
Belgium
sven.maerivoet@esat.kuleuven.ac.be

Ivan Markovsky
ESAT
K.U. Leuven
Kasteelpark Arenberg 10
B-3001 Leuven-Heverlee
Belgium
Ivan.Markovsky@esat.kuleuven.ac.be

Dr.ir Meinsma
Dept. of Applied Mathematics
University of Twente
PO BOX 217
7500 AE Enschede
The Netherlands
g.meinsma@math.utwente.nl

J. Minteer
Electrical Engineering, Mathematics, Computer Science
Delft University of Technology
PO Box 5031
2600 GA Delft
The Netherlands
J.Minteer@ewi.tudelft.nl

Agoes A. Moelja
Dept. of Applied Mathematics
University of Twente
PO Box 217
7500 AE Enschede
The Netherlands
a.a.moelja@math.utwente.nl

Dr. Ir. L. P. M. Moreau
Dept. of Mechanical Engineering
Technische Universiteit Eindhoven
PO Box 513
5600 MB Eindhoven
The Netherlands
L.P.M.Moreau@tue.nl

Prof.dr.ir. J.A. Mulder
Faculty of Aerospace Engineering. Dept. Control & Simulation
Delft University of Technology
PO Box 5058
2600 GB Delft
The Netherlands
J.A.Mulder@lr.tudelft.nl

Ir. K.M. Nauta
Dept. of Electrical Engineering
Technische Universiteit Eindhoven
PO Box 513
5600MB eindhoven
The Netherlands
maarten@stack.nl

I. Eng. Necoara
Delft Center for Systems and Control
Delft University of Technology
Mekelweg 2
2628 CD Delft
The Netherlands
i.necoara@dcsc.tudelft.nl

Prof.dr.H. Nijmeijer
Dept. of Mechanical Engineering
Technische Universiteit Eindhoven
PO Box 513
5600 MB Eindhoven
The Netherlands
h.nijmeijer@tue.nl

ir. G. Nijsse
Faculty of Engineering Technology (WB/WA)
Universiteit Twente
PO Box 217
7500AE Enschede
The Netherlands
g.nijsse@ctw.utwente.nl

Laure Ninove
Applied mathematics
Université catholique de Louvain
Av. G. Lemaître, 4
B-1348 Louvain-la-Neuve
Belgium
ninove@inma.ucl.ac.be

S.P.M. Noijen
Dept. of Mechanical Engineering
Technische Universiteit Eindhoven
PO Box 513
5600 MB Eindhoven
The Netherlands
s.p.m.noijen@student.tue.nl

Professor E.J.L. Noldus
Dept. of Electrical Energy,Systems and Automation
Universiteit Gent
Technologiepark Zwijnaarde, 913
B 9052 Zwijnaarde
Belgium
noldus@autoctrl.rug.ac.be

T.A.E. Oomen
Dept. of Mechanical Engineering
Technische Universiteit Eindhoven
Eikelenbosch 1a
5111 EL Baarle Nassau
The Netherlands
t.a.e.oomen@student.tue.nl

Ir. J. Op den Buijs
Dept. of Electrical Engineering
Technische Universiteit Eindhoven
PO Box 513
5600 MB Eindhoven
The Netherlands
j.o.d.buijs@tue.nl

M.R. Opmeer
Dept. of Mathematics
University of Groningen
PO Box 800
9400 AV Groningen
The Netherlands
opmeer@math.rug.nl

Johan Paduart
ELEC
VUB
Pleinlaan 2
1050 Brussel
Belgium
jpaduart@vub.ac.be

Ir B. Paijmans
PMA / FMTC
K.U.L.
Celestijnenlaan 300C
B-3001 Heverlee
Belgium
bart.paijmans@fmtc.be

Cédric Parloir
Service d’Automatique et d’Analyse des Systèmes
Université Libre de Bruxelles
Av FD Roosevelt 50 CP 165/55
1050 Bruxelles
Belgium
cparloir@ulb.ac.be

Ir Maria Isabel Parra Calvache
Delft Center for Systems and Control
Delft University of Technology
Mekelweg 2
2628 CD Delft
The Netherlands
n.vandenberg@dcsc.tudelft.nl

Ramkrishna Pasumarthy
Faculty of EEMCS
University of Twente
PO Box 217
7500 AE Enschede
The Netherlands
r.pasumarthy@math.utwente.nl

MSc A. Pavlov
Dept. of Mechanical Engineering
Technische Universiteit Eindhoven
PO Box 513
5600 MB Eindhoven
The Netherlands
A.Pavlov@tue.nl

K. Pelckmans
ESAT
K.U.Leuven
Kasteelpark arenberg 10
3001 Leuven (Heverlee)
Belgium
kristiaan.pelckmans@esat.kuleuven.ac.be

M Petreczky
MAS2
Centrum voor Wiskunde en Informatica
POBox 94079
1090GB Amsterdam
The Netherlands
mpetrec@cwi.nl

Patrick Philips
Mechatronics Research
PHILIPS CFT
P.O. Box 218, SAQ-2122
5600MB Eindhoven
The Netherlands
patrick.philips@philips.com

Ir. B. Pluymers
Dept. of Electrotechnical Engineering
Katholieke Universiteit Leuven
Kasteelpark 10
3000 Leuven
Belgium
bert.pluymers@esat.kuleuven.ac.be

Agnès Provost
CESAME/AUTO
UCL
4 avenue Georges Lemaître
1348 Louvain-la-Neuve
Belgium
provost@auto.ucl.ac.be

Erik Quaeghebeur
SYSTeMS research group
Universiteit Gent
Technologiepark-Zwijnaarde 914
9052 Zwijnaarde
Belgium
Erik.Quaeghebeur@UGent.be

Daan Rabijns
TW-ELEC
Vrije Universiteit Brussel
Pleinlaan 2
1050 Etterbeek
Belgium
Daan.Rabijns@vub.ac.be

Ir R. Renard
Automatic Control Laboratory
Faculté Polytechnique de Mons
31 Boulevard Dolez
7000 Mons
Belgium
frederic.renard@fpms.ac.be

CHRISTINE RENOTTE
Dept of Automatic Control
Faculté Polytechnique de Mons
Bvd Dolez, 31
7000 Mons
Belgium
christine.renotte@fpms.ac.be

Ir J. Rogge
SYSTeMS Group
Universiteit Gent
Technologiepark Zwijnaarde 914
9052 Zwijnaarde
Belgium
jonathan.rogge@ugent.be

Ir R. Ronsse
Electrical Engineering and Computer Science
Université de Liège
Montefiore Institute, B28
B-4000 Liège
Belgium
R.Ronsse@ulg.ac.be

Prof. Dr. Ir. N. B. Roozen
Dept. of Mechanical Engineering
Technische Universiteit Eindhoven
PO Box 513
5600 MB Eindhoven
The Netherlands
n.b.roozen@tue.nl

Ir. B.J.P. Roset
Dept. of Mechanical Engineering
Technische Universiteit Eindhoven
PO Box 513
5600 MB Eindhoven
The Netherlands
B.J.P.Roset@tue.nl

Ir J.H. Sandee
Dept. of Electrical Engineering
Technische Universiteit Eindhoven
PO Box 513
5600 MB Eindhoven
The Netherlands
j.h.sandee@tue.nl

Prof. Dr. C.W. Scherer
Delft Center for Systems and Control
Technische Universiteit Delft
Mekelweg 2
2628 CD Delft
The Netherlands
c.w.scherer@dcsc.tudelft.nl

ir. M.G.E. Schneiders
Dept. of Mechanical Engineering
Technische Universiteit Eindhoven
P.O. Box 513
5600 MB Eindhoven
The Netherlands
m.g.e.schneiders@tue.nl

Céline Schreiber
CESAME and NEFY
Université catholique de Louvain
4, avenue G. Lemaitre
1348 Louvain-la-Neuve
Belgium
schreiber@auto.ucl.ac.be

J.M. Schumacher
Dept. of Econometrics & OR
Tilburg University
PO Box 90153
5000 LE Tilburg
the Netherlands
jms@uvt.nl

Prof. R. Sepulchre
Electrical Engineering and Computer Science
University of Liege
Institut Montefiore, B28
4000 Liege
Belgium
r.sepulchre@ulg.ac.be

Iliyana Simeonova
Dept. of Mathematical Engineering
UCL - CESAME
Batiment Euler, Avenue G. Lemaitre, 4,
1348 LOUVAIN-LA-NEUVE
Belgium
simeonova@auto.ucl.ac.be

Dr Ir I. Smets
Dept. Chemical Engineering / BioTeC
Katholieke Universiteit Leuven
W. de Croylaan 46
3001 Leuven
Belgium
ilse.smets@cit.kuleuven.ac.be

Gabriel SOLARI
CESAME
Université Catholique de Louvain
4, Av. George Lemaître
1348 Louvain-la-Neuve
Belgium
solari@auto.ucl.ac.be

Guy-Bart Stan
Dept. of Electrical Engineering and Computer Science
University of Liege
Institut Montefiore, Grande Traverse 10
4000 Liege
Belgium
gb.stan@ulg.ac.be

Prof.dr.ir. M. Steinbuch
Dept. of Mechanical Engineering
Technische Universiteit Eindhoven
PO Box 513
5600 MB Eindhoven
The Netherlands
m.steinbuch@tue.nl

J D Stigter
Systems and Control
Wageningen UR
PO Box 43
6708 PA Wageningen
The Netherlands
hans.stigter@wur.nl

Prof.dr. A.A. Stoorvogel
Wiskunde en Informatica
Technische Universiteit Eindhoven
Postbus 513
5600MB Eindhoven
The Netherlands
A.A.Stoorvogel@tue.nl

Prof. dr. ir. G. van Straten
Dept. Agrotechnol. & Food Science
Wageningen University
Mansholtlaan 10
6708 PA Wageningen
The Netherlands
gerrit.vanstraten@wur.nl

ir. H. Super
Faculty of Engineering Technology (WB/WA)
Universiteit Twente
PO Box 217
7500AE Enschede
The Netherlands
h.super@ctw.utwente.nl

Prof. Dr. Ir. J.A.K. Suykens
Elektrotechniek, ESAT/SCD (SISTA)
K.U.Leuven
Kasteelpark Arenberg 10
3001 Leuven
Belgium
ida.tassens@esat.kuleuven.ac.be

Jacques Theys
CESAME/INMA
UCL
4-6, avenue Georges Lemaitre
B-1348 Louvain la Neuve
Belgium
theys@inma.ucl.ac.be

Ir. A.A. Tiagounov
Dept. of Electrical Engineering
Technische Universiteit Eindhoven
PO Box 513
5600 MB Eindhoven
The Netherlands
a.tiagounov@tue.nl

Ir M. C. M. Troffaes
SYSTeMS Research Group
Universiteit Gent
Technologiepark Zwijnaarde 914
9052 Zwijnaarde
Belgie
Matthias.Troffaes@UGent.be

Ir. A. T. Troffaes
ELEC
Vrije Universiteit Brussel
Pleinlaan2
B1050 Brussel
Belgium
atroffae@vub.ac.be

Peter Valk
Delft Center for Systems and Control
Delft University of Technology
Mekelweg 2
2628 CD Delft
The Netherlands
n.vandenberg@dcsc.tudelft.nl

Dr.ir. M.J.G. van de Molengraft
Dept. of Mechanical Engineering
Technische Universiteit Eindhoven
P.O. Box 513
5600 MB Eindhoven
The Netherlands
M.J.G.v.d.Molengraft@tue.nl

Jeroen Van de Wijdeven
Dept. of Mechanical Engineering
Technische Universiteit Eindhoven
PO Box 513
5600 MB Eindhoven
The Netherlands
J.J.M.v.d.Wijdeven@student.tue.nl

Nathan Van de Wouw
Department of Mechanical Engineering
TU/e
PO Box 513
5600 MB Eindhoven
The Netherlands
N.v.d.Wouw@tue.nl

ir M. van den Berg
Delft Center for Systems and Control
Delft University of Technology
Mekelweg 2
2628 CD Delft
The Netherlands
n.vandenberg@dcsc.tudelft.nl

dr.ir. Ton J.J. van den Boom
Delft Center for Systems and Control
Technische Universiteit Delft
Mekelweg 2
2628 CD Delft
The Netherlands
t.j.j..vandenboom@dcsc.tudelft.nl

Prof dr ir, P.M.J. Van den Hof
Delft Center for Systems and Control
Delft University of Technology
Mekelweg 2
2628 CD Delft
The Netherlands
n.vandenberg@dcsc.tudelft.nl

prof.dr.A.J. van der Schaft
Dept. of Applied Mathematics
Universiteit Twente
PO BOX 217
7500AE Enschede
Netherlands
a.j.vanderschaft@math.utwente.nl

G.M. van der Zalm
Dept. of Mechanical Engineering
Technische Universiteit Eindhoven
PO Box 513
5600 MB Eindhoven
The Netherlands
g.m.v.d.zalm@student.tue.nl

Ir. J.A.W.M. van Eekelen
Dept. of Mechanical Engineering
Technische Universiteit Eindhoven
W-Hoog room 0.126 PO Box 513
5600 MB Eindhoven
The Netherlands
j.a.w.m.v.eekelen@tue.nl

Ing. T. Van Herpe
ESAT - SCD
Katholieke Universiteit Leuven
K.U.Leuven, Kasteelpark Arenberg 10
B-3001 Leuven-Heverlee
Belgium
tom.vanherpe@esat.kuleuven.ac.be

Johan Van Kerckhoven
ELEC
Vrije Universiteit Brussel (VUB)
Pleinlaan 2
1050 Brussel
België
jvkerckh@vub.ac.be

Ir C.M.M. van Lierop
Dept. of Electrical Engineering
Technische Universiteit Eindhoven
PO Box 513
5600 MB Eindhoven
The Netherlands
c.m.m.v.lierop@tue.nl

M.Sc. R.J.C. van Ooteghem
Systems and Control group
Wageningen University
Mansholtlaan 10
6708 PA Wageningen
The Netherlands
Rachel.vanOoteghem@wur.nl

Dr. Ir. N.A.W. Van Riel
Dept. of Electrical Engineering
Eindhoven University of Technology
PO Box 513
5600 MB Eindhoven
The Netherlands
N.A.W.v.Riel@tue.nl

Prof. Alain Vande Wouwer
Service d'Automatique
Faculté Polytechnique de Mons
Boulevard Dolez 31
B-7000 Mons
Belgium
Alain.VandeWouwer@fpms.ac.be

Antoine Vandendorpe
CESAME/INMA
UCL
4-6, avenue Georges Lemaitre
B-1348 Louvain-la-Neuve
Belgium
vandendorpe@inma.ucl.ac.be

Prof. J. Vandewalle
Elektrotechniek, ESAT/SCD (SISTA)
K.U.Leuven
Kasteelpark Arenberg 10
3001 Leuven
Belgium
joos.vandewalle@esat.kuleuven.ac.be

Bart Vanluyten
Dept. Electrical Engineering SISTA
Katholieke Universiteit Leuven
Kasteelpark Arenberg 10
3001 Leuven
Belgium
bart.vanluyten@esat.kuleuven.ac.be

Vincent Verdult
Delft Center for Systems and Control
Technische Universiteit Delft
Mekelweg 2
2628 CD Delft
The Netherlands
v.verdult@dcsc.tudelft.nl

Prof dr ir M.H.G. Verhaegen
Delft Center for Systems and Control
Delft University of Technology
Mekelweg 2
2628 CD Delft
The Netherlands
n.vandenberg@dcsc.tudelft.nl

Javier Villegas
EEMCS
Twente University
PO Box 217
7500 AE Enschede
The Netherlands
j.a.villegas@math.utwente.nl

ir. Eveline I.P. Volcke
BIOMATH
Universiteit Gent
Coupure Links 653
9000 Gent
Belgium
eveline.volcke@biomath.ugent.be

ir. G.M. Voorsluijs
Luchtvaart- en Ruimtevaarttechniek
Technische Universiteit Delft
Kluyverweg 1
2629 HS Delft
Nederland
g.m.voorsluijs@lr.tudelft.nl

Dr. S. Weiland
Dept. of Electrical Engineering
Eindhoven University of Technology
P.O. Box 513
5600 MB Eindhoven
The Netherlands
s.weiland@tue.nl

Professor J. C. Willems
ESAT/SCD (SISTA)
K.U. Leuven
Kasteelpark Arenberg 10
B-3001 Leuven
Belgium
jan.willems@esat.kuleuven.ac.be

Dr J. J. Winkin
Dept. of Mathematics
University of Namur (FUNDP)
Rempart de la Vierge, 8
5000 Namur
Belgium
joseph.winkin@fundp.ac.be

Ir A.-C. Witsel
Automatic Control Laboratory
Faculté Polytechnique de Mons
31 Boulevard Dolez
7000 Mons
Belgium
Anne-Catherine.Witsel@fpms.ac.be

Ir M. Zandvliet
Delft Center for Systems and Control
Delft University of Technology
Mekelweg 2
2628 CD Delft
The Netherlands
n.vandenberg@dcsc.tudelft.nl

Part 4

Organizational Comments

Welcome

The Organizing Committee has the pleasure of welcoming you to the *23rd Benelux Meeting on Systems and Control*, at the "Conference Hotel Guldenberg" in Helvoirt, The Netherlands.

Aim

The aim of the Benelux Meeting is to promote research activities and to enhance cooperation between researchers in Systems and Control. This is the twenty-third in a series of annual conferences that are held alternately in Belgium and The Netherlands.

Overview of the Scientific Program

1. Plenary lectures by invited speakers
    - *Fredrik Gustafsson* (ISY, LiTH, Linköping, Sweden)
        - **Model-based filtering for automotive safety systems**
        - **The particle filter and its application to positioning**
    - *Bassam Bamieh* (Univ. of California at Santa Barbara, USA)
        - **Distributed control in large actuator/sensor arrays**
        - **Understanding and controlling turbulent shear flows**
2. Mini course on *Realization of Dynamic Systems*
    - *Bart De Moor* (ESAT-SCD, Catholic University, Leuven, Belgium)
        - **Realization from exact observations**
        - **Realizations: Examples and applications**
        - **The "noisy" realization problem and model reduction**
3. Contributed short lectures, see the list of sessions for the titles and authors of these lectures.

Directions for speakers

For a contributed lecture the available time is 25 minutes. Please leave a few minutes of this period for discussion and room changes and adhere to the indicated schedule. In each room overhead projectors and beamers will be available. Be careful with this equipment, because the beamers are supplied by some of the participating groups. When using a beamer, you have to provide a notebook yourself and you have to start your lecture with the notebook up and running and the external video port switched on.

Registration

The Benelux Meeting registration desk, located near the Hotel Reception, will be open on Wednesday, March 17, from 10:00 to 14:00. Late registrations can be made at the Benelux Meeting registration desk, when space is still available. The fee schedule is:

Arrangement	Price
single room	EUR 410.–
twin-bedded room	EUR 330.–
meals only	EUR 250.–
one day	EUR 140.–

The registration fee includes:

- Admission to all sessions.
- A copy of the Book of Abstracts.
- Coffee and tea during the breaks, and ice water and mints during the sessions.
- In the case of an accommodation arrangement: lunch and dinner on Wednesday, breakfast, lunch and dinner on Thursday and breakfast and lunch on Friday.
- In the case of a "meals only" arrangement: lunch and dinner on Wednesday and Thursday, and lunch on Friday.
- In the case of a "one day" arrangement: lunch and dinner on Wednesday or Thursday, or lunch on Friday.

The registration fee does *not* include:

- Cost of phone calls
- Special ordered drinks during lunch, dinner, in the evening, etc.

Organization

The Organizing Committee of the 23rd Benelux Meeting consists of

D. Aeyels (Univ. of Gent), G. Bastin (Univ. Catholique de Louvain), O.H. Bosgra (Delft Univ. of Technology) R.F. Curtain (Univ. of Groningen), M. Gevers (Univ. Catholique de Louvain), P.M.J. Van den Hof (Delft Univ. of Technology), Bram de Jager (Eindhoven Univ. of Technology), B.L.R. de Moor (Univ. of Leuven), H. Nijmeijer (Eindhoven Univ. of Technology) A.J. van der Schaft (Univ. of Twente), J.M. Schumacher (Tilburg Univ.), M. Steinbuch (Eindhoven Univ. of Technology), G. van Straten (Wageningen Univ.), Vincent Verdult (Delft Univ. of Technology), S. Weiland (Eindhoven Univ. of Technology), H. Zwart (Univ. of Twente).

The meeting is sponsored or supported by the following organizations:

- Dutch Institute for Systems and Control (DISC),
- Stichting Meet- en Besturingstechnologie (SMBT),
- Nederlandse Organisatie voor Wetenschappelijk Onderzoek (NWO).

The meeting has been organized by Bram de Jager (Eindhoven Univ. of Technology) and Vincent Verdult (Delft Univ. of Technology).

Conference location

All lecture rooms of "Conference Hotel Guldenberg" are situated on the ground floor. Consult the map at the back of this book to locate rooms and to avoid getting lost. During the breaks, coffee and tea will be served in the bar. Announcements and personal messages will be posted near the main conference room. Accommodation is provided in the conference hotel. Breakfast will be served between 7:30 and 8:30. Room keys can be picked up at arrival and need to be returned before 8:30 on the day of departure. Parking is free of charge. The address of "Conference Hotel Guldenberg" is

Guldenberg 12
5268 KR Helvoirt
The Netherlands
tel: +31 (0) 411 64 24 24
fax: +31 (0) 411 64 24 32

Facilities

The facilities at the center include a restaurant, bar, and recreation and sports facilities. We refer to the reception desk of the hotel for detailed information about the use of these facilities.

Best junior presentation award

Continuing a tradition begun in 1996, the Benelux meeting will close with the announcement of the winner of the Best Junior Presentation Award. This award is given for the best presentation given at the meeting by a junior researcher (i.e., someone working towards a PhD degree). The award is specifically given for quality of presentation rather than quality of research, which is judged in a different way. At the meeting, the chairs of sessions will ask three volunteers in the audience to fill out an evaluation form. After the session, the evaluation forms will be collected by the Prize Commissioners who will then compute a ranking. The winner will be announced on Friday March 19, immediately after the final lectures of the meeting and he or she will be presented with the award, which consists of a trophy that may be kept for one year and a certificate. The evaluation forms of each presentation will be returned to the junior researcher who gave the presentation. The Prize Commissioners are Karel Keesman (Wageningen University) and Rodolphe Sepulchre (Univ. of Liège). The organizing committee is counting on the cooperation of the participants to make this contest a success.

Website

An *electronic version* of the Book of Abstracts can be downloaded from the Benelux Meeting web site

http://www.wfw.wtb.tue.nl/benelux2004/boa.pdf

Meetings

The following meetings are scheduled:

- UNIT DISC on Wednesday, March 17, Restaurant, 19.00–20.30.
- Graduate School on S&C (B) on Wednesday, March 17, Restaurant, 19.00–20.30.
- Management team DISC on Wednesday, March 17, Boswilg, 20.30–22.00.
- Board DISC on Thursday, March 18, Boswilg, 20.30–22.00.

Wednesday March 17

11:20 – 11:30	P0 Auditorium *Opening*				
11:30 – 12:30	P1 Auditorium *“Model-based filtering for automotive safety systems”* Fredrik Gustafsson				
12:30 – 14:00	Lunch				
Room	Boswilg	Edelspar	Fijnspar	Zilverspar	Lijsterbes
WeM	WeM01 *Traffic*	WeM02 *Motion control*	WeM03 *Bioprocesses*	WeM04 *Modeling I*	WeM05 *System theory*
14:00 – 14:25	Maerivoet	Schneiders	Cappuyns	Guffens	Engwerda
14:25 – 14:50	Mihaylova	Boerlage	Grosfils	Schumacher	Jordan
14:50 – 15:15	Gietelink	De Kruif	Volcke	Deblauwe	Opmeer
15:15 – 15:40	Haut	Oomen	Renard	Bukkems	Julius
15:40 – 16:05	Hegyi	Sandee	Speetjens	Cloosterman	Pasumarthy
16:05 – 16:35	Break				
WeP	WeP01 *Automotive systems*	WeP02 *Signal processing*	WeP03 *Biomedical systems*	WeP04 *Modeling II*	WeP05 *Stability I*
16:35 – 17:00	Kessels	D’haene	Den Dekker	Witsel	Ronsse
17:00 – 17:25	Bonsen	Rabijns	Schreiber	Van Lierop	Rogge
17:25 – 17:50	Koot	Paduart	Musters	Van Helvoirt	Gerard
17:50 – 18:15	Klaassen	Bombois	Provost	Groot Wassink	Moreau
19:00 – 20:30	Dinner				
19:00 – 20:30	Meeting UNIT DISC				
19:00 – 20:30	Meeting Graduate School S&C				
20:30 – 22:00	Meeting Management Team DISC				

Thursday March 18

8:30 – 9:30	P2 Boswilg *"Distributed control in large actuator/sensor arrays"* Bassam Bamieh				
9:30 – 10:00	Break				
10:00 – 11:00	P3 Boswilg *Mini course part 1 on "Realization from exact observations"* Bart De Moor				
11:00 – 11:30	Break				
11:30 – 12:30	P4 Boswilg *" The particle filter and its application to positioning"* Fredrik Gustafsson				
12:30 – 14:00	Lunch				
Room	Boswilg	Edelspar	Fijnspar	Zilverspar	Lijsterbes
ThA	ThA01 *Hybrid systems*	ThA02 *Time series*	ThA03 *Observers*	ThA04 *Control I*	ThA05 *Stability II*
14:00 – 14:25	Habets	Doeswijk	Van de Wouw	Noijen	Stan
14:25 – 14:50	Petreczky	Beguin	Goffaux	Troffaes	Dietz
14:50 – 15:15	Juloski	Espinoza	Doris	Voorsluijs	Pavlov
15.15 – 15:30	Break				
ThM	ThM01 *Discrete Event Systems*	ThM02 *Identification I*	ThM03 *Mechanical systems I*	ThM04 *Control II*	ThM05 *Model predictive control I*
15:30 – 15:55	Collins	Verdult	Van der Zalm	Minteer	Van Ooteghem
15.55 – 16.20	Van Eekelen	Hoegaerts	Super	Aangenent	Lazar
16.20 – 16.45	Carbone	Hinnen	Kostic	De Graaf	Necoara
16.45 – 17:00	Break				
ThP	ThP01 *Fault detection*	ThP02 *Identification II*	ThP03 *Mechanical systems II*	ThP04 H_2 *control*	ThP05 *Model predictive control II*
17.00 – 17:25	Bos	Leskens	Den Hamer	Villegas	Tiagounov
17:25 – 17:50	Parloir	Borges	Nijsse	Moelja	Van den Berg
17:50 – 18:15	Hallouzi	Markovsky	Germay	Van de Wijdeven	Pluymers
19:00 – 20:30	Dinner				
20:30 – 21:30	Meeting board DISC				

Friday March 19

8:30 – 9:30	P5 Boswilg *Mini course part 2 on “Realizations: Examples and applications”* Bart De Moor				
9:30 – 10:00	Break				
10:00 – 11:00	P6 Boswilg *“Understanding and controlling turbulent shear flows”* Bassam Bamieh				
11:00 – 11:30	Break				
11:30 – 12:30	P7 Boswilg *Mini course part 3 on “The “noisy” realization problem and model reduction”* Bart De Moor				
12:30 – 14:00	Lunch				
Room	Edelspar	Fijnspar	Zilverspar	Lijsterbes	Vlier
FrP	FrP02 *Identification III*	FreP03 *Process control*	FrP04 *Learning control*	FrP05 *Distributed systems*	FrP06 *Computation and control*
14:00 – 14:25	Parra Calvache	Nauta	Pelckmans	Grosfils	Delvenne
14:25 – 14:50	De Block	Anthonis	Fancois	Aksikas	Chahlaoui
14:50 – 15:15	Gins	Lepore	Quaeghebeur	Levrie	Blondel
15:15 – 15:40	Fritz	Bex		Logist	Blondel
15:45 – 16:00	Best Junior Presentation Award				
16:00	Closure of 23rd Benelux Meeting				

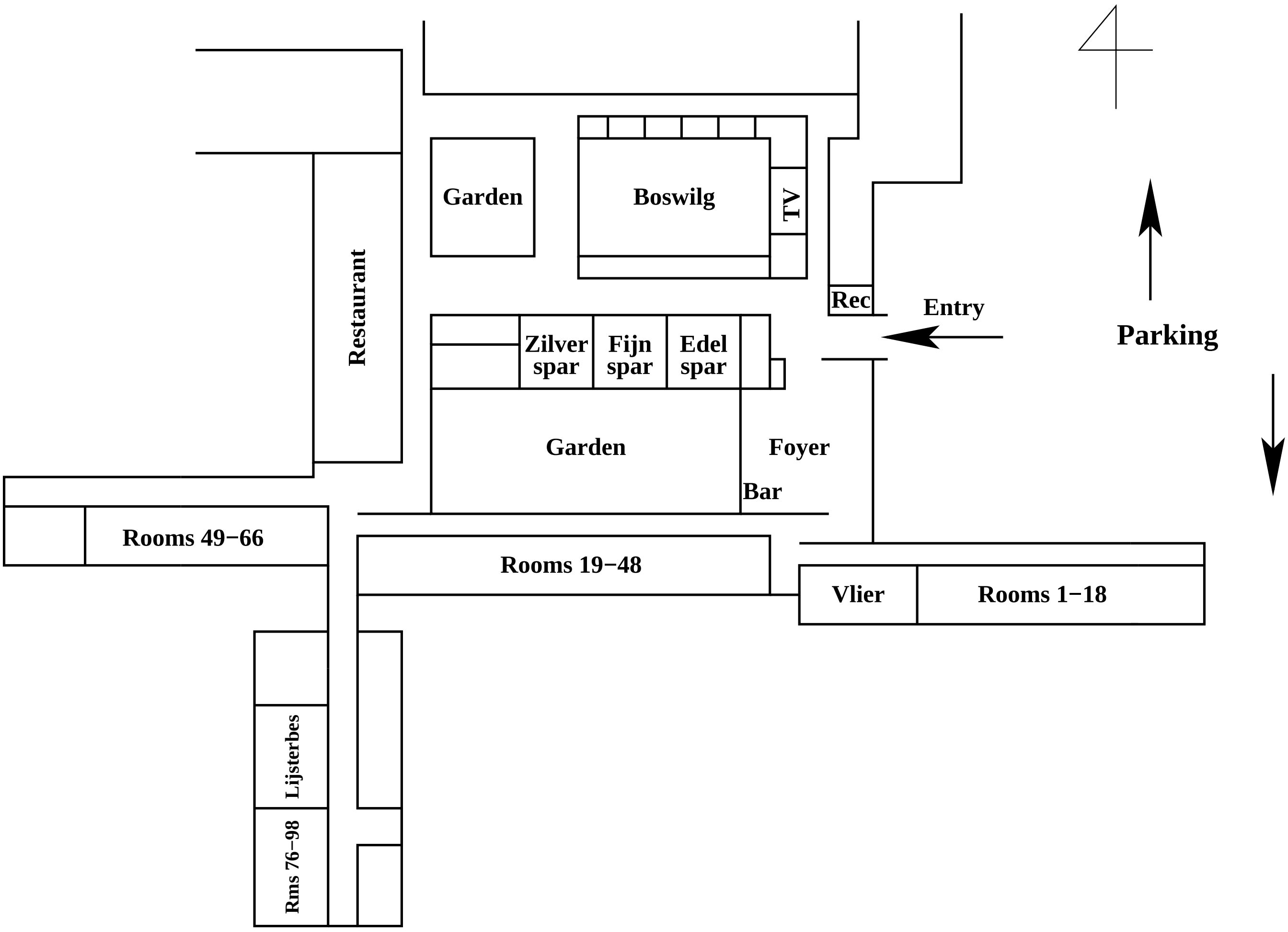
Garden
Boswilg
TV
Restaurant
Rec
Entry
Parking
Zilver spar
Fijn spar
Edel spar
Garden
Foyer
Bar
Rooms 49−66
Rooms 19−48
Vlier
Rooms 1−18
Lijsterbes
Rms 76−98